A NON-METALLIC APPROACHES FOR C–H AND C–Si BOND ACTIVATIONS

THESIS

Submitted To The

UNIVERSITY OF PUNE

For The Degree Of

DOCTOR OF PHILOSOPHY

In

CHEMISTRY

By

Sujit Pal

Research Supervisor

Dr. GANESH PANDEY

DIVISION OF ORGANIC CHEMISTRY

NATIONAL CHEMICAL LABORATORY

PUNE – 411008

June 2013

To my parents

CERTIFICATE

This is to certify that the work incorporated in the thesis entitled "**A Non-Metallic Approaches for C-H and C-Si bond Activations**" which is being submitted to the **University of Pune** for the award of **Doctor of Philosophy in Chemistry** by **Mr. Sujit Pal** was carried out by her under my supervision at the **National Chemical Laboratory**, **Pune**. A material that has been obtained from other sources has been duly acknowledged in the thesis.

Date:

Dr. Ganesh Pandey

(Research Guide)

DECLARATION

I hereby declare that the work presented in the thesis entitled **"A non-metallic approaches for C-H and C-Si bond activations"** submitted for Ph. D. Degree to the **University of Pune**, has been carried out by me at the **National Chemical Laboratory**, **Pune**, under the supervision of **Dr. Ganesh Pandey**. The work is original and has not been submitted in part or full by me for any degree or diploma to this or any other University/Institute.

Date: (**Sujit Pal**)

Division of Organic Chemistry

National Chemical Laboratory

Pune 411008,

India.

Acknowledgement

This work has been completed with the generous help and encouragement of several people. I would like to thank all of them for their support they have rendered for the accomplishment of the work presented in this dissertation.

I would like to express my deep sense of gratitude to my research guide, Dr. Ganesh Pandey for introducing me to the fascinating area of organic photochemistry. This work presented in this thesis could not have been accomplished without his unconditional guidance, encouragement and undiminished enthusiasm. I am especially thankful to him for constant helping me to improve my expression power in proper words.

I must acknowledge the moral support, motivation and motherly affection showed by Dr. (Mrs) S. R. Gadre (madam). Apart from scientific discussion, I am thankful to her for giving me a better insight and guiding me always to a right direction.

I am very much grateful to Dr. Anil Kumar for his constant encouragement and support throughout my research period.

Special thanks are due to my senior colleagues Dr. Prabal Banerjee, Dr. Sanjay Raikar, , Dr. Balakrishna, Dr. Kishore Bharadwas, Dr. Kesarinath Tiwari, Dr.Nishant Gupta, Dr.Debasish grahacharya, Dr. Ravindra Kumar, Dr. Prasanna kumara Chikkade, Shrikant, Dr. P. Siva Swaroop, Dr. Rajendar Salla, Dr. Dharmendra Tiwari and Dr. Amrut Gaikwad for their sincere advice and guidance during the course of study.

I am thankful to my senior Dr. Shrinivas Dumbre for teaching me a discipline work culture and fine experimental skills. Shrinivas ji who actually initiated the project related to the Conformationally Restricted Azasugars and success of this project is entirely based on his valuable observation. I would like to convey my special thanks to Ramakrishna for his untiring effort during later stage of my research work. Dr. Samuel Shikuku from Keneya who had joined our group for a short term research programme and I feel privilege that I got

opportunity to work with him. I am thankful to Jagadish and Dr. Mantu Rajbanshi for helping me to bring out this dissertation into reality. I was thankful to Rajesh and Dr. Nishant Gupta for helping me in making slides in many instances. I am really grateful to my contemporary labmates Debasis Dey and Priyanka. A. Adate for their unconditional supports, in whatever situation I was. I was really enjoyed the company of Deepak, Binoy, Animesh, Shiva kumar, Janakiram, Durga Prasad, Pradip, Akash, Rushil, Sandeep, Sahani, Ajay, Pushpendra, Divya, Dr. Bhawna Singh, Dr. Atish Chandra, Dr. Navnath. I will always cherish memories of these days.

Special thanks to Dr. Kumar Vanka and Miss. Nishamol Kuriakose for solving my theoretical calculations. Dr. Rajmohan, Srikant and Snehal (NMR), who went out of their way in helping me out whenever I needed an urgent analysis. I am especially grateful to Dr. Rahul Banerjee and Mr. Arijit mallick for helping me with crystallographic analysis. I would also like to convey my thanks to the GC-MS, HPLC and HRMS analyzing people for their assistance.

The cooperation and supports from entire NCL GJ hostel friends and few of my close people like Amrita, Ritu, Bimalendu, Dinesh, Manjit Nandi, Sutapa and Paromita di which I will never forget.

I simply do not have the words to thank my parents, sister, brother and all of my family members whose everlasting encouragement, support and patience during my seemingly unending education have helped me to reach this juncture.

I thank CSIR, New Delhi, for the award of Research Fellowship and Director, N. C. L., for the infra-structural facilities.

Sujit

Contents

Abbreviations

aq.	aqueous	NMR	Nuclear magnetic resonance
mL	Milliliter	*p*-TSA	*p*-Toluenesulfonic acid
mmol	Millimole	TBS	*tert*-Butyldimethylsilyl
m.p.	melting point	COSY	Correlation Spectroscopy
DBU	1,8- Diazabicyclo [5.4.0]undec-7-ene	NOE	Nuclear overhauser effect/enhancement
DEPT	Distortionless enhancement by polarization transfer	HSQC	Heteronuclear Single Quantum Coherence)
DMAP	*N*,*N*-Dimethylaminopyridine	HMBC	*Heteronuclear Multiple Bond Correlation*
DMF	*N*,*N*-dimethylformamide	THF	Tetrahydrofuran
DMSO	Dimethylsulfoxide	TLC	Thin layer chromatography
DCE	1, 2 -dichloroethane		
g	gram	PMB	*p*-methoxy benzyl
GC	Gas chromatography	SM	Starting material
h	hour	Ac	Acetyl
Hz	Hertz	HMDS	Hexamethyldisilazane
M	Molarity (molar)	LDA	Lithium diisopropylamide
N	Normality	TMEDA	Tetramethylethylenediamine
TMS	Trimethylsilyl	IBX	2-Iodoxybenzoic acid
MS	Mass spectrum	MPO	4-Methoxy pyridine N-oxide
		EDCI.HCl	1-(3-Dimethylaminopropyl)-3-ethylcarbodiimide hydrochloride

General Remarks

- All the solvents were purified according to literature procedure.[1]
- Petroleum ether used in the experiments was of 60−80 ˚C boiling range.
- Column chromatographic separations were carried out by gradient elution with suitable combination of two solvents and silica gel (60−120 mesh/100−200 mesh/230−400 mesh).
- The irradiation was performed by using 450-W Havonia medium pressure lamp and pyrax filter (>300 nm).
- Reaction progress was monitored by TLC or GC. TLC was performed E-Merck pre-coated 60 F254 plates and the spots were rendered visible by exposing to UV light, Iodine, phosphomolibdic acid, *o*-Anisol, KMnO4. GC analysis was performed on Perkin Elmer 8700 and Varian CP 3800 GCs using SGE BP1, BP20 and Varian Chromopack CP-Sil-5CB columns.
- IR spectra were recorded on FTIR instrument, for solid either as nujol mull, neat in case of liquid compounds or their solution in chloroform.
- NMR spectra were recorded on Bruker AV 200 (200 MHz ^{1}H NMR and 50 MHz ^{13}C NMR), Bruker AV 400 (400 MHz ^{1}H NMR and 100 MHz ^{13}C NMR) and Bruker DRX 500 (500 MHz ^{1}H NMR and 126 MHz ^{13}C NMR).
- ^{13}C peak multiplicity assignments were made based on DEPT data.
- Mass spectra were recorded on PE SCIEX API QSTAR pulser (LC-MS) and Shimadzu QP 5000 GC/MS coupled to Shimadzu 17A GC using a DBI column.
- High resolution mass (HR-ESI-MS) spectra was recorded on a Thermo scientific make Q-exactive model spectrometer using electrospray ionization
- Optical rotations were measured on a JASCO P-1020 polarimeter.
- HPLC were performed on Shimadzu Class-VP V6.12 SP5 with UV detector.
- All the melting points recorded are uncorrected and were recorded using electrothermal melting point apparatus.
- Numbering of compounds, schemes, tables, referencing and figures for each chapter as well as abstract are independent.

1. Perrin, D. D.; Armarego, W. L. F. Purification of Laboratory Chemicals, 4th ed. Butterworth Heinemann, **1999.**

Thesis Abstract

A Non-Metallic Approaches for C–H and C–Si Bond Activations

The present dissertation is divided into three chapters.

<u>Chapter I:</u>Direct Benzylic C–H Activation for C–O Formation by Photoredox Catalysis.

This chapter starts with a brief account on the importance of C-H activation strategy in the modern research interest. In this context, Intense research activities by several research groups in this area have resulted in the development of some very useful protocols for regioselective C_{sp2}-H activation through transition metal catalyses, however, corresponding C_{sp3}-H activation is still in its infancy. The benzyl group being an important motif in organic syntheses, its direct activations has been achieved by using either hetero-atom chelated transition metal catalyst or non-directed oxidative activations. In spite of impressiveprogress made in this area, the reported protocols are far frombeing environmentally benign as they either require moisture-sensitive and expensive metal catalysts or special structuralrequirements along with excessive use of chemical oxidants.Therefore, further research in this area is still warranted. With this endeavor, we envisioned an unprecedented benzylic C–H bond activation protocol *via* photoredox cycle as shown in **Fig. 1** and report herein the success of our concept for direct benzylic C–H activation for C–O bond formation which requires neither a metal catalyst nor any chemical oxidant.

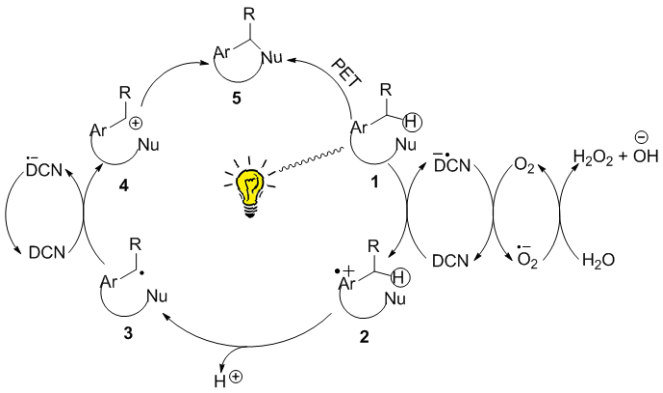

Figure 1.Concept of benzylic C–H activation *via* photoredox catalysis.

Initally, to test the feasibility of the proposed concept for the intramolecular benzylic C–O bond formation was examplified through the cyclizations of substrates (**6**-**8**) as depicted in **Table-1**.

Table -1

Entry	Substarte	Product	Time	Yield (%)[a]
1	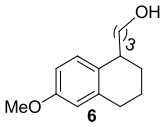 **6**	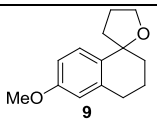 **9**	3 h	62
2	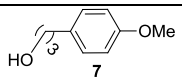 **7**	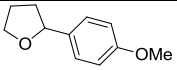 **10**	3 h	51
3	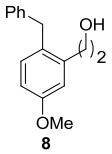 **8**	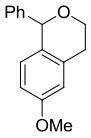 **11**	5 h	72

[a] yield was calculated based on starting materials consumption.

Having successfully activated benzylic C–H bond for cycloetherification reaction, we turned our attention towards trapping benzylic radical **13** (**Scheme 1**). Towards this end, we carried out PET activation of **12** with the hope that radical **13** would be stabilized by α-ester group and might add on to the tethered olefin to produce corresponding indane derivative **14**. However, identical activation of **12** produced **17** (52%) instead of expected **14**. This result could only be explained by implicating the intermediacy of distonic carbocation **16**.

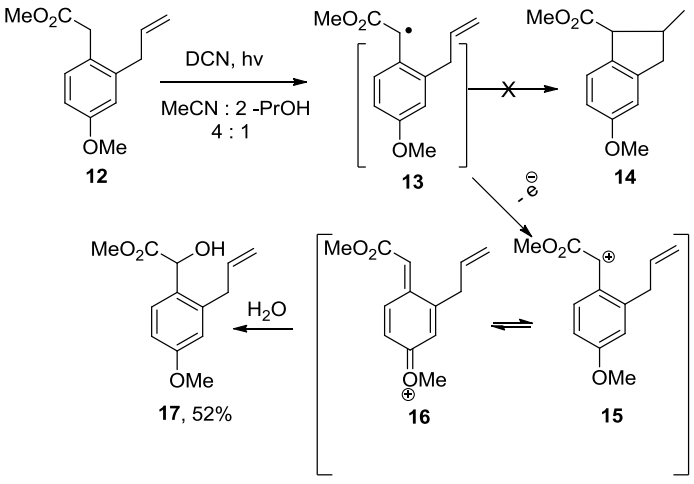

Scheme 1

Towards an effort to generalize this reaction, we studied several substrates **18-20** and results are shown in **Table 2**.

Table 2

Entry	Substrate	Product	Time	Yield(%)[a]
1	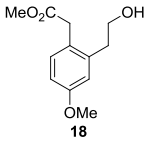 **18**	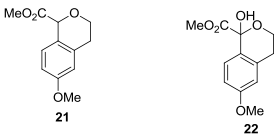 **21** **22**	4 h	**21** (15), **22** (65)
2	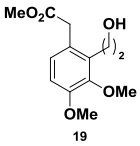 **19**	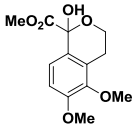 **23**	5 h	52
3	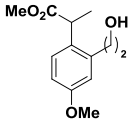 **20**	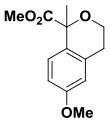 **24**	4 h	46

[a] yield was calculated based on starting materials consumption.

After successfully realizing benzylic C–H bond activation for intramolecularcycloetherification reaction, we enthusiastically turned our attention of introducing oxygen functionality at benzylic position intermolecularly as shown in **Scheme 2**.

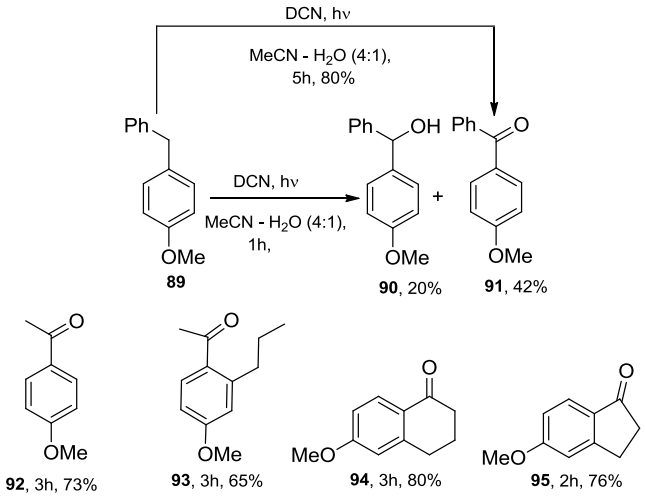

Scheme 2

Chapter II: Metal free C – Si bond activation and its synthetic application

This chapter deals with the photocatalyticC–Si bond cleavage of α-silyltrimethylamine radical cation intermediateas shown in **Scheme 1.** Thus this methodology was recognized as useful for stereoselective constructing of nitrogen containing heterocyclic moiety comprising of bi-cyclic amines and biologically important polyhydroxylated cyclic amines i. e. ***azasugars***.

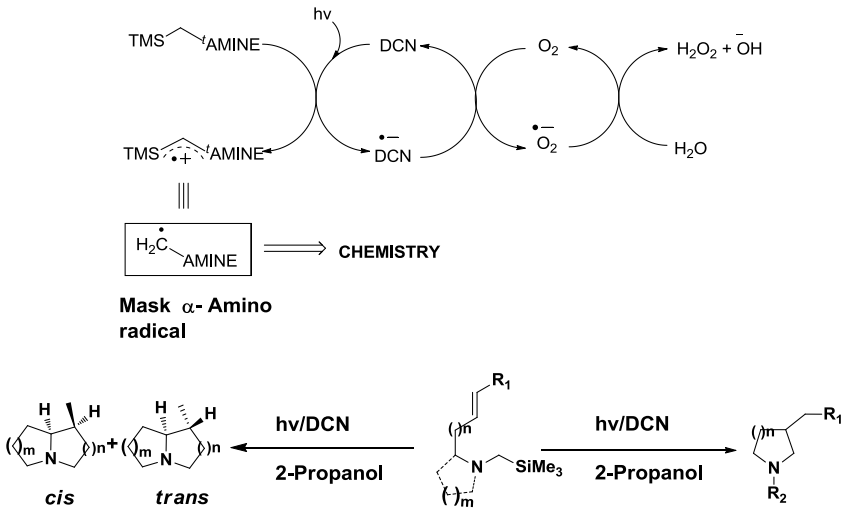

Scheme 1

As a part of our ongoing interest in the design and synthesis of new potent azasugars and less explored potential of polyhydroxylated 1-azabicyclo[4.2.0]octaneframeworkas a glycosidase inhibitor, we designed and synthesized hydrochloride salt of (3*S*,4*R*,5*S*,6*R*)-1-azabicyclo[4.2.0]octane-3,4,5-triol **(6. HCl)** as shown in **Scheme 2**.

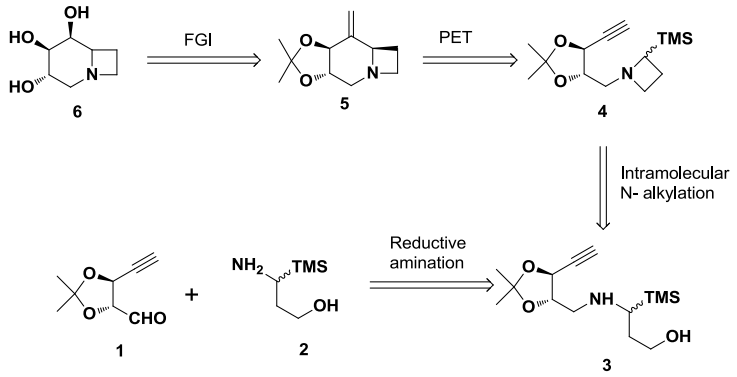

Scheme 2

The inhibitory activities of **6.HCl** was screened against β-galactosidase (*Aspergillusoryzae*), *α*-galactosidase (coffee beans), *β*-glucosidase / *β*-mannosidase (almonds), *α*-glucosidase (yeast) and α-mannosidase (jack beans). It is apparent that **6. HCl** exhibited good (*ki* = 7.6*μM*), competitive and specific inhibition against *β* – glucosidase only.

Chapter III:Protecting group free Synthetic effort towards the (+) 223A

In this chapter we have discussed all the precedents synthetic strategies have been used for the synthesis of indolizidine alkaloid **223A**. The unexplored biological activity and in search for its more concise synthesis, have prompted us to design a synthetic strategy for the asymmetric synthesis of **(+)-223A** as shown in **Scheme 1**.

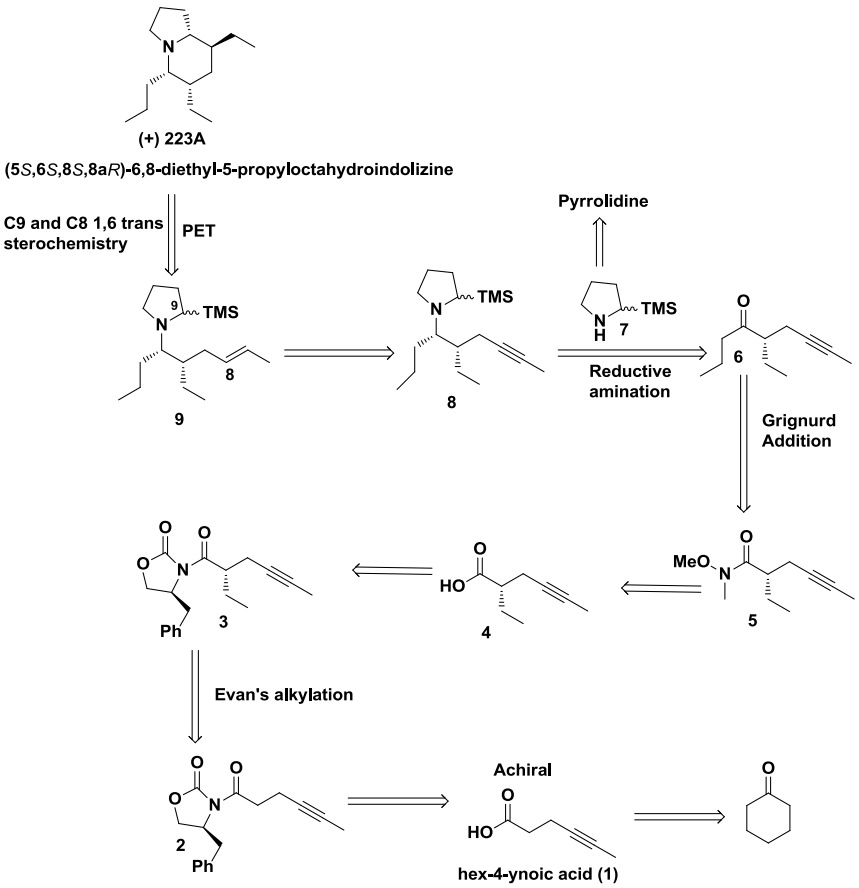

Scheme 1

Towards this planned strategy, **2** was synthesized from **1** and was subjected to asymmetric alkylation by using ethyltriflate (EtOTf) and NaHMDS at - 78° C. However, the unanticipated failure in the reductive amination reaction between **6** and **7**, led us to utilize **10** as a precursor for reductive amide alkylation to obtain **11** by following steps as shown in **Scheme 2**. The required **10** was synthesized by coupling of **4** and **7** utilizing EDCI. HCl as an amidating reagent (**Scheme 2**). Reaction of **10** with *n*-propylmagnesium at -78° C followed by sodium borohydride reduction of resultant imine produced **11** as a mixture of diastereomers.

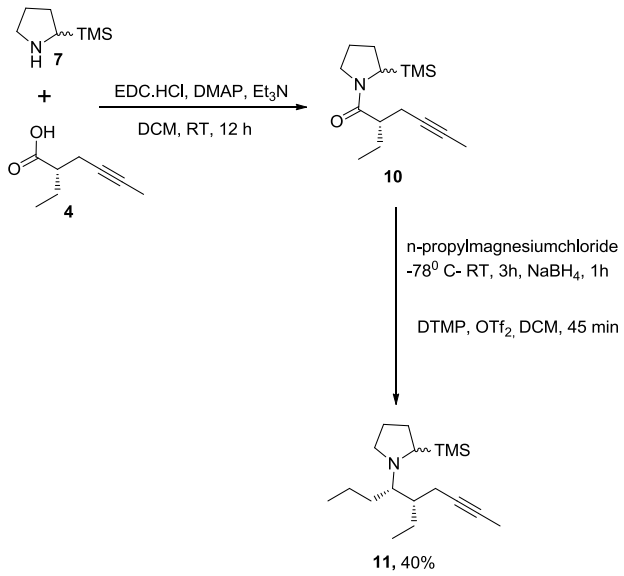

Scheme 2

Due to time constrains, the synthesis of **(+)-223A** has to be curtailed at this stage for the time being.

In summary, we have developed a conceptually new metal free benzylic C-H activation strategy for the construction of C-O bond by both intra and intermolecularly. Similar activation of C-Si bond of *α*-silyltrimethylamine radical cation intermediate has been successfully utilized in the synthesis of bio-active azasugars.

Note: Compounds numbers in the abstract are different from those in the thesis.

CHAPTER 1

Direct Benzylic C–H Activation for C–O Bond Formation by Photoredox Catalysis

1.1 Introduction:

Organic synthesis relies on functional group transformations or structural features exhibiting relatively high reactivity. Thus, installing a new bond requires the presence of either a heteroatom, such as oxygen, nitrogen, halogen or unsaturation in carbon backbone. This is illustrated by the sequence of several steps that converts compound **1** to product **2** (**Scheme 1**).

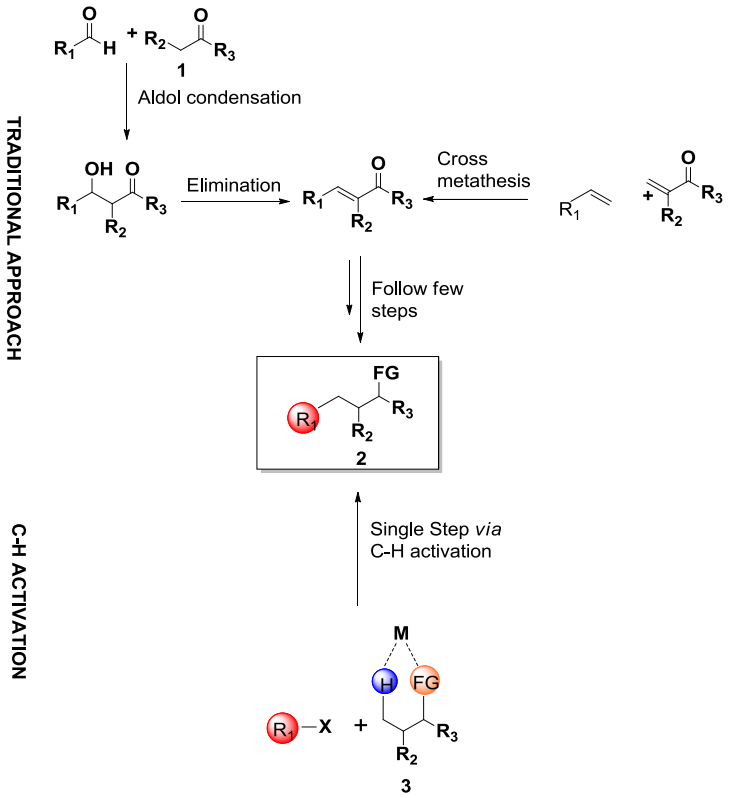

Scheme 1

However, discovery of new methodologies that either improves the step and atom economy of existing processes or introduces novel and innovative transformation to construct complex molecules is the long-standing goal of the synthetic chemists. In this regard, the fast-growing field of C–H activation represents one of the most promising approaches of the last decades[1-3]. The direct transformation of C–H bonds into C–C or C–heteroatom bond reduces needless pre-functionalization of starting materials and represents a more atom and step economy strategy than traditional bond forming reactions[4-5].

Historically, selective functionalization of C–H bond was observed in Hofmann-Löffler-Freytag and Barton reaction[6] (**Scheme 2**). The critical regioselectivity was dictated by the proximity between the radical and the corresponding C–H bond; however, this was not recognized by the terminology of "C–H activation" at that time.

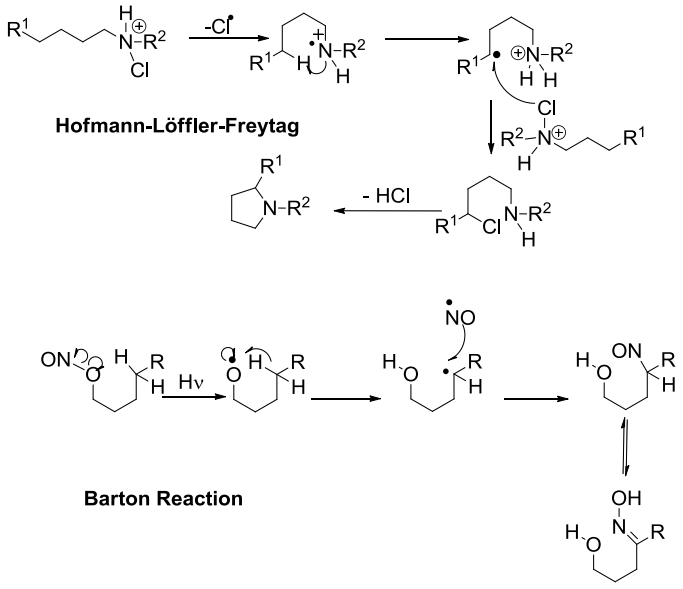

Scheme 2

The field took off during the 1980s, when there was a dramatic increase in the number of metal salts and complexes that were found to initiate direct C–H bond functionalization by oxidative addition[7-8]. But the drawback was that most of these transformations required equal amounts, in moles, of the hydrocarbon and the metal and both partners were consumed during the reaction. This was not acceptable for large-scale chemistry, as the metals involved are generally more expensive than the products. There has been an explosion of interest in developing catalytic reactions for bringing about oxidative addition of metal catalysts for C–H activation[9-12]. In this context, direct C_{sp2}-H activation by the use of directing groups (DG), such as amides, pyridines, or acetanilides, have become the strategies of choice to allow site-selective arene functionalization[13-16] (**Scheme 3**).

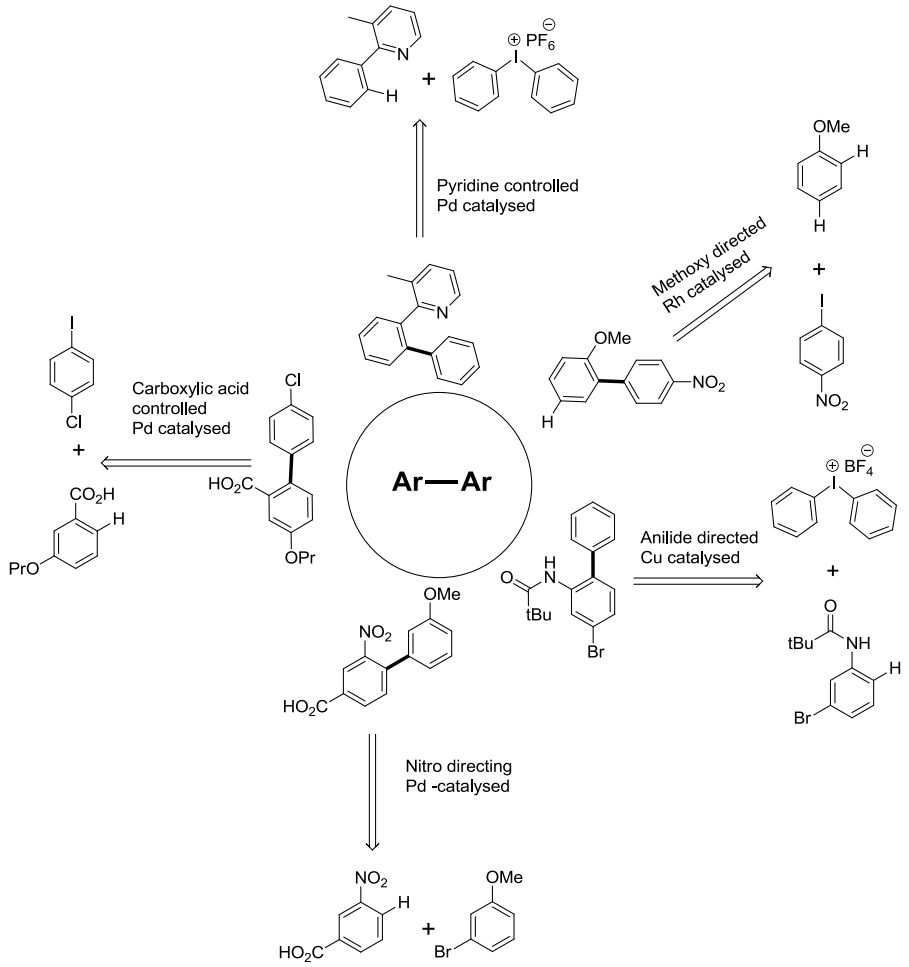

Scheme 3

Because of the coordination ability of the DG, it directs the transition metal into close proximity of the C–H bond to be activated, resulting in high levels of regioselectivity and increased reactivity because of the higher effective concentration of the catalyst at the site of interest.

However, despite these advantages, the use of DGs has certain limitations. In most cases, functionalization of the arenes occurs only at the C–H bond *ortho* to the DG, thus, restricting the scope of accessible products. Furthermore, additional synthetic steps are often required to both install the DG into the starting material and to manipulate it after C–H functionalization.

A more appealing strategy for the C–H activation of benzene derivatives would be to avoid using DGs altogether. To date, only a few examples of non-directed transition metal catalyzed regioselective C_{Sp2}–H activation of benzene derivatives have been

disclosed, although recent reports demonstrate a rapidly growing interest in this class of transformation[17-20] (**Scheme 4**).

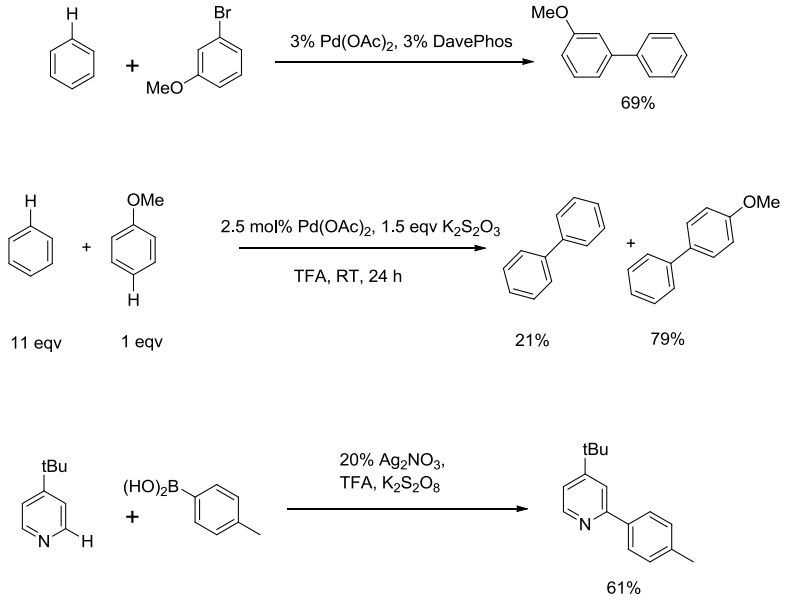

Scheme 4

Intense research activities by several research groups on the above strategies have resulted in the development of useful protocols for regioselective C_{sp2}–H activation through transition metal catalyses, however, corresponding C_{sp3}–H activation is still in its infancy[21-22]. The reason behind is that most transition metal-catalyzed C–H activations involve cleavage of the C–H bond to form a C–M bond. But this is generally more difficult to achieve with C_{sp3}–H bonds compared to C_{sp2}–H bond because the former are less acidic and lack proximal empty low – energy filled orbitals that readily interact with orbitals of the metal.

Amongst the few novel approaches in the C–hetero or C–C bond formation through remote un-activated aliphatic C_{sp3}–H bond functionalization, using Mn(III) and Fe(III) porphyrins, Breslow[23] and his co-workers were able to demonstrate first metal mediated nitrene insertion into C_{sp3}–H. By recognizing the strengths of this concept, Du Bois[24] and co-workers subsequently have developed several intramolecular amination methodologies by using $Rh_2(OAc)_4$ as catalyst and $Pd(OAc)_2$ as oxidant (**Scheme 5**).

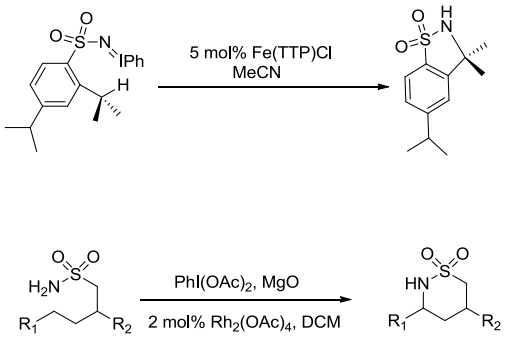

Scheme 5

In the area of direct intermolecular C–O bond formation, Fe- catalyzed hydroxylation of an un-activated and remote C_{sp3}–H bond is also reported[25-26] (**Scheme 6**).

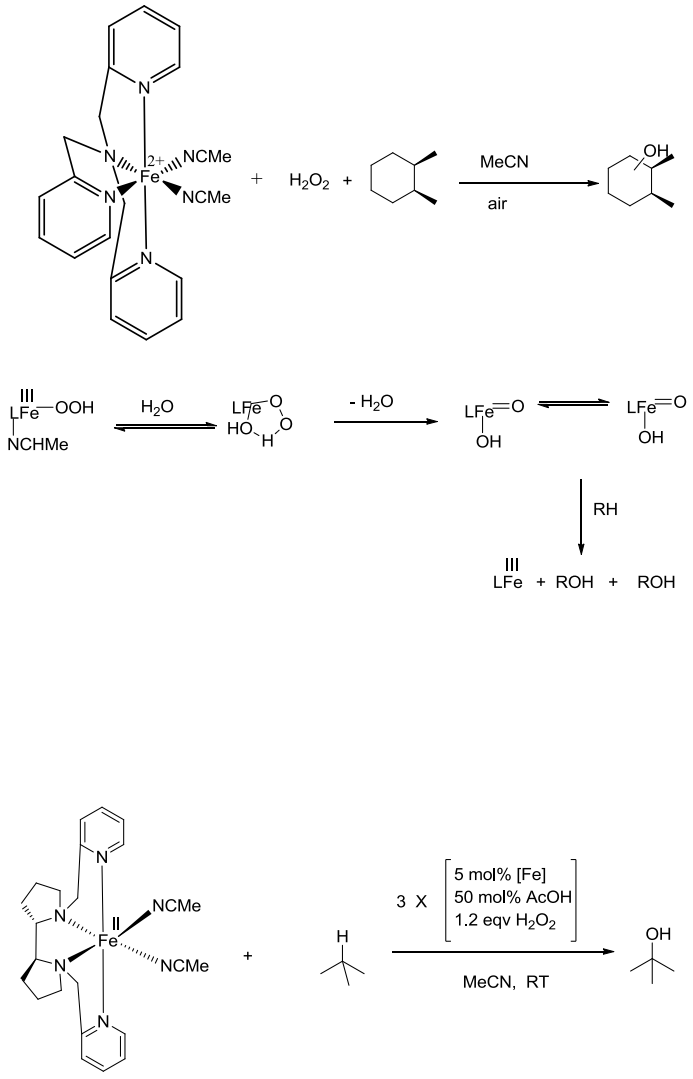

Scheme 6

Stanforfd *et al.*[27]have also reported acetoxylation of C_{sp3}–H by imine directed Pd-catalysed activation (**Scheme 7**).

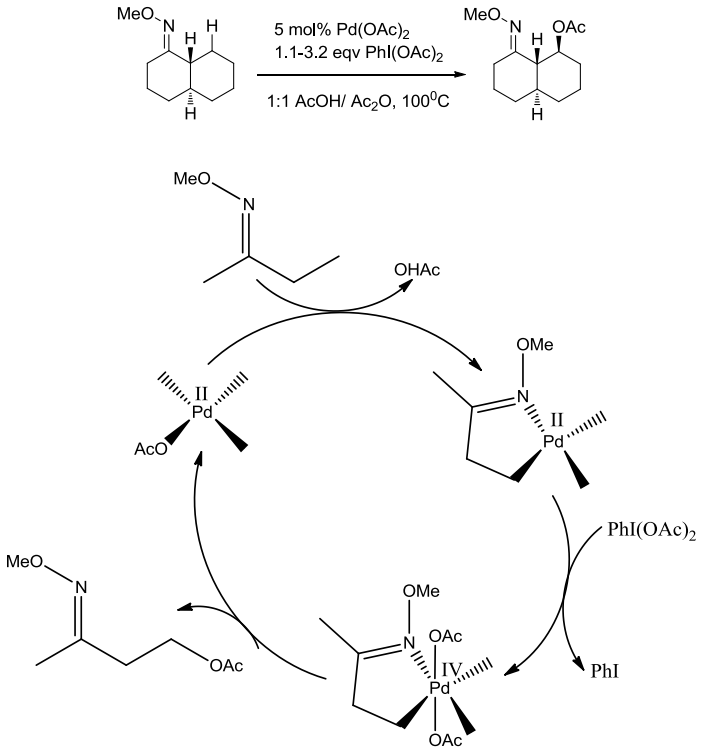

Scheme 7

Pd-catalysed carboxyl group directed remote C_{sp3}–H arylation has been reported[28] by Yu group where aryl iodide was used as a coupling partner (**Scheme 8**).

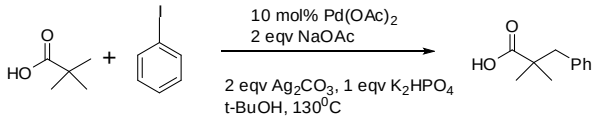

Scheme 8

Similarly, benzylic C_{sp3}-H bond functionalizations also being an important reaction in organic syntheses (**Figure 1**), direct activations have been achieved by following strategies of 1) hetero-atom chelated transition metal catalysed[29-33], 2) non-directed oxidative activations[34-39], 3) acid catalysed activations[40-42].

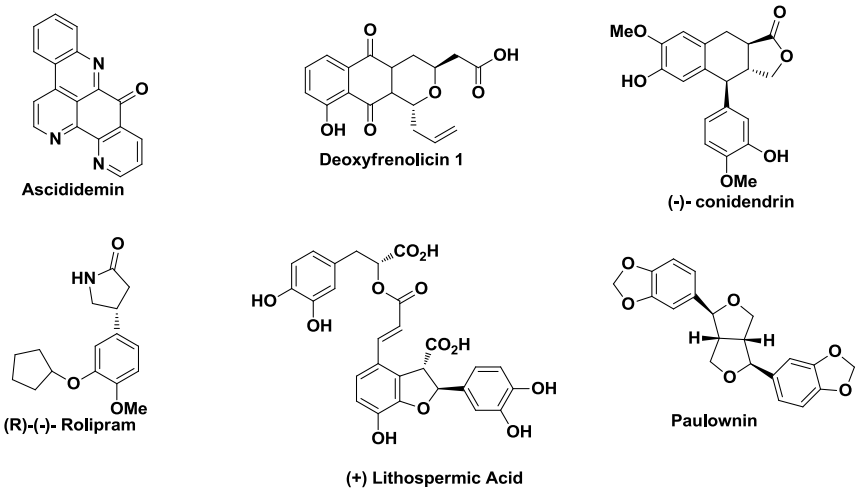

Figure 1

Since this dissertation concerns with the benzylic C_{sp3}–H bond activation, it would be imperative to discuss the methodologies are reported in this area to put the work in proper perspectives.

1.2 Strategies for Benzylic C_{sp3}-H bond activation: Literature reports

Heteroatom chelated transition metal catalyzed approaches

Similar to C_{sp2}–H bond activations of arenes, directing groups (DG) have also played significant role in benzylic C_{sp3}-H bond activations. For illustration, a compound such as **4** which possesses a pyridine moiety and an amide group has been used for chelation controlled palladium catalyzed benzylic C–H arylation/oxidation reaction[29]as shown in **Scheme 9**.

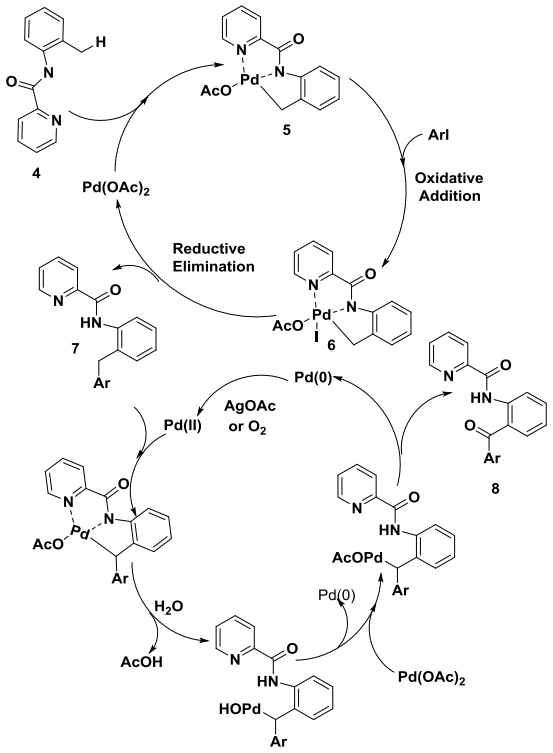

Scheme 9

Another example of Ru(0) catalyzed pyridine controlled direct benzylic C–H arylation[30] of acyclic amine with aryl boronates is reported for highly regioselective and efficient synthesis of **13**. The catalytic process is initiated by the coordination of ruthenium(0) to the nitrogen of pyridine moiety, followed by oxidative addition to **10**. Subsequently, the ketone is reduced to the corresponding alcohol, followed by formation of a metal-alkoxy (Ru-OR) species **11**. This intermediate facilitates the transmetalation with $ArB(OR)_2$ to **12**. The ketone simultaneously works as a hydrogen and boron scavenger. Reductive elimination of **12** finally delivers product **13** and re-generates the catalyst as shown in **Scheme 10**.

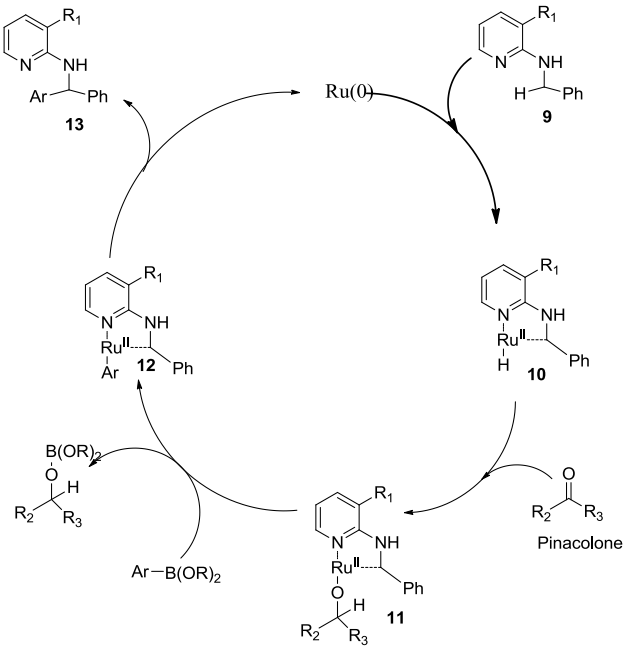

Scheme 10

Benzylic C–H bond activation by Cu (I) chelated oxy insertion between benzylic C–H and oxygen of *ortho*-methylbenzanilides (**14**) is reported for C–O bond formation reaction[31]. It was suggested that reaction proceeds by hydrogen abstraction by Cu(III) chelated intermediate (**17**) produced *in situ* by selectfluor (**Scheme 11)**.

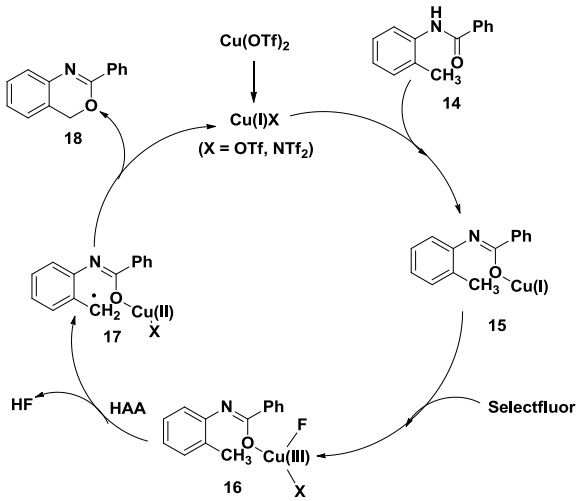

Scheme 11

Martin *et al.*[32] have reported carboxyl group directed Pd (II) chelated benzylic C–H bond activation of multi-substituted benzoic acid **19** for intramolecular C–O bond formation in presence of amino acid ligand **23** as shown in **Scheme 12**.

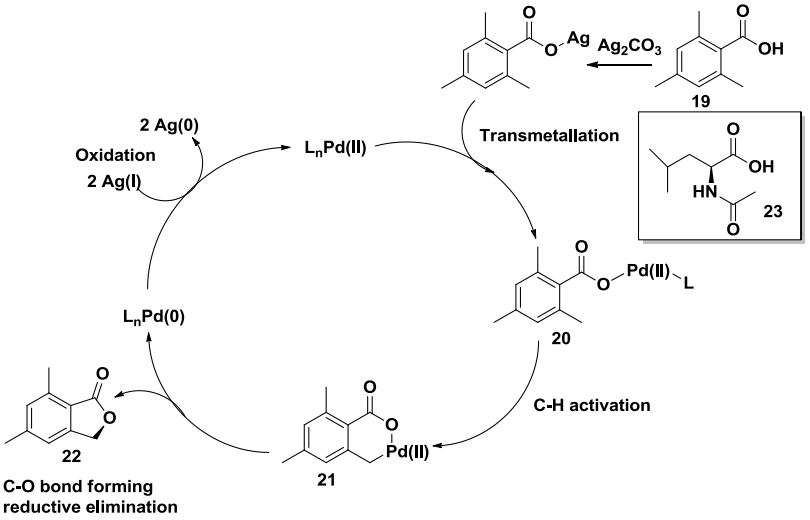

Scheme 12

Recently a palladium catalysed cascade process[33] between *o*-methyl phenylisocyanide (**24**) and aryl iodide is reported for the synthesis of 2-arylindoles (**27**) derivatives. The reaction is initiated by the insertion of aryl palladium species into the isocyanide followed by regioselective benzylic C–H bond activation as shown in **Scheme 13**.

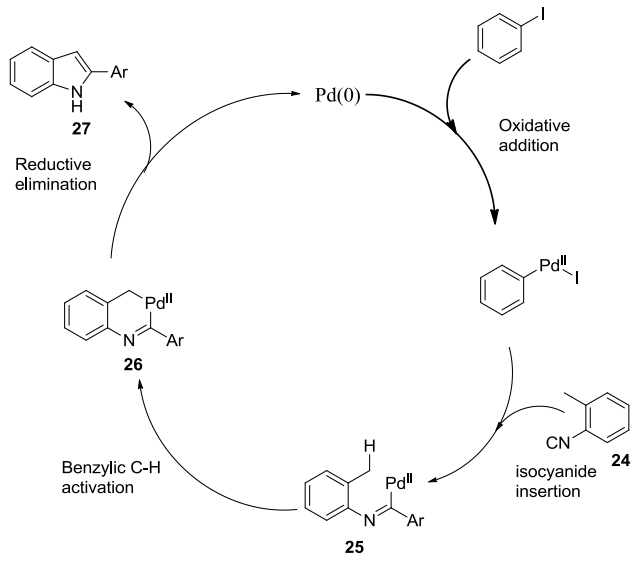

Scheme 13

Non-directed benzylic C-H activation

In the context of non-directed benzylic C–H activations, pioneering work by Li *et al.*[34] of iron (II) catalysed intermolecular C–C bond formation between diphenylmethane (**29**) and 1, 3-diketone **28** in presence of TBHP is worth mentioning.

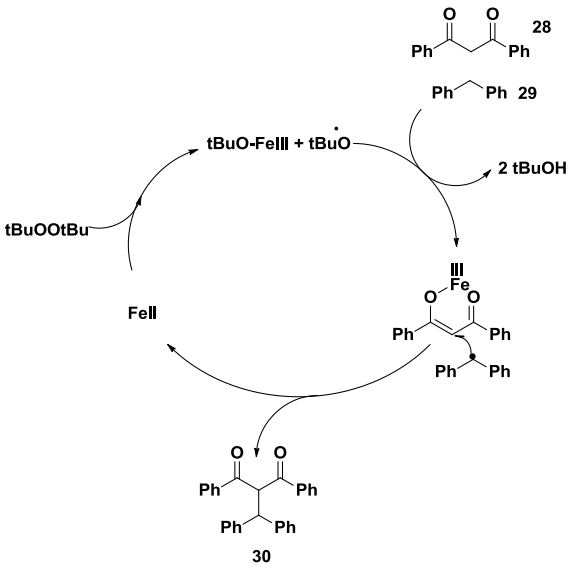

Scheme 14

Un-activated benzylic C–H carbonylation to synthesize benzylcarboxylate esters **34** has also been reported[35] by CO insertion to an organopalladium species **32,** generated by oxidative addition of Pd(0) to the benzylic radical as shown in **Scheme 15**.

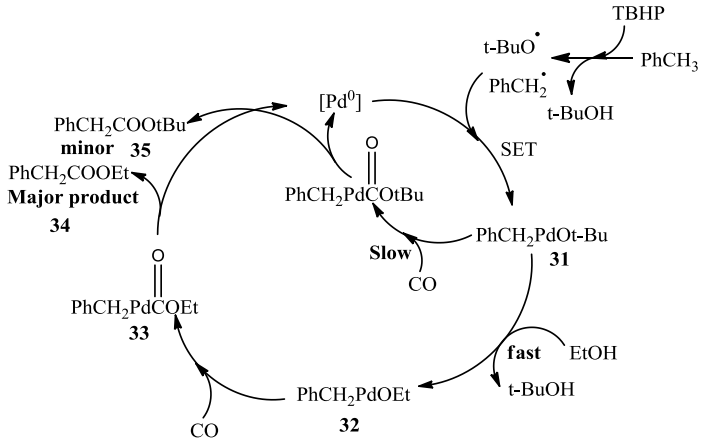

Scheme 15

Beside the use of transition metal catalysts in presence peroxides (*e.g.* TBHP), 2, 3-dichloro-5, 6-dicyano-1, 4-benzoquinone (DDQ) has been utilized as an excellent oxidative reagent for benzylic C–H bond activations where benzylic moiety is substituted by a heteroatom (oxygen or nitrogen). For example, intermolecular C–C bond formation with various carbon nucleophiles have been reported[36-37] by DDQ mediated oxidation of cyclic and acyclic benzylic ethers (**Scheme 16**)

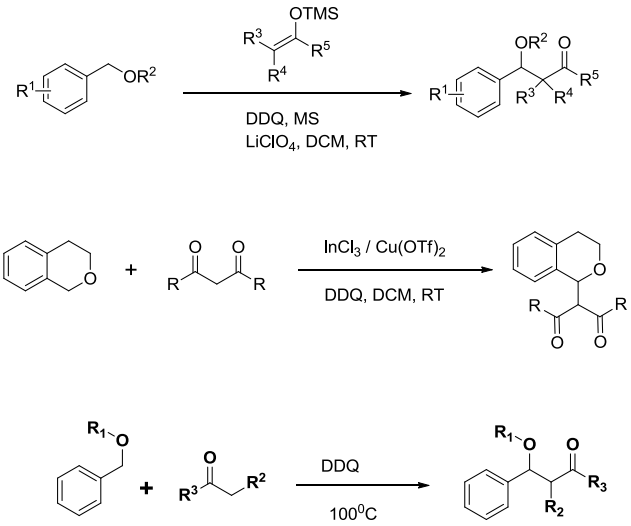

Scheme16

Recently, Floreancig *et al.*[38] have reported that oxocarbenium ion intermediate generated by DDQ oxidation of benzylic ethers, can be also captured by nucleophiles appended in the molecules (**Scheme 17)**.

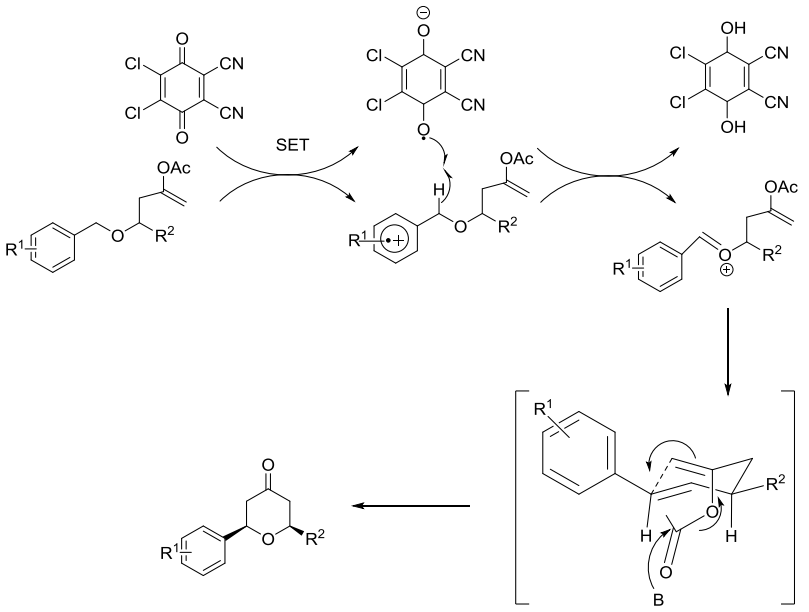

Scheme 17

A similar report has also appeared[39], where oxocarbenium ion intermediate **37** is trapped by an un-activated olefin in the presence of lewis acid $SnBr_4$ to produce 2,4,6-*cis*-tetrahydropyran derivative (**39**) as shown in **Scheme 18**.

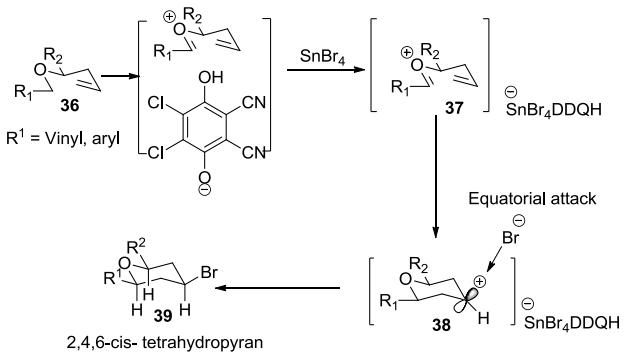

Scheme 18

Acid catalysed benzylic C-H activation

Metal free catalytic activation for C–C bond formation of acridines and xanthenes has been achieved[40] by the Brönsed acid (triflic acid) catalysed cleavage of hydroperoxide intermediate (**41**) to produce active intermediate **42** which is subsequently intermolecularly trapped by enolizable ketone to produce net coupled product **43** as shown in **Scheme 19**.

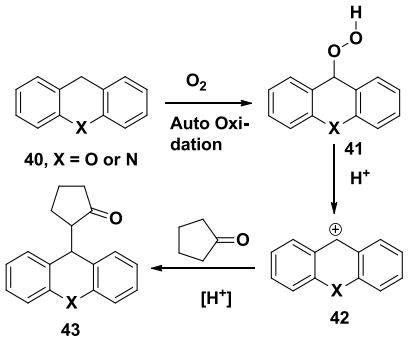

Scheme 19

Similarly, Lewis acid catalysed activation of C–H bond of 2-alkylazaarenes (**44**) is also reported[41] for direct addition to enones to obtain 2-alkyl substituted azarenes of type **47** as shown in **Scheme 20**.

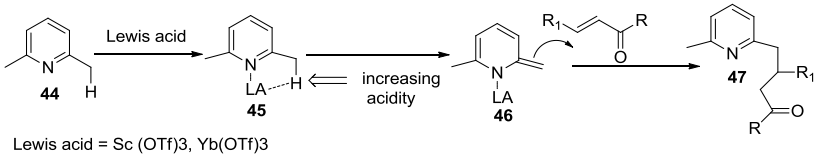

Scheme 20

A conceptually new strategy of benzylic C–H bond activation is reported by Sames *et al.*[42] where cyclic acetal of **48** on treatment with boron trifluoride etherate generates oxocarbenium intermediate **49**, which activates 1, 5 hydride transfer from the benzylic site. The resultant oxocarbenium-enolether intermediate **50** undergoes rapid C-C bond formation producing **51** stereoselectively (**Scheme 21)**. The observed stereochemistry is explained by considering the favourable six-member chair conformation of intermediate **50** where all substituents lie in equatorial positions.

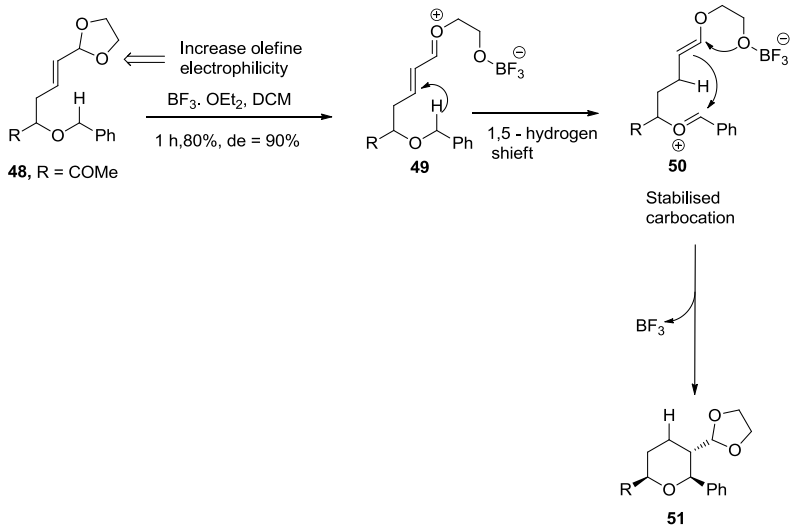

Scheme 21

In spite of impressive progress made in this area, the reported protocols are far from being environmentally benign as they either require moisture sensitive and expensive metal catalysts or special structural requirements along with excessive use of chemical oxidants. Therefore, further development in this area is still warranted. Based on our previous work on photoinduced electron transfer (PET) reactions[43-45], we sought to develop a new PET initiated 1, 4-dicyanonaphthalene (DCN) photocatalysed benzylic C_{sp3}–H activation for nucleophilic carbon –hetero atom bond (C–X) formation as shown in **Scheme 22**.

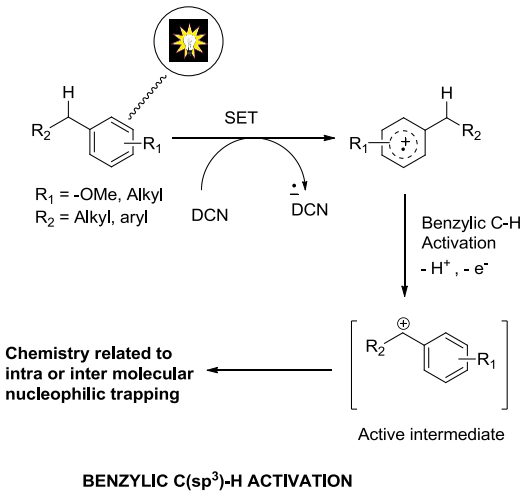

Scheme 22

However, before describing our current designed strategy of benzylic C-H activation, it may be imperative to introduce the concept of PET reactions in general.

1.3 Concept of Photo-induced Electron Transfer Reaction:

Promotion of an electron from the highest occupied molecular orbital (HOMO) in the ground state to an unoccupied molecular orbital (LUMO) makes that molecule both highly oxidizable and reducible. That is the energetically high lying electron can be transferred to the vacuum (or to an acceptor of constant reduction potential) with smaller activation than any electron can have in a ground state occupied molecular orbital (HOMO). Similarly, the vacuum created in the ground state HOMO which is generated upon photoexcitation allows far more effective reduction, since the electron affinity of the excited state is significantly enhanced compared with the ground state. Thus photoexcitation of electron acceptor (A) or electron donor (D) substrates lead to well defined changes in their redox properties in a well defined manner.

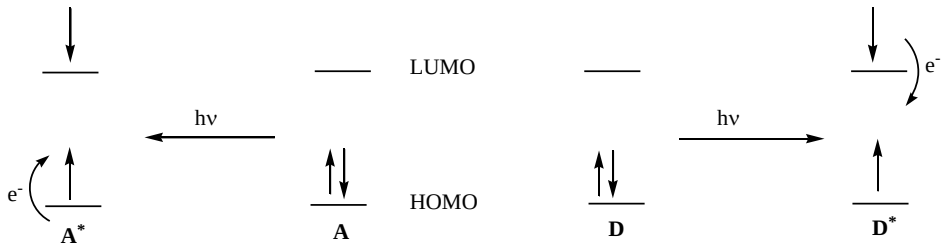

The donor property of D increases proportionally with the excitation energy [ΔE (D*) = hν] i.e the ionization energy. IP (D) is reduced by the promotion of an electron from the HOMO to the LUMO (Eq. 1). The electron affinity of the acceptor EA (A) behaves similarly (Eq 2).

$$IP(D^*) = IP(D) - \Delta E(D^*) \quad \text{.....(Eq 1)}$$

$$EA(A^*) = EA(A) - \Delta E(A^*) \quad \text{.....(Eq 2)}$$

Thus electron transfer between donor and acceptor substrates should occur more easily after

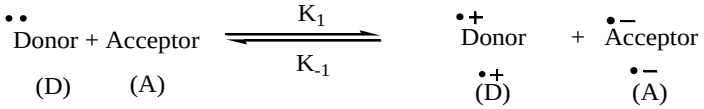

photochemical excitation of one of the reducing species if either IP (D*) < EA(A) or IP (D) < EA(A*) holds true **Figure 3**.

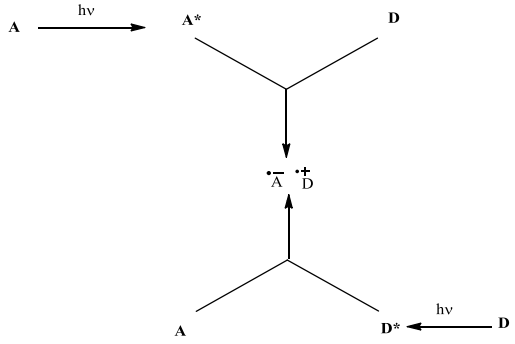

Figure 3 Photochemically induced electron transfer between donor(D) and acceptor (A) molecules

IP and EA are valid only for the gas phase. However, the oxidation and reduction potentials [$E_{1/2}$ (Ox) of D and [$E_{1/2}$ (Red) of A], which are the corresponding parameters in solution are obtained experimentally. The conditions for the electron transfer between D and A after irradiation have been formulated by Rehm – Weller[46] as shown in **Eq 3**.

$$\Delta G[A_s^{-\cdot} D_s^{+\cdot}] = F[E_{1/2\,(Ox)} \text{ of } D - E_{1/2\,(red)} \text{ of } A] - \Delta E_{EXC} + \Delta E_{CO} \quad \text{.....Eq 3.}$$

Where ΔE_{EXC} is the excitation energy of the electronically excited species and ΔE_{COU} is the Coulomb interaction energy of the two radical ions at a distance 'a' from each other in a given solvent. The free energy (ΔG) for the formation of solvent separated ion pairs [$A_s^{-\cdot}$ $D_s^{+\cdot}$]in a solvent can thus be obtained. The Weller equation therefore predicts the feasibility of electron transfer within a donor – acceptor system. ΔG negative (exothermic process) indicates that the electron transfer process is thermodynamically allowed, whereas ΔG positive (endothermic process) indicates that the electron transfer process is thermodynamically forbidden. The ET process is highly endothermic in ground state, however when either D or A is electronically excited, the free energy change for ET from D to A becomes exothermic. After initial PET processes, the ability or propensity of the

intermediates, *e.g.* exciplexes, radical ions and their chemistry depends upon several factors such as redox potential of donor – acceptor and solvent polarity. Since these intermediates are short lived, they successively get transformed into another intermediate of lower energy. PET between donor and acceptor pair leads to the formation of either radical ion pairs or exciplexes depending upon the nature of the solvent.

1.4 Origin of benzylic C-H activation concept by photoredox catalysis:

During the exploration of new reactions of photoinduced electron transfer (PET) generated radical cations, we had developed a regioselective C_{sp2}–H activation by via arene radical cation for intramolecular C–heteroatom and C–C bond forming reactions[43,45] as shown in **Scheme 23**.

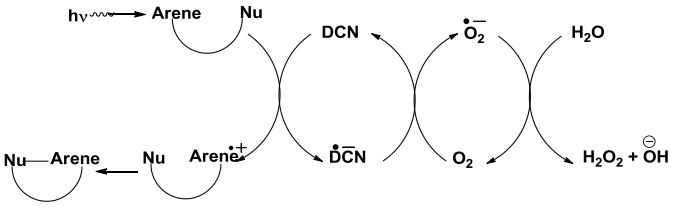

Scheme 23

In another study, C_{sp3}–H activation was also realized by sequential electron-proton-electron (E-P-E) loss to generate iminium ion from PET oxidation of tertiary amines[44] as shown in **Scheme 24**. The resultant iminum cation was *in situ* trapped by a nucleophile.

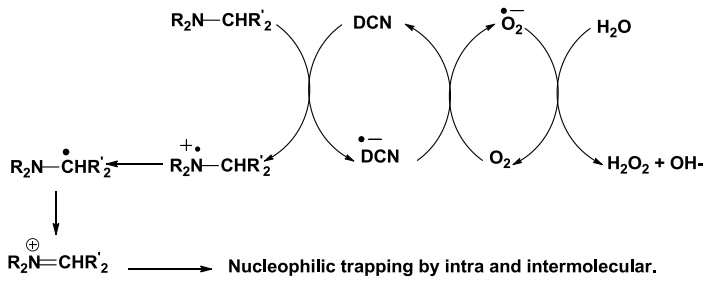

Scheme 24

These two critical observations led us to envisage an unprecedented benzylic C_{sp3}–H bond activation protocol *via* photoredox cycle as shown in **Scheme 25.** The reaction was envisioned by considering the generation of arene radical cation **40** by photoinduced SET from the singlet arene to ground state DCN[45]. Furthermore, it was also visualized that

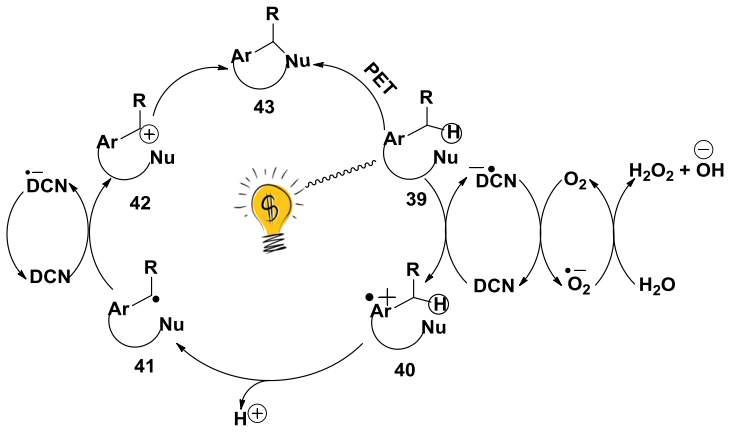

Scheme 25

increased acidity of benzylic proton due to adjacent arene radical cation would render easy deprotonation of **40** producing **41.** This intermediate radical species**41** may undergoes another electron loss to DCN owing to enhanced oxidation potential generating benzylic cation **42** akin to the phenomena observed in iminium ion formation (see **Scheme 24**). This benzylic cation could in turn be trapped by a nucleophile either intra- or intermolecularly.

1.5 Results and discussion:

Initially to test the feasibility of the proposed concept, a mixture of alkylarene **44** (1mmol) and 1,4-dicyanonaphthalene (DCN, 0.05 mmol) in acetonitrile was photolysed using 450-W Hanovia medium pressure lamp housed in a Pyrex glass immersion well (> 300 nm) for 3 h (55 % conversion, monitored by GC, all light absorbed by **44** only). Usual work-up and purification of the reaction mixture produced 6-methoxy-1-methylisochroman **(49)** in 51% yield (calculated based on consumptions of starting material).

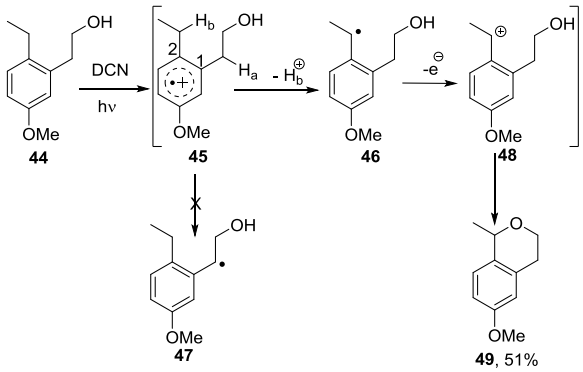

Scheme 26

Longer irradiation (< 5 h) produced complex mixture of products. The regioselective formation of **46** by H_b^+ loss from **47** is explained by natural bond orbital (NBO) analysis of the natural charge density on each carbon atom of**45** using Gaussian 09 suite of programs[47]. The more positive charge residing on C-2 (+0.2598) in comparison to C-1 (+0.0593) plausibly makes H_b more acidic for accelerated deprotonation. Furthermore, the free energies of two optimized geometries of radical intermediates **46** and **47** at the same level of theory have shown that **46** is more stable than **47** by at least 1.07 kcal / mol (Δ G).

Investigation of substrate scope for intramolecular C-O bond forming reaction:

Encouraged by this result, alkylarenes **50** and **51** were activated in identical manner as described for **44** which produced corresponding cyclic ethers **56 (**62%**)** and **57 (**51%), respectively (**Table 1**).

Table 1: Generality of intramolecular cycloetherification reaction.

Entry	Substarte	Product	Time	Yield[a] (%)
1	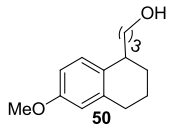 **50**	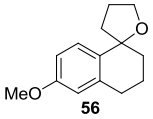 **56**	3 h	62
2	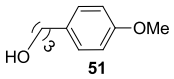 **51**	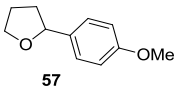 **57**	3 h	51
3	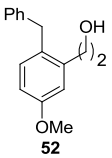 **52**	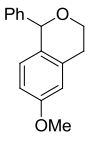 **58**	5 h	72
4	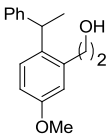 **53**	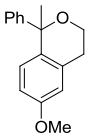 59	5 h	61
5	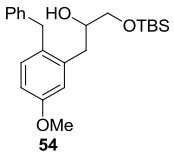 **54**	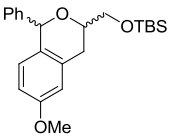 **60**	4 h	58
6	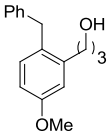 **55**	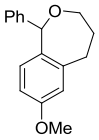 **61**	4 h	55

[a] isolated yield, calculated based on consumption of starting material.

We observed that substrates (**52-55**) having phenyl ring at the activated benzylic center produced cyclic product (**58-61**) with better yield (60-70%).

Attempts to trap benzylic radical intermediate by tethered olefin

Having successfully activation of benzylic C-H bond for cycloetherification reaction, we turned our attention towards the trapping of benzylic radical **41** (see **Scheme 24**), the first intermediate formed in this reaction. Towards this end, we carried out PET activation of **62** with the hope that radical **63** would be stabilized by α-ester group and might add on to the tethered olefin to produce corresponding indane derivative **64**. However, identical activation of **62** produced **67** (52%) instead of expected **64**. This result could only be explained by implicating the intermediacy of distonic carbocation **66**. The trace amount of moisture present in the solvent reacted with **66** to produce **67** as shown in **Scheme 27**.

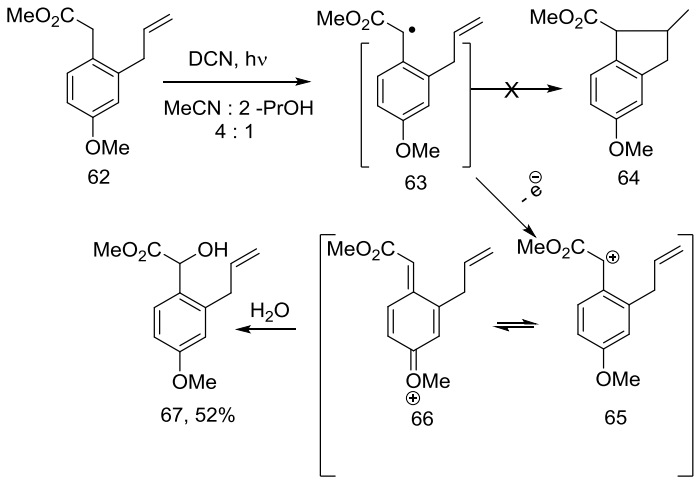

Scheme 27

To the best of our knowledge, this interesting and unprecedented reaction can only parallel to Ishihara's[48-49]report of intramolecular oxylactonization of ketocarboxylic acid by using hypervalent iodine as a catalyst in the presence of peroxides. However, this protocol sometimes suffers from low chemoselectivity due to competing Baeyer–Villiger oxidations[49] (**Scheme 28**).

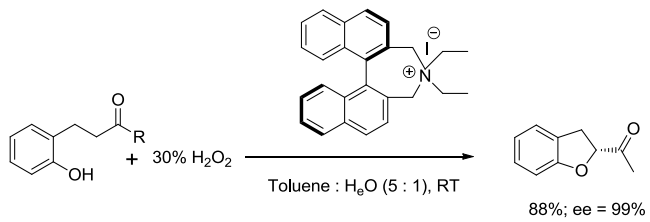

Scheme 28

In order to provide further evidence to the formation of intermediate **66**, we evaluated to study PET activation of **69** which was easily synthesized as shown in **Scheme 29**.

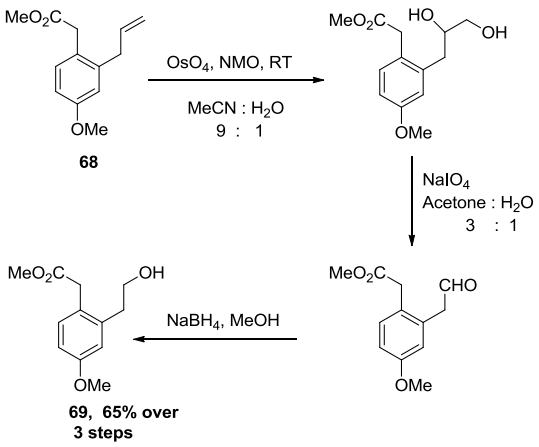

Scheme 29

Usual PET activation of **69**, surprisingly, produced cyclic hemiacetal **73 (**65 % yield, crystalline solid, m.p.= 255° C – 265° C) along with expected **70** (15% yield). The structure of **72** was deduced on the basis of detailed ^{1}H NMR, ^{13}C NMR, mass spectroscopy which was also confirmed by X–ray crystallography. The existence of two intermolecular O-H…O hydrogen bonds in the crystal structure may possibly explain the unusual stability of **72** even at room temperature (**Scheme 30**).

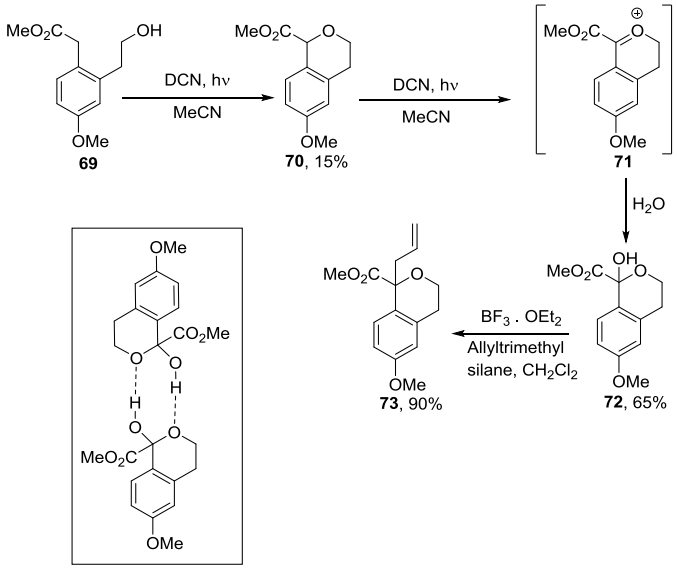

Scheme 30

The structure of **72** was further confirmed by transforming it to **73** by carrying out allylation (90% yield) reaction with allyltrimethylsilane in the presence of $BF_3.OEt_2$.

Towards an effort to generalize this reaction, we studied several substrates **74**-**81** and results are shown in **Table 2**.

Table 2. Substrate scope studies for cyclic hemiacetal formation.

Entry	Substrate	Product, Time (h)	Yield[a] (%)
1	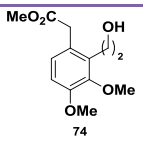 74	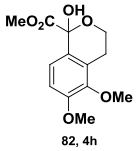 82, 4h	55
2	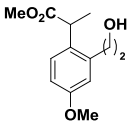 75	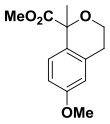 83, 5h	52
3	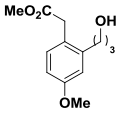 76	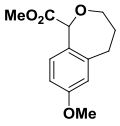 84, 4h	44
4	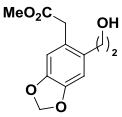 77	Complex mixture	
5	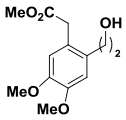 78	Complex mixture	
6	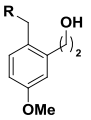 R= CN, 79 R= OMe, 80	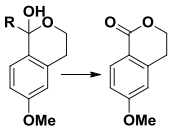 R= CN, 85 R= OMe, 86 87, 1h	85 75
7	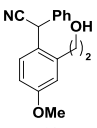 81	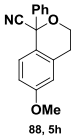 88, 5h	72

[a] isolated yield, calculated based on consumption of starting material.

It was observed that **74** produced only corresponding hemiacetal (**82**, 55% yield) as expected whereas **76** gave **84** (44% yield) as the sole product possibly due to unfavorable cyclic seven membered oxocarbenium ion geometry. Unfortunately, **77**and **78** produced unidentified mixture of products possibly due to competing benzylic C–H activations. Furthermore, to broaden the scope of this reaction, we studied the activation of **79** and **80** and isolated interestingly same cyclic lactone **87** in each case, possibly by the decomposition of unstable cyclic cyano hemiacetal **85** or methoxy hemiacetal **86** intermediates, respectively. The involvement of **85** and **86** type of intermediate for the formation of **87** is suggested based on the isolation of **88** from the activation of **81**, respectively.

Investigation of Intermolecular C-O bond formation

After successfully realizing benzylic C-H bond activation for intramolecular cycloetherification reaction, we enthusiastically turned our attention of introducing oxygen functionality at benzylic position intermolecularly. The synthesis of aryl ketones that are used in synthesis of fine chemicals as well as pharmaceuticals[50] is considered as a fundamental chemical reaction in organic synthesis. Friedel–Crafts acylation[51] of aromatic compounds is the most common practical route for the synthesis of aromatic ketones. However, the air sensitive nature of acylating agents (acyl chloride or anhydride) and lack of regioselectivity (*o:p* ratio) imposes a severe limitation to this strategy. To overcome these drawbacks, Nicolaou *et al.*[52] reported direct arylalkyl oxidation to corresponding carbonyls by utilizing stoichiometric amount of IBX. However, due to very low solubility and reactivity of organoiodine reagents in water these methods are restricted only in organic solvent which renders it very slow. Subsequently, same reaction was modified for aqueous medium by using catalytic iodobenzene in the presence of *m*-CPBA[53].

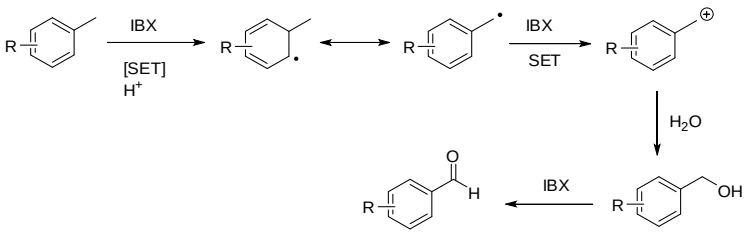

Scheme 31

The heavy metal catalyzed oxidation of arylalkenes using *m*-CPBA or TBHP as oxidants is also explored by several groups[54-59], but most of them have employed toxic metals like Mn, Co, Ru, Rh and Bi and therefore, their applicability is limited.

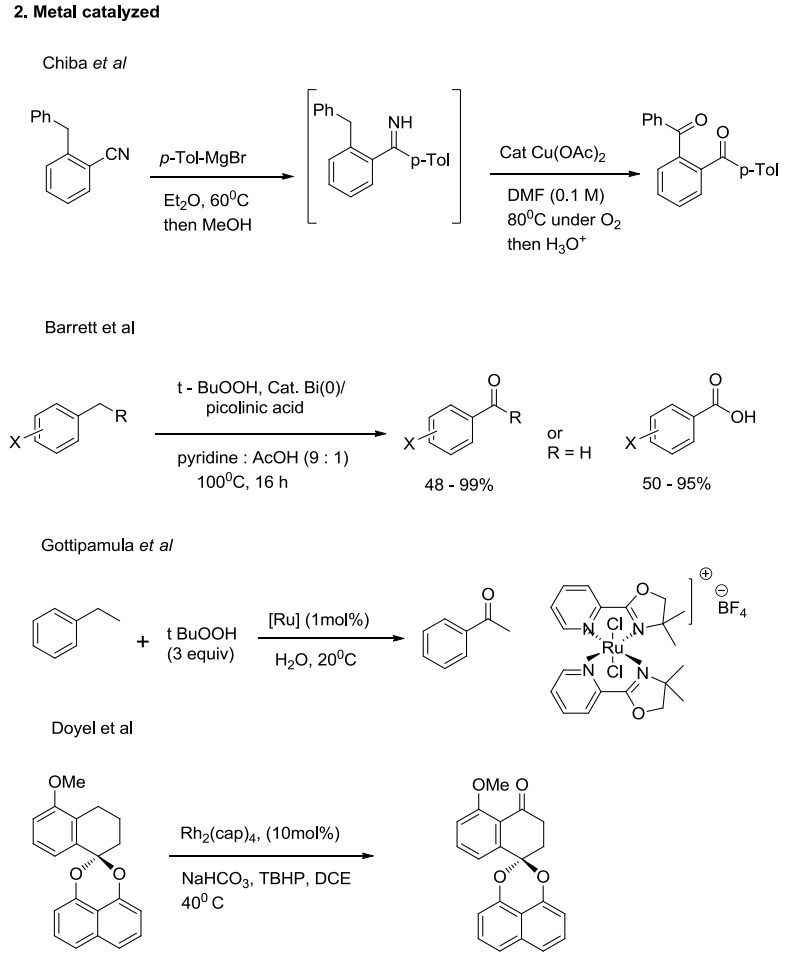

Scheme 32

Recently, phthalimide N-oxyl radical (PINO), generated by the reaction of N-hydroxyphthalimide with oxygen in the presence anthraquinone derivatives, is also reported for arylalkene autooxidation[60] producing mixture of both corresponding alcohol and ketone in low to moderate yields (**Scheme 33**).

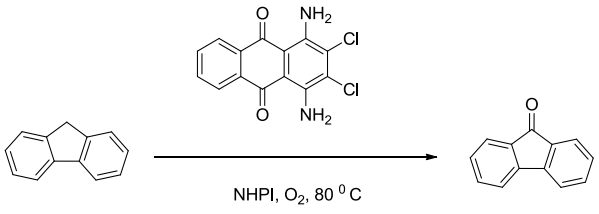

Scheme 33

In contrast to precedence reports, we hypothesized that freely available water could be used as a source of oxygen for benzylic oxidation through current concept as shown in **Scheme 34.** Initially to substantiate our hypothesis, we activated **89** in acetonitrile- water (4:1) mixture for 5 h and isolated **91** in high yield (80%), presumably involving benzylic alcohol **90** as an intermediate. To prove the intermediacy of **90** in this reaction, authentic sample of **90** was irradiated in the identical manner which produced **91** in quantitative yield.

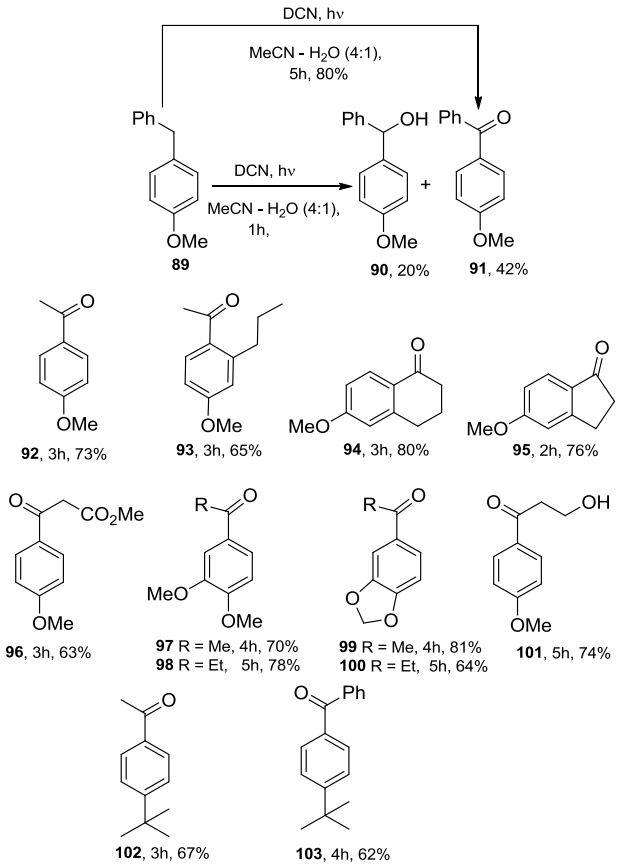

Scheme 34

Furthermore, a control experiment by irradiating **89** only for 1 h, afforded a mixture of **90** (42%) and **91** (20%) supporting the mechanism of direct transformation of **89** to **91**. To generalize the current protocol of arylalkyl oxidation, several arylalkyls were studied and results (**92-103**) are shown in **Scheme 28**. Besides having established high regioselectivity, a unique chemoselectivity was also established by PET activation of **101**.

1.6 Summary:

In conclusion, we have successfully developed a new concept of benzylic C-H activation for intramolecular cycloetherification reactions as well direct oxidation to aryl ketones (**Figure 4**).

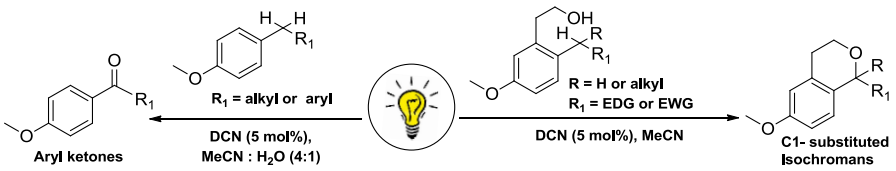

Figure 4

This new concept of direct C-H bond activation holds promise to be extremely useful in for the synthesis of pharmacologically important. Further studies for C–C as well as C–N bond forming reaction is presently being pursued in the group.

1.7 References

1) a) R. G. Bergman, *Nature***2007**, *446*, 391 – 393.

2) K. Godula, D. Sames, *Science***2006**, *312*, 67.

3) J. A. Labinger, J. E. Bercaw, *Nature***2002**, *417*, 507 – 514.

4) R. H. Crabtree, *Chem. Rev*. **2010**, *39*, 575-575.

5) W. R. Gutekunst, P. S. Baran, *Chem. Soc. Rev*. **2011**,*40*, 1976–1991.

6) Barton, D. H. R.; Beaton, J. M.; Geller, L. E.; Pechet, M. M., *J. Am. Chem. Soc.* **1961**,*83*, 4076.

7) N. Miyaura, A. Suzuki, *Chem. Rev*. **1995**, *95*, 2457–2483.

8) N. J. Whitcombe, K. K. Hii, S. E. Gibson, *Tetrahedron***2001**, *57*, 7449 – 7476.

9) Prof. Dr. Piet W. N. M. van Leeuwen and Dr. John C. Chadwick in the title of *Homogeneous Catalysts: Activity-Stability–Deactivation*, Published online:18 JUN **2011**, DOI: 10.1002/9783527635993.ch9.

10) Xiao Chen, Keary M. Engle, Dong-Hui Wang, Jin-Quan Yu, *Angew. Chem.***2009**, *121*, 5196–5217; *Angew. Chem. Int. Ed.***2009**, *48*, 5094–5115.

11) Naohiko Yoshikai, Ye Wei, *Asian J. Org. Chem.* Mar 14, **2013**, DOI:*10.1002/ajoc.201300016*.

12) L. Ackermann, *Chem. Rev*. **2011**, *111*, 1315 – 1345.

13) Daugulis, O.; Do, H.-Q.; Shabashov, D. *Acc. Chem. Res.* **2009**, *42*, 1074.

14) Colby, D. A.; Tsai, A. S.; Bergman, R. G.; Ellman, J. A. *Chem. Res.* **2012**, *45*, 814.

15) Engle, K. M.; Mei, T.-S.; Wasa, M.; Yu, J.-Q. *Acc. Chem. Res.* **2012**, *45*, 788.

16) N. Kuhl, M. N. Hopkinson, J. Wencel-Delord, F. Glorius, *Angew. Chem. Int. Ed*. **2012**, *51*, 10236 – 10254.

17) H.-Q. Do, R. M. K. Khan, O. Daugulis, *J. Am. Chem. Soc*. **2008**, *130*, 15185.

18) K. Ueda, S. Yanagisawa, J. Yamaguchi, K. Itami, *Angew. Chem*. **2010**, *122*, 9130; *Angew.Chem. Int. Ed*. **2010**, *49*, 8946.

19) S. I. Gorelsky, D. Lapointe, K. Fagnou, *J. Org. Chem.* **2012**, *77*, 658; e) F. Bellina, R. Rossi, *Tetrahedron* **2009**, *65*, 10269.

20) L-C. Campeau, K. Fagnou, *Chem. Commun.*,**2006**, 1253-1264.

21) a) O. Baudoin, *Chem. Soc. Rev*. **2011**, *40*, 4902 – 4911.

22) S.-Y. Zhang, F.-M.Zhang, Y.-Q. Tu, *Chem. Soc. Rev*. **2011**, *40*, 1937 – 1949.

23) Breslow, R.; Gellman, S. H., *J. Am. Chem. Soc*. **1983**, *105*, 6728.

24) Zalatan, D. N.; Du Bois, *J. Top. Curr.Chem*. **2010**, *292*, 347.

25) Que, L.; Tolman, W. B., *Nature***2008**, *455*, 333.

26) Chen, M.; White, M. C., *Science***2007**, *318*, 783.

27) Desai, L. V.; Hull, K. L.;Sanford, M. S., *J. Am. Chem. Soc*. **2004**, *126*, 9542.

28)Giri, R.; Maugel, N.; Li, J.-J.; Wang, D.-H.;Breazzano, S. P.; Saunders,L. B.; Yu,J.-Q., *J. Am. Chem. Soc*. **2007**, *129*, 3510.

29) Y. Xie, Y. Yang, L. Huang, X. Zhang, Y. Zhang, *Org. Lett*. **2012**, *14*, 1238 – 1241.

30) N. Dastbaravardeh , M. Schnürch, M. D. Mihovilovic, *Org. Lett*. **2012**, *14*, 1930 – 1933.

31) Y. Li, Z. Li, T. Xiong, Q. Zhang, X. Zhang, *Org. Lett*. **2012**, *14*, 3522 – 3525.

32) P. Nov_k, A. Correa, J. G. Donaire, R. Martin, *Angew. Chem. Int. Ed*. **2011**, *50*, 12236.

33) T.Nanjo, C. Tsukano, Y. Takemoto, *Org. Lett*. **2012**, *14*, 4270 – 4273.

34) C. J. Li, *Acc. Chem. Res*. **2009**, *42*, 335 – 344.

35) P. Xie, Y. Xie, B. Qian, H. Zhou, C. Xia, H. Huang, *J. Am. Chem. Soc*. **2012**, *134*, 9902 – 9905.

36) Z. Li, Li. Cao, C.-J. Li, *Angew. Chem. Int. Ed*. **2007**, *46*, 6505 – 6507.

37) a) Z. Li, C. J. Li, *J. Am. Chem. Soc*. **2005**, *127*, 3672 – 3673.; b) Y. Zhang, C. J. Li, *J. Am. Chem. Soc*.**2006**, *128*, 4242 – 4243.; c) S. J. Park, J. R. Price,M. H. Todd, *J. Org. Chem*. **2012**, *77*, 949 – 955.

38) L. Liu, P. E. Floreancig., *Angew. Chem. Int. Ed*. **2010**, *49*, 5894 – 5897.

39) B. Yu, T. Jiang, Y. Su, X. Pan, X. She, *Org. Lett*.**2009**, *11*, 3442 – 3445.

40) a) B. Zhang, S. K. Xiang, L. H. Zhang, Y. Cui, N. Jiao, *Org. Lett*. **2011**, *13*, 5212 – 5215; b) A. Pinter, A. Sud, D. Sureshkumar, M. Klussmann, *Angew. Chem. Int. Ed.***2010**, *49*, 5004 –5007.

41) H. Komai, T. Yoshino, S. Matsunaga, M. Kanai *Org. Lett*. **2011**, *13*, 1706;.

42) K. M. McQuaid, D. Sames, *J. Am. Chem. Soc*. **2009**, *131*, 402–403.

43) a) G. Pandey, A. Murugan, M. Balakrishnan, *Chem. Commun*. **2002**, 624 – 625; b) G. Pandey, M. Karthikeyan, A. Murugan, *J. Org. Chem*. **1998**, *63*, 2867 – 2872; c) G. Pandey, A. Krishna, K. Girija, M. Karthikeyan, *Tetrahedron Lett*. **1993**, *34*, 6631 – 6634; d) G. Pandey,M. Sridhar, U. T. Bhalerao, *Tetrahedron Lett*. **1990**, *31*, 5373 – 5376; e) G.Pandey,A. Krishna,U. T.Bhalerao, *Tetrahedron Lett.***1989**, *30*, 1867-1870.

44) (a) G. Pandey, *Synlett***1992**, *7*, 546 – 552; (b) G. Pandey, *Topics in Current Chemistry***1993**, *168*, 175-221.

45) A. Krishna, Ph. D. Thesis entitled, *´Photoinduced SET initiated reactions: Generation and synthetic application of arene radical cations´* submitted to Osmania University, Hyderabad, India, **1989**.

46) D. Rehm, A. Weller, *Isr. J. Chem*. **1970**, *8*, 259.

47)(a) Gaussian 09, Revision A.01, M. J. Frisch, G. W. Trucks, H. B. Schlegel, G. E. Scuseria, M. A. Robb, J. R. Cheeseman, G. Scalmani, V. Barone, B. Mennucci, G. A. Petersson, H. Nakatsuji, M. Caricato, X. Li, H. P. Hratchian, A. F. Izmaylov, J. Bloino, G. Zheng, J. L. Sonnenberg, M. Hada, M. Ehara, K. Toyota, R. Fukuda, J. Hasegawa, M. Ishida, T. Nakajima, Y. Honda, O. Kitao, H. Nakai, T. Vreven, J. A. Montgomery, Jr., J. E. Peralta, F. Ogliaro, M. Bearpark, J. J. Heyd, E. Brothers K. N. Kudin, V. N. Staroverov, R. Kobayashi, J. Normand, K. Raghavachari, A. Rendell, J. C. Burant, S. S. Iyengar, J. Tomasi, M. Cossi, N. Rega, J. M. Millam, M. Klene, J. E. Knox, J. B. Cross, V. Bakken, C. Adamo, J. Jaramillo, R. Gomperts, R. E. Stratmann, O. Yazyev, A. J. Austin, R. Cammi, C. Pomelli, J. W. Ochterski, R. L. Martin, K. Morokuma, V. G. Zakrzewski, G. A. Voth, P. Salvador, J. J. Dannenberg, S. Dapprich, A. D. Daniels, O Farkas, J. B. Foresman, J. V. Ortiz, J. Cioslowski, D. J. Fox, Gaussian, Inc., *Wallingford CT*, **2009**; (b) Calculation was performed using the DFT method where

B3LYPfunctional and **6 – 31+g*** basis sets were used, D. B.Axel, *J. Chem. Phys.***1993**, *98*, 5648-5652.

48) M. Uyanik, H. Okamoto, T. Yasui, K. Ishihara, *Science***2010**, *328*, 1376-1379,

49) M. Uyanik, T. Yasui, K. Ishihara, *Bioorg. Med. Chem. Lett.* **2009**, *19*, 3848-3851.

50) Sheldon, R. A.; Kochi, J. K. *Metal Catalyzed Oxidations of Organic Compounds* Academic Press: New York, **1981**; (b) Cainelli, G.; Cardillo, G. Chromium *Oxidations in Organic Chemistry*; Springer: Berlin, **1984**; (c) Hudlicky, M. *Oxidation in Organic Chemistry*; American Chemical Society: Washington, DC, **1990**; (d) M. Recupero, C. Punta, *Chem. Rev*. **2007**, *107*, 3800–3842.

51) Smith, Michael B.; March, Jerry, *Advanced Organic Chemistry: Reactions, Mechanisms, and Structure* (6th ed.), New York: Wiley-Interscience, **2007**, ISBN 0-471-72091-7.

52) K. C. Nicolaou,P. S. Baran, Y-Li. Zhong,*J. Am. Chem. Soc*. **2001**, *123*, 3183-3185.

53) Y. Xu, J. T. Hu, J. Yan, *Chinese. Chem. Lett.* **2012**, *23*, 891-894.

54) a) L. Zhang, G. Y. Ang, S. Chiba, *Org. Lett.***2011**, *13*, 1622-1625.

55) T. Nagano, S. Kobayashi, *Chem. Lett*. **2008**, *37*, 1042-1045.

56) C. S. Yi, K. H. Kwon, D. W. Lee, *Org. Lett.* **2009**, *11*, 1567-1570.

57) A. J. Catino, J. M. Nichols, H. Choi, S. Gottipamula, M. P. Doyle, *Org. Lett*. **2005**, *7*, 5167-5170.

58) Y. Bonvin, E. Callens, I. Larrosa, D. A. Henderson, J. Oldham, A. J. Burton, A. G. M. Barrett, *Org. Lett*. **2005**, *7*, 4549-4552.

59) N. H. Lee, C. S. Lee, D. S. Jung, *Tetrahedron Lett*. **1998**, *39*, 1385-1388.

60) a) G. Yang, Qia. Zhang, H. Miao,Xi. Tong, Jie Xu**,** *Org. Lett.***2005**, *7*, 263-266; b) K. Ohkubo, S. Fukuzumi, *Org. Lett.***2000**, *2*, 3647-3650; c) R. Lechner, S. Kümmel, B. König, *Photochem.Photobiol. Sci.* **2010**, *9*, 1367-1377.

1.8 EXPERIMENTAL

A) General approach for the synthesis of substrates (44, 52 – 55):

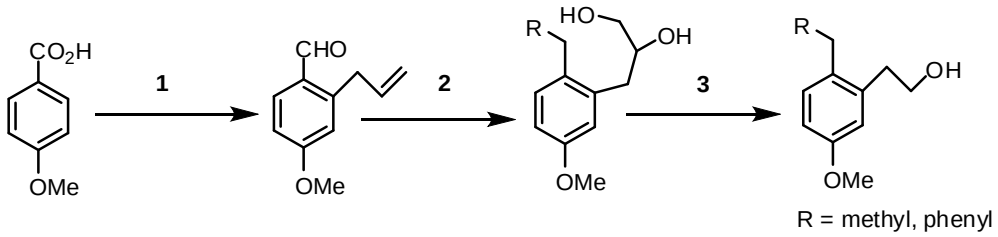

Reagent and Condition: 1. (a) TMDEA. *s*-BuLi,THF, -78°C, allyl-Br, 55%, (b) $SOCl_2$, MeOH, reflux, 95% ,(c) LAH , THF, 90%, (d) IBX, ethylacetate, reflux, 95%; **2**. (a) phenyl or methyl Grignard , THF, 90%, (b) OsO_4, NMO, acetonitrile : water (9:1), 85%, (c) H_2, Pd/C, 5% AcOH-MeOH, 90%; **3**. (a) $NaIO_4$, acetone :water (3:1), 95%, (b) $NaBH_4$, MeOH, 95%.

B) General approach for the synthesis of substrates (69, 74-81):

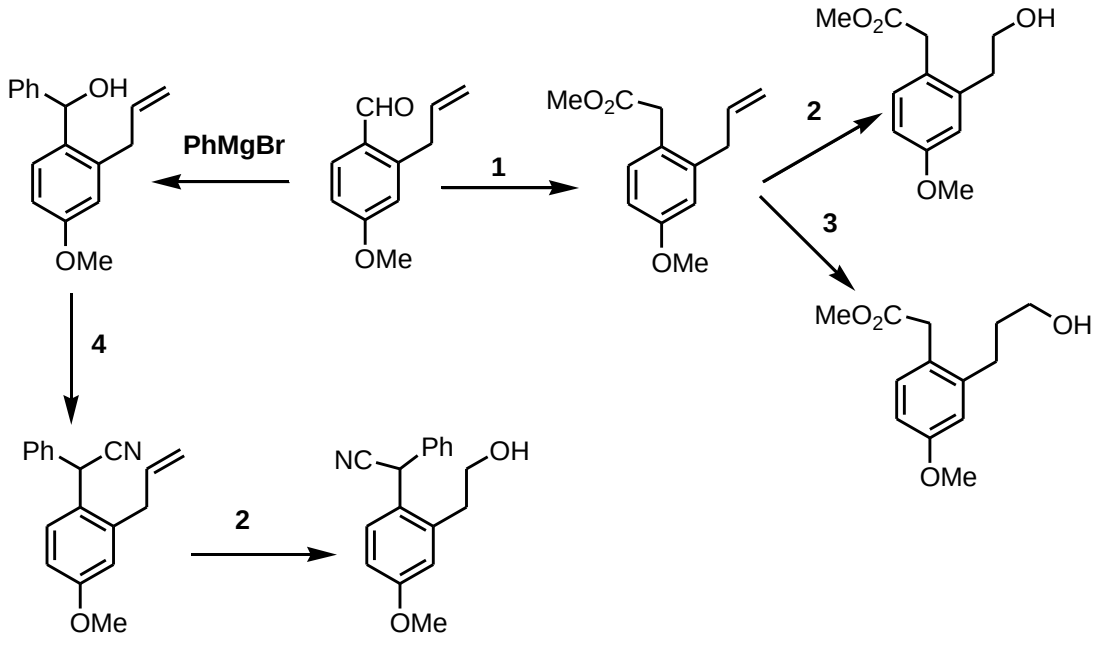

Reagents and conditions:1. (a) MOM-PPh_3, *n*- BuLi, 0^OC, (b) 2N HCl- THF reflux, 65% after two steps, (c)NaH_2PO_4, $NaClO_2$, DMSO – H_2O, 70% (d) $SOCl_2$, MeOH, reflux, 95%; **2**. (a) OsO_4, NMO, acetonitrile : water (9:1), 86%, (b) $NaIO_4$, acetone :water (3:1), 95%, (c) $NaBH_4$, MeOH, 95%; **3**. (a) BH_3. DMS, THF, O^0C, then H_2O_2, 72%; **4.**(a) $InCl_3$, TMSCN, DCM, 10h, 83%.

General irradiation procedure:

A solution of substrates (1.0 mmol) and DCN (0.05 mmol) in 150 mL acetonitrile/ acetonitrile – water (4:1) was irradiated using 450-W Hanovia medium pressure lamp housed in a Pyrex glass immersion well (> 300 nm). The reaction was monitored by GC [column CP – Sil 5 CB, 100 Deg (1min) 10 Deg/min - 150 Deg (0min) 20 Deg/min - 250 Deg (9min) on Varian CP-3800] periodically. After maximum starting material was consumed, the photolysed solution was concentrated under vacuo. The crude residue was purified over silica gel (100-200 mesh) to obtain desired cyclised product. Unreacted starting material and DCN were recovered at the end of the reaction. The yield was calculated based on the consumption of starting material.

Characterization details of substrates and products:

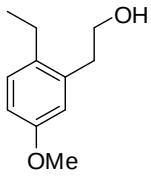

2-(2-Ethyl-5-methoxyphenyl)ethanol (44):

^{1}H NMR (200 MHz, $CDCl_3$) δ ppm: 7.13 (d, J = 9.2 Hz, 1H), 6.71 - 6.77 (m, 2H), 3.82 (t, J = 6.9 Hz, 2 H), 3.77 (s, 3H), 2.87 (t, J = 7.0 Hz, 2H), 2.59 (q, J = 7.6 Hz, 2H), 1.74 (brs, 1H), 1.19 (t, J = 7.6 Hz, 3H); ^{13}C NMR (50 MHz, $CDCl_3$) δ ppm: 157.5, 136.9, 134.6, 129.4, 115.3, 111.7, 63.0, 55.0, 35.8, 24.7, 15.5.

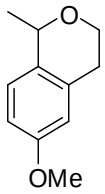

6-Methoxy-1-methylisochroman (49):

R_f = 0.4, Pet – ether : ethyl acetate (95: 05), colourless liquid;^{1}H NMR (400 MHz, $CDCl_3$) δ ppm:6.96 (d, J = 8.5 Hz, 1H), 6.74 (dd, J = 8.3, 2.7 Hz, 1H), 6.63 (d, J = 2.5 Hz, 1H), 4.81 (q, J = 6.7 Hz, 1H), 4.08 – 4.20 (m, 1H), 3.78 (s, 3H), 3.66 - 3.81 (m, 1H), 2.88 - 3.09 (m, 1H), 2.54 - 2.69 (m, 1H), 1.49 (d, J = 6.6 Hz, 3H); ^{13}C NMR (100 MHz, $CDCl_3$) δ ppm: 157.8, 134.7, 131.9, 125.9, 113.3, 112.3, 72.1, 63.6, 55.2, 31.9, 22.7; HR-MS (EI) m/z: calcd. for $C_{11}H_{15}O_2$ $[M + H]^+$: 179.1072; found: 179.1067.

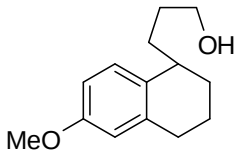

3-(6-Methoxy-1,2,3,4-tetrahydronaphthalen-1-yl)propan-1-ol (50):

^{1}H NMR (400 MHz, $CDCl_3$) δ ppm:7.08 (d, J = 8.5 Hz, 1H), 6.69 (dd, J = 8.4, 2.6 Hz, 1H), 6.59 (d, J = 2.4 Hz, 1H), 3.76 (s, 3H), 3.61 - 3.70 (m, 2H), 2.69 - 2.77 (m, 3H), 1.52 - 1.87 (m, 8H), 1.52 (brs, 1H); ^{13}C NMR (100 MHz, $CDCl_3$) δ ppm: 157.3, 138.2, 133.2, 129.4, 113.5, 111.8, 63.3, 55.2, 36.6, 32.9, 30.5, 30.0, 27.8, 19.9.

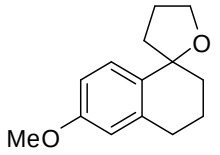

6'-Methoxy-3',4, 4, 5 - tetrahydro-2'H,3H-spiro[furan-2,1'-naphthalene] (56):

R_f = 0.4, Pet – ether : ethyl acetate (90:10), colourless liquid; ^{1}H NMR (400 MHz, $CDCl_3$) δ ppm:7.33 (d, J = 8.8 Hz, 1H), 6.76 (dd, J = 8.8, 2.7 Hz, 1H), 6.56 (d, J = 2.5 Hz, 1H), 4.05 - 4.12 (m, 1H), 3.93 - 4.01 (m, 1H), 3.76 (s, 3H), 2.66 - 2.84 (m, 2H), 1.65 - 2.15 (m, 8H); ^{13}C NMR (100 MHz, $CDCl_3$) δ ppm: 158.1, 138.3, 134.8, 127.7, 112.7, 112.5, 82.5, 68.1, 55.1, 40.3, 36.1, 29.8, 26.5, 21.1; HR-MS (EI) m/z: calcd. for $C_{14}H_{19}O_2$ $[M + H]^+$: 219.1385; found: 219.1381.

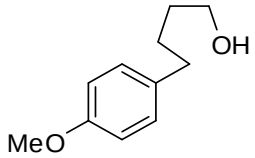

4-(4-Methoxyphenyl)butan-1-ol (51):

^{1}H NMR (200 MHz, $CDCl_3$) δ ppm: 7.11 (d, J = 8.6 Hz, 2H), 6.84 (d, J = 8.7 Hz, 2H), 3.78 (s, 3H), 3.64 (t, J = 6.2 Hz, 2H), 2.49 - 2.66 (m, 2H), 1.56 - 1.75 (m, 4H), 1.55 (brs, 1H); ^{13}C NMR (50 MHz, $CDCl_3$) δ ppm: 157.6, 134.4, 129.2, 113.6, 62.6, 55.1, 34.6, 32.1, 27.7.

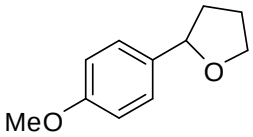

2-(4-Methoxyphenyl)tetrahydrofuran (57):

R_f = 0.3, Pet – ether : ethyl acetate (95: 05), colourless liquid;^{1}H NMR (400 MHz, $CDCl_3$) δ ppm: 7.23 (d, J = 8.6 Hz, 2H), 6.88 (d, J = 8.8 Hz, 2H), 4.81 (t, J = 7.1 Hz, 1H), 3.90 – 4.12 (m, 2H), 3.79 (s, 3H), 2.16 – 2.34 (m, 1H), 1.92 – 2.07 (m, 2H), 1.72 – 1.86 (m, 1H);^{13}C NMR (100 MHz, $CDCl_3$) δ ppm: 158.7, 135.3, 126.9, 113.6, 80.4, 68.4, 55.2, 34.4, 26.0 ppm; HR-MS (EI) m/z: calcd. for $C_{11}H_{15}O_2$ $[M + H]^+$: 179.1072; found: 179.1066.

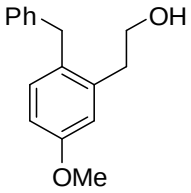

2-(2-Benzyl-5-methoxyphenyl)ethanol (52):

^{1}H NMR (200 MHz, $CDCl_3$) δ ppm: 7.06 - 7.42 (m, 6H), 6.77 - 6.89 (m, 2 H), 4.07 (s, 2H), 3.87 (s, 3H), 3.78 (t, J=6.8 Hz, 2H), 2.88 (t, J=6.8 Hz, 2H); ^{13}C NMR (50 MHz, $CDCl_3$) δ ppm: 158.2, 141.1, 138.0, 131.7, 131.2, 128.5, 128.4, 126.0, 115.7, 111.7, 62.9, 55.2, 38.2, 36.2.

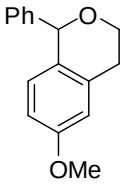

6-Methoxy-1-phenylisochroman (58):

R_f = 0.4, Pet – ether : ethyl acetate (95: 05), colourless liquid; ^{1}H NMR (400 MHz, $CDCl_3$) δ ppm: 7.23 -7.35 (m, 5H), 6.64 - 6.69 (m, 3H), 5.67 (s, 1H), 4.14 - 4.19 (m, 1H), 3.87 – 3.95 (m, 1H), 3.78 (s, 3H), 3.03 – 3.16 (m, 1H), 2.80 (dt, J = 6.8, 3.26 Hz, 1H); ^{13}C NMR (100 MHz, $CDCl_3$) δ ppm: 158.1, 142.4, 135.1, 130.0, 128.8, 128.3, 128.04, 128.03, 113.17, 112.30, 79.4, 63.7, 55.2, 29.16; HR-MS (EI) m/z: calcd. for $C_{16}H_{17}O_2$ $[M + H]^+$: 241.1229; found: 241.1221

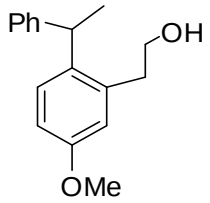

2-(5-Methoxy-2-(1-phenylethyl)phenyl)ethanol (53):

^{1}H NMR (200 MHz, $CDCl_3$) δ ppm: 7.17 - 7.32 (m, 6H), 6.76 - 6.87 (m, 2H), 4.36 (q, J = 7.1 Hz, 1H), 3.78 (s, 3 H), 3.65 - 3.75 (m, 2H), 2.77 – 3.01 (m, 2H), 1.52 (d, J = 7.1 Hz, 3H); ^{13}C NMR (50 MHz, $CDCl_3$) δ ppm: 159.4, 138.3, 135.8, 130.3, 128.9, 127.9, 127.5, 126.3, 120.1, 115.7, 111.7, 63.1, 55.1, 39.7, 35.9, 22.7.

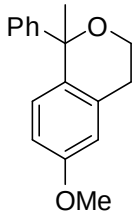

6-Methoxy-1-methyl-1-phenylisochroman (59):

R_f = 0.3, Pet – ether : ethyl acetate (95: 05) colourless liquid; ^{1}H NMR (400 MHz, $CDCl_3$) δ ppm: 7.21 - 7.33 (m, 5H), 7.03 (d, J = 8.6 Hz, 1H), 6.80 (dd, J = 8.5, 2.4 Hz, 1H), 6.69 (d, J = 2.3 Hz, 1H), 3.84 - 3.92 (m, 1H), 3.81 (s, 3H), 3.57 - 3.70 (m, 1H), 2.95 - 3.11 (m, 1H), 2.61 - 2.70 (m, 1H), 1.85 (s, 3H); ^{13}C NMR (100 MHz, $CDCl_3$) δ ppm: 157.9, 146.6, 135.0, 132.5, 128.4, 127.9, 127.1, 113.3, 112.0, 78.1, 59.8, 55.2, 30.1, 29.3 ; HR-MS (EI) m/z: calcd. for $C_{17}H_{19}O_2$ $[M + H]^+$: 255.1385; found: 255.1380.

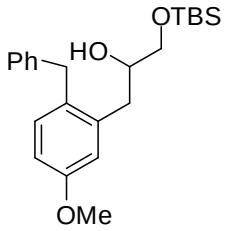

1-(2-Benzyl-5-methoxyphenyl)-3-(tert-butyldimethylsilyloxy)propan-2-ol (54):

^{1}H NMR (400 MHz, $CDCl_3$) δ ppm: 7.01 - 7.29 (m, 6H), 6.82 (d, *J* = 2.7 Hz, 1H), 6.75 (d, *J* = 2.3 Hz, 1H), 3.99 (s, 2H), 3.78 (s, 3H), 3.75 - 3.78 (m, 1H), 3.37 - 3.56 (m, 2H), 2.69 (d, *J*=6.6 Hz, 2H), 0.85 (s, 9H), 0.03 (s, 6H). ^{13}C NMR (100 MHz, $CDCl_3$) δ ppm: 158.1, 141.1, 138.0, 131.6, 128.5, 128.3, 125.9, 115.9, 111.7, 72.2, 66.3, 55.1, 38.1, 36.4, 25.8, - 5.39.

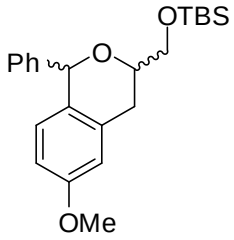

***Tert*-Butyl((6-methoxy-1-phenylisochroman-3-yl)methoxy)dimethylsilane (60):**

R_f = 0.4, Pet – ether : ethyl acetate (94: 06), isolated as mixture of diasteromers; ^{1}H NMR (400 MHz, $CDCl_3$) δ ppm (Only for major isomers): 7.21 – 7.35 (m, 5H), 6.86 (d, *J* = 8.7 Hz, 1H), 6.68 – 6.73 (m, 2H), 5.89 (s, 1H), 3.87 – 3.98 (m, 1H), 3.81 (s, 3H), 3.58 – 3.72 (m, 2H), 2.72 – 2.94 (m, 2H), 0.84 (s, 9H), 0.01(s, 6H); ^{13}C NMR (100 MHz, $CDCl_3$) δ ppm: 158.35, 142.19, 134.98, 128.96, 128.64, 128.37, 128.05, 127.65, 113.4, 112.08, 80.6, 68.6, 66.1, 55.1, 30.5, 25.5, 18.3, - 5.4; HPLC: Kromasil RP18 column (MeOH : H_2O 80:20, flow rate = 1 ml /min, 230nm), major diastereomer: R_{t1} = 50.92 min and minor diastereomer: R_{t2} = 54.45 min; HR-MS (EI) m/z: calcd. for $C_{23}H_{32}O_3NaSi$ $[M + Na]^+$: 407.2018; found: 407.2014.

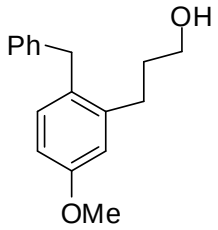

3-(2-Benzyl-5-methoxyphenyl)propan-1-ol (55):

^{1}H NMR (400 MHz, $CDCl_3$) δ ppm: 7.14 - 7.37 (m, 5H), 7.13 (d, J = 8.3 Hz, 1H), 6.86 (d, J = 2.5 Hz, 1H), 6.80 (dd, J = 8.3, 2.5 Hz, 1H), 4.07 (s, 2H), 3.88 (s, 3H), 3.69 (t, J = 6.1 Hz, 2H), 2.67 - 2.76 (m, 2H), 1.77 - 1.87 (m, 2H); ^{13}C NMR (100 MHz, $CDCl_3$) δ ppm: 158.2, 141.5, 141.3, 131.5, 130.6, 128.6, 128.3, 125.9, 115.1, 111.0, 62.4, 55.2, 38.1, 33.5, 29.2.

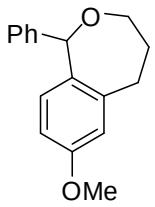

7-Methoxy-1-phenyl-1,3,4,5-tetrahydrobenzo[c]oxepine (61):

R_f = 0.3, Pet – ether : ethyl acetate (95: 05), white solid; ^{1}H NMR (400 MHz, $CDCl_3$) δ ppm: 7.19 - 7.33 (m, 5H), 6.67 (d, J = 1.8 Hz, 1H), 6.41 - 6.45 (m, 2H), 5.61 (s, 1H), 4.25 (dt, J = 12.2, 3.8 Hz, 1H), 3.79 – 3.92 (m, 1H), 3.65 (s, 3H), 3.01 - 3.17 (m, 1H), 2.79 – 2.91 (m, 1H), 1.73 – 1.87 (m, 2H); ^{13}C NMR (100 MHz, $CDCl_3$) δ ppm: 158.7, 143.7, 141.1, 135.0, 129.1, 128.2, 127.3, 115.7, 109.9, 83.1, 73.0, 55.1, 35.0, 29.8; HR-MS (EI) m/z: calcd. for $C_{17}H_{19}O_2$ $[M + H]^+$: 255.1385; found: 255.1380.

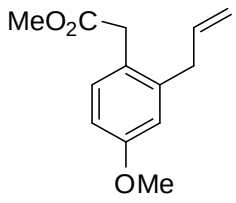

Methyl 2-(2-allyl-4-methoxyphenyl)acetate (62):

^{1}H NMR (400 MHz, $CDCl_3$) δ ppm: 7.15 (d, J = 9.2 Hz, 1H), 6.70 - 6.75 (m, 2H), 5.82 - 6.01 (m, 1H), 4.90 - 5.13 (m, 2H), 3.77 (s, 3H), 3.66 (s, 3H), 3.59 (s, 2H), 3.38 (d, J = 6.2 Hz, 2H); ^{13}C NMR (100 MHz, $CDCl_3$) δ ppm: 172.2, 158.8, 139.6, 136.2, 131.5, 124.6, 115.9, 115.3, 111.5, 54.9, 51.7, 37.5.

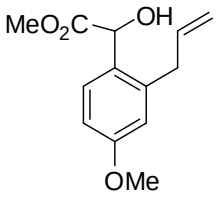

Methyl 2-(2-allyl-4-methoxyphenyl)-2-hydroxyacetate (67):

R_f = 0.3, Pet – ether : ethyl acetate (90: 10) colourless liquid; ^{1}H NMR (400 MHz, $CDCl_3$) δ ppm: 7.23 (d, *J* = 9.2 Hz, 1H), 6.73 – 6.80 (m, 2H), 5.87 – 6.07 (m, 1H), 5.34 (s, 1H), 4.99 – 5.12 (m, 2H), 3.77 (s, 3H), 3.73 (s, 3H), 3.50 (m, 2H); ^{13}C NMR (100 MHz, $CDCl_3$): δ 174.7, 159.6, 139.7, 136.5, 128.8, 128.5, 116.3, 115.72, 111.92, 69.64, 55.16, 52.80, 36.80.

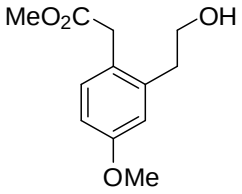

Methyl 2-(2-(2-hydroxyethyl)-4-methoxyphenyl)acetate (69):

^{1}H NMR (400 MHz, $CDCl_3$) δ ppm: 7.11 (d, *J* = 8.5 Hz, 1H), 6.75 (d, *J* = 2.6 Hz, 1H), 6.70 (dd, *J* = 8.3, 2.5 Hz, 1H), 3.79 (t, *J* = 6.55 Hz, 2H), 3.76 (s, 3H), 3.65 (s, 3H), 3.62 (s, 2H), 2.84 (t, *J* = 6.6 Hz, 2H), 2.22 (brs, 1H); ^{13}C NMR (100 MHz, $CDCl_3$) δ ppm: 172.7, 158.8, 138.62, 131.5, 124.3, 115.6, 111.9, 62.9, 55.1, 52.0, 37.5, 36.1.

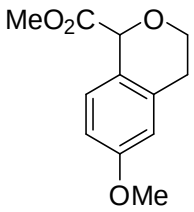

Methyl 6-methoxyisochroman-1-carboxylate (70):

R_f = 0.5, Pet – ether : ethyl acetate (94:06) colourless liquid; ^{1}H NMR (400 MHz, $CDCl_3$) δ ppm: 7.29 (d, *J* = 8.5 Hz, 1H), 6.77 (dd, *J* = 8.5, 2.5 Hz, 1H), 6.66 (d, *J* = 2.5 Hz, 1H), 5.31 (s, 1H), 4.24 - 4.30 (m, 1H), 3.95 - 3.99 (m, 1H), 3.78 (s, 3 H), 3.77 (s, 3H), 2.82 – 2.87 (m, 2H); ^{13}C NMR (100 MHz, $CDCl_3$) δ ppm: 171.8, 158.8, 135.1, 127.2, 123.1, 113.5, 112.7, 74.5, 62.7, 55.2, 52.3, 28.3; HR-MS (EI) m/z: calcd. for $C_{12}H_{14}O_4$ Na[M + Na]$^+$: 245. O790; found: 245.0784.

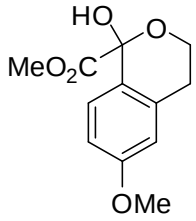

Methyl 1-hydroxy-6-methoxyisochroman-1-carboxylate (72):

R_f = 0.3, Pet – ether : ethyl acetate (80:20) white, crystalline solid; ^{1}H NMR (400 MHz, $CDCl_3$) δ ppm:7.13 (d, *J* = 8.5 Hz, 1H), 6.77 (dd, *J* = 8.5, 2.5 Hz, 1H), 6.66 (d, *J* = 2.5 Hz, 1H), 4.55 (s, 1H for -OH), 4.05 - 4.15 (m, 2H), 3.78 (s, 3H), 3.74 (s, 3H), 3.02 – 3.11 (m, 1H), 2.65 (dt, *J* = 16.4, 2.1 Hz, 1H); ^{13}C NMR (100 MHz, $CDCl_3$) δ ppm:172.0, 159.5, 136.1, 128.0, 125.3, 113.1, 112.8, 94.2, 60.1, 55.2, 53.5, 28.5. HR-MS (EI) m/z: calcd. for $C_{12}H_{14}O_5$ Na[M + Na]$^+$: 261.0739; found: 261.0733.

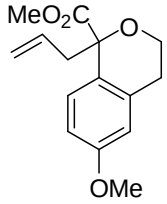

Methyl 1-allyl-6-methoxyisochroman-1-carboxylate (73):

To a solution of **33** (0.12 g, 0.5 mmol) in dry DCM (15 mL) was added BF_3. OEt_2 (0.084 g, 0.6 mmol) at 0°C. The mixture was stirred for 5 minutes. Allyl silane (0.091 g, 0.8 mmol) diluted by 5 mL of dry DCM was added drop wise to the reaction mixture at 0°C and it was allowed to warm to room temperature and stirred for an additional 4 h. After the completion of the reaction (monitored by TLC), it was quenched by adding 5 mL of water. The reaction mixture was extracted by ethylacetate (2 X 50 mL), washed with water and brine, dried over anhydrous Na_2SO_4, concentrated under reduced pressure. The residue was column chromatographed over silica gel using pet ether:ethyl acetate (95 :5) as eluant to obtain **34** (0.11 g, 90%) as a colorless liquid.

R_f = 0.4, Pet – ether : ethyl acetate (95:05) colourless liquid;^{1}H NMR (400 MHz, $CDCl_3$) δ ppm: 7.45 (d, *J* = 8.8 Hz, 1H), 6.79 (dd, *J* = 8.7, 2.8 Hz, 1H), 6.61 (d, *J* = 2.7 Hz, 1H), 5.59 - 5.80 (m, 1H), 5.01 - 5.08 (m, 2H), 4.06 (dd, *J* = 8.1, 3.0 Hz, 2H), 3.72 (s, 3H), 3.66 (s, 3H), 2.86 - 3.05 (m, 2H), 2.55 - 2.76 (m, 2H); ^{13}C NMR (100 MHz, $CDCl_3$) δppm:173.6, 158.4, 135.9, 132.6, 128.3, 126.7, 118.5, 113.1, 112.7, 80.6, 62.2, 55.2, 52.4, 45.3, 29.1. HR-MS (EI) m/z: calcd. for $C_{15}H_{18}O_4$ Na[M + Na]$^+$: 285.1103; found: 285.1097.

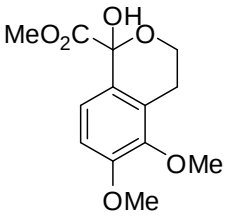

Methyl 1-hydroxy-5,6-dimethoxyisochroman-1-carboxylate (82):

R_f = 0.3, Pet – ether : ethyl acetate (80:20) colourless liquid; ^{1}H NMR (400 MHz, $CDCl_3$) δ ppm: 6.93 (d, *J* = 8.5 Hz, 1H), 6.82 (d, *J* = 8.5 Hz, 1H), 4.09- 4.12 (m, 1H + 1H brs), 3.86 (s, 3H), 3.82 (s, 3H), 3.81 – 3.77 (m, 1H), 3.76 (s, 3H), 2.85- 2.90 (m, 2H); ^{13}C NMR (100 MHz, $CDCl_3$) δppm: 172.0, 152.4, 145.2, 129.1, 125.9, 122.4, 110.7, 93.9, 60.2, 60.0, 55.7, 53.6, 22.7. HR-MS (EI) m/z: calcd. for $C_{13}H_{16}O_6$ Na $[M + Na]^+$: 291.0845; found: 291.0839.

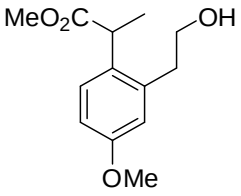

Methyl 2-(2-(2-hydroxyethyl)-4-methoxyphenyl)propanoate (75):

^{1}H NMR (400 MHz, $CDCl_3$) δ ppm: 7.19 (d, *J* = 8.5 Hz, 1H), 6.75 - 6.80 (m, 2H), 3.98 (q, *J* = 7.1 Hz, 1H), 3.86 - 3.90 (m, 2H), 3.78 (s, 3H), 3.63 (s, 3H), 2.93 (t, *J* = 6.6 Hz, 2H), 1.45 (d, *J* = 7.1 Hz, 3H).

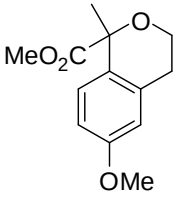

Methyl 6-methoxy-1-methylisochroman-1-carboxylate (83):

^{1}H NMR (400 MHz, $CDCl_3$) δ ppm: 7.35 (d, *J* = 8.5 Hz, 1H), 6.79 (dd, *J* = 8.7, 2.6 Hz, 1H), 6.62 (d, *J* = 2.4 Hz, 1H), 4.05 - 4.11 (m, 2H), 3.78 (s, 3H), 3.73 (s, 3H), 2.90 – 3.06 (m,1H), 2.71 (dt, *J* = 16.2, 3.4 Hz, 1H), 1.71 (s, 3H); ^{13}C NMR (100 MHz, $CDCl_3$) δ ppm: 174.3, 158.5, 135.0, 128.5, 128.1, 113.1, 112.7, 78.1, 62.1, 55.2, 52.4, 29.0, 27.9. HR-MS (EI) m/z: calcd. for $C_{13}H_{16}O_4$ Na$[M + Na]^+$: 259.0946; found: 259.0941.

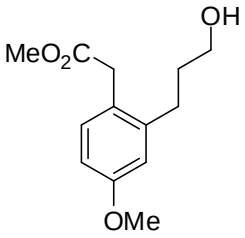

Methyl 2-(2-(3-hydroxypropyl)-4-methoxyphenyl)acetate (76):

^{1}H NMR (400 MHz, $CDCl_3$) δ ppm: 7.12 (d, J = 8.5 Hz, 1H), 6.74 (d, J = 2.4 Hz, 1H), 6.72 (dd, J = 8.3, 2.4 Hz, 1H), 3.76 (s, 3H), 3.66 (s, 3H), 3.65 (t, J = 6.3 Hz, 2H), 3.60 (s, 2H), 2.68 (m, 2H), 2.22 (brs, 1H), 1.82 (m, 2H); ^{13}C NMR (100 MHz, $CDCl_3$) δppm: 172.6, 158.7, 141.7, 131.5, 124.3, 114.9, 111.3, 61.8, 55.0, 51.9, 37.4, 33.2, 28.9.

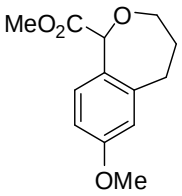

Methyl 7-methoxy-1,3,4,5-tetrahydrobenzo[c]oxepine-1-carboxylate (84):

^{1}H NMR (400 MHz, $CDCl_3$) δ ppm: 6.93 (d, J = 8.3 Hz, 1 H), 6.73 (d, J = 2.5 Hz, 1 H), 6.62 - 6.69 (m, 1 H), 5.27 (s, 1 H), 4.28 (dt, J = 12.4, 3.8 Hz, 1 H), 3.85 (m, 1H), 3.84 (s, 3 H), 3.78 (s, 3 H), 2.91 - 3.02 (m, 2 H), 1.73 - 2.00 (m, 2 H); ^{13}C NMR (100 MHz, $CDCl_3$) δppm: 171.2, 159.5, 143.6, 129.4, 127.9, 115.9, 110.5, 81.1, 72.7, 55.2, 52.2, 34.2, 29.6; HR-MS (EI) m/z: calcd. for $C_{13}H_{16}O_4$ Na $[M + Na]^+$: 259.0946; found: 259.0941.

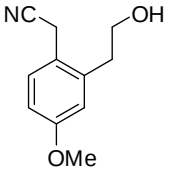

2-(2-(2-Hydroxyethyl)-4-methoxyphenyl)acetonitrile (79):

^{1}H NMR (200 MHz, $CDCl_3$) δ ppm: 7.31 (d, J = 8.6 Hz, 1H), 6.79 (m, 2H), 3.89 (t, J = 6.6 Hz, 2H), 3.79 (s, 3H), 3.72 (s, 2H), 2.85 (t, J = 6.6 Hz, 2H).

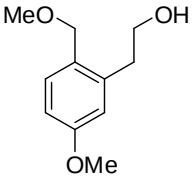

2-(5-Methoxy-2-(methoxymethyl)phenyl)ethanol (80):

^{1}H NMR (200 MHz, $CDCl_3$) δ ppm: 7.21 (d, J = 8.5 Hz, 1H), 6.79 – 6.71 (m, 2H), 4.39 (s, 2H), 3.84 (t, J = 6.8 Hz, 2H) 3.79 (s, 3H), 3.36 (s, 3H), 2.88 (t, J = 6.6 Hz, 2H).

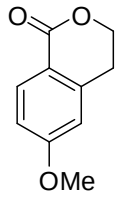

6-Methoxyisochroman-1-one (87):

R_f = 0.3, Pet – ether : ethyl acetate (90:10) colourless liquid; ^{1}H NMR (200 MHz, $CDCl_3$) δ ppm: 8.05 (d, J = 8.4 Hz, 1H), 6.90 (dd, J = 8.5, 2.5 Hz, 1H), 6.71 (d, J = 2.4 Hz, 1H), 4.49 (t, J = 8.6 Hz, 2H), 3.85 (s, 3H), 3.01 (t, J = 8.6 Hz, 2H); ^{13}C NMR (100 MHz, $CDCl_3$) δ ppm: 165.2, 163.7, 141.8, 132.7, 117.8, 113.6, 111.9, 67.1, 55.5, 28.2; HR-MS (EI) m/z: calcd. for $C_{10}H_{10}O_3$ Na[M + Na]$^+$: 201.0528; found: 201.0522.

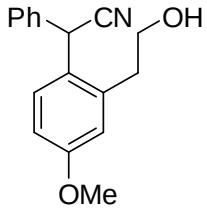

2-(2-(2-Hydroxyethyl)-4-methoxyphenyl)-2-phenylacetonitrile (81):

^{1}H NMR (200 MHz, $CDCl_3$) δ ppm: 7.11 - 7.36 (m, 6 H), 6.76 - 6.84 (m, 2H), 5.48 (s, 1H), 3.79 (s, 3H), 3.76 (t, J = 6.6, Hz 2 H), 2.74 – 2.85 (m, 2H); ^{13}C NMR (100 MHz, $CDCl_3$) δ ppm: 159.5, 138.2, 135.8, 130.5, 129.1, 128.4, 127.6, 126.3, 120.2, 116.2, 112.3, 62.8, 55.2, 38.7, 35.7.

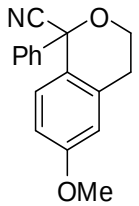

6-Methoxy-1-phenylisochroman-1-carbonitrile (88):

R_f = 0.3, Pet – ether : ethyl acetate (90:10) white crystalline solid; ^{1}H NMR (200 MHz, $CDCl_3$) δ ppm: 7.50 - 7.55 (m, 2H), 7.37 - 7.44 (m, 3H), 6.86 (d, *J* = 8.6 Hz, 1H), 6.69 - 6.75 (m, 2H), 4.24 - 4.30 (m, 2H), 3.79 (s, 3H), 3.15 - 3.33 (m, 1H), 2.83 (dt, *J* =16.5, 2.5 Hz, 1 H); ^{13}C NMR (100 MHz, $CDCl_3$) δ ppm: 159.4, 139.6, 134.7, 129.4, 129.0, 128.7, 127.2, 126.1, 119.4, 113.6, 113.4, 78.33, 62.5, 55.3, 28.18; HR-MS (EI) m/z: calcd. for $C_{17}H_{15}O_2NNa[M + Na]^+$: 288.1000; found: 288.0995.

Characterization of products of arylalkyl oxidation :

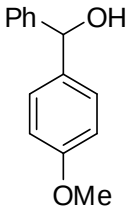

(4-Methoxyphenyl)(phenyl)methanol (90):

R_f = 0.3, Pet – ether : ethyl acetate (85:15) colourless liquid; ^{1}H NMR (200 MHz, $CDCl_3$) δ ppm: 7.25 – 7.39 (m, 7H), 6.88 (d, *J* = 8.6 Hz, 2H), 5.80 (s, 1H), 3.78 (s, 3H).

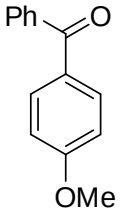

(4-Methoxyphenyl)(phenyl)methanone (91):

R_f = 0.5, Pet – ether : ethyl acetate (85:15) colourless liquid; ^{1}H NMR (200 MHz, $CDCl_3$) δ ppm: 7.71 - 7.85 (m, 4H), 7.42 – 7.60 (m, 3H), 6.97 (d, *J* = 8.8 Hz, 2H), 3.79 (s, 3H); ^{13}C NMR (100 MHz, $CDCl_3$) δ ppm: 195.5, 163.1, 138.2, 132.5, 131.8, 129.7, 128.1, 113.5, 55.4.

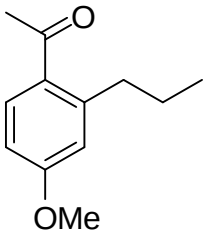

1-(4-Methoxy-2-propylphenyl)ethanone (92):

R_f = 0.5, Pet – ether : ethyl acetate (90:10) colourless liquid; ^{1}H NMR (200 MHz, $CDCl_3$) δ ppm: 7.72 (d, *J* = 9.3 Hz, 1H), 6.66 - 6.78 (m, 2H), 3.84 (s, 3H), 2.81 - 2.91 (m, 2 H), 2.54 (s, 3H), 1.57 - 1.63 (m, 2H), 0.96 (t, *J* =7.3 Hz, 3H); ^{13}C NMR (100 MHz, $CDCl_3$) δ ppm: 199.9, 161.8, 146.6, 132.4, 130.0, 116.8, 110.4, 55.3, 36.7, 29.4, 24.7, 14.2.

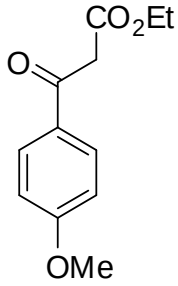

Ethyl 3-(4-methoxyphenyl)-3-oxopropanoate (93):

R_f = 0.4, Pet – ether : ethyl acetate (85:15) colourless liquid; ^{1}H NMR (200 MHz, $CDCl_3$) δ ppm: 7.93 (d, *J* = 8.8 Hz, 2H), 6.95 (d, *J* = 8.8 Hz, 2H), 4.21 (q, *J* = 6.42 Hz, 2H), 3.92 (s, 2H), 3.85 (s, 3H), 1.24 (t, *J* = 6.42 Hz, 3H).

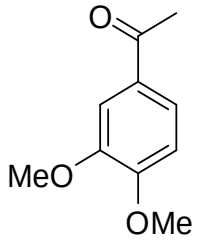

1-(3,4-Dimethoxyphenyl)ethanone (94):

R_f = 0.5, Pet – ether : ethyl acetate (90:10) colourless liquid; ^{1}H NMR (200 MHz, $CDCl_3$) δ ppm: 7.59 (dd, *J* = 8.4, 2.4 Hz, 1H), 7.51 (d, *J* = 2.4 Hz, 1H), 6.89 (d, *J* = 8.4, Hz, 1H) , 3.94 (s, 3H), 3.92 (s, 3H), 2.56 (s, 3H).

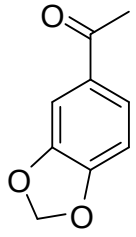

1-(Benzo[d][1,3]dioxol-5-yl)ethanone (95):

R_f = 0.5, Pet – ether : ethyl acetate (90:10) colourless liquid; ^{1}H NMR (200 MHz, $CDCl_3$) δ ppm: 7.56 (dd, *J* = 8.6, 2.4 Hz, 1H), 7.43 (d, *J* = 2.4 Hz, 1H), 6.86 (d, *J* = 8.4 Hz, 1H), 6.03 (s, 2H), 2.53 (s, 3H).

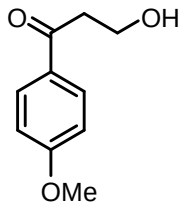

3-Hydroxy-1-(4-methoxyphenyl)propan-1-one (101):

R_f = 0.3, Pet – ether : ethyl acetate (80:20) colourless liquid; ^{1}H NMR (200 MHz, $CDCl_3$) δ ppm: 7.96 (d, *J* = 8.9 Hz, 2H), 6.95 (d, *J* = 8.9 Hz, 2H), 4.01 (t, *J* = 5.3 Hz, 2H), 3.87 (s, 3H), 3.17 (t, *J* = 5.3 Hz, 2H); ^{13}C NMR (100 MHz, $CDCl_3$) δ ppm: 199.1, 163.8, 130.3, 129.6, 113.8, 58.2, 55.2, 39.8.

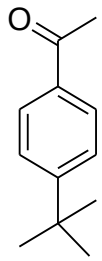

(4-tert-butylphenyl)(phenyl)methanone (102):

R_f = 0.3, Pet – ether : ethyl acetate (90:10) colourless liquid; ^{1}H NMR (200 MHz, $CDCl_3$) δ ppm: 7.92 (d, *J* = 8.5 Hz, 2 H), 7.49 (d, *J* = 8.5 Hz, 2 H), 2.59 (s, 3 H), 1.36 (s, 9 H).

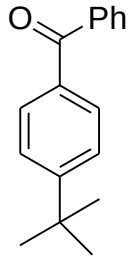

(4-tert-butylphenyl)(phenyl)methanone (103):

R_f = 0.4, Pet – ether : ethyl acetate (90:10) colourless liquid; ^{1}H NMR (200 MHz, $CDCl_3$) δ ppm: 7.96 - 7.72 (m, 4 H), 7.66 - 7.44 (m, 5 H), 1.41 (s, 9 H)

1.9 Spectra of all new compounds:

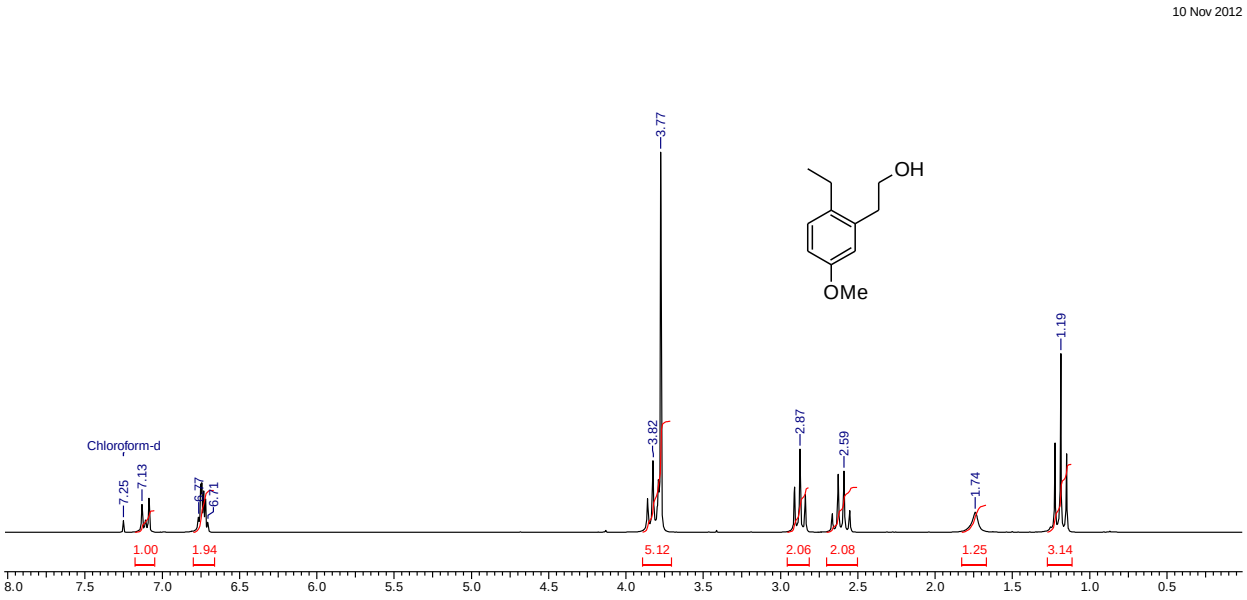

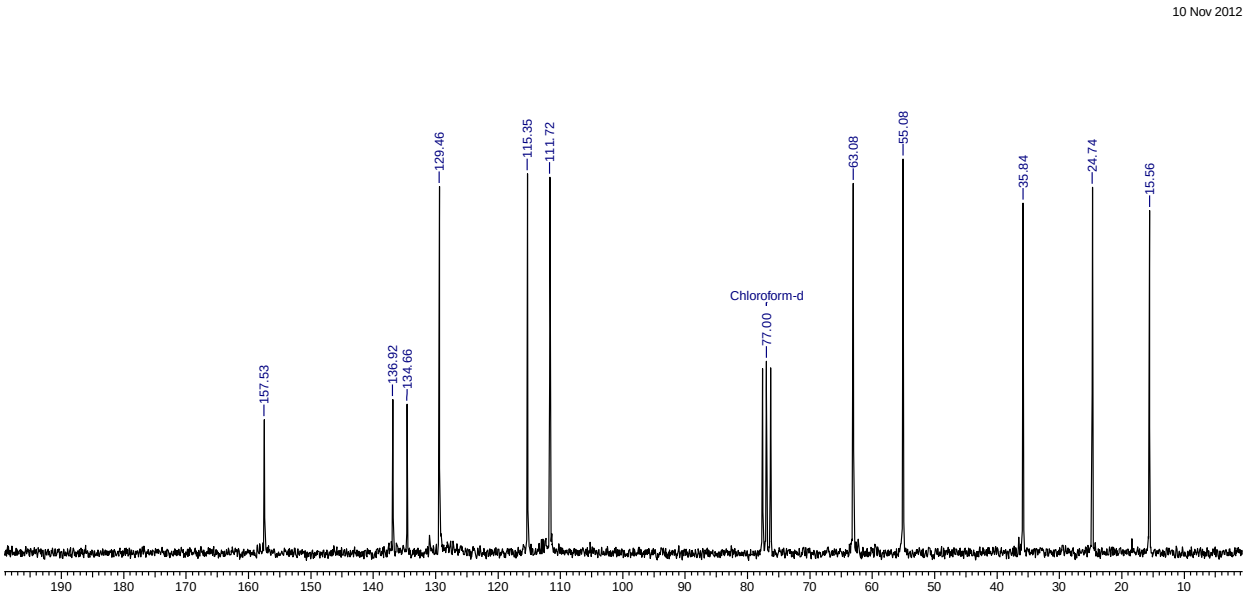

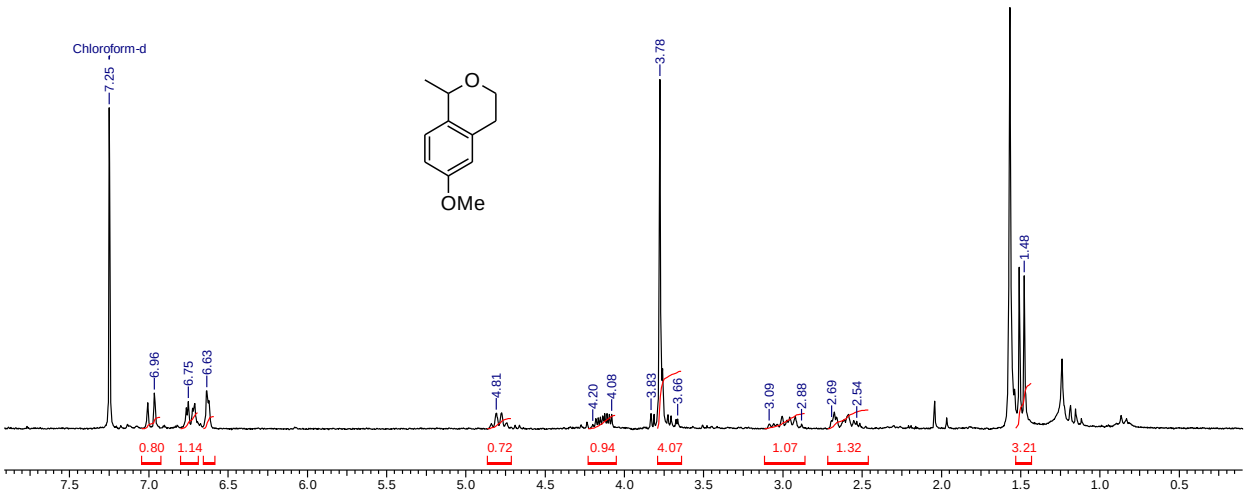
10 Nov 2012
Chloroform-d
7.25
6.96
6.75
6.63
4.81
4.20
4.08
3.83
3.78
3.66
3.09
2.88
2.69
2.54
1.48
OMe
0.80
1.14
0.72
0.94
4.07
1.07
1.32
3.21

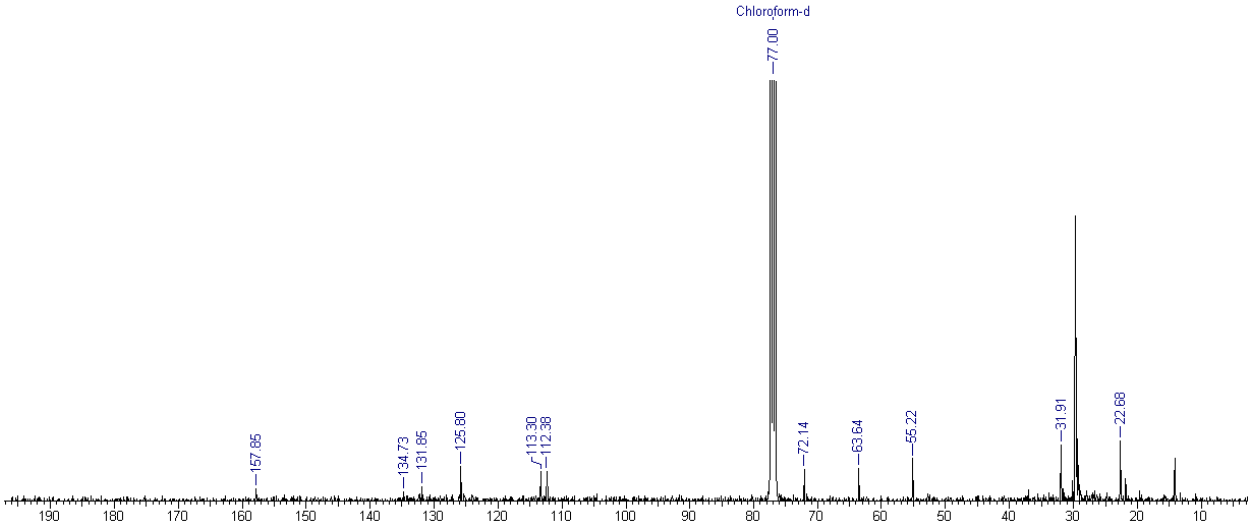
Chloroform-d
77.00
157.85
134.73
131.85
125.80
113.30
112.38
72.14
63.64
55.22
31.91
22.68

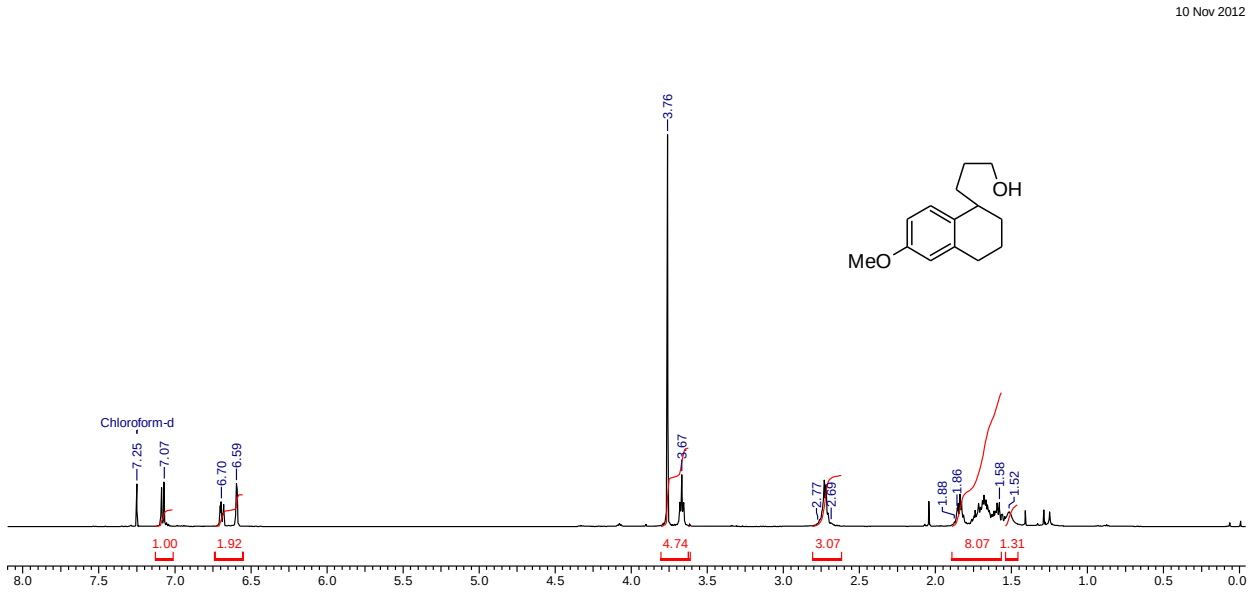
10 Nov 2012
3.76
OH
MeO
Chloroform-d
7.25
7.07
6.70
6.59
3.67
2.77
2.69
1.88
1.86
1.58
1.52
1.00
1.92
4.74
3.07
8.07
1.31

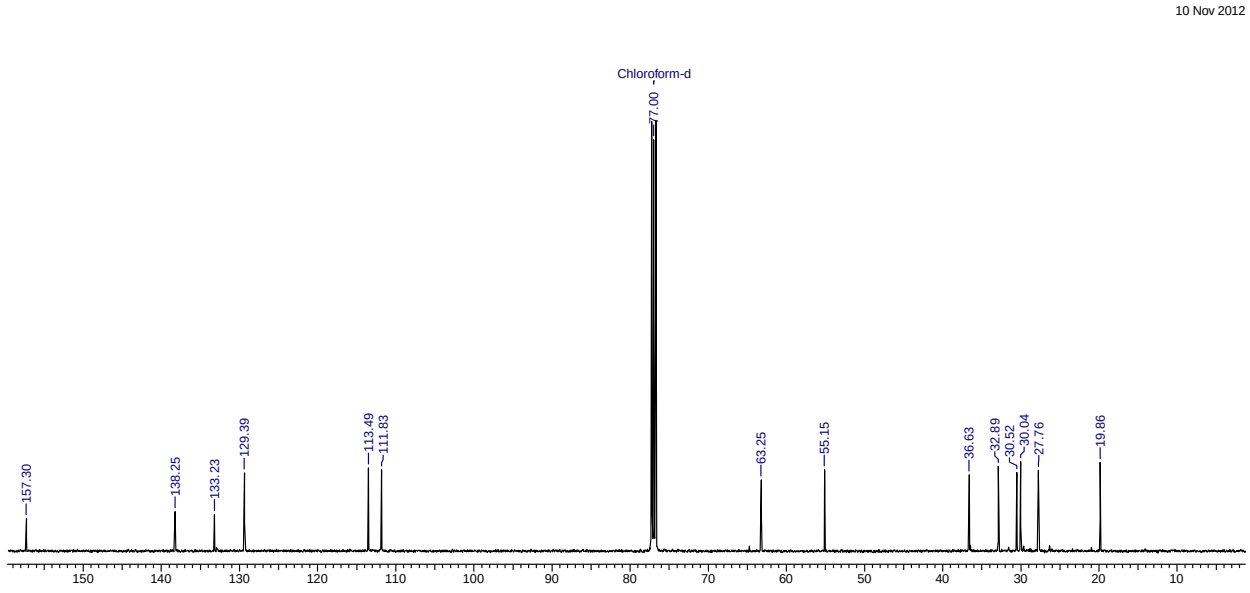
10 Nov 2012
Chloroform-d
77.00
157.30
138.25
133.23
129.39
113.49
111.83
63.25
55.15
36.63
32.89
30.52
30.04
27.76
19.86

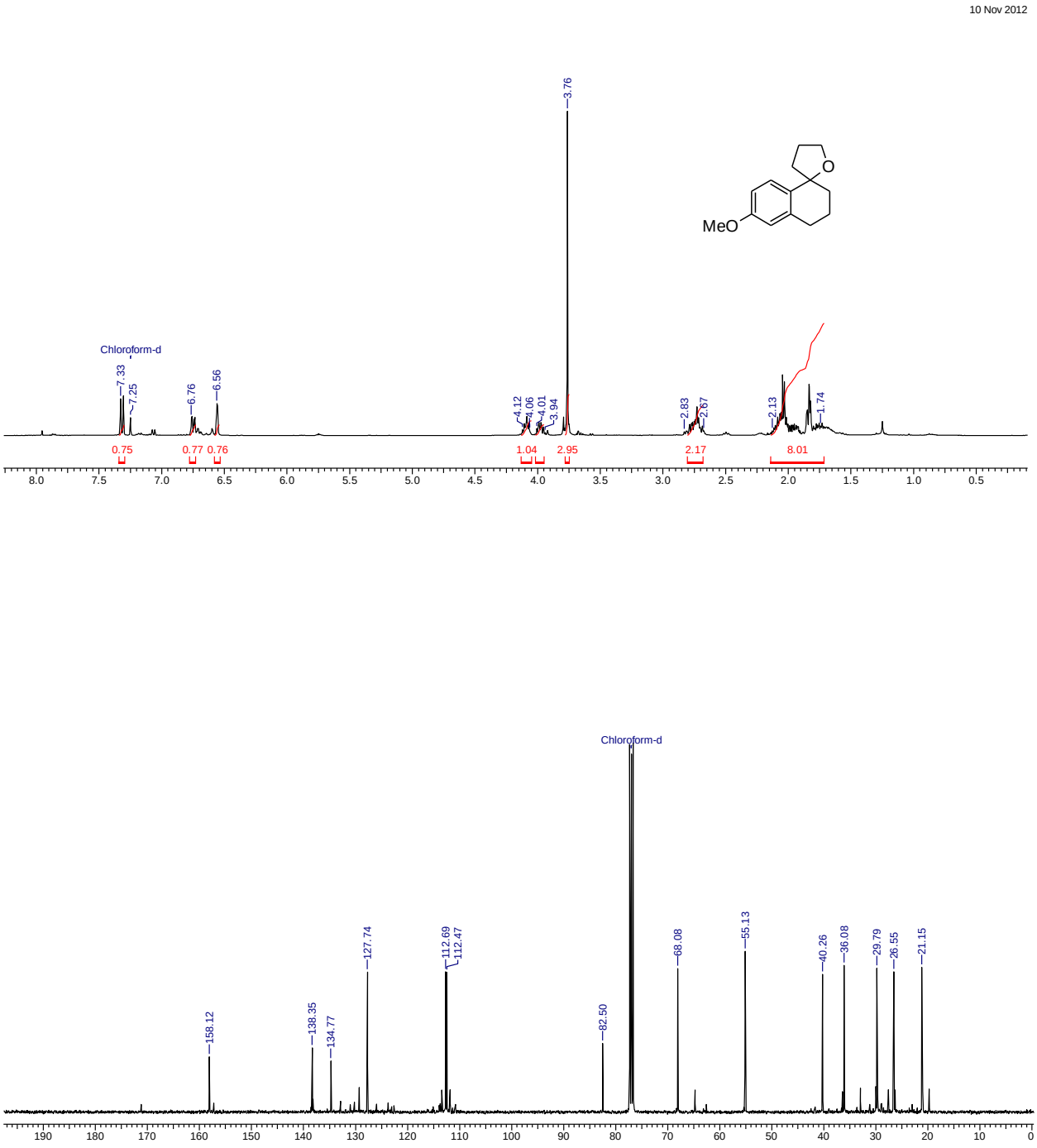
10 Nov 2012
3.76
O
MeO
Chloroform-d
7.33
7.25
6.76
6.56
4.12
4.06
4.01
3.94
2.83
2.67
2.13
1.74
0.75
0.77
0.76
1.04
2.95
2.17
8.01
Chloroform-d
158.12
138.35
134.77
127.74
112.69
112.47
82.50
68.08
55.13
40.26
36.08
29.79
26.55
21.15

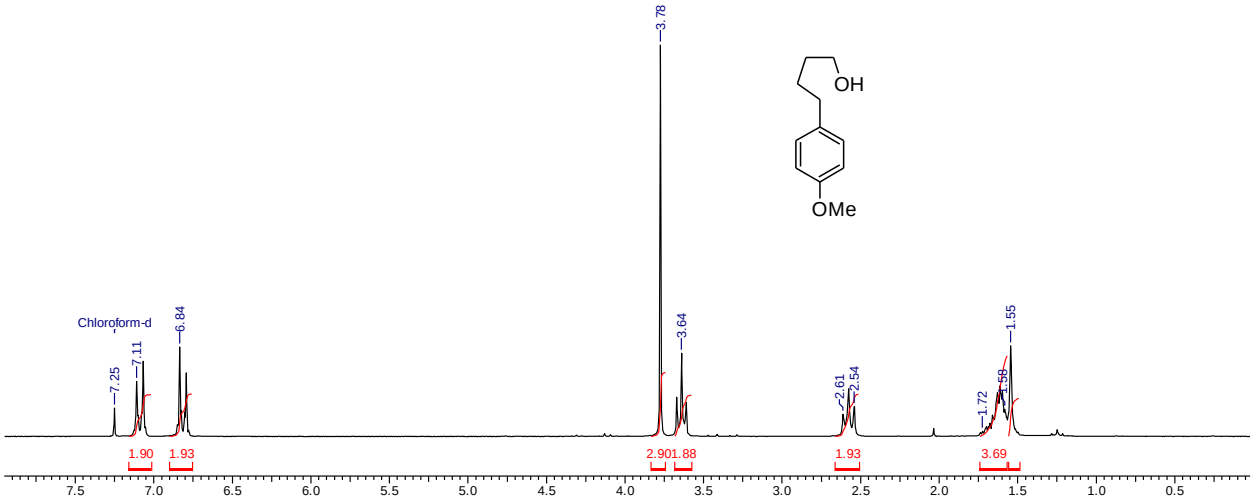
3.78
OH
OMe
Chloroform-d
7.25
7.11
6.84
3.64
2.61
2.54
1.72
1.58
1.55
1.90
1.93
2.90
1.88
1.93
3.69
7.5
7.0
6.5
6.0
5.5
5.0
4.5
4.0
3.5
3.0
2.5
2.0
1.5
1.0
0.5

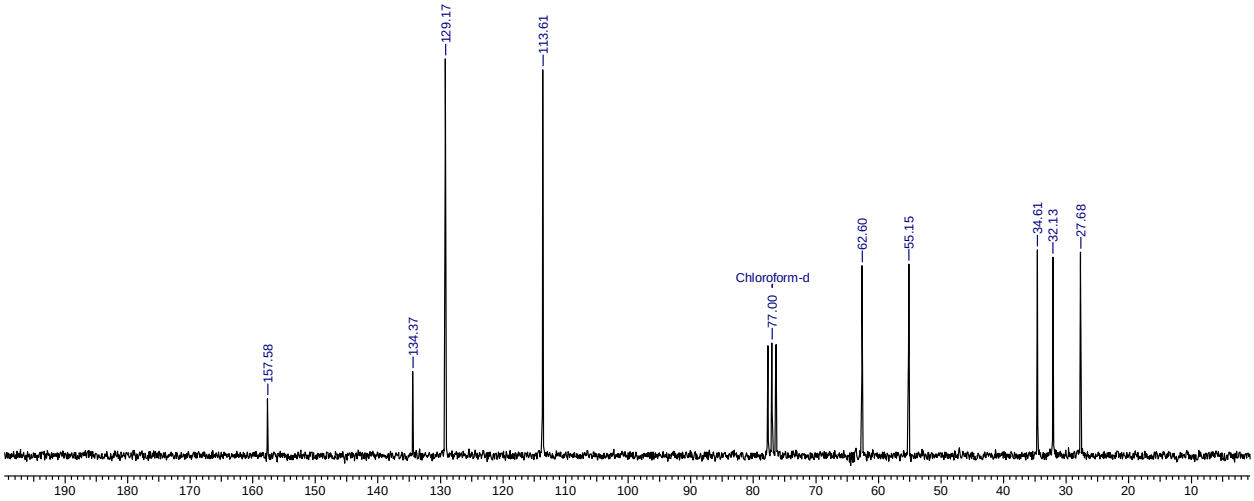
129.17
113.61
157.58
134.37
Chloroform-d
77.00
62.60
55.15
34.61
32.13
27.68
190
180
170
160
150
140
130
120
110
100
90
80
70
60
50
40
30
20
10

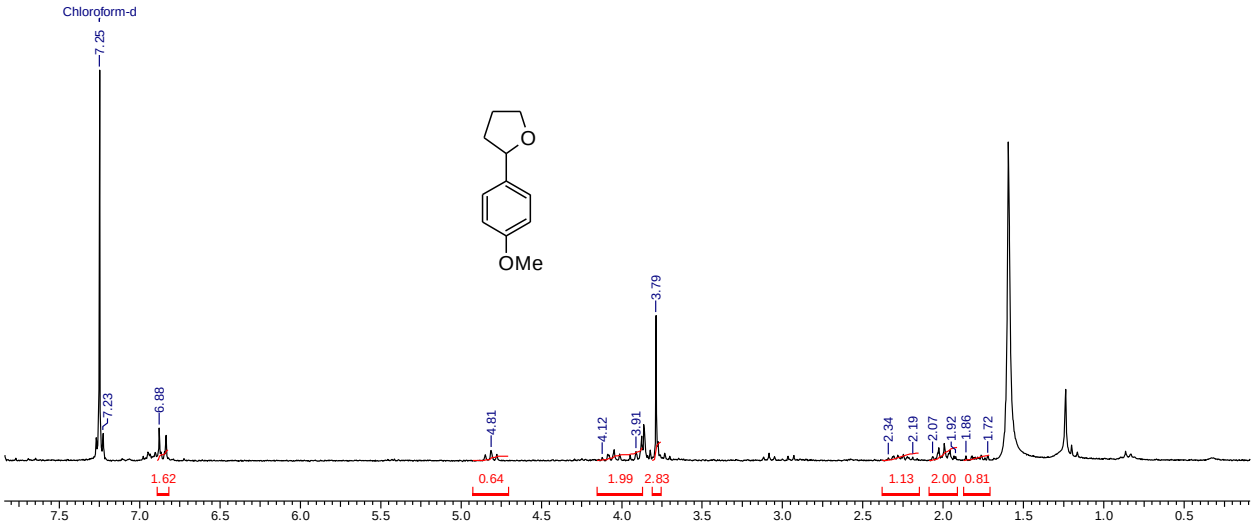
Chloroform-d
7.25
7.23
6.88
4.81
4.12
3.91
3.79
2.34
2.19
2.07
1.92
1.86
1.72
O
OMe
1.62
0.64
1.99
2.83
1.13
2.00
0.81

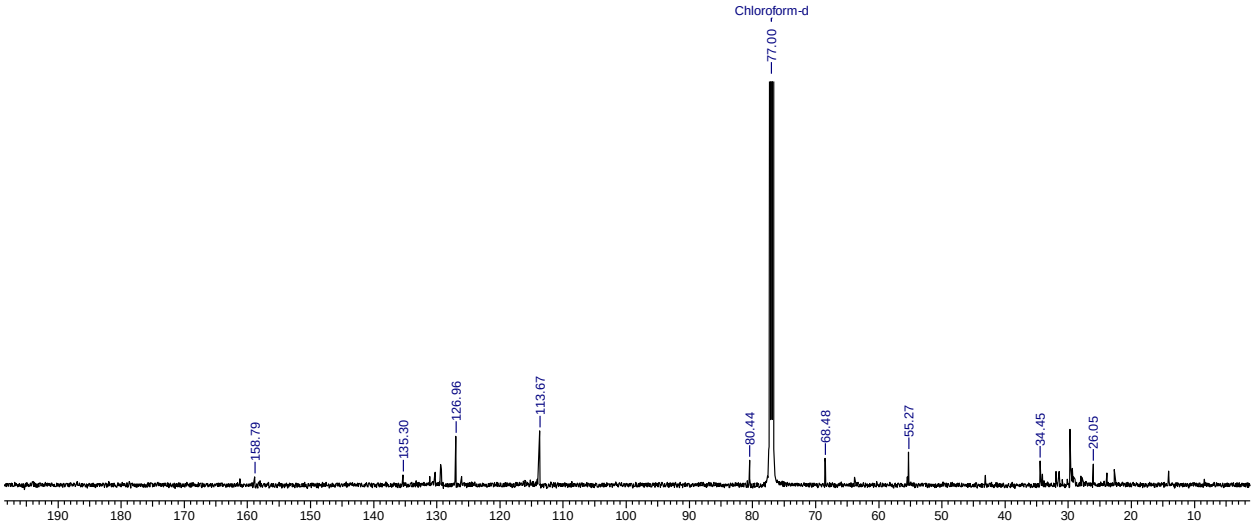
Chloroform-d
77.00
158.79
135.30
126.96
113.67
80.44
68.48
55.27
34.45
26.05

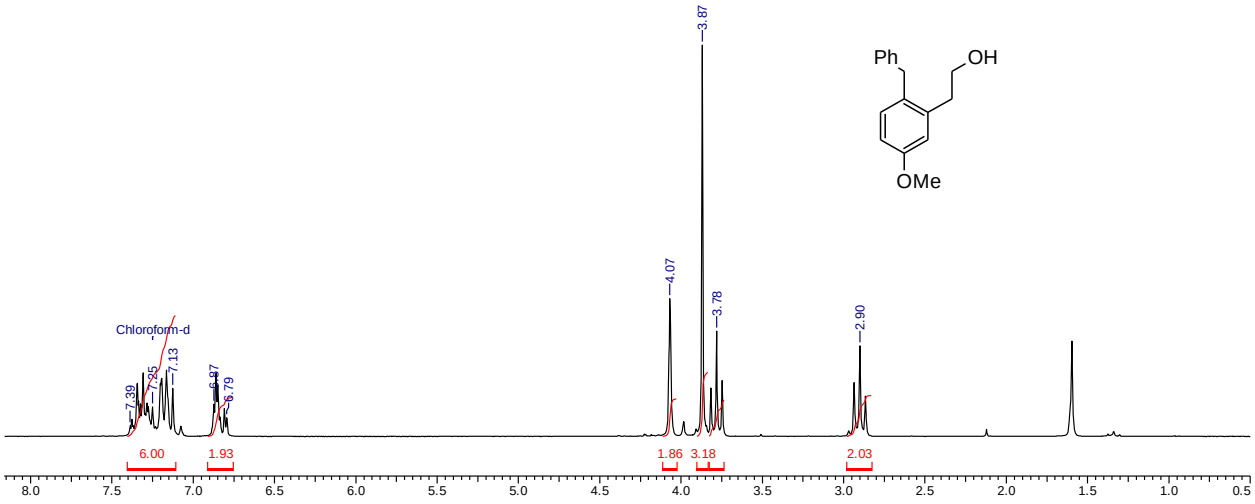
Ph
OH
OMe
Chloroform-d
7.39
7.35
7.13
6.87
6.79
4.07
3.87
3.78
2.90
6.00
1.93
1.86
3.18
2.03

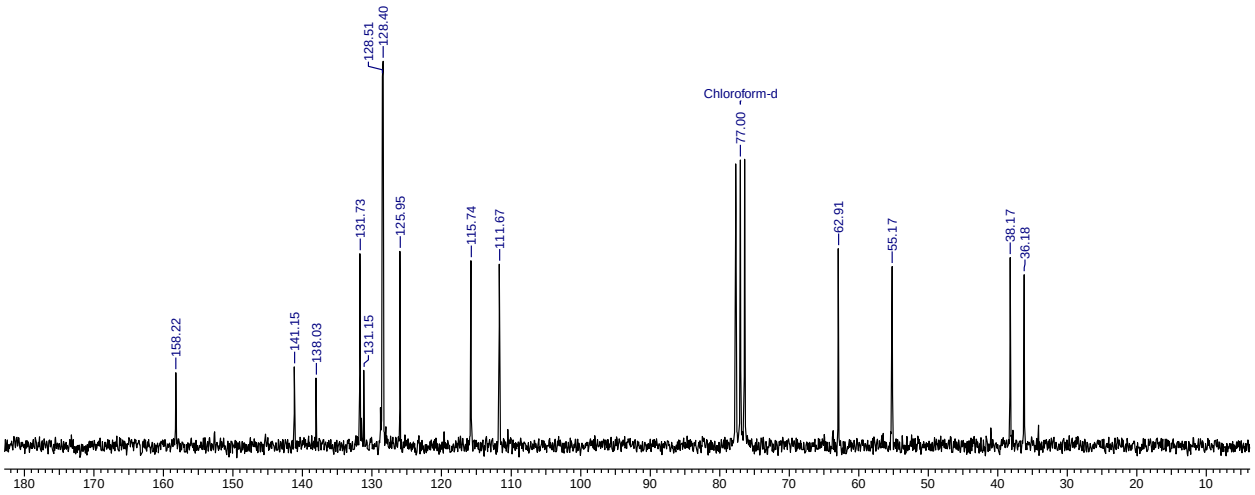
158.22
141.15
138.03
131.73
131.15
128.51
128.40
125.95
115.74
111.67
Chloroform-d
77.00
62.91
55.17
38.17
36.18

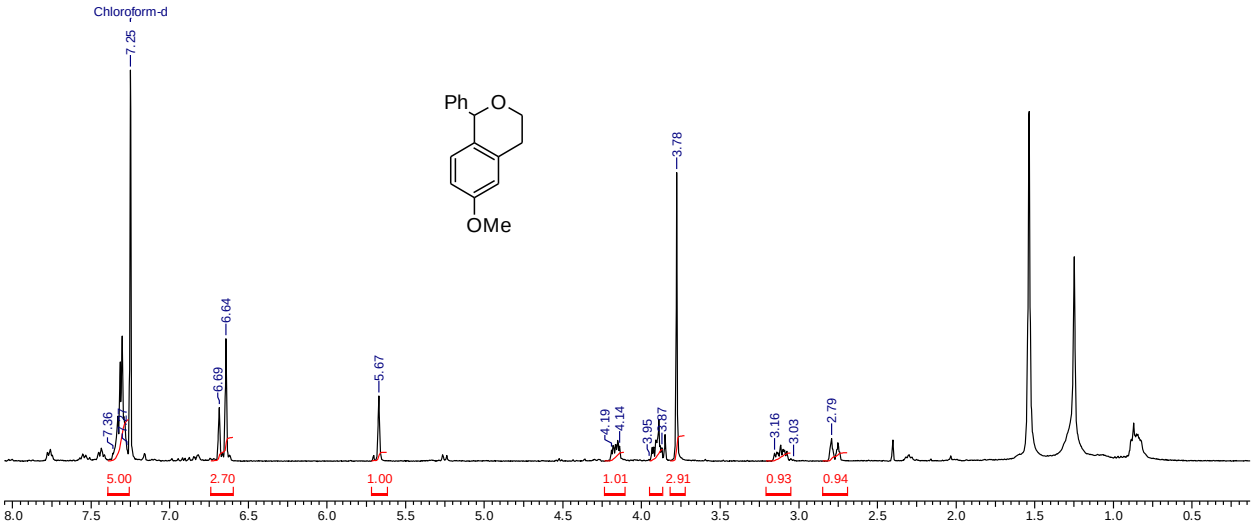
Chloroform-d
7.25
Ph
O
OMe
3.78
6.64
6.69
5.67
7.36
7.27
4.19
4.14
3.95
3.87
3.16
3.03
2.79
5.00
2.70
1.00
1.01
2.91
0.93
0.94

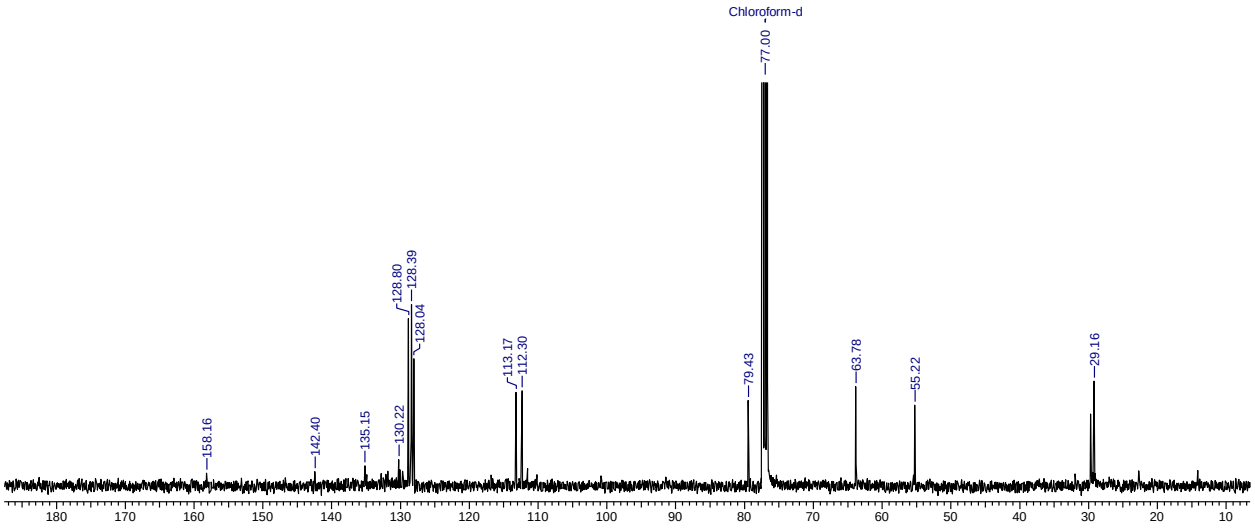
Chloroform-d
77.00
128.80
128.39
128.04
113.17
112.30
158.16
142.40
135.15
130.22
79.43
63.78
55.22
29.16

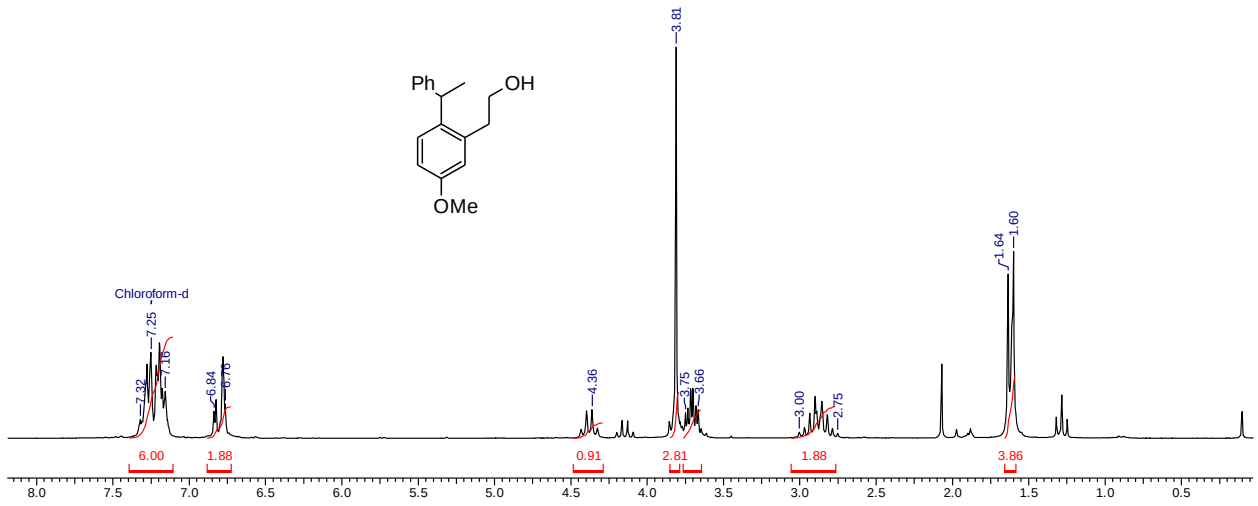
Ph
OH
OMe
Chloroform-d
7.32
7.25
7.16
6.84
6.76
4.36
3.81
3.75
3.66
3.00
2.75
1.64
1.60
6.00
1.88
0.91
2.81
1.88
3.86
8.0
7.5
7.0
6.5
6.0
5.5
5.0
4.5
4.0
3.5
3.0
2.5
2.0
1.5
1.0
0.5

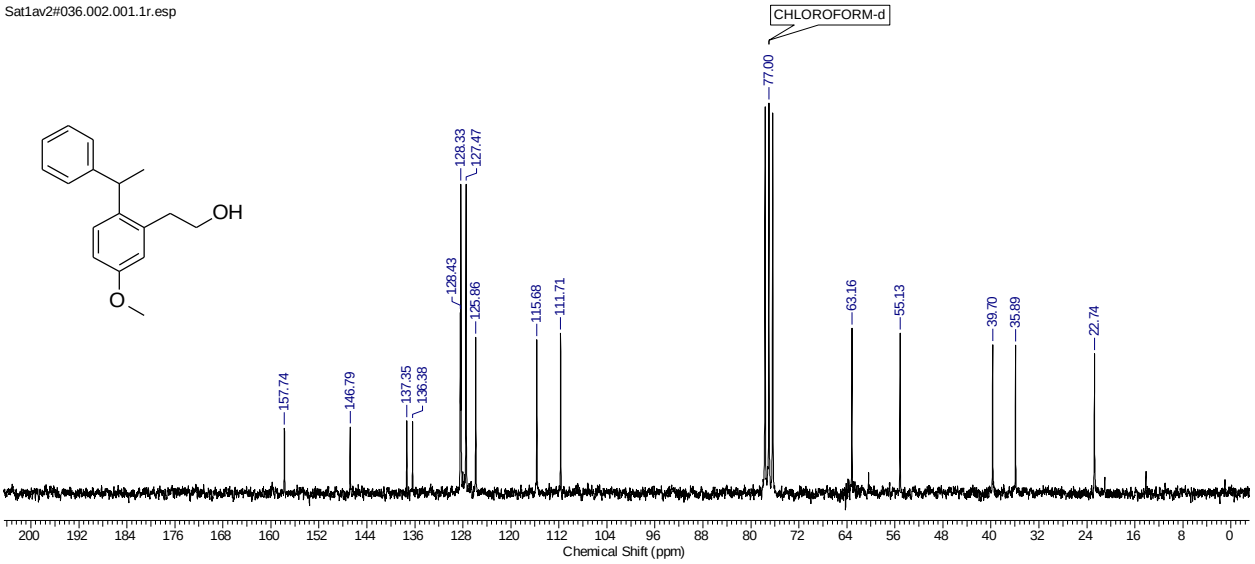
Sat1av2#036.002.001.1r.esp
CHLOROFORM-d
77.00
OH
O
128.33
127.47
128.43
125.86
115.68
111.71
157.74
146.79
137.35
136.38
63.16
55.13
39.70
35.89
22.74
200
192
184
176
168
160
152
144
136
128
120
112
104
96
88
80
72
64
56
48
40
32
24
16
8
0
Chemical Shift (ppm)

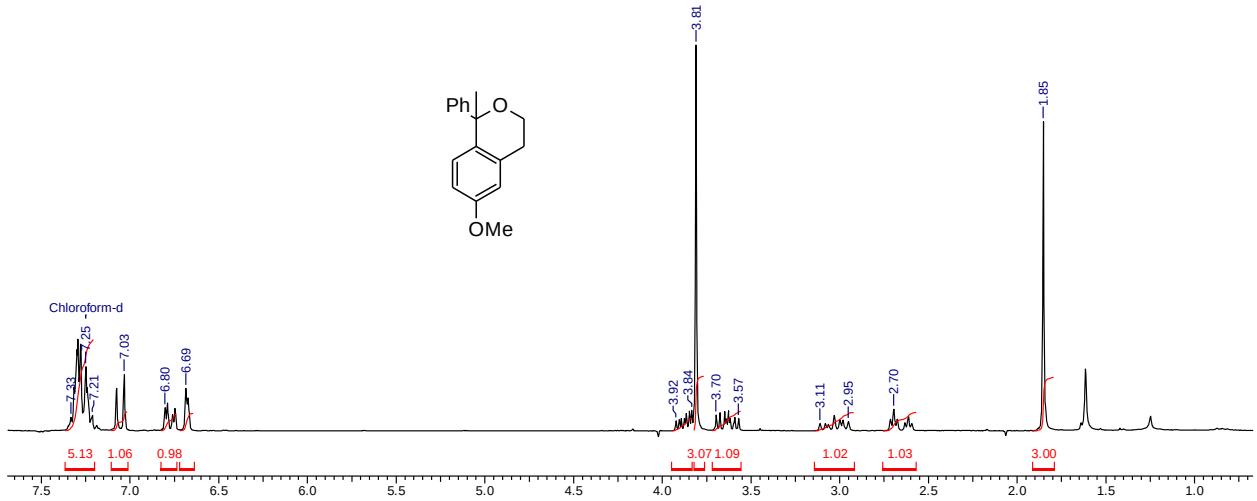
Ph
O
OMe
Chloroform-d
7.33
7.25
7.21
7.03
6.80
6.69
3.92
3.84
3.81
3.70
3.57
3.11
2.95
2.70
1.85
5.13
1.06
0.98
3.07
1.09
1.02
1.03
3.00

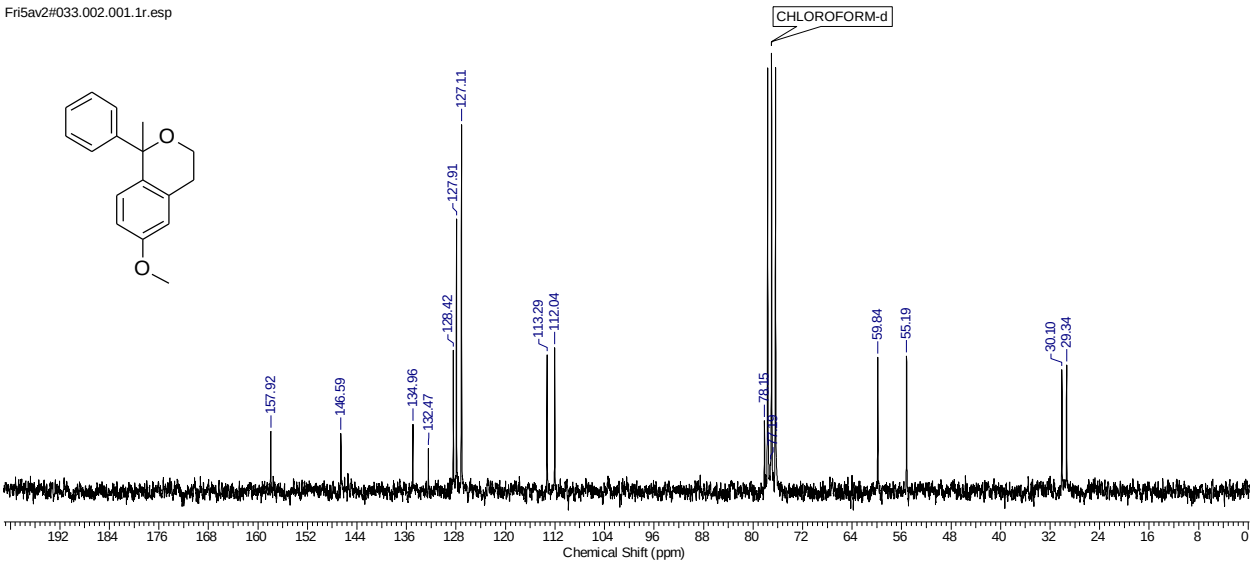
Fri5av2#033.002.001.1r.esp
CHLOROFORM-d
O
O
157.92
146.59
134.96
132.47
128.42
127.91
127.11
113.29
112.04
79.15
77.16
59.84
55.19
30.10
29.34
Chemical Shift (ppm)

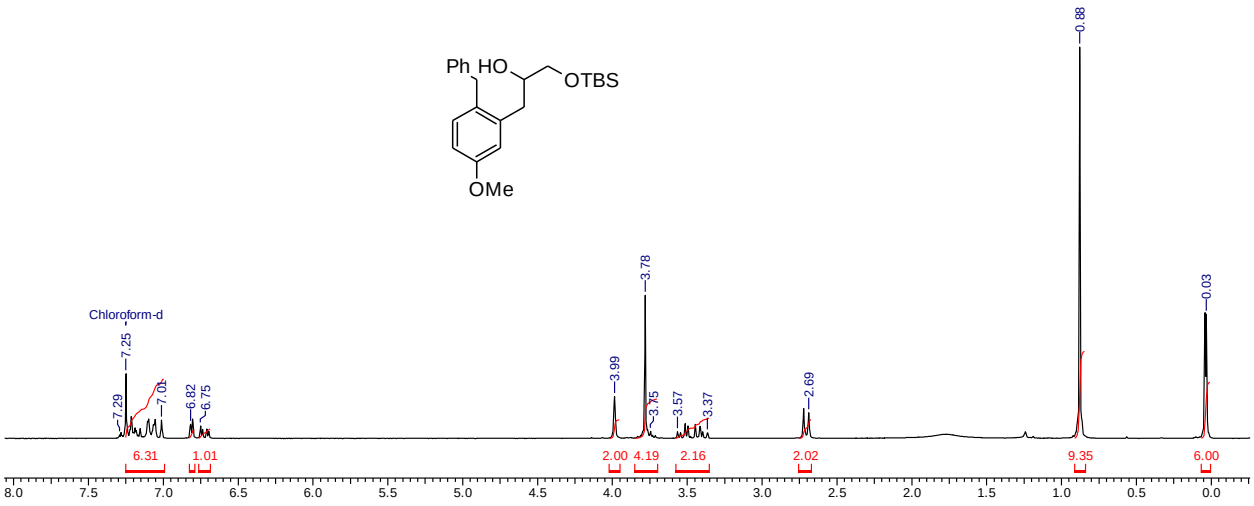
Ph
HO
OTBS
OMe
Chloroform-d
7.25
7.29
7.01
6.82
6.75
3.99
3.78
3.75
3.57
3.37
2.69
0.88
0.03
6.31
1.01
2.00
4.19
2.16
2.02
9.35
6.00

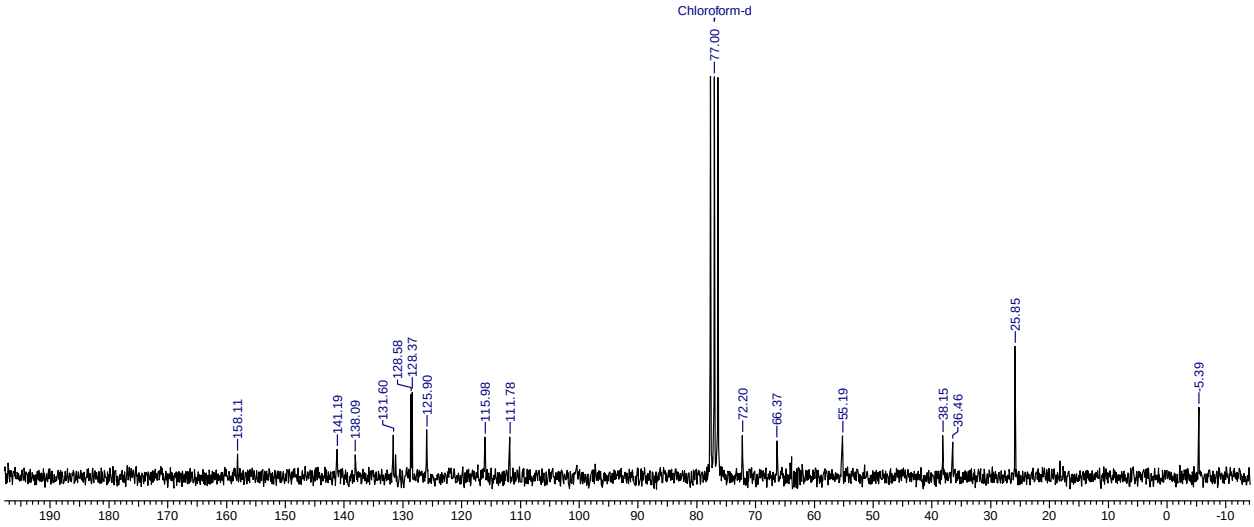
Chloroform-d
77.00
158.11
141.19
138.09
131.60
128.58
128.37
125.90
115.98
111.78
72.20
66.37
55.19
38.15
36.46
25.85
5.39

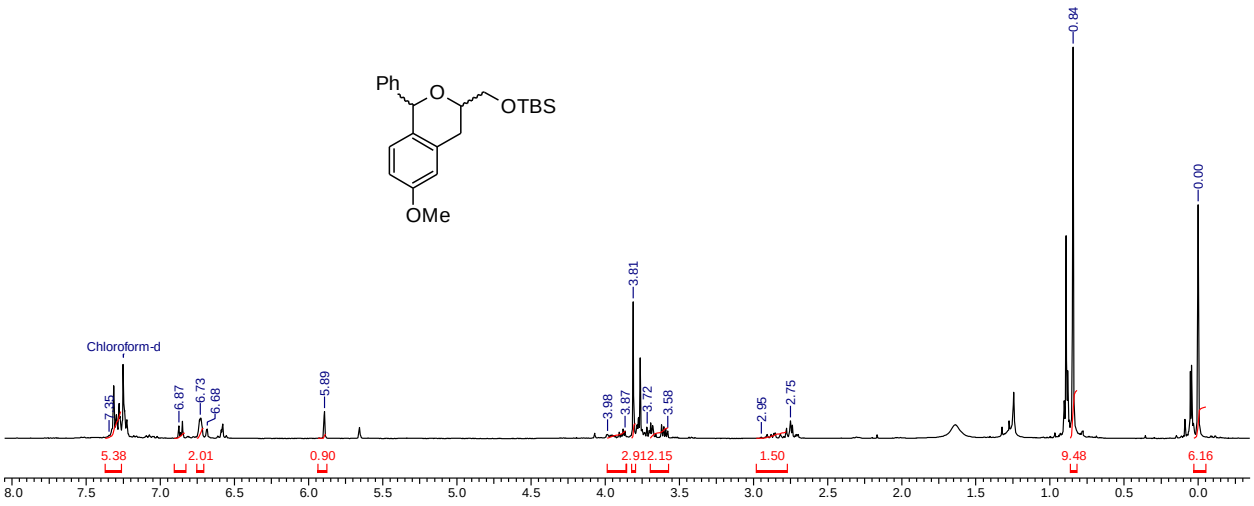
Ph
O
OTBS
OMe
Chloroform-d
7.35
6.87
6.73
6.68
5.89
3.98
3.87
3.72
3.58
3.81
2.95
2.75
0.84
0.00
5.38
2.01
0.90
2.91
2.15
1.50
9.48
6.16

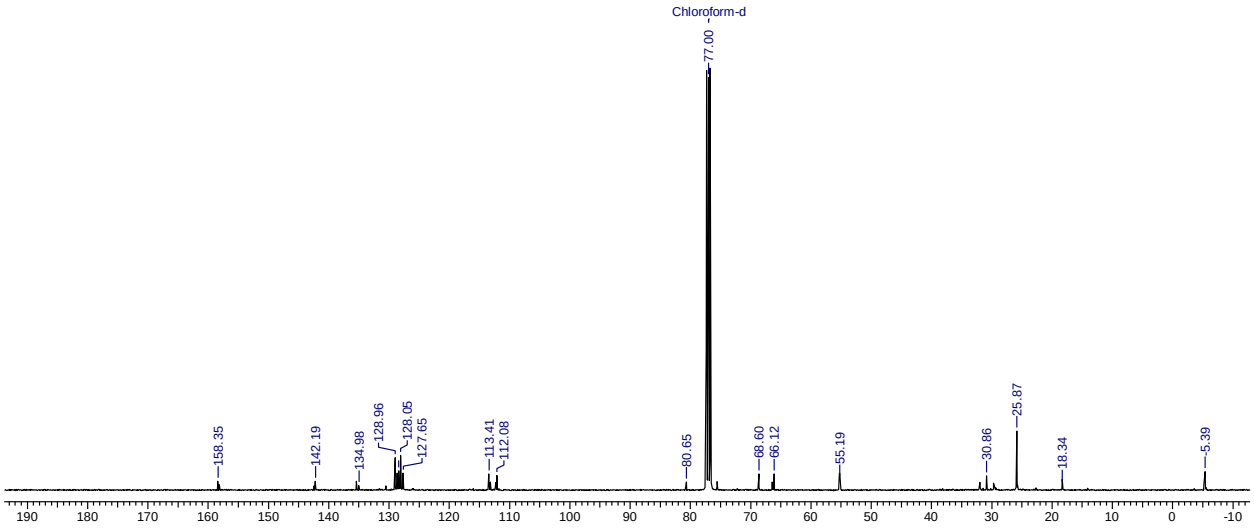
Chloroform-d
77.00
158.35
142.19
134.98
128.96
128.05
127.65
113.41
112.08
80.65
68.60
66.12
55.19
30.86
25.87
18.34
-5.39

HPLC data of 60.

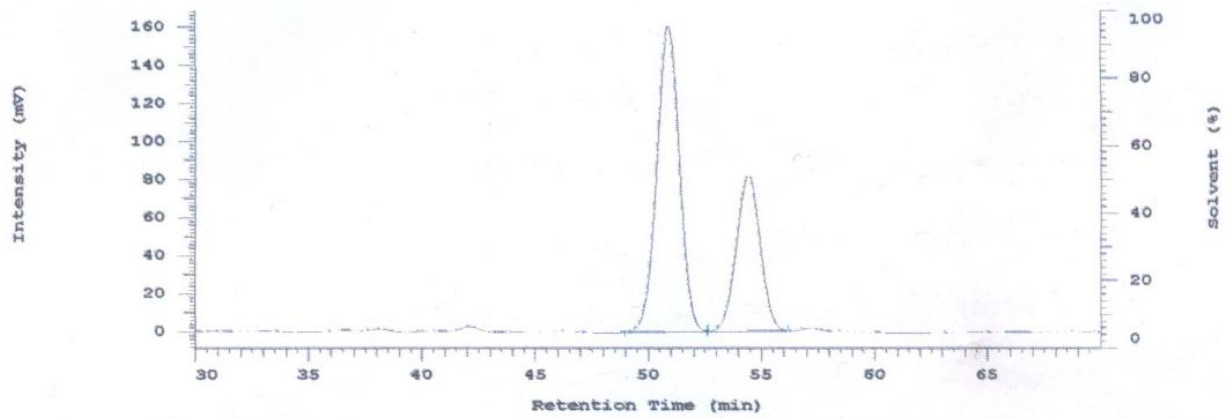

Peak Quantitation: AREA Calculation Method: AREA%

No.	RT	Height	Area	Area %
1	50.92	160583	11156100	64.918
2	54.45	82023	6028725	35.082
		242606	17184825	100.000

Column : Kromasil RP18 (150 x 4.6 mm)
M.P. : MeoH:H2O (80:20)

Flow Rate : 1 ml/min (1208 psi)
Sample conc: 2.5mg/2ml
Inj vol: 2 ul
WAVELENGTH : 230 nm

LCMS data [M + Na]:

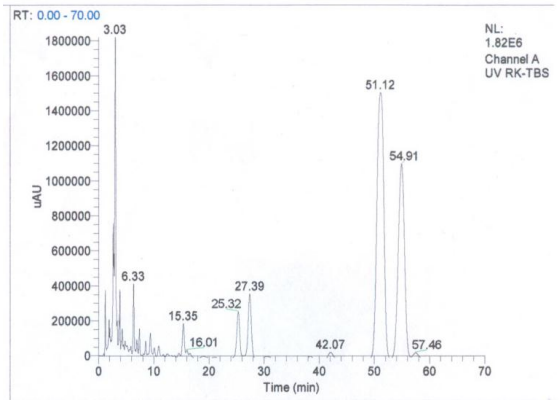

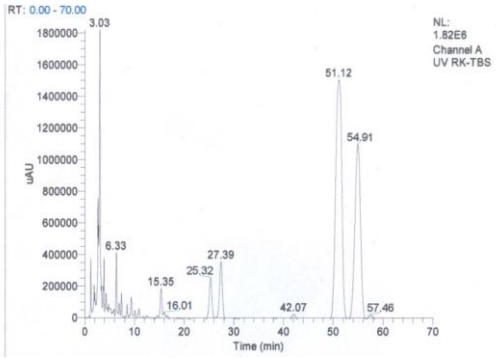

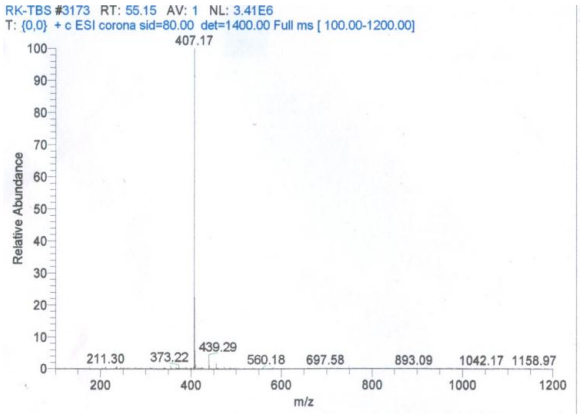

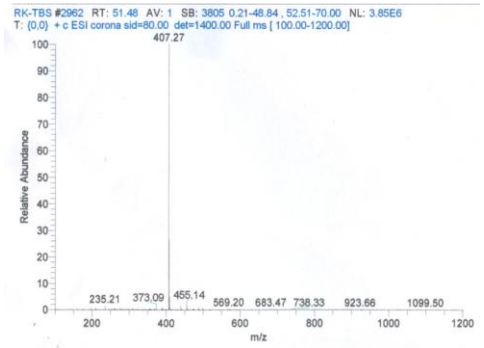

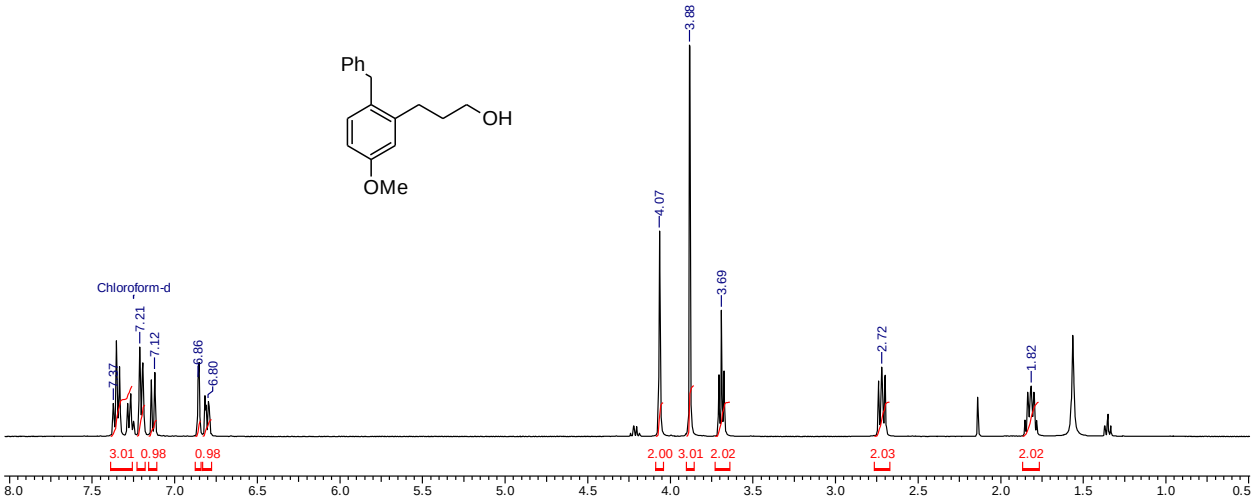
Ph
OH
OMe
Chloroform-d
7.37
7.21
7.12
6.86
6.80
4.07
3.88
3.69
2.72
1.82
3.01
0.98
0.98
2.00
3.01
2.02
2.03
2.02

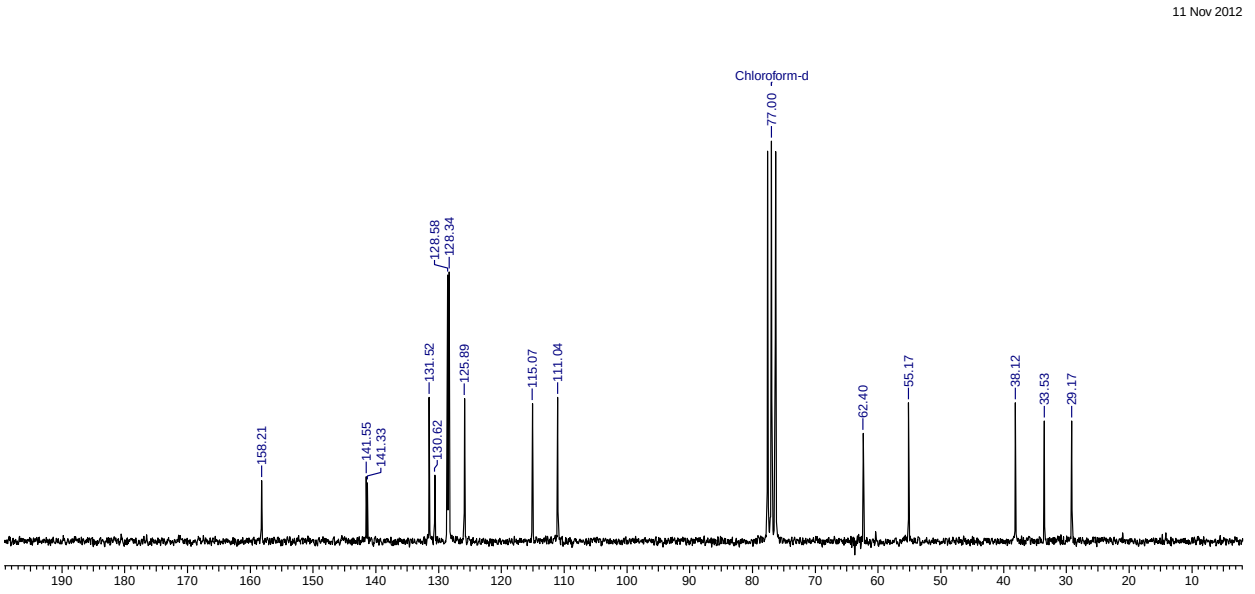
11 Nov 2012
Chloroform-d
77.00
158.21
141.55
141.33
131.52
130.62
128.58
128.34
125.89
115.07
111.04
62.40
55.17
38.12
33.53
29.17

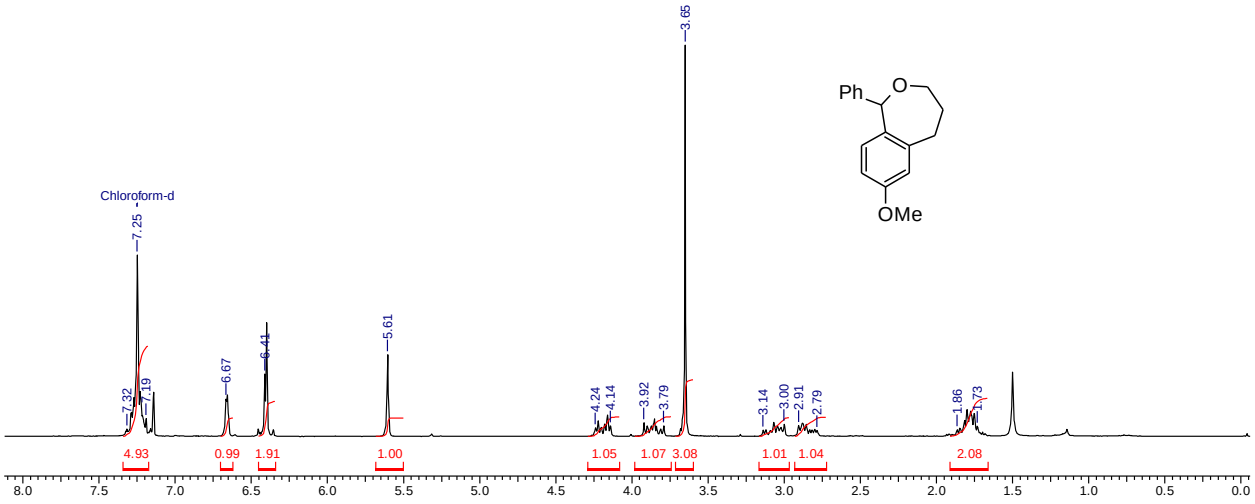
Chloroform-d
7.25
7.32
7.19
6.67
6.41
5.61
4.24
4.14
3.92
3.79
3.65
3.14
3.00
2.91
2.79
1.86
1.73
4.93
0.99
1.91
1.00
1.05
1.07
3.08
1.01
1.04
2.08
Ph
O
OMe

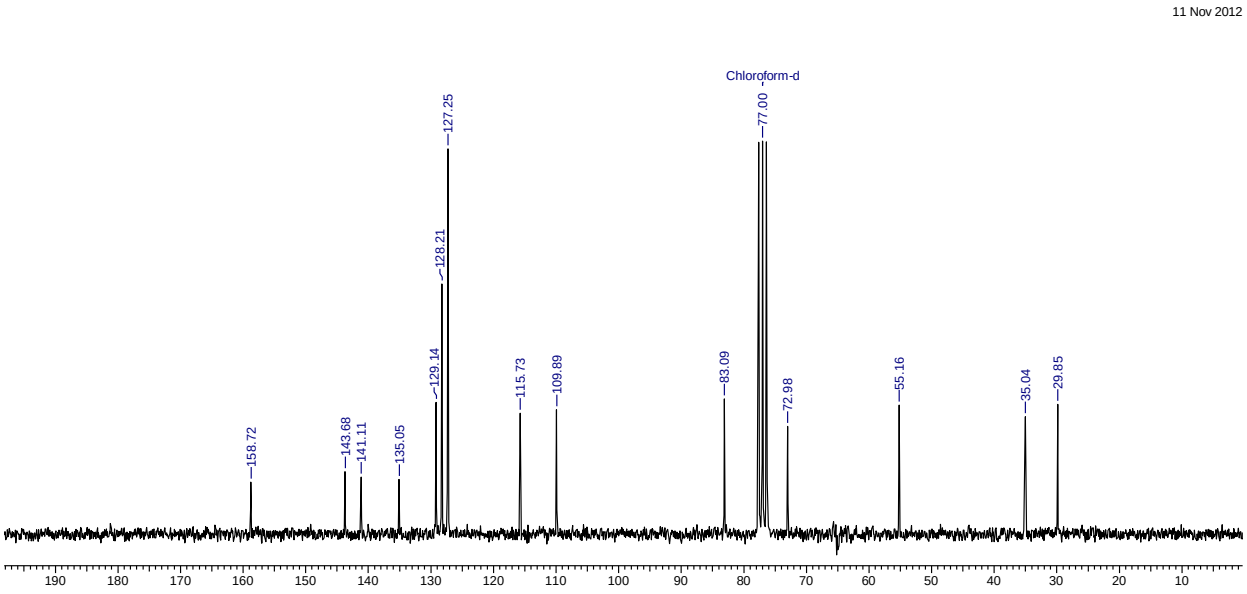
11 Nov 2012
Chloroform-d
127.25
128.21
129.14
158.72
143.68
141.11
135.05
115.73
109.89
83.09
77.00
72.98
55.16
35.04
29.85

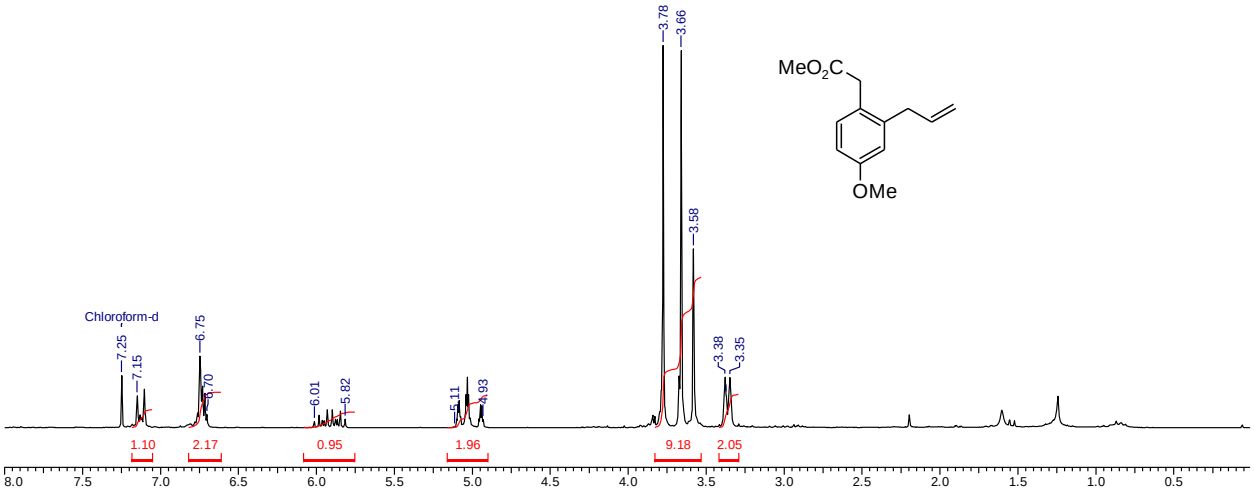
MeO2C
OMe
Chloroform-d
7.25
7.15
6.75
6.70
6.01
5.82
5.11
4.93
3.78
3.66
3.58
3.38
3.35
1.10
2.17
0.95
1.96
9.18
2.05

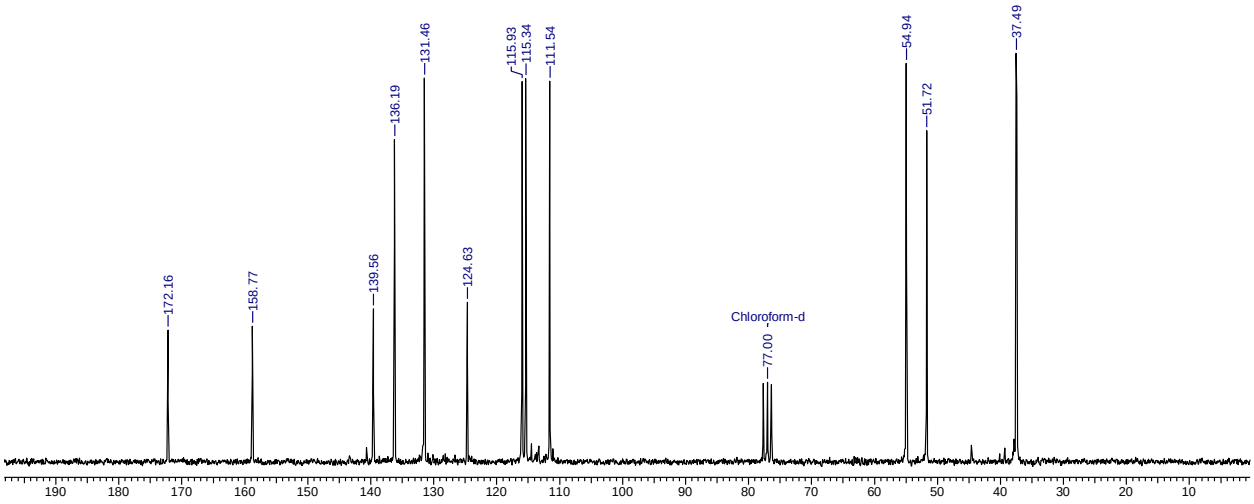
172.16
158.77
139.56
136.19
131.46
124.63
115.93
115.34
111.54
Chloroform-d
77.00
54.94
51.72
37.49

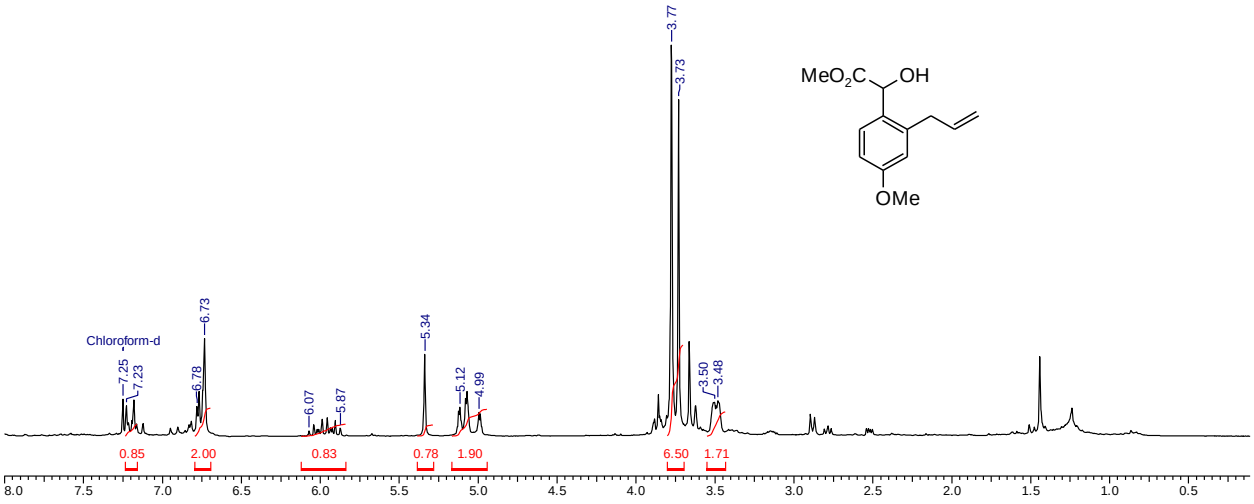
MeO2C
OH
OMe
Chloroform-d
7.25
7.23
6.78
6.73
6.07
5.87
5.34
5.12
4.99
3.77
3.73
3.50
3.48
0.85
2.00
0.83
0.78
1.90
6.50
1.71

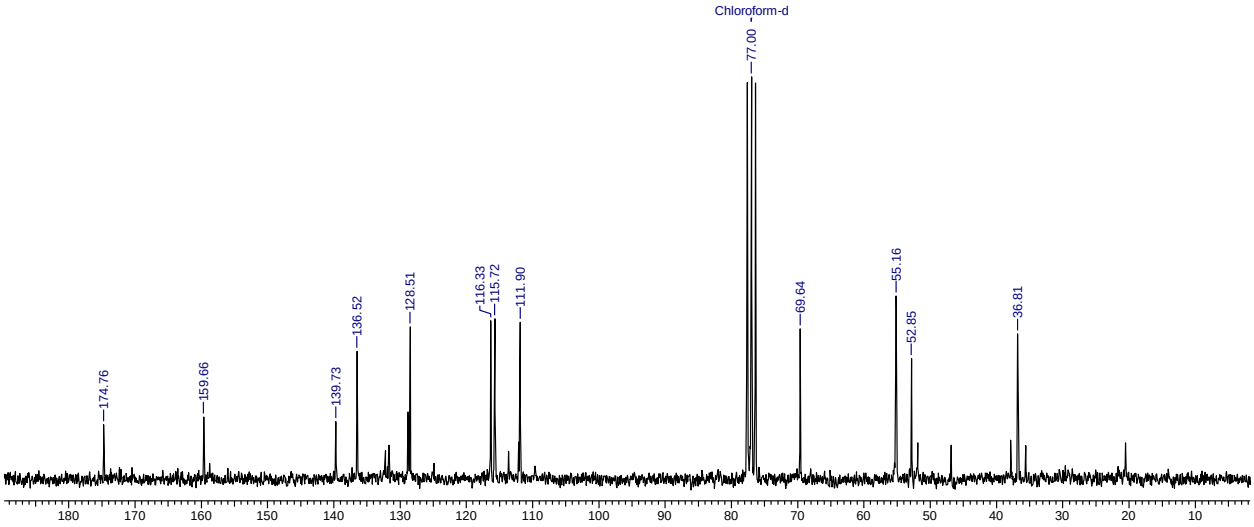
Chloroform-d
77.00
174.76
159.66
139.73
136.52
128.51
116.33
115.72
111.90
69.64
55.16
52.85
36.81

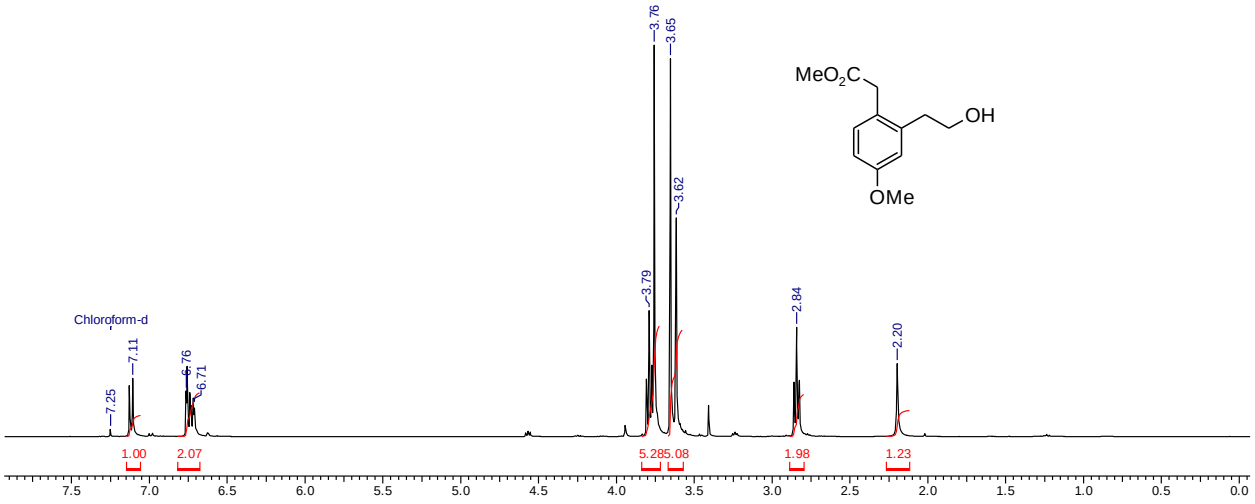
MeO2C
OH
OMe
Chloroform-d
7.25
7.11
6.76
6.71
3.76
3.65
3.62
3.79
2.84
2.20
1.00
2.07
5.28
5.08
1.98
1.23

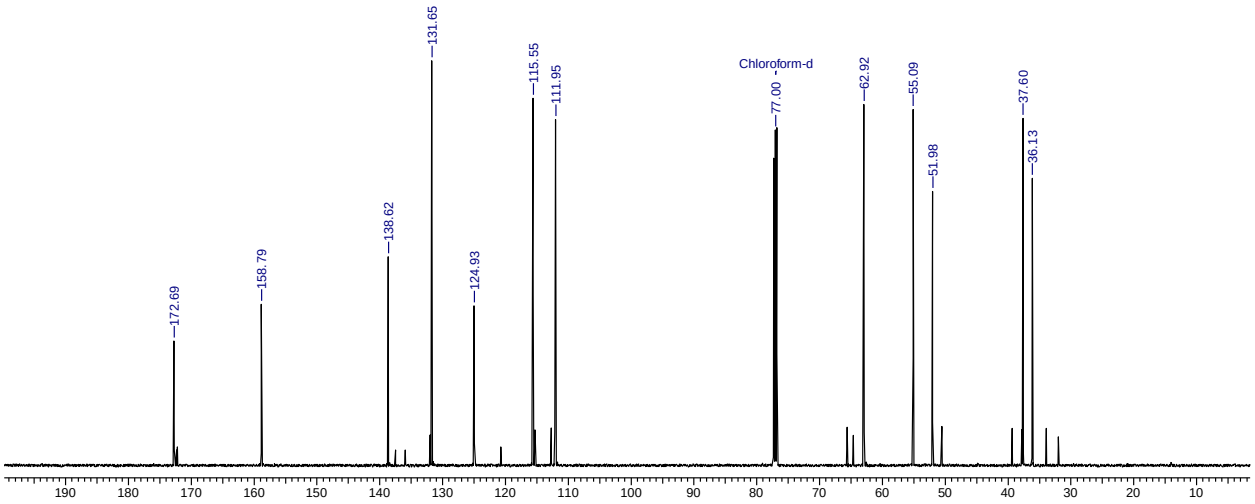
172.69
158.79
138.62
131.65
124.93
115.55
111.95
Chloroform-d
77.00
62.92
55.09
51.98
37.60
36.13

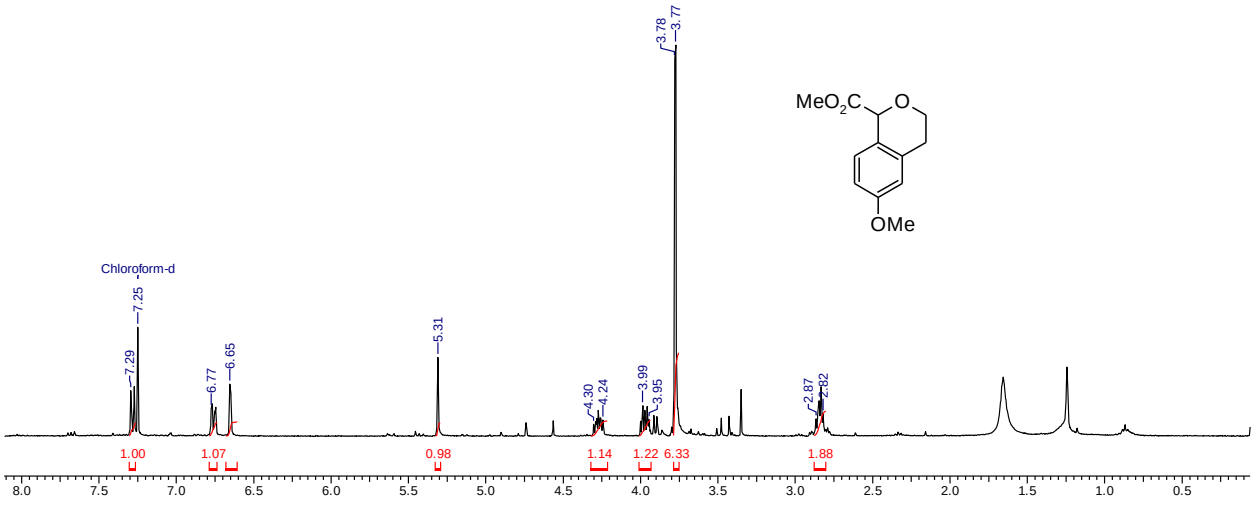
MeO2C
O
OMe
Chloroform-d
7.25
7.29
6.77
6.65
5.31
4.30
4.24
3.99
3.95
3.78
3.77
2.87
2.82
1.00
1.07
0.98
1.14
1.22
6.33
1.88

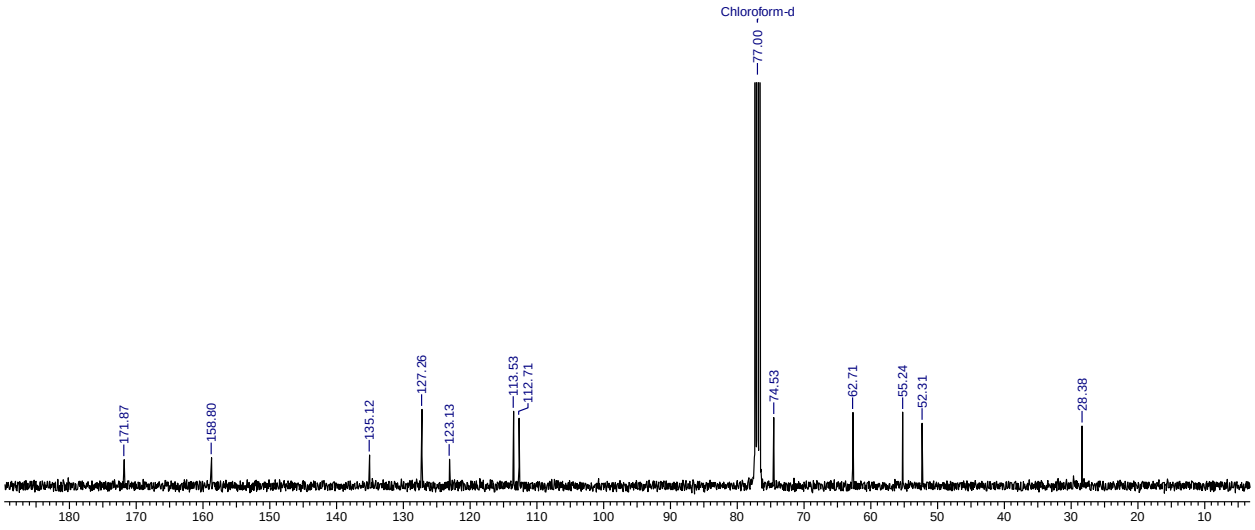
Chloroform-d
77.00
171.87
158.80
135.12
127.26
123.13
113.53
112.71
74.53
62.71
55.24
52.31
28.38

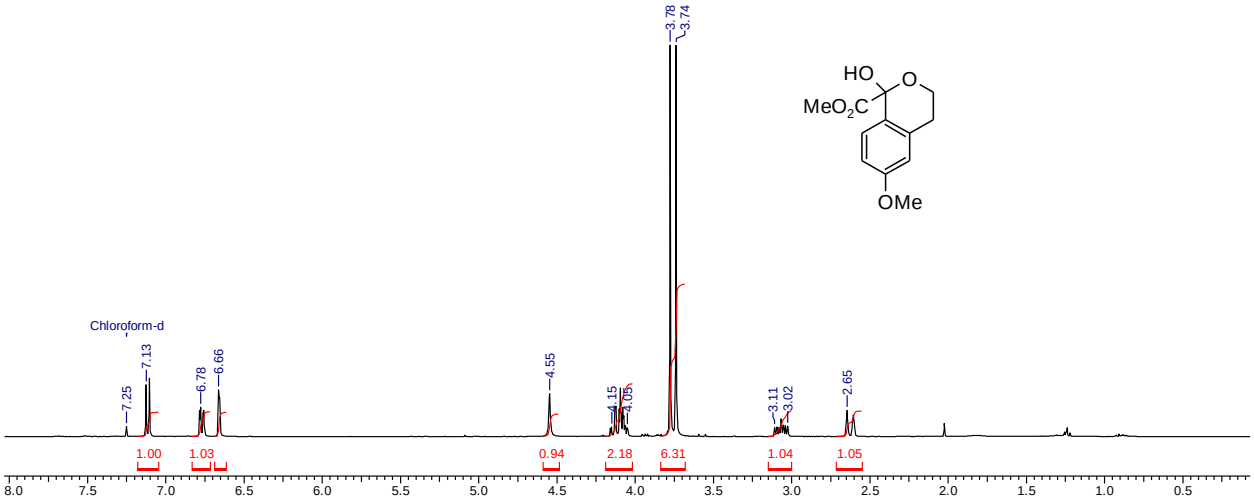
HO
O
MeO2C
OMe
Chloroform-d
7.25
7.13
6.78
6.66
4.55
4.15
4.05
3.78
3.74
3.11
3.02
2.65
1.00
1.03
0.94
2.18
6.31
1.04
1.05

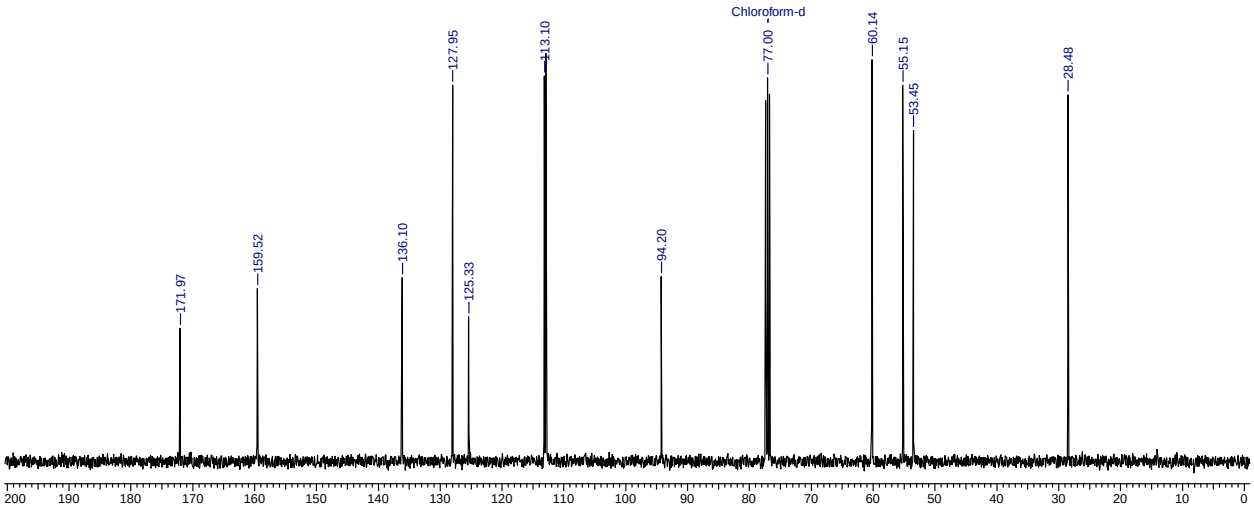
Chloroform-d
171.97
159.52
136.10
127.95
125.33
113.10
94.20
77.00
60.14
55.15
53.45
28.48

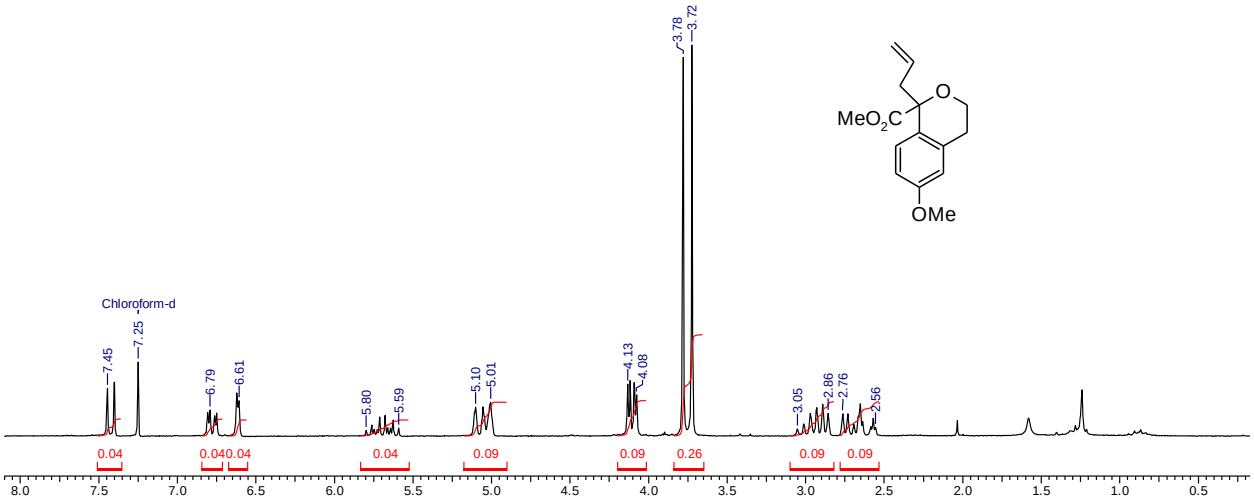
3.78
3.72
MeO2C
O
OMe
Chloroform-d
7.45
7.25
6.79
6.61
5.80
5.59
5.10
5.01
4.13
4.08
3.05
2.86
2.76
2.56
0.04
0.04
0.04
0.04
0.09
0.09
0.26
0.09
0.09

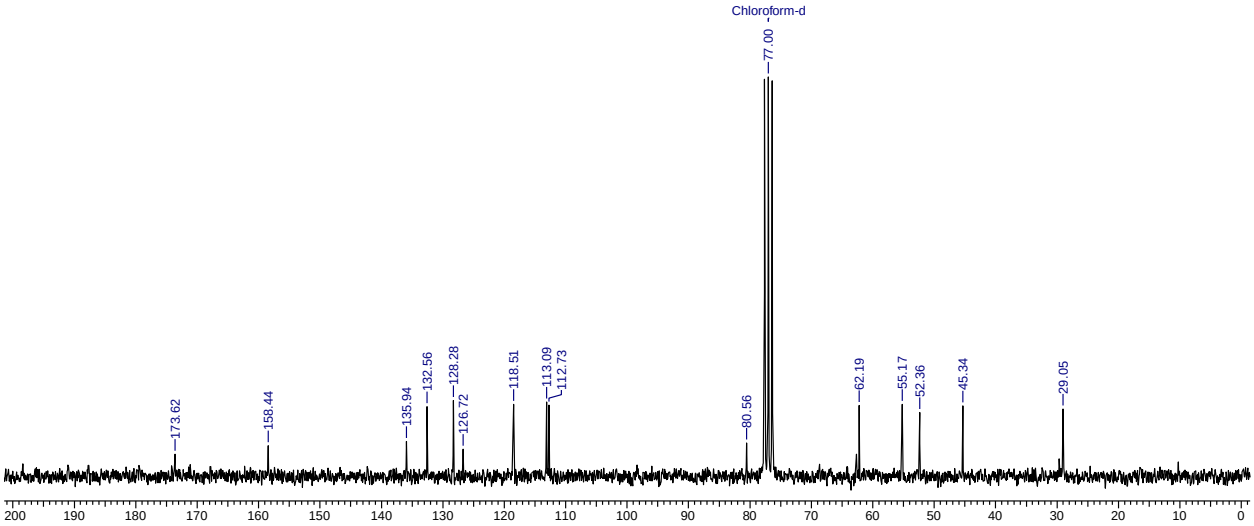
Chloroform-d
77.00
173.62
158.44
135.94
132.56
128.28
126.72
118.51
113.09
112.73
80.56
62.19
55.17
52.36
45.34
29.05

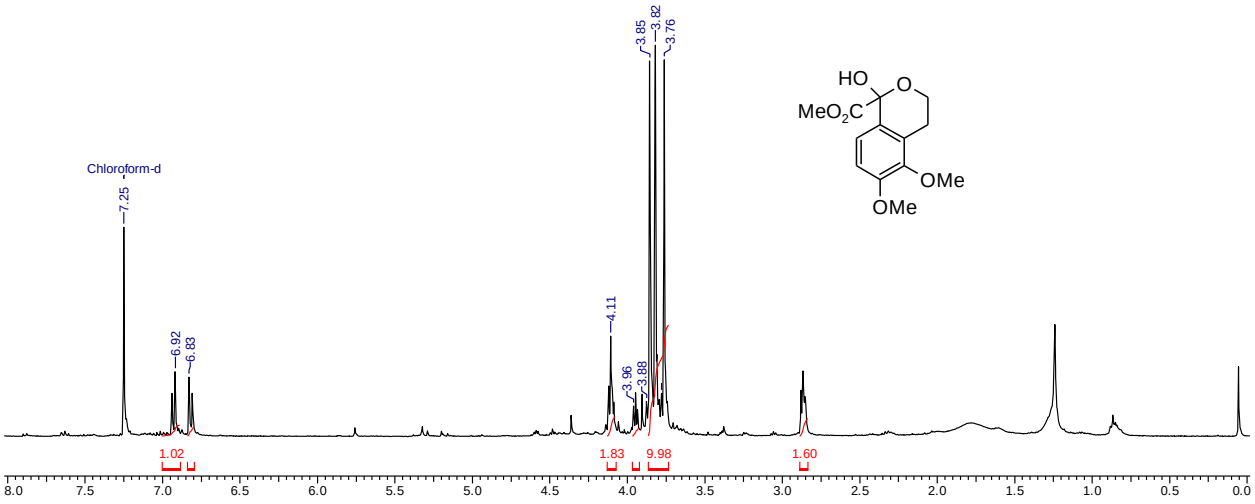
Chloroform-d
7.25
6.92
6.83
4.11
3.96
3.88
3.85
3.82
3.76
HO
O
MeO2C
OMe
OMe
1.02
1.83
9.98
1.60

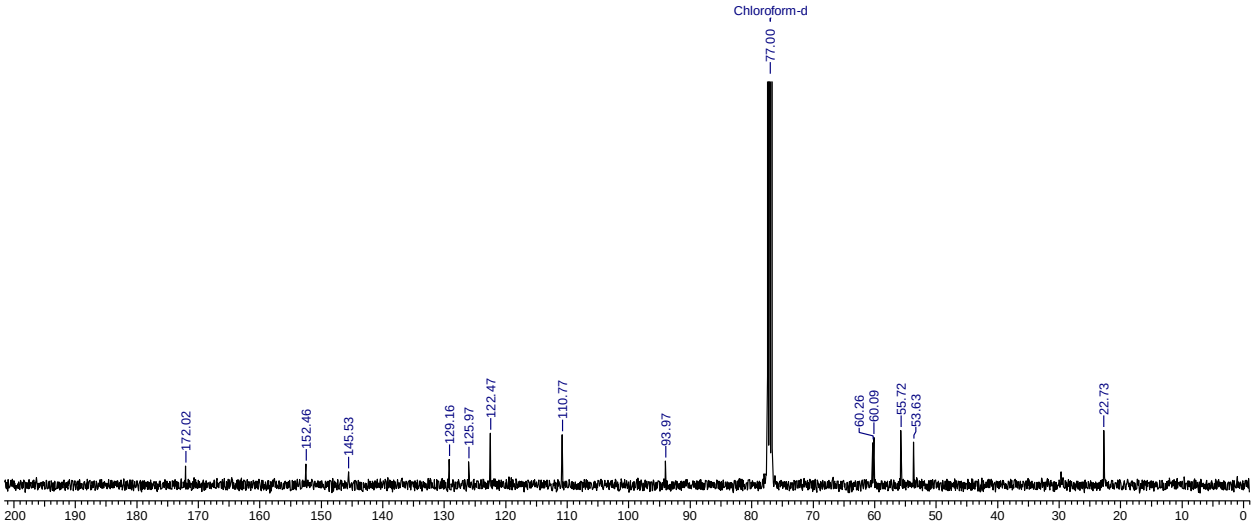
Chloroform-d
77.00
172.02
152.46
145.53
129.16
125.97
122.47
110.77
93.97
60.26
60.09
55.72
53.63
22.73

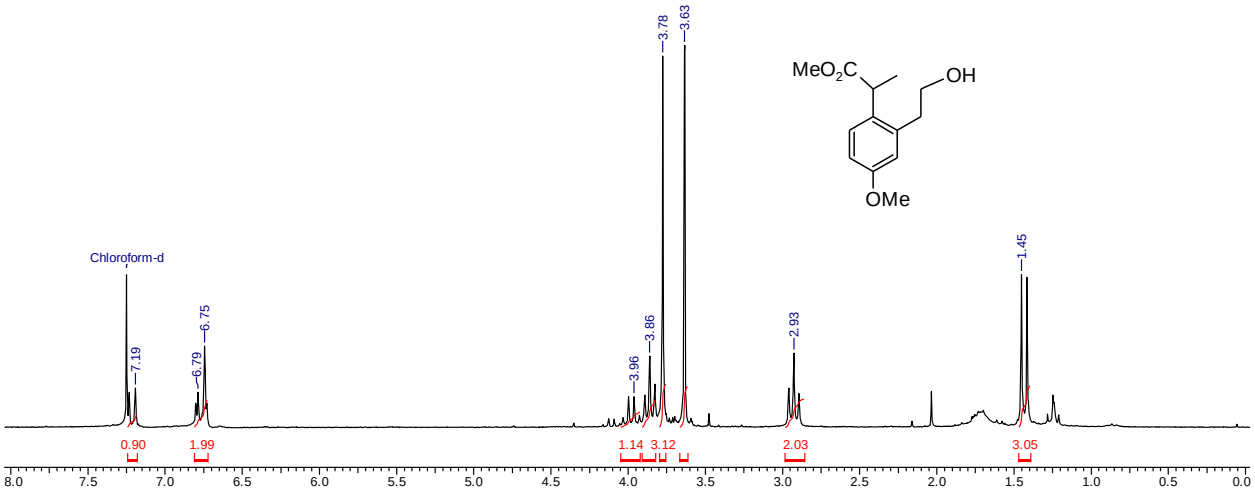
MeO2C
OH
OMe
Chloroform-d
7.19
6.79
6.75
3.96
3.86
3.78
3.63
2.93
1.45
0.90
1.99
1.14
3.12
2.03
3.05
8.0
7.5
7.0
6.5
6.0
5.5
5.0
4.5
4.0
3.5
3.0
2.5
2.0
1.5
1.0
0.5
0.0

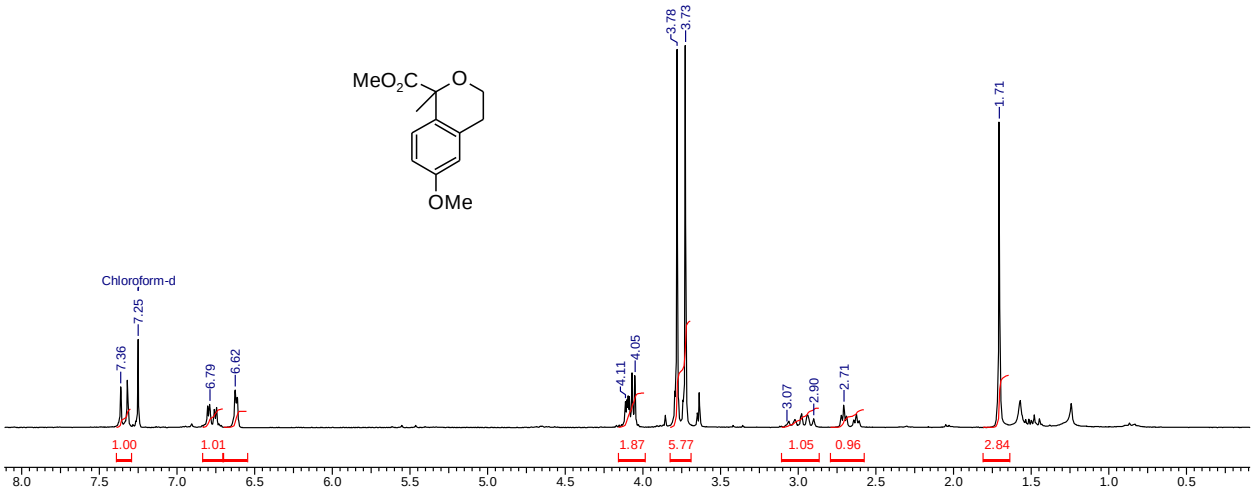
MeO2C
O
OMe
Chloroform-d
7.36
7.25
6.79
6.62
4.11
4.05
3.78
3.73
3.07
2.90
2.71
1.71
1.00
1.01
1.87
5.77
1.05
0.96
2.84

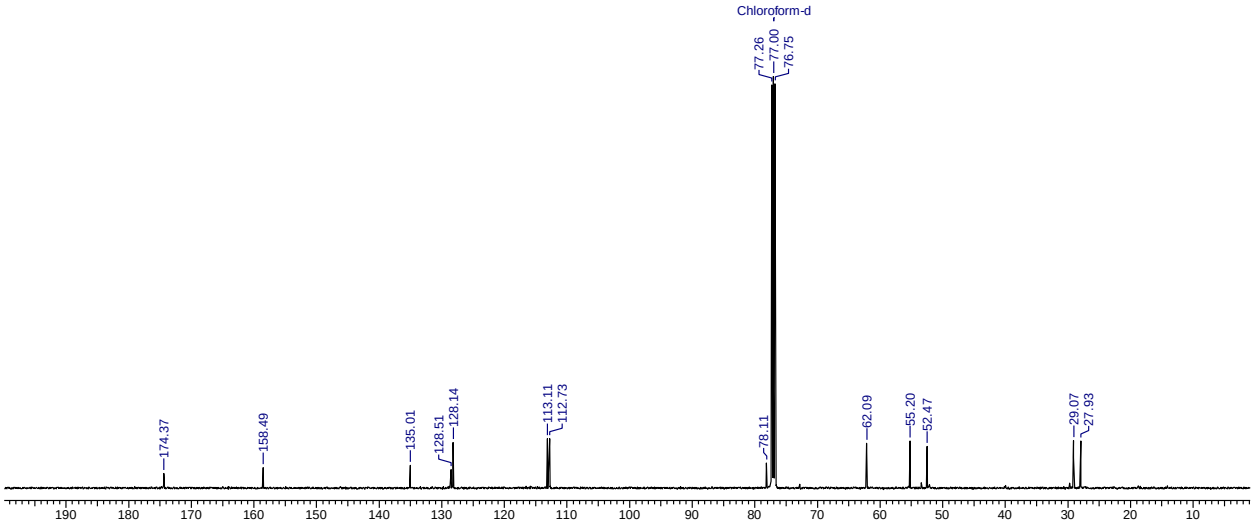
Chloroform-d
77.26
77.00
76.75
174.37
158.49
135.01
128.51
128.14
113.11
112.73
78.11
62.09
55.20
52.47
29.07
27.93

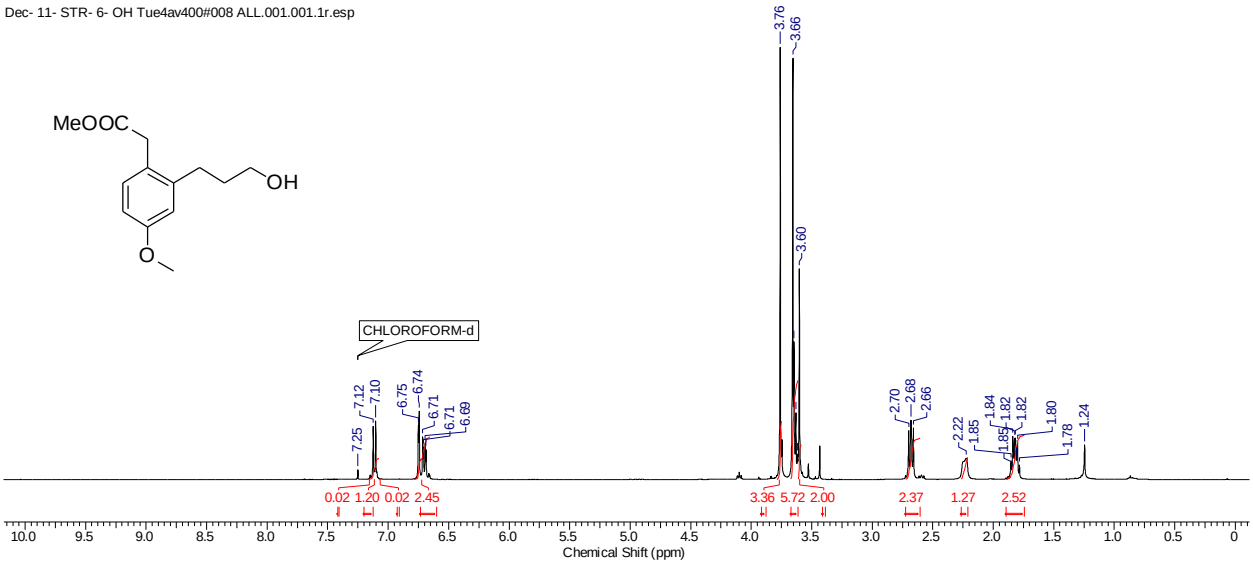
Dec- 11- STR- 6- OH Tue4av400#008 ALL.001.001.1r.esp
MeOOC
OH
O
CHLOROFORM-d
7.25
7.12
7.10
6.75
6.74
6.71
6.71
6.69
3.76
3.66
3.60
2.70
2.68
2.66
2.22
1.85
1.84
1.82
1.82
1.80
1.78
1.24
0.02 1.20 0.02 2.45
3.36 5.72 2.00
2.37
1.27
2.52
Chemical Shift (ppm)

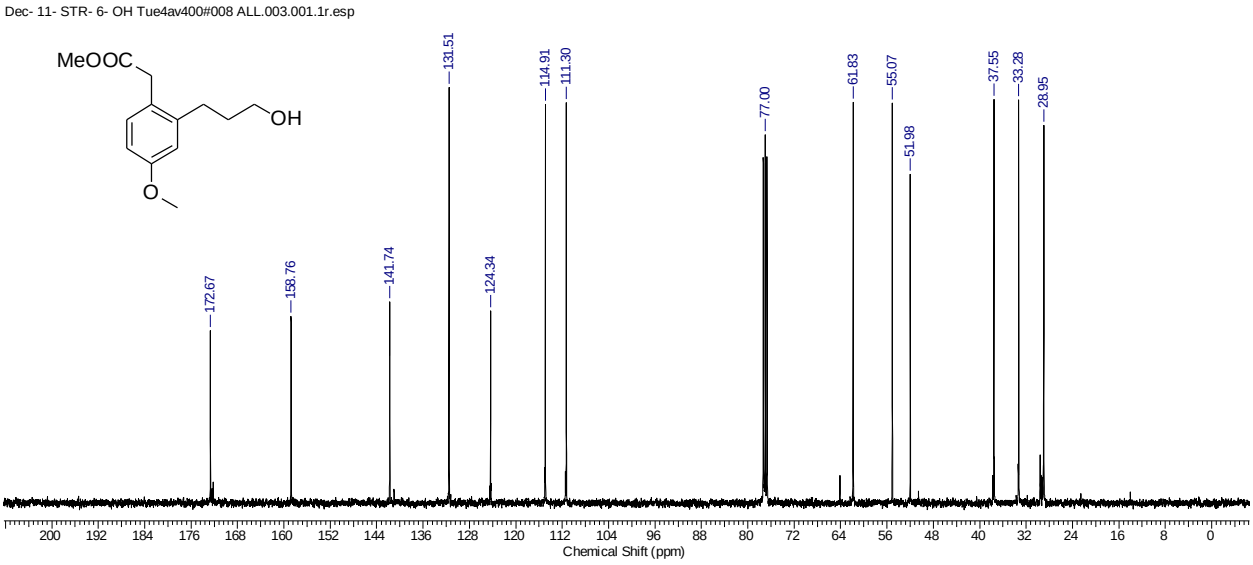
Dec- 11- STR- 6- OH Tue4av400#008 ALL.003.001.1r.esp
MeOOC
OH
O
172.67
158.76
141.74
131.51
124.34
114.91
111.30
77.00
61.83
55.07
51.98
37.55
33.28
28.95
Chemical Shift (ppm)

27 Dec 2012

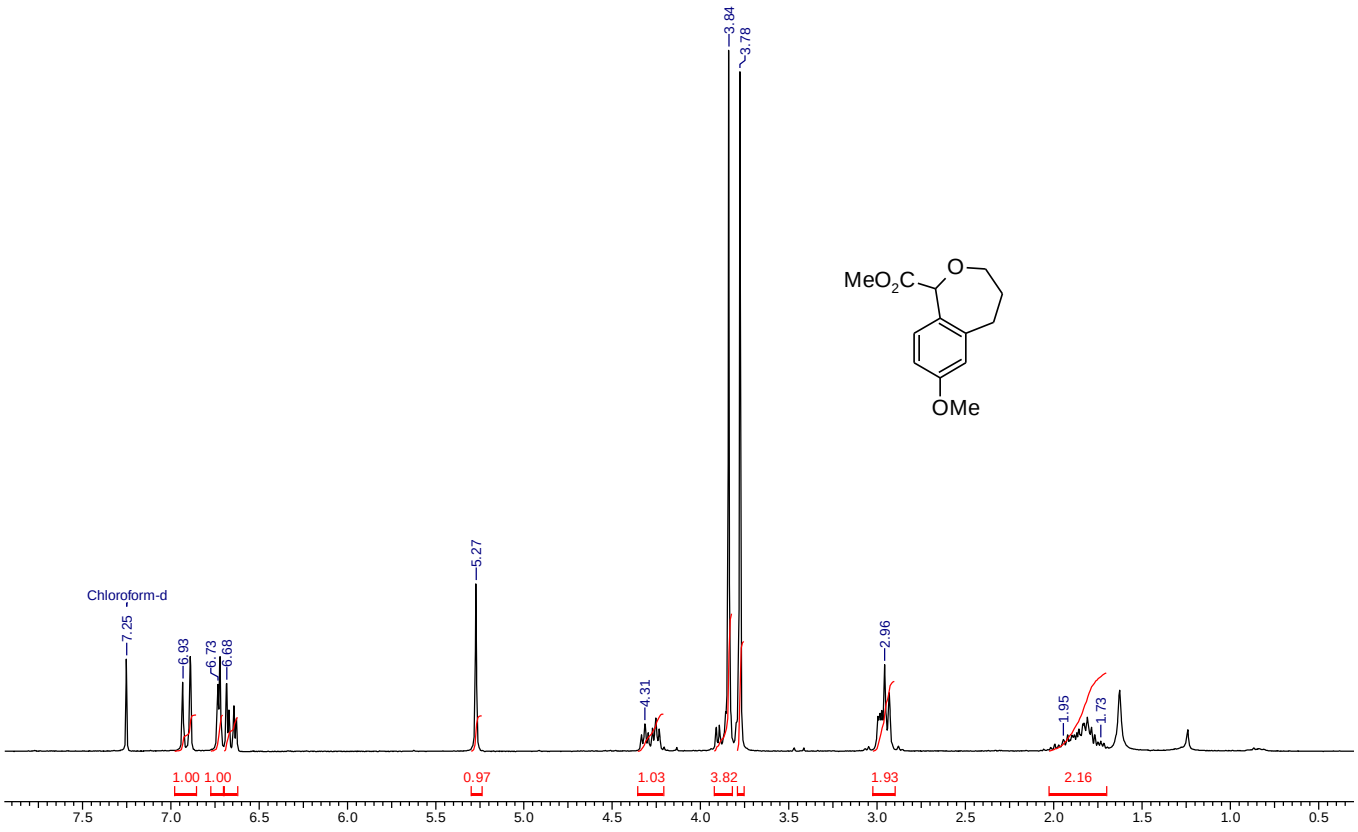
3.84
3.78
MeO2C
O
OMe
Chloroform-d
7.25
6.93
6.73
6.68
5.27
4.31
2.96
1.95
1.73
1.00 1.00
0.97
1.03
3.82
1.93
2.16
7.5
7.0
6.5
6.0
5.5
5.0
4.5
4.0
3.5
3.0
2.5
2.0
1.5
1.0
0.5

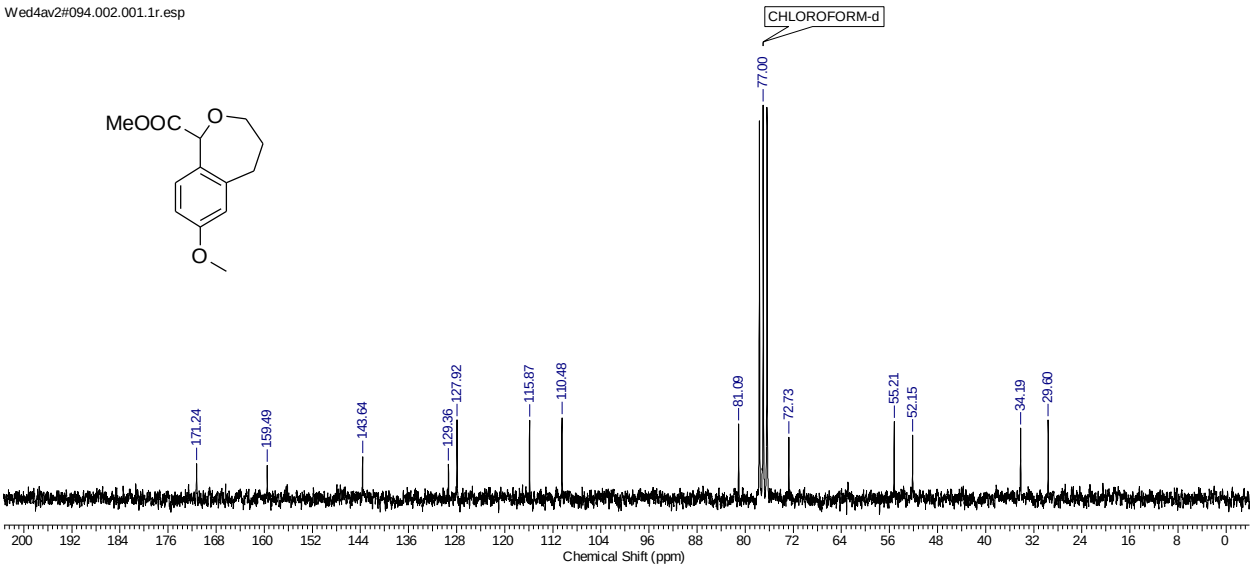
Wed4av2#094.002.001.1r.esp
CHLOROFORM-d
77.00
MeOOC
O
O
171.24
159.49
143.64
129.36
127.92
115.87
110.48
81.09
72.73
55.21
52.15
34.19
29.60
200
192
184
176
168
160
152
144
136
128
120
112
104
96
88
80
72
64
56
48
40
32
24
16
8
0
Chemical Shift (ppm)

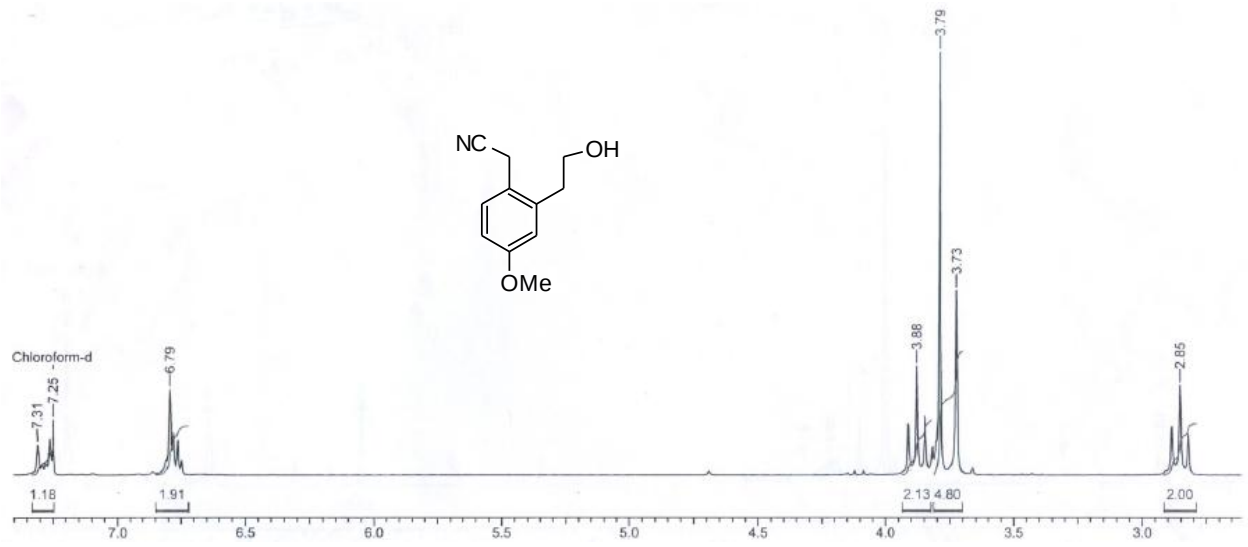
NC
OH
OMe
Chloroform-d
7.31
7.25
6.79
3.88
3.79
3.73
2.85
1.18
1.91
2.13
4.80
2.00
7.0
6.5
6.0
5.5
5.0
4.5
4.0
3.5
3.0

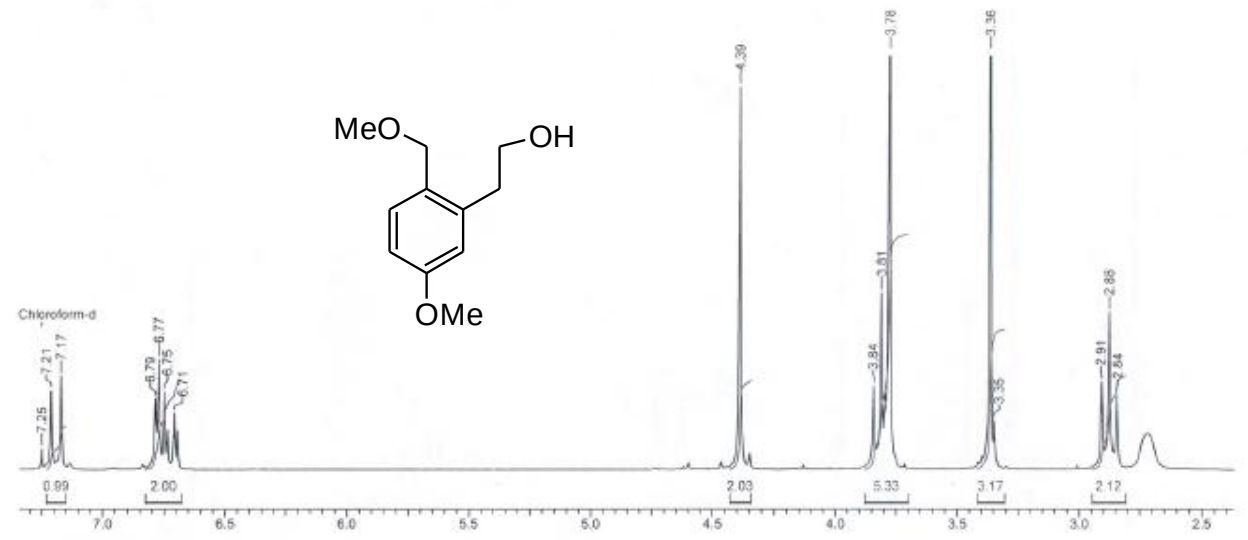
MeO
OH
OMe
Chloroform-d
7.25
7.21
7.17
6.79
6.77
6.75
6.71
4.39
3.84
3.81
3.78
3.36
3.35
2.91
2.86
2.84
0.99
2.00
2.03
5.33
3.17
2.12
7.0
6.5
6.0
5.5
5.0
4.5
4.0
3.5
3.0
2.5

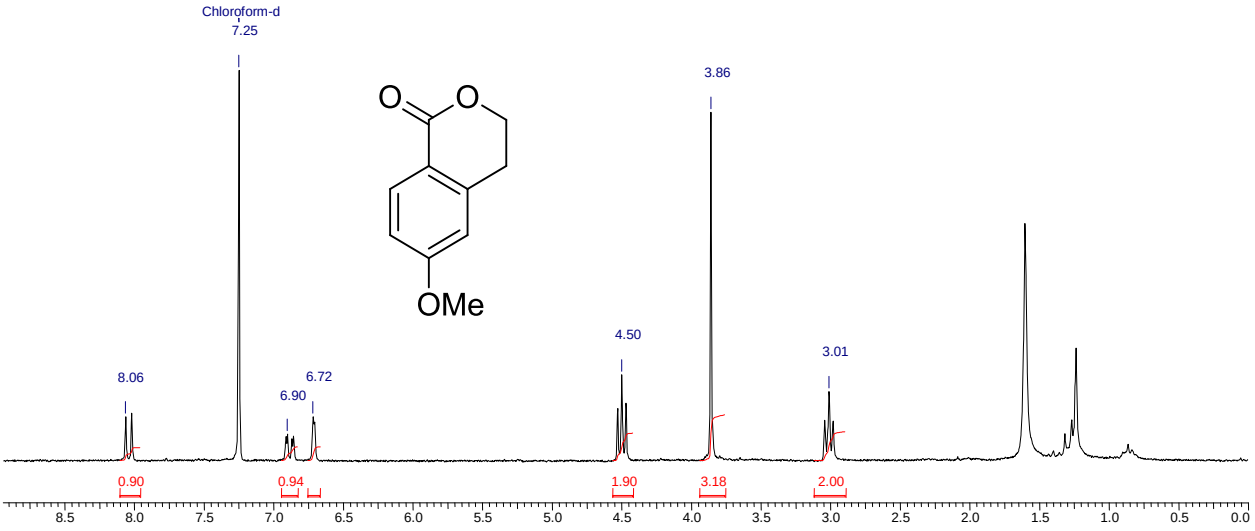
Chloroform-d
7.25
O
O
OMe
3.86
4.50
3.01
8.06
6.72
6.90
0.90
0.94
1.90
3.18
2.00
8.5
8.0
7.5
7.0
6.5
6.0
5.5
5.0
4.5
4.0
3.5
3.0
2.5
2.0
1.5
1.0
0.5
0.0

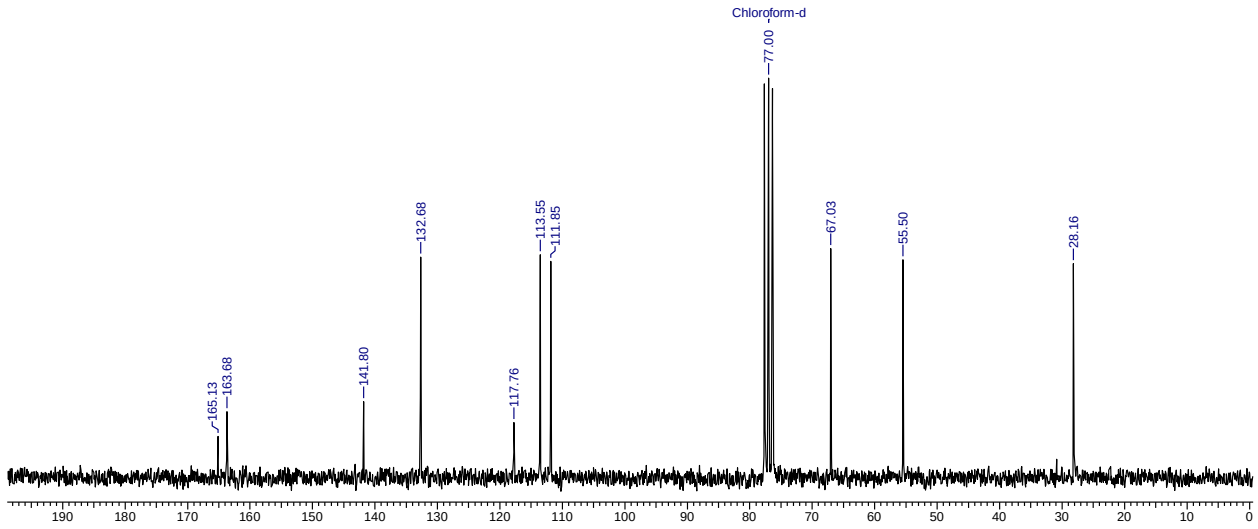
Chloroform-d
77.00
132.68
113.55
111.85
67.03
55.50
28.16
165.13
163.68
141.80
117.76
190
180
170
160
150
140
130
120
110
100
90
80
70
60
50
40
30
20
10
0

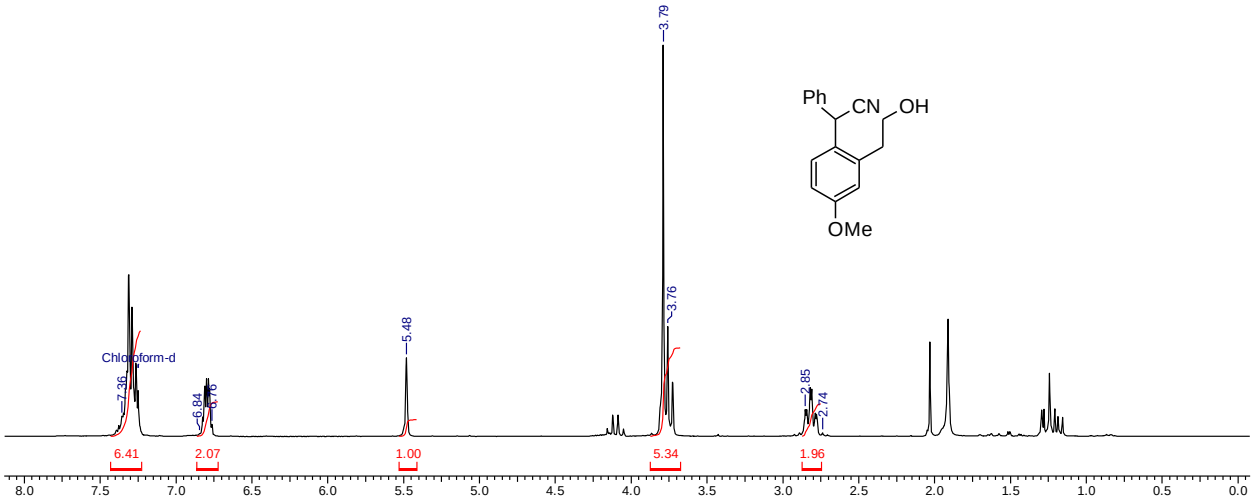
Ph
CN
OH
OMe
Chloroform-d
7.36
6.84
6.76
5.48
3.79
3.76
2.85
2.74
6.41
2.07
1.00
5.34
1.96

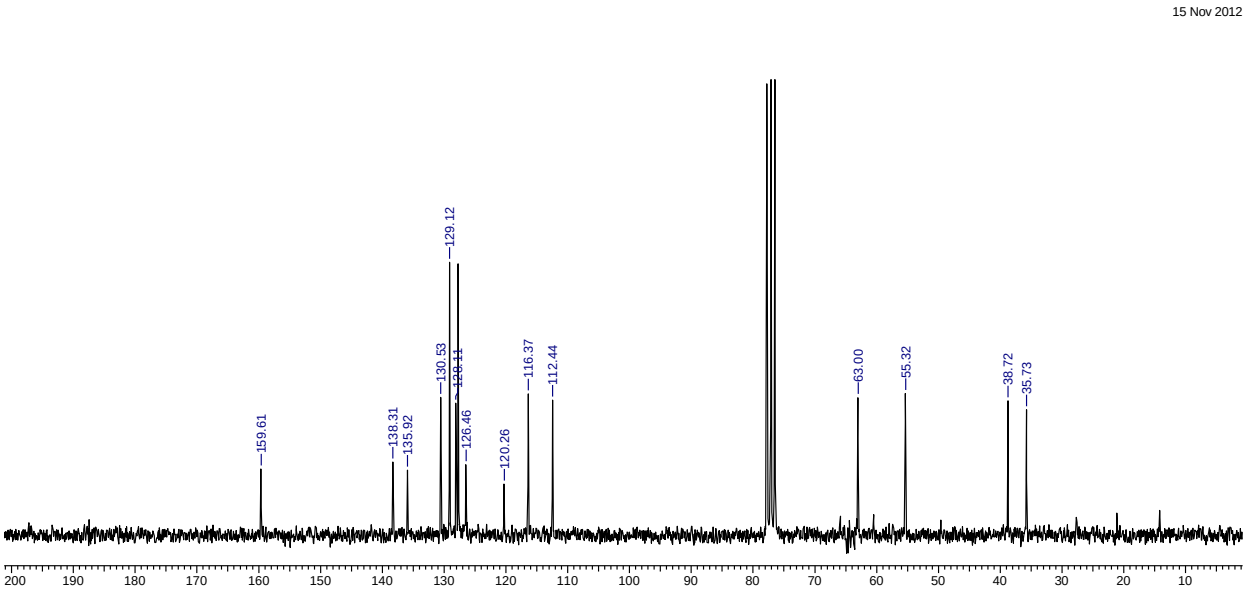
15 Nov 2012
159.61
138.31
135.92
130.53
129.12
128.11
126.46
120.26
116.37
112.44
63.00
55.32
38.72
35.73

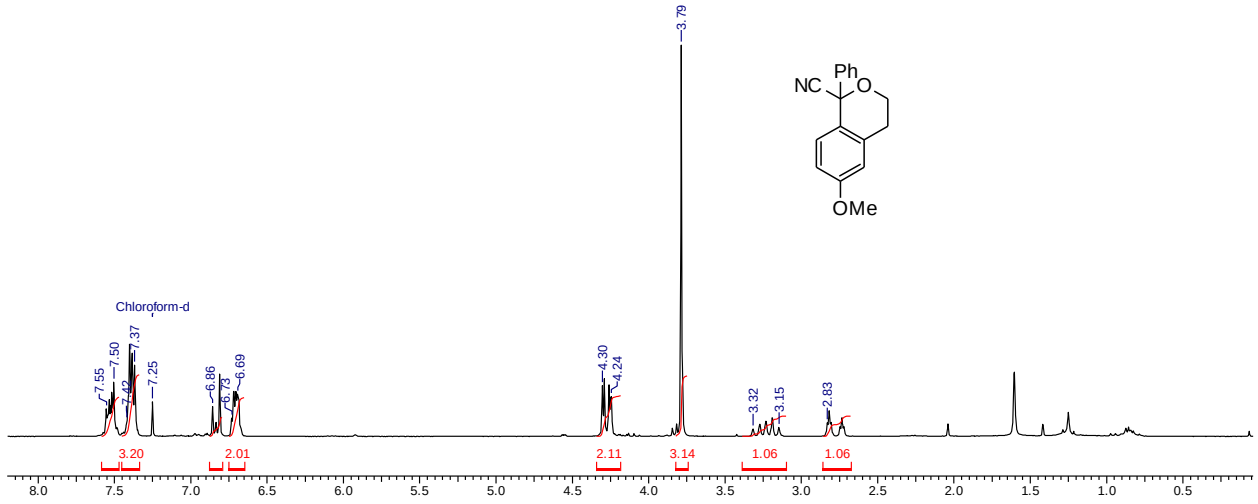
3.79
Ph
NC
O
OMe
Chloroform-d
7.55
7.50
7.37
7.42
7.25
6.86
6.73
6.69
4.30
4.24
3.32
3.15
2.83
3.20
2.01
2.11
3.14
1.06
1.06

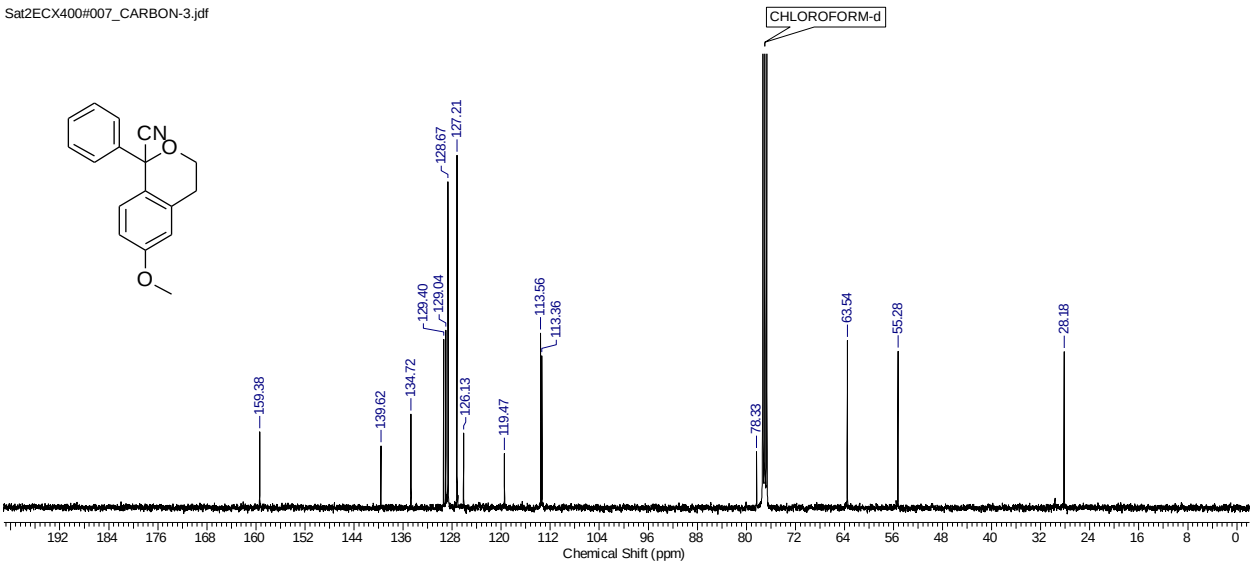
Sat2ECX400#007_CARBON-3.jdf
CHLOROFORM-d
CN
O
O
159.38
139.62
134.72
129.40
129.04
128.67
127.21
126.13
119.47
113.56
113.36
78.33
63.54
55.28
28.18
Chemical Shift (ppm)

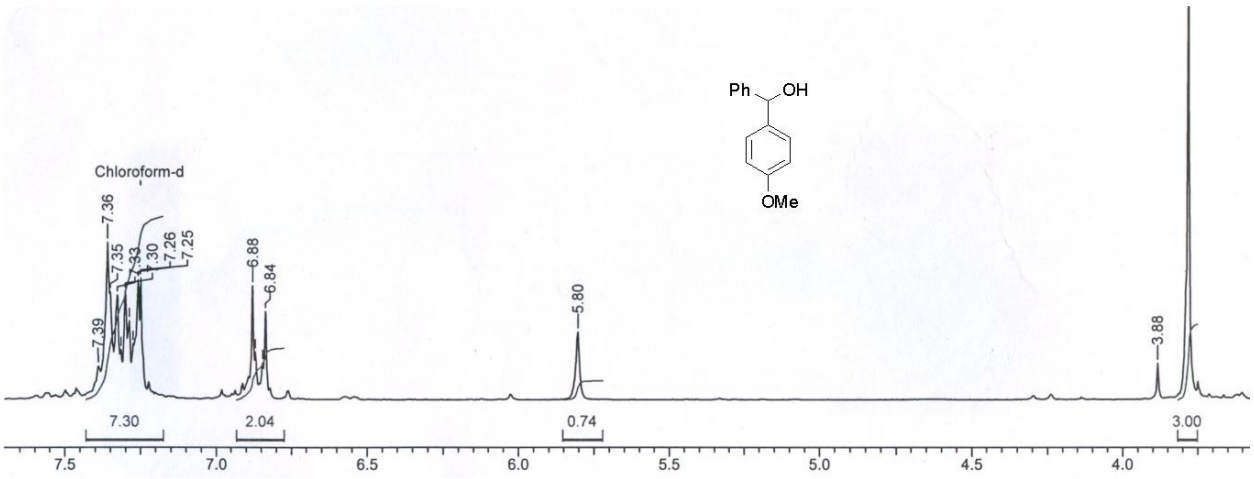
Ph
OH
OMe
Chloroform-d
7.36
7.35
7.33
7.30
7.26
7.25
7.39
6.88
6.84
5.80
3.88
7.30
2.04
0.74
3.00
7.5
7.0
6.5
6.0
5.5
5.0
4.5
4.0

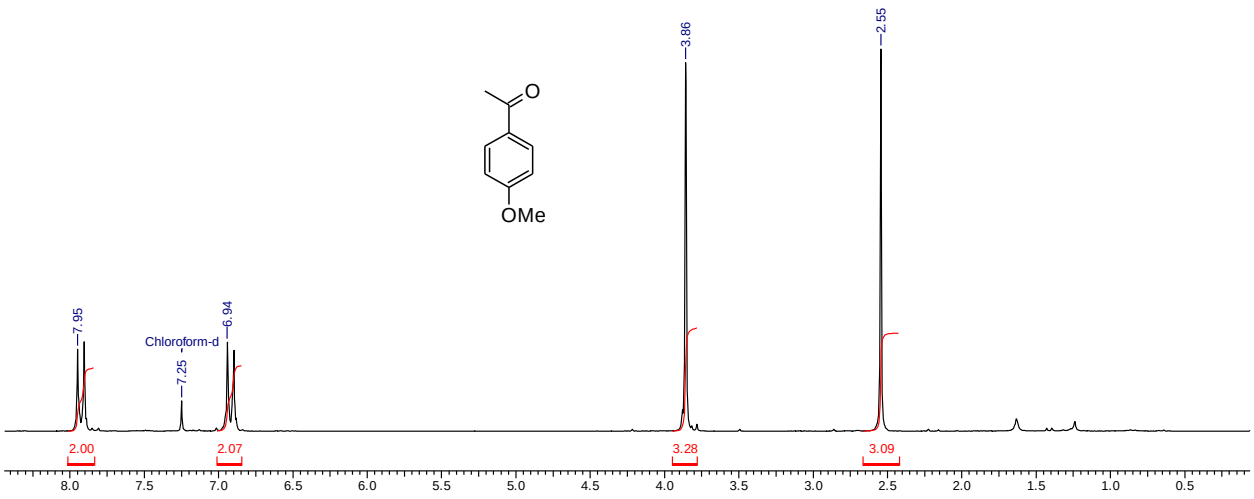
O
OMe
3.86
2.55
7.95
Chloroform-d
7.25
6.94
2.00
2.07
3.28
3.09
8.0
7.5
7.0
6.5
6.0
5.5
5.0
4.5
4.0
3.5
3.0
2.5
2.0
1.5
1.0
0.5

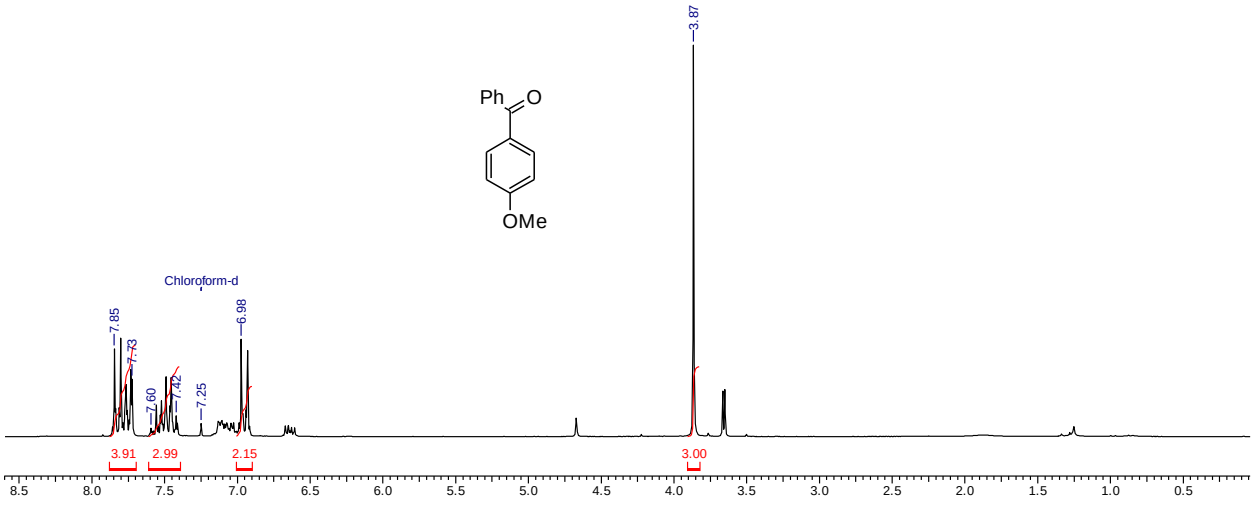
3.87
Ph
O
OMe
Chloroform-d
7.85
7.73
7.60
7.42
7.25
6.98
3.91
2.99
2.15
3.00
8.5
8.0
7.5
7.0
6.5
6.0
5.5
5.0
4.5
4.0
3.5
3.0
2.5
2.0
1.5
1.0
0.5

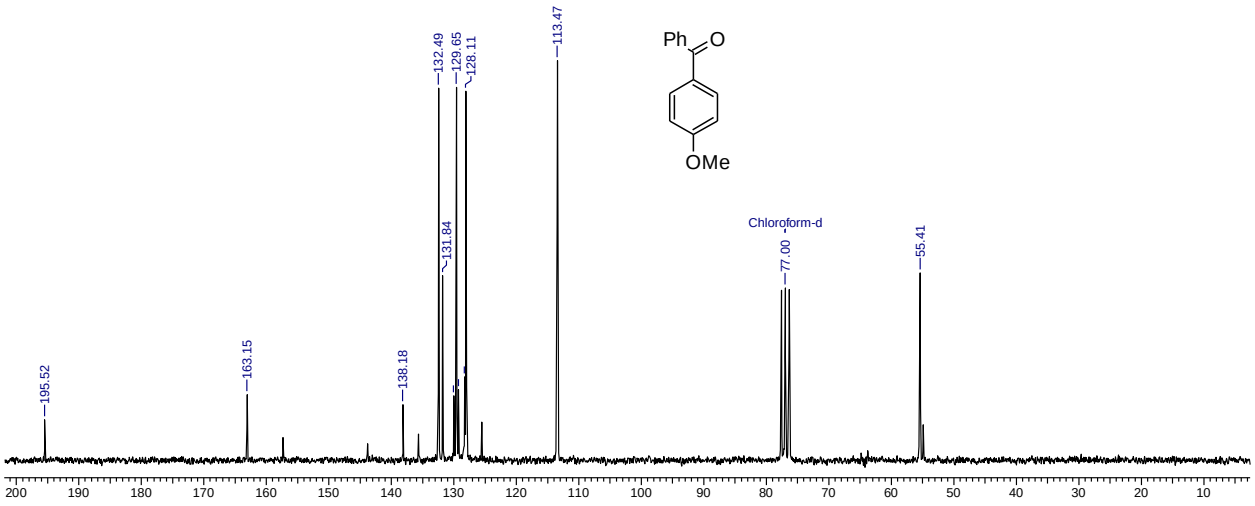
132.49
129.65
128.11
113.47
Ph
O
OMe
131.84
Chloroform-d
77.00
55.41
195.52
163.15
138.18
200
190
180
170
160
150
140
130
120
110
100
90
80
70
60
50
40
30
20
10

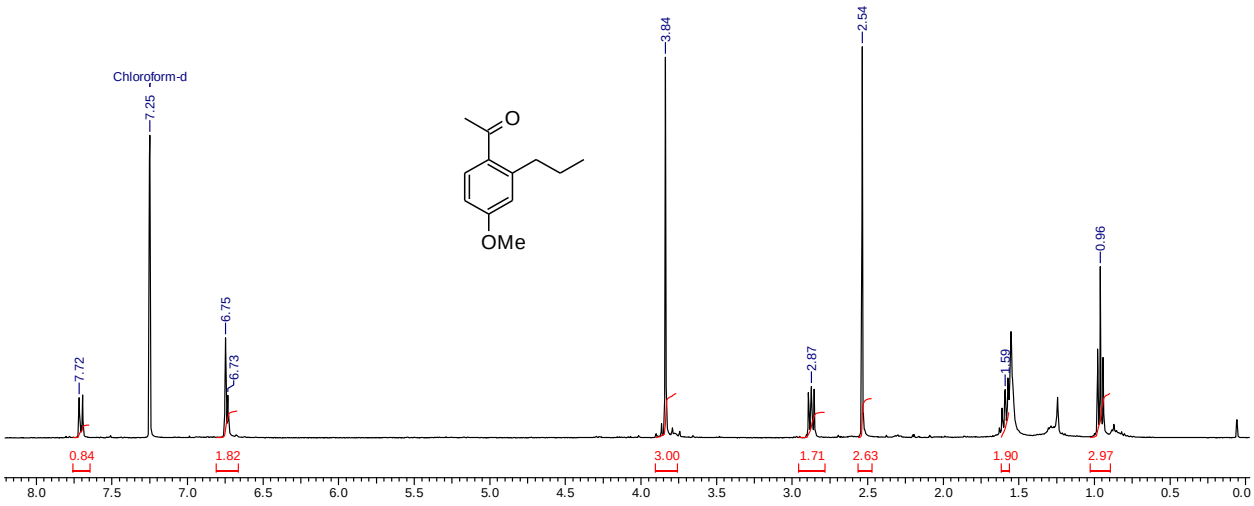
Chloroform-d
7.25
7.72
6.75
6.73
3.84
2.87
2.54
1.59
0.96
O
OMe
0.84
1.82
3.00
1.71
2.63
1.90
2.97
8.0
7.5
7.0
6.5
6.0
5.5
5.0
4.5
4.0
3.5
3.0
2.5
2.0
1.5
1.0
0.5
0.0

15 Nov 2012

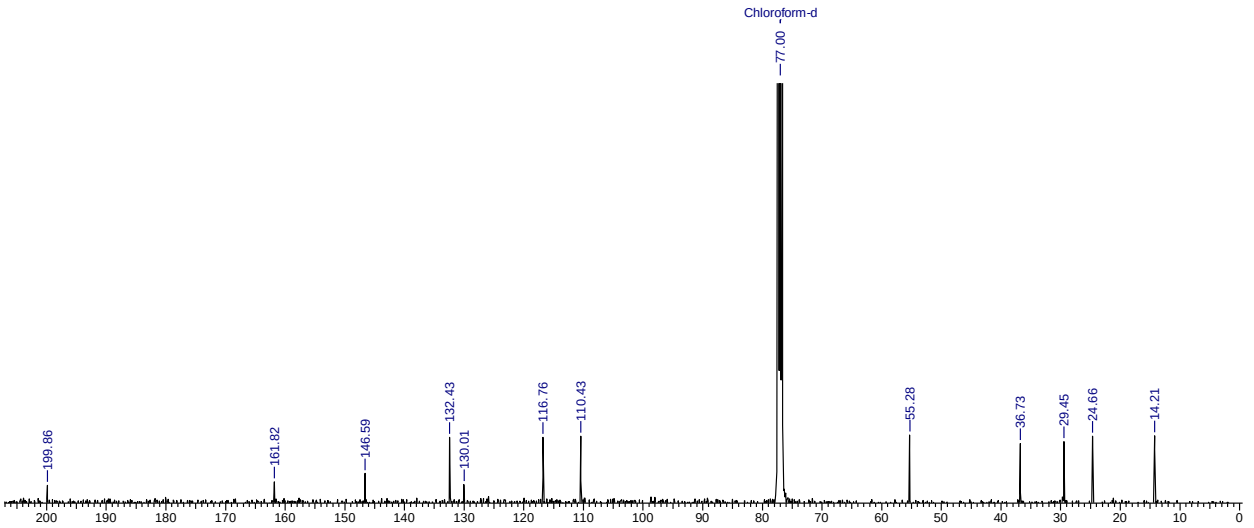
Chloroform-d
77.00
199.86
161.82
146.59
132.43
130.01
116.76
110.43
55.28
36.73
29.45
24.66
14.21
200
190
180
170
160
150
140
130
120
110
100
90
80
70
60
50
40
30
20
10
0

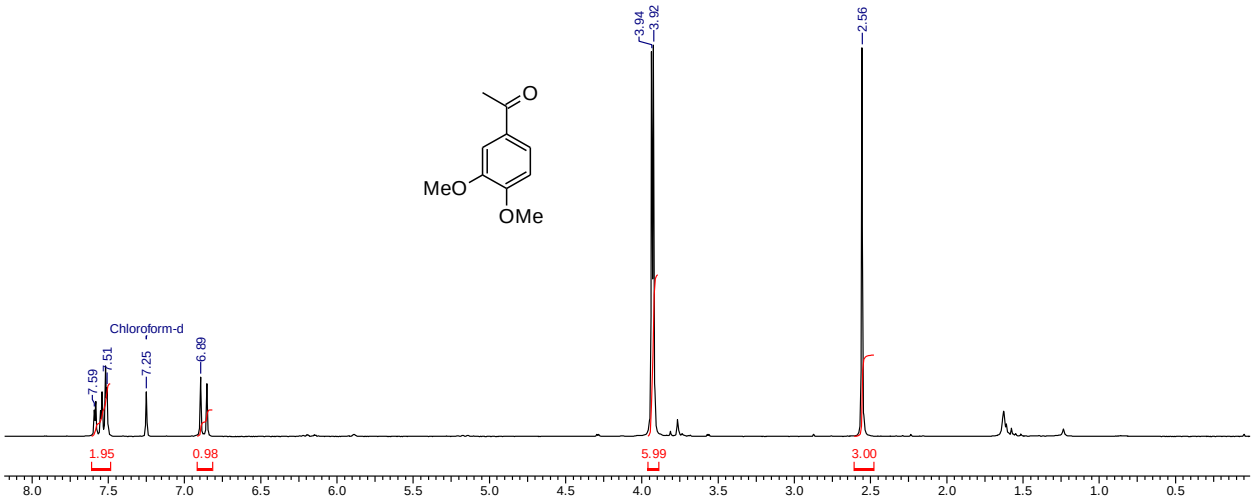
3.94
3.92
2.56
O
MeO
OMe
Chloroform-d
7.59
7.51
7.25
6.89
1.95
0.98
5.99
3.00
8.0
7.5
7.0
6.5
6.0
5.5
5.0
4.5
4.0
3.5
3.0
2.5
2.0
1.5
1.0
0.5

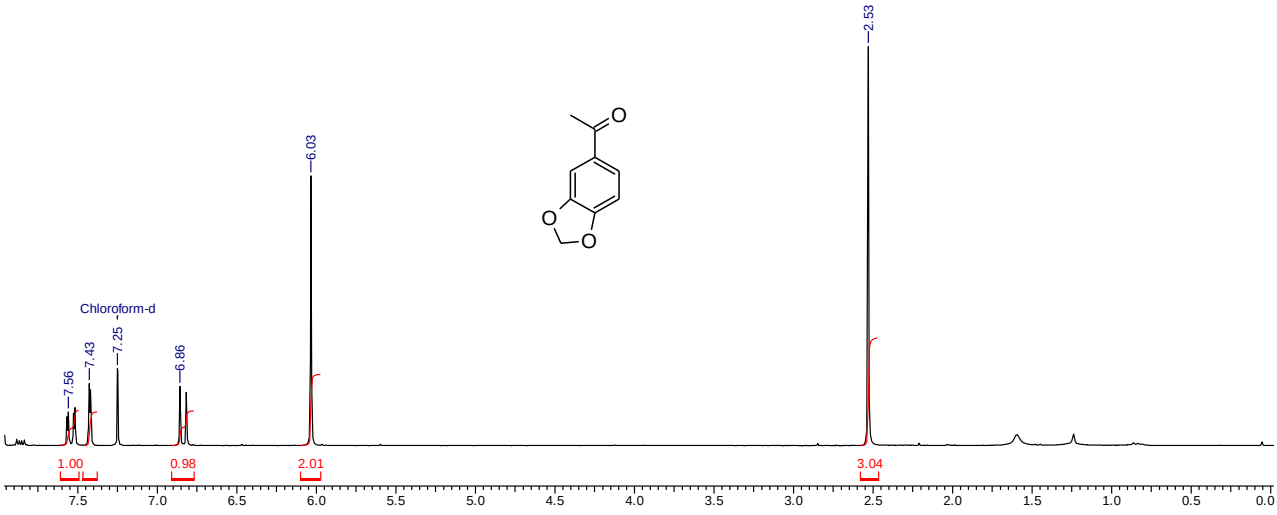
2.53
6.03
O
O
O
Chloroform-d
7.56
7.43
7.25
6.86
1.00
0.98
2.01
3.04
7.5
7.0
6.5
6.0
5.5
5.0
4.5
4.0
3.5
3.0
2.5
2.0
1.5
1.0
0.5
0.0

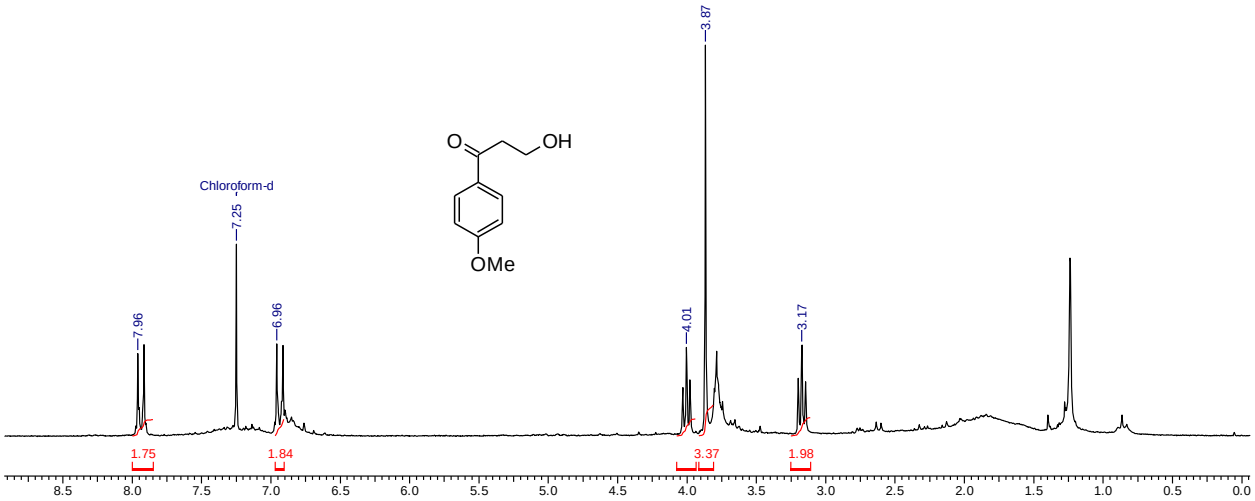
O
OH
OMe
Chloroform-d
7.25
3.87
7.96
6.96
4.01
3.17
1.75
1.84
3.37
1.98
8.5
8.0
7.5
7.0
6.5
6.0
5.5
5.0
4.5
4.0
3.5
3.0
2.5
2.0
1.5
1.0
0.5
0.0

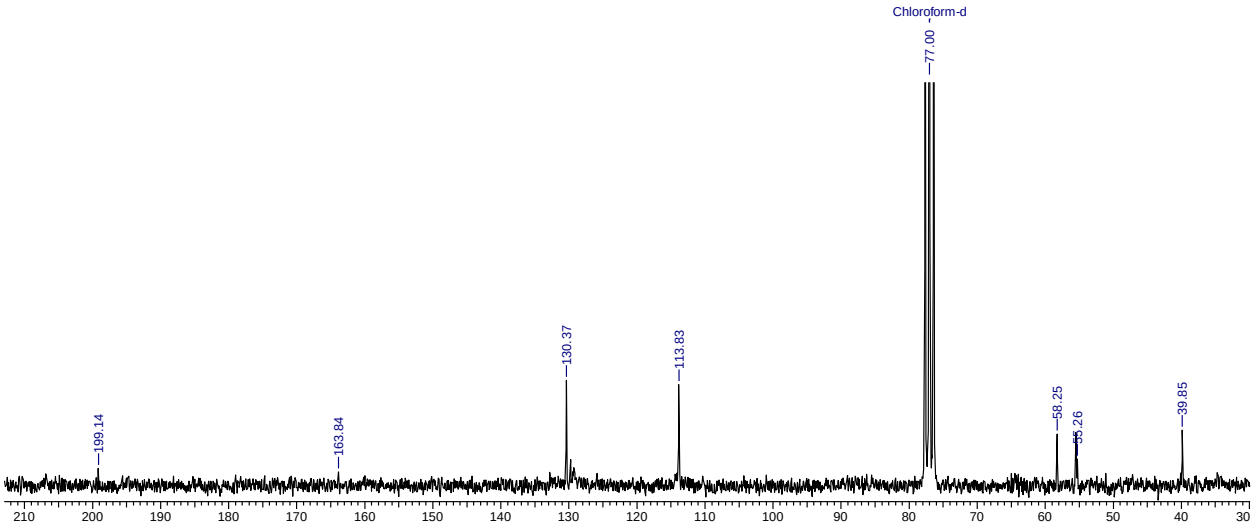
Chloroform-d
77.00
199.14
163.84
130.37
113.83
58.25
55.26
39.85
210
200
190
180
170
160
150
140
130
120
110
100
90
80
70
60
50
40
30

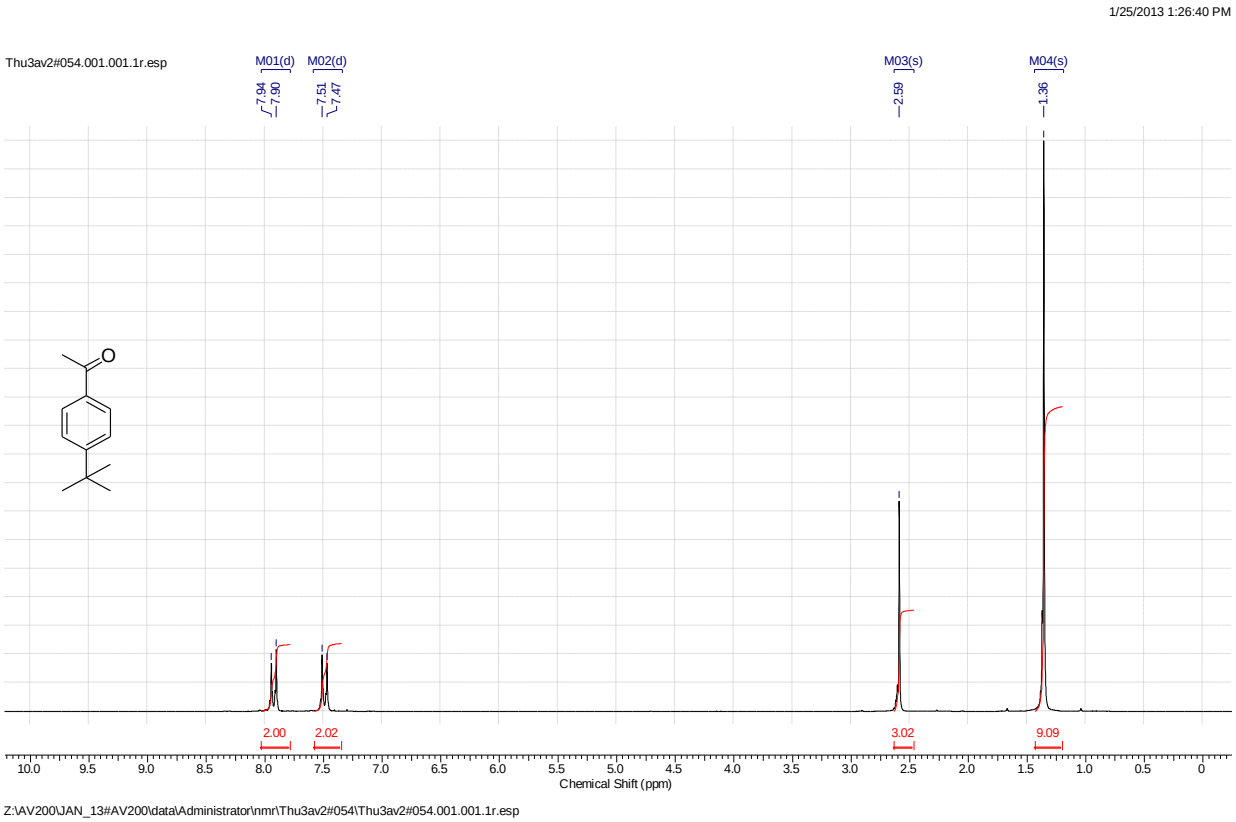
1/25/2013 1:26:40 PM
Thu3av2#054.001.001.1r.esp
M01(d)
M02(d)
M03(s)
M04(s)
7.94
7.90
7.51
7.47
2.59
1.36
O
2.00
2.02
3.02
9.09
10.0
9.5
9.0
8.5
8.0
7.5
7.0
6.5
6.0
5.5
5.0
4.5
4.0
3.5
3.0
2.5
2.0
1.5
1.0
0.5
0
Chemical Shift (ppm)
Z:\AV200\JAN_13#AV200\data\Administrator\nmr\Thu3av2#054\Thu3av2#054.001.001.1r.esp

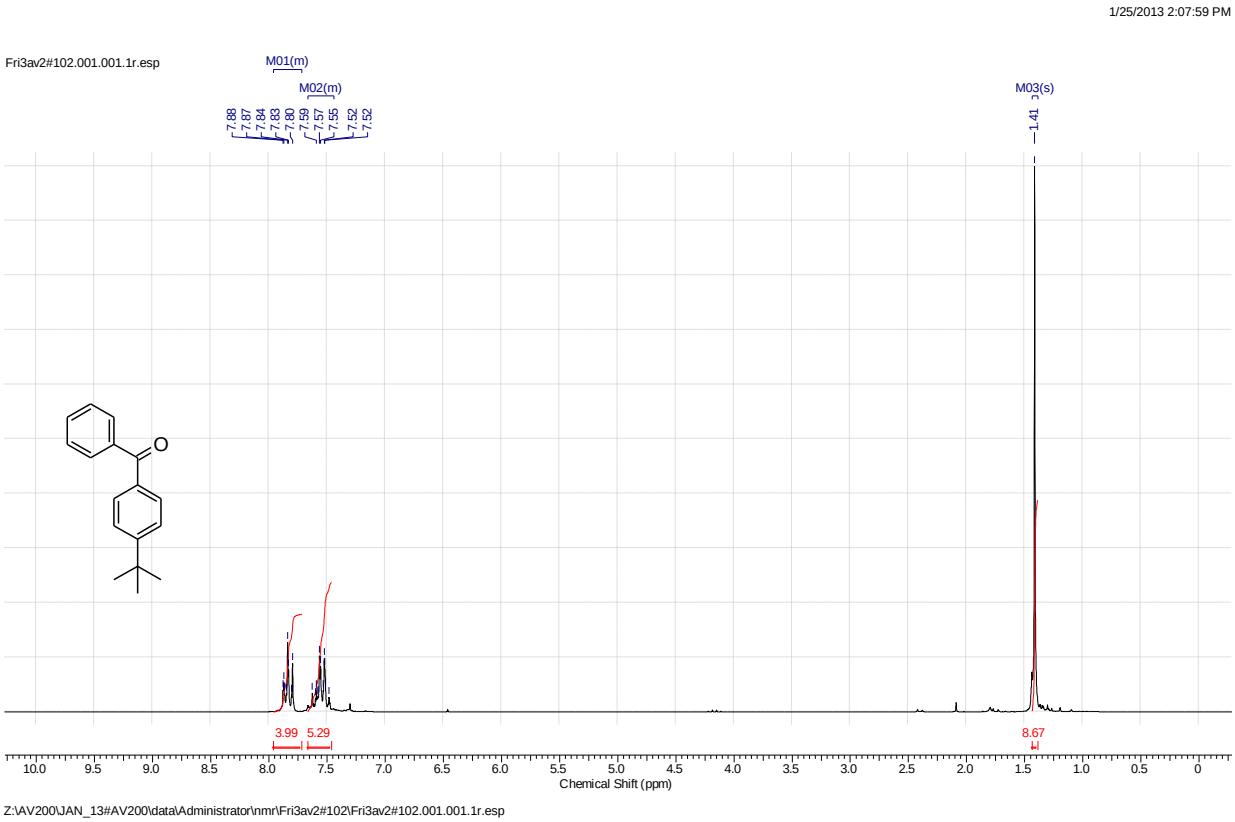
1/25/2013 2:07:59 PM
Fri3av2#102.001.001.1r.esp
M01(m)
M02(m)
M03(s)
7.88
7.87
7.84
7.83
7.80
7.59
7.57
7.55
7.52
7.52
1.41
O
3.99
5.29
8.67
10.0
9.5
9.0
8.5
8.0
7.5
7.0
6.5
6.0
5.5
5.0
4.5
4.0
3.5
3.0
2.5
2.0
1.5
1.0
0.5
0
Chemical Shift (ppm)
Z:\AV200\JAN_13#AV200\data\Administrator\nmr\Fri3av2#102\Fri3av2#102.001.001.1r.esp

CHAPTER 2

METAL FREE C – Si BOND ACTIVATION AND ITS SYNTHETIC APPLICATIONS

2.1 Introduction:

Radical cations often undergo loss of electrofugal group from positions either -α or -β to charged centers producing stabilized radical and cation species, as shown below (**Scheme 1**). The loss of electrofugal group depends on the structure of the radical ion and polarity of the solvents[1-2].

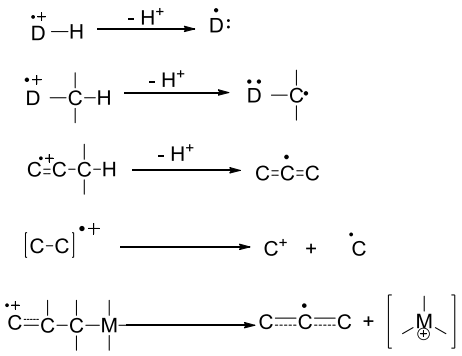

Scheme 1

Proceeding section would discuss few examples from literature to put the study presented in this Chapter in proper perspectives.

Carbon – carbon bond cleavage through radical cations

Pioneering work by Arnold *et al.*[3-4] have demonstrated that 2, 2-diphenyl ether (**1**) undergoes C–C bond cleavage via its corresponding radical cation **1**$^{\cdot+}$, effected by electron transfer to excited cyano-aromatics as shown in **Scheme 2**.

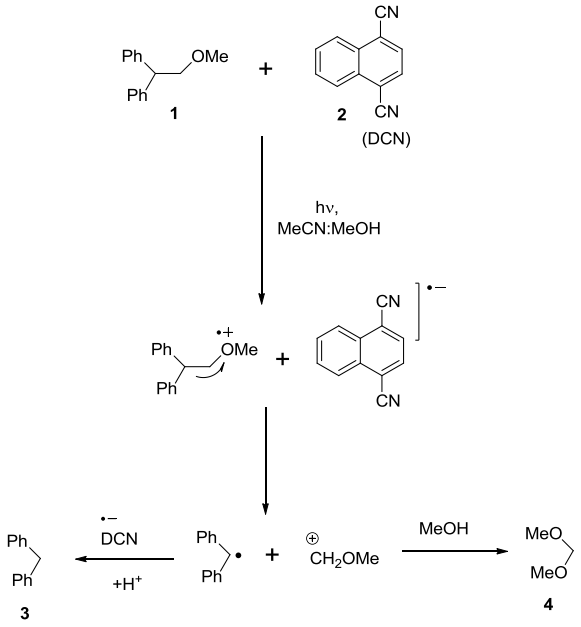

Scheme 2

Similar C–C cleavage of 1, 1, 2, 2-tetraphenylethane radical cation is also reported[5] (**Scheme 3**).

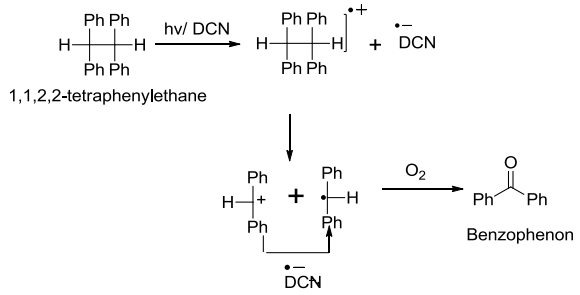

Scheme 3

In another study C–C bond cleavage of benzopinacols radical cation $\mathbf{5}^{+\cdot}$, produced by irradiating the CT-complex of **5** and chloranil (**6**), is also demonstrated[6] (**Scheme 4**).

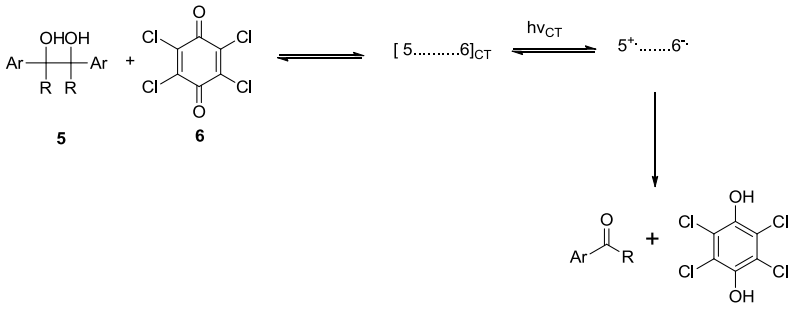

Scheme 4

Metal – Metal bond cleavage through radical cations

Similar to C–C bond cleavage, corresponding radical cations from 4A organometallics (M–M; M = M = Si, Sn, Ge) possessing low energy of ionization for M–M bond, is also reported[7] to undergo M–M bond dissociation. One of the early examples in this category may be found in the work of Sakurai *et al* [8] where dissociation of Si–Si bond is reported when CT complex between **7** and TCNE was irradiated in ESR cavity at room temperature.

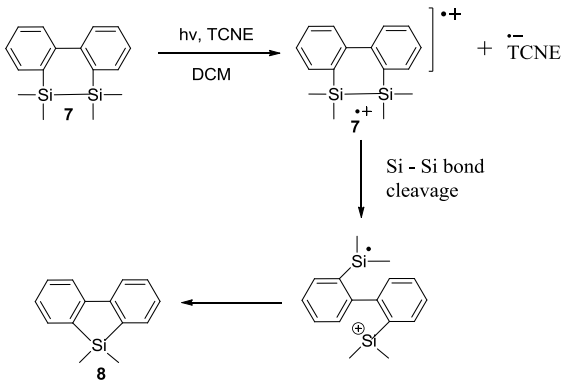

Scheme 5

Si-Si bond fragmentation of $Me_3Si\text{-}SiMe_3$ (**10**$^{\cdot+}$), generated by using 10-methyl acridinium ion (**9**, Acr H^+) excited state as NAD^+ analogue is also demonstrated[9] as described in **Scheme 6**.

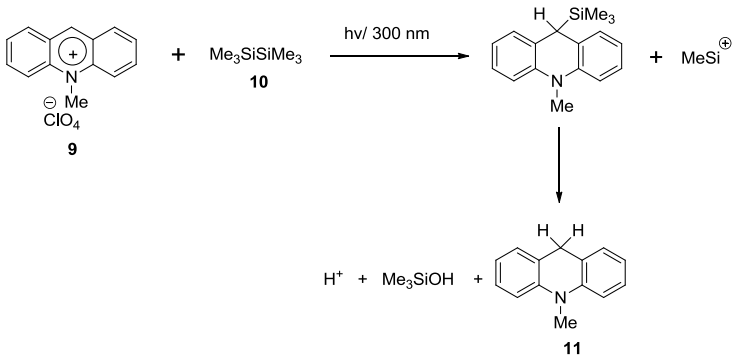

Scheme 6

Similar dissociation was noticed in Se–Se bond cleavage from corresponding $PhSeSePh^{+\cdot}$ (**12**$^{+\cdot}$), leading to the formation of eletrophilic selenium species ($PhSe^+$), is also reported[10-11] (**Scheme 7)** from our group.

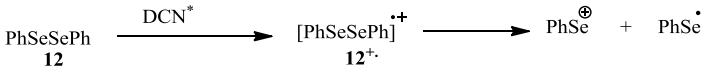

Scheme 7

Carbon-metal bond activation

It has been observed that radical cation formed after ionization on π-system which is stabilized by releasing σ- electron density to a deficient center (*i.e.***13**$^{\cdot+}$), undergoes eletrofugal loss of R_3M[12] (M= Si, Sn, Ge), as shown in **Scheme 8**.

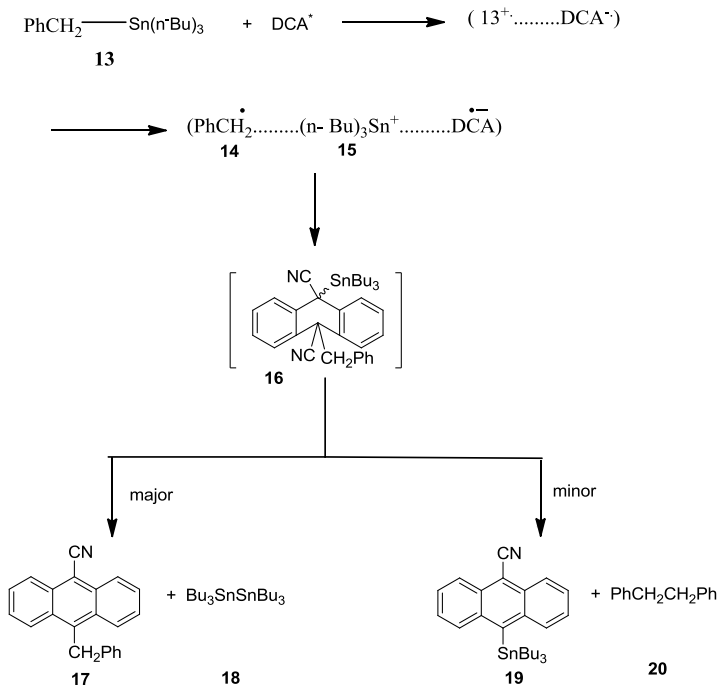

Scheme 8

Authors have explained that the formation of **16** is a direct consequence of recombination of **14** and **15** with $DCA^{-\cdot}$, after the fragmentation of $\mathbf{13}^{+\cdot}$ in the solvent cage.

Dissociation of C–Si bond from *α*-trimethylsilylamine radical cation $\mathbf{23}^{+\cdot}$, produced by single electron transfer from corresponding amine to excited state of enone **21**, is reported from Mariano's group[13] where α- amino radical coupled product **24** was isolated (**Scheme 9)**.

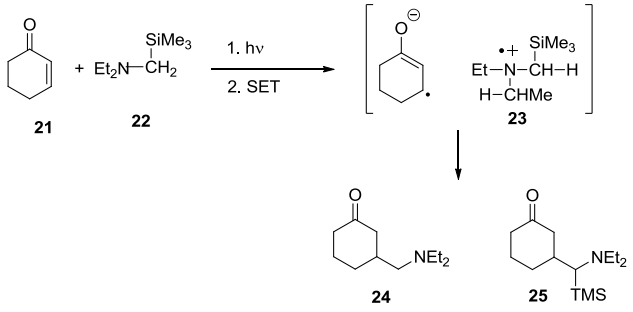

Scheme 9

The same group have also noticed that C–TMS *Vs* C–H bond dissociation from $\mathbf{23}^{\cdot+}$ depends on the polarity of the solvent. The application of this observation is shown by synthesizing few alkaloids[14].

However, since Padwa's group[15] had failed to cyclize *α*-amine radicals **36**, generated through conventional cleavage of C-Se bond *α*-to nitrogen by tributyltin hydide (**Scheme 10**), the Mariano's[13] hypothesis of involvement of free α-amino radical, owing to the electronic assistance of the amino nitrogen to radical, in his reaction demanded further research.

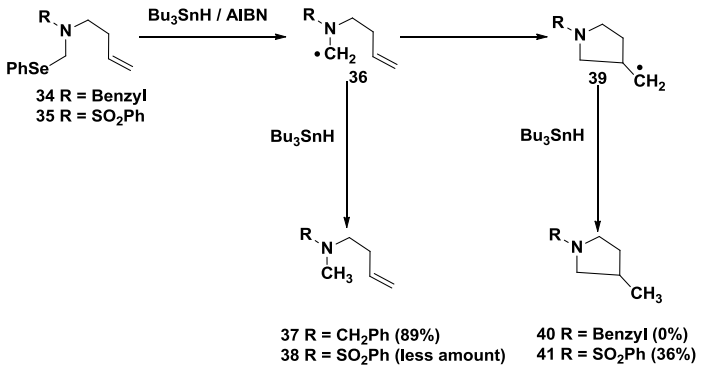

Scheme 10

In this context, our group reported[16-18] that *α*-silyltrimethylamine radical cation intermediate **44**, generated by SET from **42** to an excited 1, 4-dicyanonapthalene (DCN) in high polar solvent (like acetonitrile, *iso*-propanol) follows a concerted process of elimination of TMS group and simultaneous cyclization to produce **46** in excellent yield (**Scheme 11**).

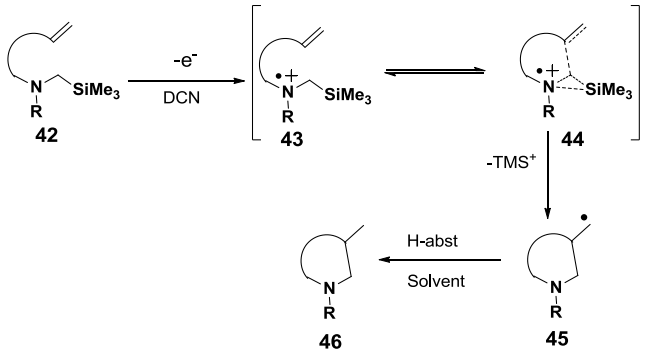

Scheme 11

Thus, this methodology was recognized as useful strategy for constructing of nitrogen containing heterocyclic moiety employing a photoredox cycle as shown in **Scheme 12**.

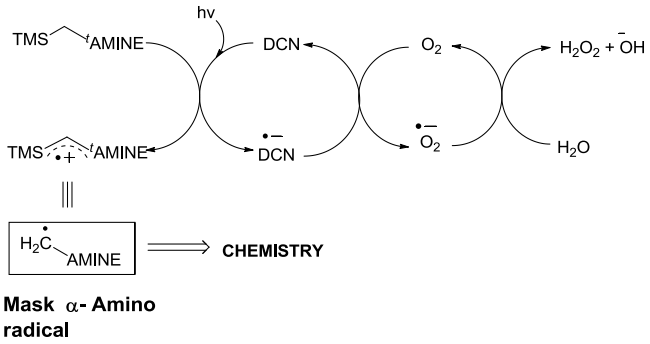

Scheme 12

2.2 Developing a new concept of C-Si bond activation: Stereoselective synthesis of 1 – Azabicyclo (m:n:o) alkane system:

The suitability of this strategy was adequately established for the construction of monocyclic (where n =0, m = 1, 2 etc.) and bicyclic amines[16] (where n = m = 1, 2 etc.) as depicted in **Scheme 13**.

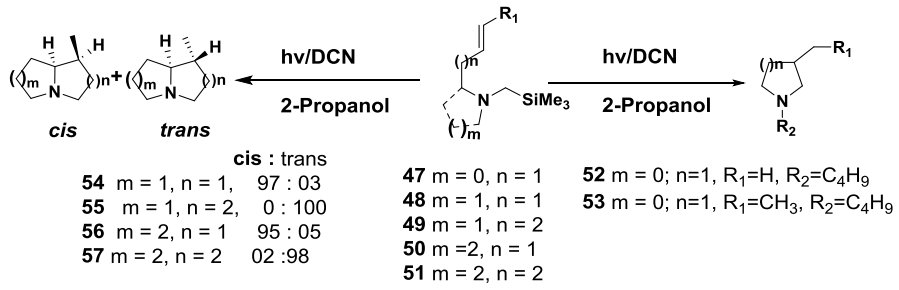

Scheme 13

The stereochemical aspects of such cyclization was established to be dependent upon the ring size being formed[17]. In case of **58** where the new ring formed was five membered, 1,5-*cis* stereochemistry was predominant, whereas in case of **61** where six membered ring is formed, 1,6-*trans* stereochemistry emerged (**Scheme 14**).

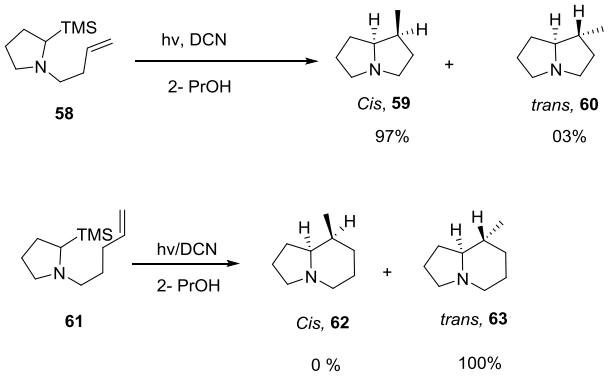

Scheme 14

Having established an efficient strategy for the construction of steroselective bicyclic amines, several biologically important polyhydroxylated cyclic amines *i. e.* ***azasugars*** were also synthesized by employing this methodology[19].

Since in the proceeding section, the synthesis of conformationally restricted azasugars is going to be discussed, it would be pertinent to introduce here azasugars (iminosugars) and their importance.

2.3 An introduction to Azasugars as Glycomimetics:

Glycosides are compounds containing a carbohydrate and non–carbohydrate residue in the same molecule, whereas glycosidases are the enzymes that cleave linkages between the carbohydrate part and non-carbohydrate part. Glycosidases (glycoside hydrolases/glycosyl hydrolases, E.C. number 3.2.1.x) and glycosyltransferases (EC 2.4) are omnipresent protein macromolecules which catalyze glycosyl group transfer reaction that assemble, trim and shape carbohydrates into bioactive glycoprotein and glycolipid conjugates. Largely, these processes involve the cleavage of the glycosidic bond linking a sugars anomeric carbon with an oligo- or polysaccharide or a nucleoside diphosphate group. The liberated glycosyl group is further transferred to water (by glycosidases) or to some other nucleophilic acceptor (by transferases[20]) as shown in **Figure 1**. This means glycosidases and glycosyltransferases are responsible for the hydrolysis and formation, respectively, of glycosidic bond.

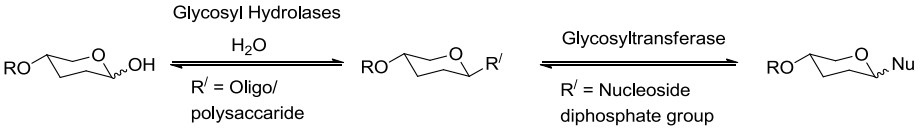

Figure 1

Based on the above mentioned role of glycosidases, it would not be exaggeration to mention that glycosidases are essential for the survival and existence of all living organisms as it has an ability to lower the energy of the transition state for the corresponding reactions. For example digestive glycosidases break down large sugar-containing molecules to release monosaccharides which can be more easily taken up and used metabolically by the organism. Lysosomal glycosidases catabolise glycoconjugates intracellularly and a wide range of glycosidases are involved in the biosynthesis of the oligosaccharide portions of glycoprotein's and glycolipids which play vital roles in mammalian cellular structure and functions[21].

Thus, ***glycosidase inhibitors*** are chemical entity which are capable of mimicking either the charge or shape (or both) of the substrate or that of any of the transition states (*e.g.***TS – 1** or **TS- 2** in **Scheme 15**) and therefore, these can act as a reversible inhibitor of that particular glycosidase.

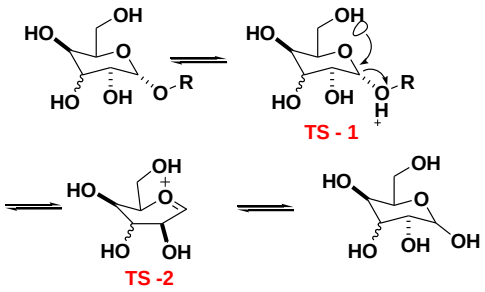

Scheme 15

Ever since the revolutionary work by Paulsen *et al.*[22] on analogues of monosaccharides in which the ring oxygen is replaced by nitrogen perhaps became the best-known azasugar glycomimetics (**Scheme 16**). This modification provided these analogues (polyhydroxylated azasugar alkaloids) metabolic inertness, retaining the recognition by glycosidases and other carbohydrate-recognizing proteins. Nojirimycin (NJ) was the first polyhydroxylated piperidine alkaloid belonging to this class isolated in 1966[23-24]. However, in the same year 1-deoxynojirimycin (DNJ) was also synthesized and later in 1976 was isolated from *Mulberry trees*[25], *Bacillus*[26] and *Streptomyces* cultures. Both NJ and DNJ, if protonated at the basic nitrogen atom, become the charge mimic of **TS- 2** (as shown in **Scheme 15)**.

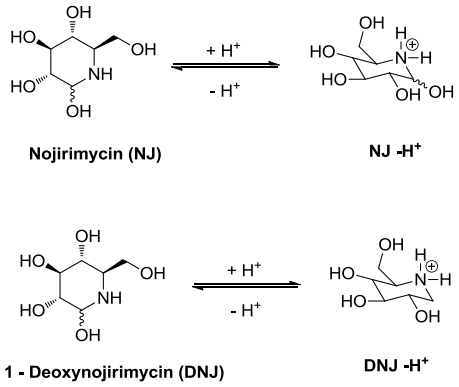

Scheme 16

With the hope of discovering glycosidase-inhibiting azasugars, rigorous research work has been continuing with the isolation and development of synthetic strategy for such polyhydroxylated pyrrolidine, piperidine, indolizidines, pyrrolizidines[27-28].

In order to provide a general and flexible strategy for the syntheses of 1N-iminosugars, our group introduced a new concept of synthesizing these classes of molecules through a synthon **69** (**Scheme 17**) easily accessible by the cyclization of (**68**) α-trimethylsilylmethylamine radical cation to a tethered acetylene functionality[29]. The acetonide moiety was chosen in order to lock the conformation for better diastereoselection during the functionalization of the exocyclic olefin.

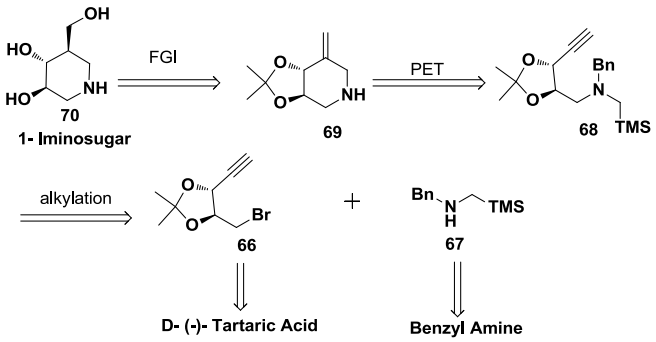

Scheme 17

In an effort to extend the scope of this strategy and to discover more potent and biologically important azasugars, we have also synthesized indolizidine class of polyhydroxylated 1-azabicyclo [4.3.0] nonane azasugars such as (+)-6-*epi*-castanospermine[30] (**83**) and additional

two more analogues **85** and **84** by employing similar α-silyltrimethylamine radical cation cyclization to tethered acetylene moiety as shown in **Scheme 18**.

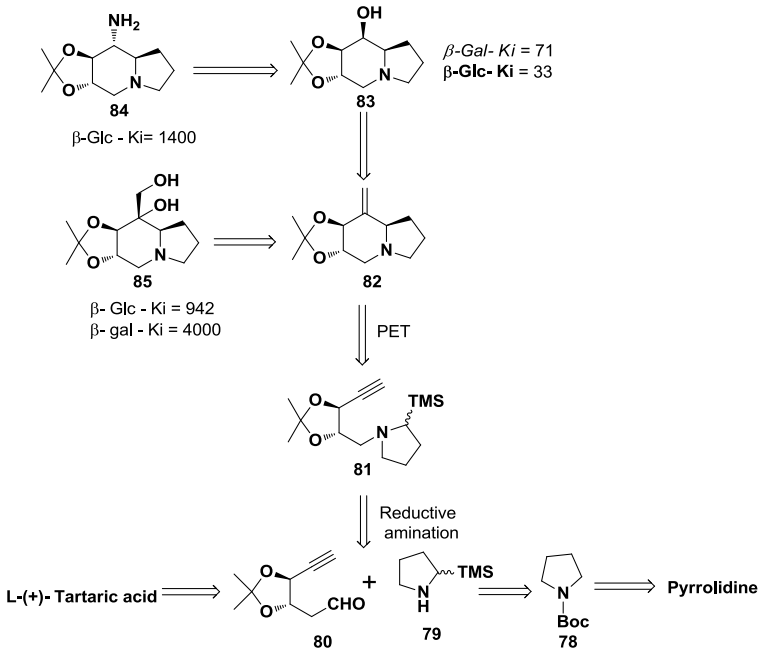

Scheme 18

1-Deoxy-8-*epi*-castanospermine **83** showed nonspecific mild inhibition against α-galactosidase ($K_i/\mu M$ = 71, *α-galactoidase*), β-galactosidase ($K_i/\mu M$ = 73, *β-galactosidase*) and β-glucosidase ($K_i/\mu M$= 33, *β-glucosidase*). Based on the enzyme inhibition studies, it was concluded that due to the presence of structural flexibility in these azasugars (**83**-**85**), they lose some degree of selectivity towards a particular enzyme.

Thus, we realised that if any entity (binding species) that possesses lesser degree of freedom, it would bind more effectively to the active site of the enzyme and moreover, if it resembles also with the charge of oxo-carbenium ion intermediate (**TS- 2** in **Scheme 19**), enhanced inhibition and selectivity towards the corresponding enzyme could emerge. As a part of our ongoing interest in the design and synthesis of new potent azasugars[19] and less explored potential of polyhydroxylated 1-azabicyclo[4.2.0]octane framework as a glycosidase inhibitor[31-32], we designed **86** with a hope that it may be an active azasugar. The reason behind this design was that the six-membered ring of azasugar **86** will be forced into a half-

chair conformation at physiological pH= 5 due to constrained azetidine ring which will mimic the oxo-carbenium ion intermediate of the enzyme transition state (**Scheme 19**).

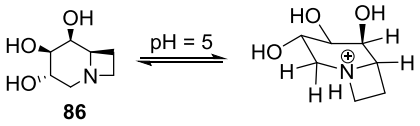

Scheme 19

In regard to the synthesis of **86**, we visualized the construction of polyhydroxylated 1-azabicyclo[4.2.0]octane framework (**92**) by retrosynthetic analysis as shown in **Scheme 20**.

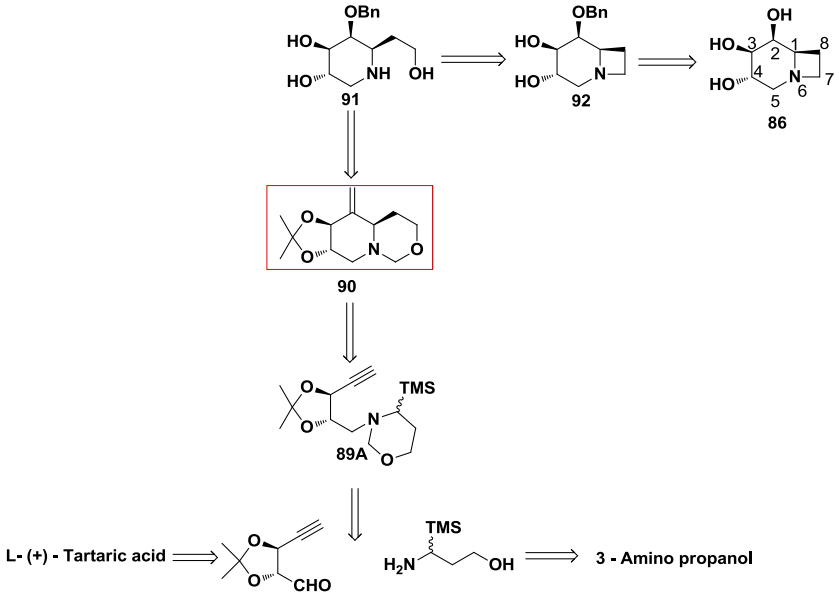

Scheme 20

However, before going into the details of our synthetic efforts towards this molecule, it will be pertinent to update few synthetic approaches available in literature for such conformationally restricted glycosidase inhibitors.

2.4 Literature approaches for the synthesis of conformationally restricted azasugars:

A) Ganem's approach[33]:

Ganem's *et al*. reported a new class of potent active site –directed glycosidase inhibitor **96** with the speculation that protonated aziridine analogues like **96** might preferentially interfere with α- glycoside hydrolysis by S_N2 esterification of the enzyme's β'-face carboxylate anion. The **96** was synthesized from known 1–deoxy nojirimycine derivative **93** in five steps with 27% overall yield (**Scheme 21)**. It displayed a potent inhibitor activity selectively against green coffee bean α-galacosidase (7.1 μM, pH = 5-6).

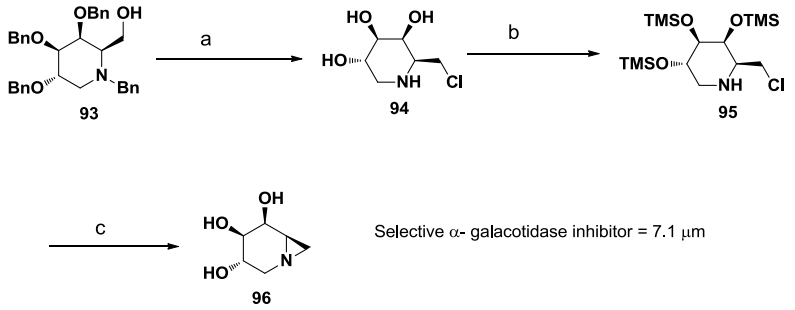

Scheme 21

Reagents and conditions: (a) i) Mesylation and displacement (76%, *conditions are not provided*); ii)hydrogenolysis (100%, *conditions are not provided*); (b) $(TMS)_2NH$, TMSCl, py then H_2O (88%); (c) i) *n*-BuLi (1 eq), THF, −78 °C (36–40%); ii) K_2CO_3, MeOH, rt (100%).

B) Bols's approach[34]:

Bols's group synthesized **101** from methyl D-glucopyranoside (**97**) by following the route outlined in **Scheme 22**.

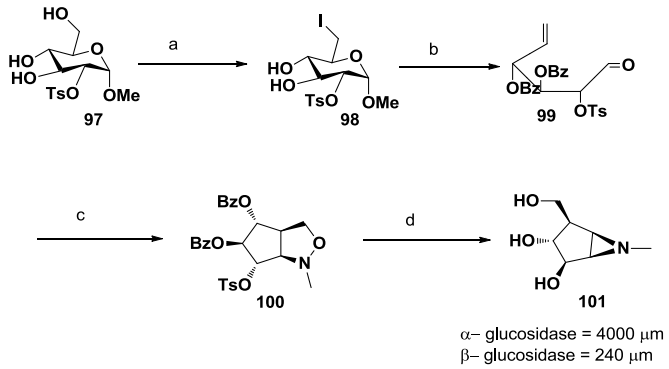

Scheme 22

Reagents and conditions: (a) i) TsCl, py; ii) BzCl, py; iii) NaI, Ac_2O, reflux; (b) Zn, EtOH, reflux; (c)MeNHOH, EtOH, py, 45 °C; (d) i) H_2, Ni, 1 atm; ii) NaOMe (78% over two steps).

C) Dhavale's approach[32]:

Recently Dhavale's group has synthesized new bicyclic conidine iminosugars **106A** and **106B** starting from D-glucose as shown in **Scheme 23**. The enzymes inhibitory studies have revealed that **106A** moderate inhibition with α-galactosidase and α- mannosidase, while **106B** shows selective inhibition with α- mannosidase.

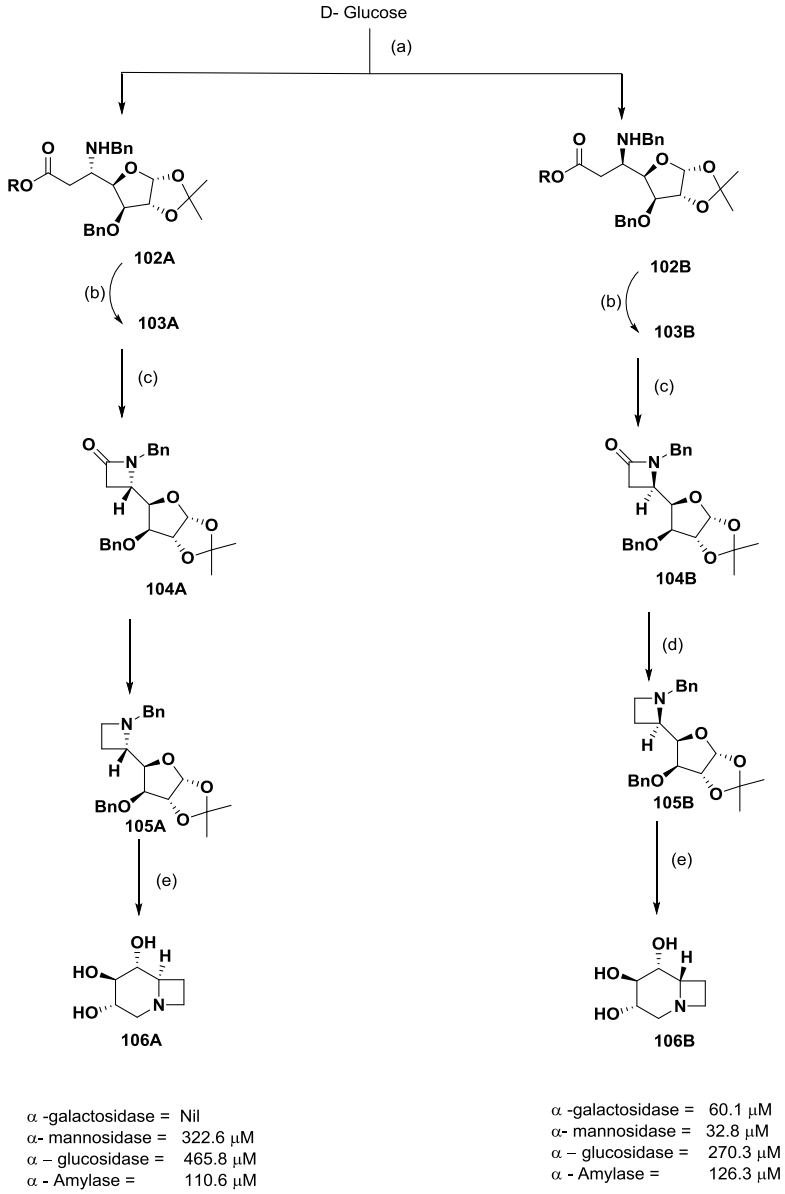

Scheme 23

Reagents and condition: (a) N- benzylamine, 24 h, RT, b) LiOH, H_2O, MeOH-H_2O, 0°C to RT, 2h; (c)2-chloro-1-methylpyridiniumiodide, Et_3N, DCM, 2 h; (d) $LiAlH_4$, THF, -10° to 0°C 10 min; (e) (i) TFA/H_2O (3:2), 0°C to RT 4h; (ii) H_2, 10% Pd/C, MeOH, 80 psi, RT, 5 days.

Considering the importance of conformationally restricted azasugars and limited scope of the diversity by above synthetic routes, we have designed a new strategy of synthesizing **86** from the key intermediate **90** which was assumed to be synthesized by PET initiated *α*-silyltrimethylamine radical cation cyclization of **89A** as shown in retrosynthetic analysis (**Scheme 20**).

2.5 Result and Discussion:

The synthesis began by synthesizing precursor **89** by coupling **88** and **87**, synthesized by based on the protocol already developed from our group[29,35]. Since our PET cyclization strategy required *N*-alkylated α-trimethylsilylmethyl amine moiety, we transformed **89** into the cyclic 1, 3-oxazine derivative **89A** by refluxing with paraformaldehyde. PET activation of **89A,** employing our established protocol produced **90** as a single diastereomer[36] in 60 % yield (**Scheme 24**).

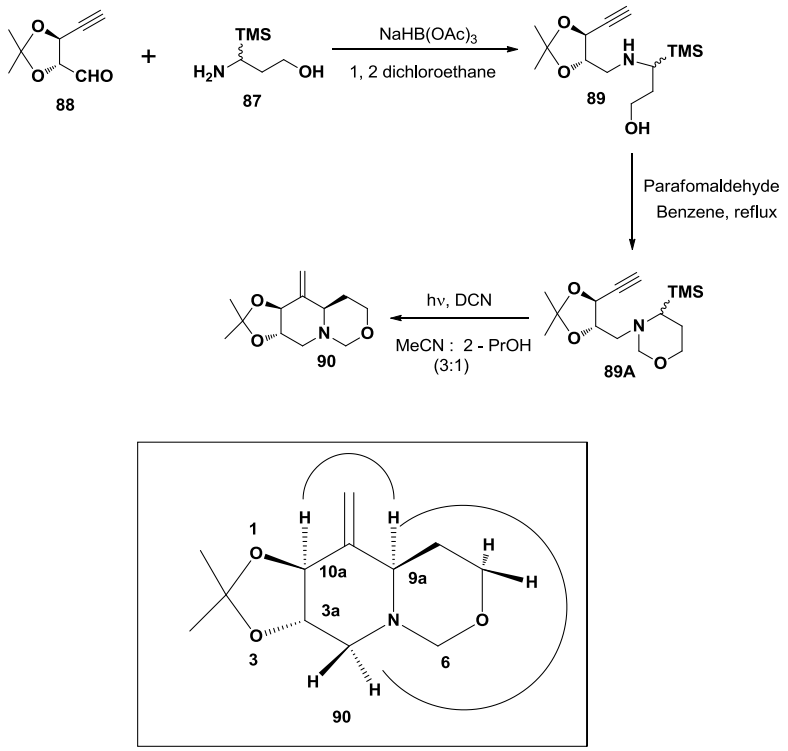

Scheme 24

The product **90** displayed two olefinic protons at δ 4.9 (bs, 1H,) and δ 5.1 (bs, 1H,). The doublet at δ 2.65 (d, J = 5.8 Hz, 1H) was assigned to H_{9a}proton whereas other doublets at δ 3.86 (d, 1H, J = 8.0 Hz) and δ 4.48 (d, 1H, J = 8.0 Hz) were assigned to H_{-6}. ^{13}C NMR indicated the presence of 12 non-equivalent carbons. DEPT spectrum characterized two acetonide methyl signals at δ 26.6, 26.8; 5 CH_2carbons at δ 27.7, 51.2, 67.1, 86.5, 103.6; three CH carbons at δ 60.4, 76.5, 81.5 and two quaternary carbons at δ 111.0, 142.7. The observed NOE between H_{10a} and H_{9a} suggested that they are *cis* to each other.

To proceed further along the proposed synthetic route, **90** was dihydroxylated using OsO_4 which gave **107** as a crystalline solid (m.p.= 165°- 168°) in 90 % yield as an exclusive diastereomer (**Scheme 25**). Oxidative cleavage of **107** with sodium periodate adsorbed on silica gel afforded **108** which upon sodium borohydride reduction gave **109** in 85% yield as a single diastereoisomer. The benzyl protection of **109** afforded **110** followed by global deprotection by treating with 6 (N) HCl gave **91** in 95% yield[37].

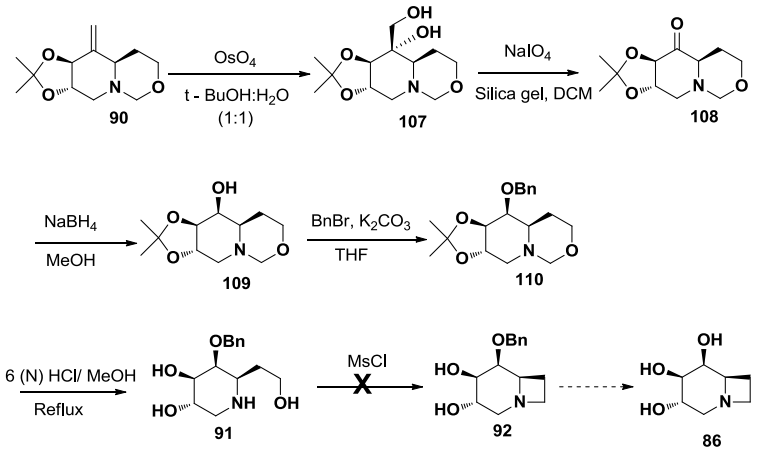

Scheme 25

An attempted cyclization of **91** to obtain **92** via mesylation of free primary –OH, however, failed. Further attempts for this cyclization as mentioned in **Table-1** unfortunately also did not succeed.

Table 1

Method	Remark
DEAD, PPh_3, DCM	Required compound not isolated
PPh_3, I_2, DCM	Same as above
Consecutive tri hydroxyl group of piperidine ring was converted to –OBn and then methylene deprotection by 6 (N) HCl followed by treating with MsCl/ Et_3N.	Very messy TLC was observed, desired product could not able to isolate.

The observed failure of such cyclization may be due to the constrain experienced in forming the 1-azabicyclo[4.2.0] octane bi-cyclic system. Therefore, we planned the synthesis of **86** directly by the photoredox activation of **115** as described in **Scheme 26**.

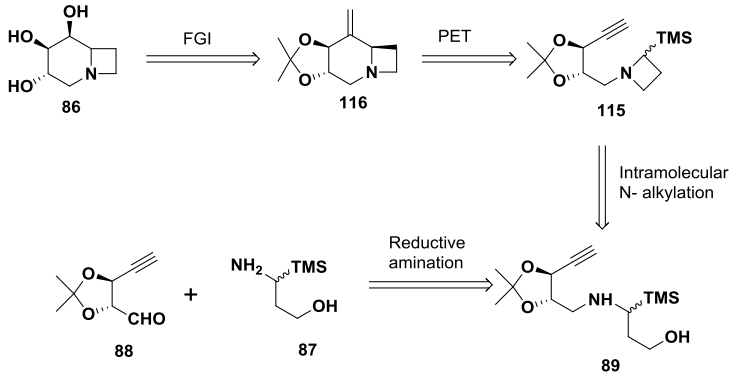

Scheme 26

To this end, **115** was synthesized as a 1:1 diasteromeric mixture by intramolecular N-alkylation of **89** by heating it with MsCl in presence of triethylamine in toluene (70°C). In the ^{1}H NMR spectrum of **115**, the protons appeared in two sets with same intensity. For example, TMS protons appeared at δ -0.02 and -0.01 as two singlets. The methylene protons of azetidine ring (N–CH(TMS)–$\underline{CH_2}$) appeared at δ 1.86 and δ 1.96 as multiplets. The acetylinic proton and methylene (N–$\underline{CH_2}$) protons of piperidine ring merged together at δ 2.62-2.45 (3H, m). The other methylene (N-CH_2) protons of azetidine ring appeared at δ 3.15-2.82 (2H, m). The methine proton (N–C$\underline{H}$–TMS) appeared as doublet of doublet at δ 4.24 and 4.71 (two sets, dd, *J* = 7.3, 2.2 Hz, 1H).

The PET cyclization of **115** in 2-PrOH under standard photo-irradiation conditions[20], produced **116** as a single diastereomer. The ^{1}H NMR spectrum of **116** showed disappearance of acetynilic proton and the appearance of two olefinic (C=C$\underline{H_{8a}}\underline{H_{8b}}$) protons at δ 4.77 (bs, 1H) and δ 5.19 (bs,1H). The four protons of azatidine ring appeared at δ 2.46-2.49 (m, H_{1a}), δ 2.51-2.52 (m, H_{1b}), δ 3.26-3.29 (m, H_{2a}) and δ 3.44-3.47 (m, H_{2b}) respectively. The other two protons of methylene group (H_{3a} and H_{3b}) appeared at δ 2.73 (dd, *J* = 13.3, 11.4 Hz, 1H) and δ 2.92 (dd, *J* = 13.3, 4.7 Hz, 1H).The newly generated bi-cyclic ring junction proton (H_7) appeared at δ 4.03-4.04 (m, 1H). In ^{13}C NMR, the two olefinic carbons appeared at δ 103.6, 146.5. The NOESY cross correlation between H_5–H_7 suggested that they are *cis* to each other.

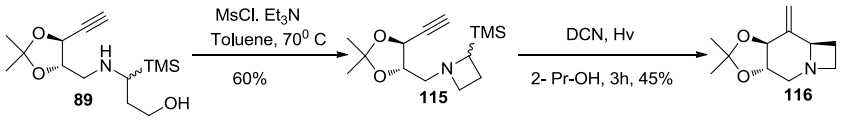

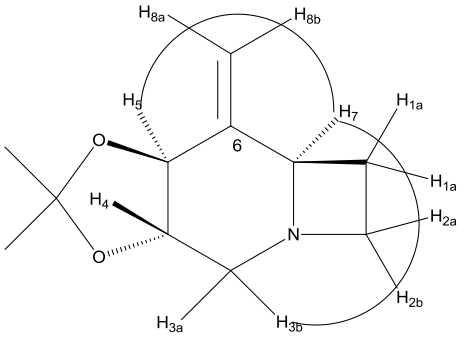

NOE correlation of cyclized product **116**

Scheme 34

After constructing 1-azabicyclo[4.2.0]octane framework successfully, we turned our attention towards functionalizing the *exo*-olefinic bond by following the same protocol as discussed above (**Scheme 35**). The ^{1}H NMR of **117** [C(OH)-C<u>HH</u>-OH] protons appeared as doublets at δ 4.24 (d, *J* = 11.5 Hz, 1H) and δ 3.80 (d, *J* = 11.5 Hz, 1H), respectively. The H_{7a} and H_{5a} appeared at at δ 3.82- 3.80 (m, 1H) and δ 3.51 (d, *J* = 9.4 Hz, 1H). The H_{4a} and H_{3e} protons appeared by merged together at δ 3.25-3.31 (m, 2H). The strong NOESY cross correlation between H_{4a}–H_{8b}, suggested that they are *cis* to each other.

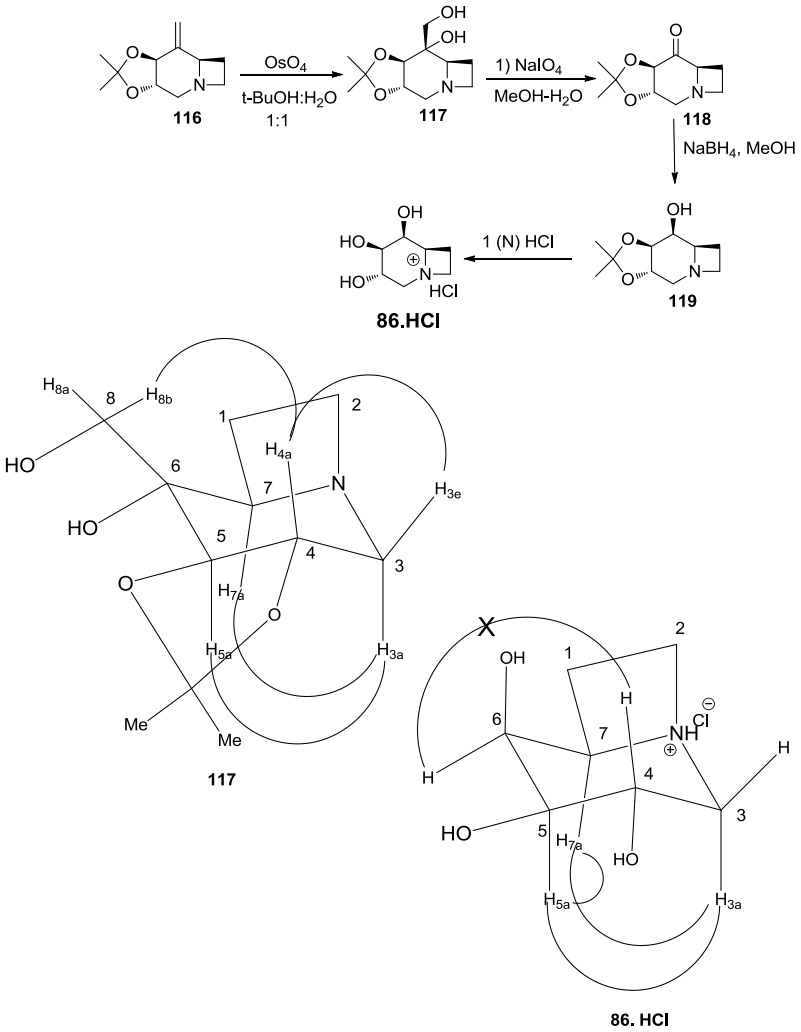

NOE experiments over **117** and **86. HCl**

Scheme 35

Finally, treating **119** with 1 (N) HCl afforded **86** as a hydrochloride salt (**86.HCl)**. The ^{1}H NMR analysis of **86**.**HCl** displayed ten distinguished protons. For example, the three *α*–hydroxy protons (H_9, H_{10} and H_{11}) appeared as multiplets at δ 4.18, δ 4.10 and δ 4.05, respectively, whereas bicyclic ring junction proton (H_{12}) appeared at δ 4.27. The four azetidine ring protons (H_1, H_2, H_5, H_6) appeared at δ 2.33-2.35 (m, 1H), δ 2.75-2.77 (m, 1H), δ 3.42-3.44 (m, 1H) and δ 3.49 (dd, *J* = 8.2, 5.2 Hz, 1H), respectively. In ^{13}C NMR the two azetidine CH_2 carbons (C_1 and C_2) appeared at δ 21.9 and δ 58.63, respectively. The other CH_2 carbon (C_3) appeared at δ 49.10. The remaining four CH carbons appeared at δ 62.70, 68.09, 71.32 and 73.5, respectively. From NOESY analysis it was observed that there is no cross correlation between H_6 and H_{4a} confirming *trans* relationship between them.

2.6 Enzyme inhibition study:

The inhibitory activities of **86. HCl** was screened against β-galactosidase (*Aspergillus oryzae*), *α*-galactosidase (coffee beans), *β*-glucosidase / *β*-mannosidase (almonds), *α*-glucosidase (yeast) and *α*-mannosidase (jack beans). The results are summarized in the **Table 1**.

Table 1. Screening with different enzymes

Enzymes	Azasugar **86. HCl** (*ki* = *μM*)
β - galactosidase	114
α - galactosidase	Nil
β - glucosidase	7.6
α - glucosidase	Nil
β - mannosidase	Nil
α - mannosidase	Nil

From the above results, it is apparent that **86. HCl** exhibited good (*ki* = 7.6*μM*), competitive and specific inhibition against *β* – glucosidase only.

2.7 Summary:

In conclusion, we have designed synthesized and evaluated **86** as a potent and selective *β* - glucosidase inhibitor. Fairly good and specific glycosidase inhibition activity exhibited by **86.HCl** is expected to encourage further research towards the improving its potency by incorporating minor structural variation to its core or by increasing the polarity of the molecule.

2.8 Reference

1) a) R. S. Davison, *Adv. Photochem*. **1986**, *13*, 165.

2) V. F. Travern, r. west, *J. Am. Chem. Soc*. **1973**, *95*, 6824.

3) a) D. R. Arnold, A. J. Maroulis, *J. Am. Chem. Soc*. **1976**, *98*, 5931.

4) Okamoto. A.; Snow. M. S. Arnold. D. R. *Tetrahedron* **1986**, *42*, 6175.

5) L. W. Reichel, G. W. Griffin, A. J. Mullar, P. K. Das, S. N. Ege, *Can. J. Chem*. **1984**, *62*, 424.

6) S. Sankararaman, S. Perrier, J. K. Kochi, *J. Am. Chem. Soc*. **1989**, *111*, 6448.

7) L. Szepes, T. Koranyi, G. Naray-szabo, A. Modelli, G. Distefano, *J. Orgmet. Chem*. **1981**, *35*, 217.

8) Sakurai. H.; Kira.M.; Uchida.T. *J. Am. Chem. Soc*. **1973**, *95*, 6826.

9) Fukuzumi. S.; Kitano.T.; Mochida. K. *Chem. Lett*. **1989**, 2177.

10) a) Pandey. G.; Soma Sekar.B. B. V. *J. Org. Chem*. **1992**, *57*, 4019.

11) Pandey. G.; Soma Sekar.B. B. V.; Bhalerao. U. T. *J. Am. Chem. Soc.***1990**, *112*, 5650.

12) Eaton. D. F. *J. Am. Chem. Soc*. **1980**, *102*, 3280

13) Zhang. X-M.; Mariano. P. S. *J. Org. Chem*. **1991**, *113*, 8847

14) Jeon. T. Y.; Lee. C-P.; Mariano.P. S. *J. Am. Chem. Soc*. **1991**, *113*, 8847.

15) Padwa, A.; Nimmesgern, H.; Wong, G. S. K. *J. Org. Chem.***1985**, *50*, 5620.

16) a) Pandey. G.; Devi Reddy. G. *Tetrahedron Lett*. *33*(43), 6533, **1992**.

17) Pandey. G.; Devi Reddy.G.; Chakrabarti. D. *J. Chem. Soc., Perkin Trans. 1*, **1996**, 219.;

18) The Thesis of Dr. G. Devi Reddy of National Chemical Laboratory, Pune, **1994**, in title of 'Mechanistic And Synthetic Aspect of PET promoted photocyclisation of α- Silyl amine: Synthesis of Biologically Active Compounds.

19) Pandey. G.; Dey.D.; Gadre, S. R. *Chimia. Int. J. Chem*. **2013**, *67*, 30 – 38.

20) Niwa. T.; Inouye, S.; Tsuruoka, T.; Koaze.Y.; Niida. T. *Agric. Bio. Chem*. **1970**, *34*, 966.

21) Watson, A. A.; Fleet, G. W. J.; Asano, N.; Molyneux, R. J. Nash. R. J. *Photochemistry*, **2001**, *56*, 265.

22) a) Paulsen, H.; Sangster, I.; Heyns, K. *Chem. Ber.* **1967**, *100*, 802.

23) Inouye, S.; Tsuruoka, T.; Nida, T. *J. Antibiot.* **1966**, *19*, 288.

24) Niwa, T.; Inouye, S.; Tsuruoka, T.; Koaze, Y.; Niida, T. *Agric. Biol. Chem.* **1970**, *34*, 966.

25) Yagi, M.; Kouno, T.; Aoyagi, Y.; Murai, H. *Nippon Nogel Kagaku Kalshi***1976**, *50*, 571.

26) Schmidt, D.D.; Frommer, W.; Mullar, L.; Truscheit, E. *Naturwissenschaften***1979**, *66*, 584.

27) Stütz, A. E. *Iminosugas as glycosidase inhibitors: nojirimycine and beyond; Wiley-VCH: Weibheim*, **1999**.

28) Y. D. Vankar, R. lahiri, A. A. Ansari, *Chem. Soc. Rev*. **2013**, DOI. 10. 1039/c3cs35525j.

29) Pandey, G.; Kapur, M**.***Org. Lett.***2002**, *4*, 3883-3886.

30) Pandey, G.; Dumbre, S. G.; Pal, S.; Khan, M. I.; Shabab, M. *Tetrahedron*, **2006**,*63*, 4756.

31) Pandey, G.; Dumbre, S. G.; Khan, M. I.; Shabab, M. *Tetrahedron Lett*, **2006**,*45*, 7923.

32) Sanap. S. P.; Ghosh. S.; Jabgunde.Amit; pinjari.R; Gejji.S.; Shing.S.; Chopade.B.; Dhavale. D. *Org. Biomol. Chem.***2010**, *8*, 3307.

33) Tong, M. K.; Ganem, B. *J. Am. Chem. Soc.* **1988**, *110*, 312.

34) Lopez, O. L.; Fernandez-Bolanos, J. G.; Lillelund, V. H.; Bols, M. *Org. Biomol. Chem.* **2003**, *1*, 478.

35) Pandey. G.; Banerjee.P.; Kumar.R.; Puranik. V. G.; *Org. Lett*, **2005**, *7*, 3713.

36) G. Pandey, G. D. Reddy, G. Kumaraswamy, *Tetrahedron***1994**, *50*, 8185.

37) The thesis of S. G. Dumbre of National Chemical Laboratory, Pune, **2006**, in title of, *´Design and synthesis of new azasugars: β- lactam azasugar hybrids, 1 – deoxy- D- Galacto-homonojirimycine and 1 – deoxy – D Gluco-homonojirimycin as glycosidase inhibitors´*

2.9 Experimental

15. Preparation of 1-((5-ethynyl-2,2-dimethyl-1,3-dioxolan-4-yl)methyl)-2-(trimethylsilyl)azetidine (115):

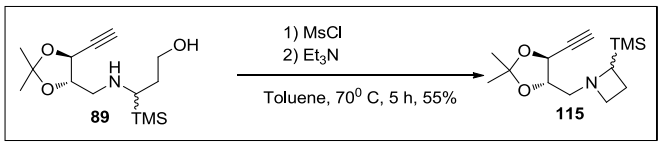

To a solution of **89** (2.8 g, 9.46 mmol) in dry toluene (200 mL), Et_3N (1.92 g, 20 mmol, 2.63 mL) and MsCl (1.18g, 10.4 mmol, 0.8 mL) was added at 0° C. The reaction mixture was allowed to come at room temperature and was further stirred for 4 h at 70°C. After maximum starting materials was found consumed (monitored by GC and TLC) the reaction mixture was cooled to room temperature. Toluene was removed under reduced pressure and the sticky residue was purified by column chromatography (silica, 2 % ethylacetate – pet ether) to afford pure **115** (1.44 g, 55%) as a colourless liquid.

^{1}H NMR (200 MHz, $CDCl_3$) δ:0.26 (s, 9H), 1.38 - 1.49 (three peaks, 3:2:1, 6H), 1.82- 1.86 (m, 1H), 1.87 – 2.10 (m, 1H), 2.45 – 2.61 (m, 3H), 2.81 – 2.92 (m, 1H), 2.93 – 3.10 (m, 1H), 3.51- 3.64 (m, 1 H), 3.86 - 4.07 (m, 1H), 4.24 – 4.71 (two peaks, dd, *J* = 7.3, 2,2 Hz, 1H).; **^{13}C NMR (50MHz, $CDCl_3$) δ** : -5.0, 17.8 + 18.1, 24.6 + 25.4+ 25.7, 56.1 + 57.0 + 58.0, 58.4 + 58.6, 61.3, 65.9 + 67.9, 78.5 + 79.6; **Mass (m/z): 268** $(M+H)^+$**.**

Preparation of (3a*S*,7a*R*,8a*S*)-2,2-dimethyl-8-methylenehexahydro-3aH-azeto[1,2-a][1,3]dioxolo[4,5-d]pyridine(116):

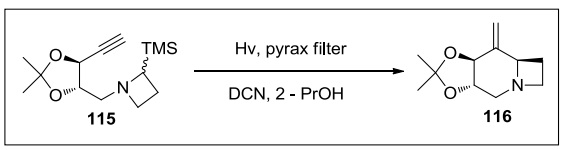

A solution containing **115** (1g, 3.58 mmol) and 1,4 – dicyanonaphthalene (0.150 g, 0.75 mmol) in *iso*- propanol (200 mL) was irradiated in an open specially designed irradiation vessel using

450- W Havonia medium pressure mercury lamp. The lamp was immersed in a pyrax water – jacketed immersion well which allowed only wavelength greater the 300 nm to pass through. After 3 h of irradiation, the consumption of the starting material was found to be almost complete (monitored by GC and TLC) and at this stage the irradiation was discontinued. The solvent was removed under reduced pressure and the residue was column chromatographed (2 % MeOH - ethylacetate) to afford pure **116** (silica, 0.26 g, 45%) as a colourless liquid.

^{1}H NMR (200 MHz, $CDCl_3$) δ :1.38 (s, 3H), 1.39 (s, 3H), 1.84-1.87 (m, 1H), 2.49 - 2.52 (m, 1H), 2.73 (dd, *J* = 13.3, 11.1 Hz, 1H), 2.88 – 2.93 (dd, *J* = 13.4, 4.7 Hz, 1H), 3.28 (m, 1H), 3.46(m, 1H), 3.65 (m, 1H), 3.75 (m, 1H), 4.07 (m, 1H), 4.77 (bs, 1H), 5.19 (bs, 1H).; **^{13}C NMR (50MHz, $CDCl_3$) δ :**22.8, 26.9, 27.1, 51.8, 52.0, 63.1, 75.3, 80.2, 103.6, 110.5, 146.9.; **α $^{27}_D$** = + 91.7°(in $CHCl_3$).; **Mass (m/z %):** 196 $(M+H)^+$.

Preparation of (3a*S*,7a*R*,8*S*,8a*R*)-8-(hydroxymethyl)-2,2-dimethylhexahydro-3aH-azeto[1,2-a][1,3]dioxolo[4,5-d]pyridin-8-ol(117):

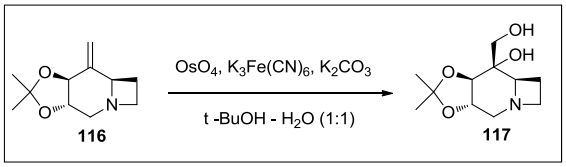

To a mixture of potassium ferricyanide (0.81 g, 2.44 mmol) and potassium carbonate (0.34 g, 2.4 mmol) in 10 mL water at 0^0C, **116** (0.12 g, 0.61 mmol) dissolved in *t*–BuOH (10 mL) followed by osmium tetraoxide (1mL of 1 % solution of OsO_4 in *t*-BuOH) was added. The reaction mixture was stirred for 24 h at room temperature. After overnight stirring, solid of Na_2SO_3 (0.2 g, 1.3 mmol) was added and a clear separation of the two layers was noticed. Aqueous layer was extracted with ethyl acetate (4 X 40 mL) and the combine organic extracts were dried over anhydrous of Na_2SO_4. The solvent was evaporated under reduced pressure and the residue was purified by column chromatography (silica, 10 % MeOH- ethylacetate) to afford **117** (0.78 g, 72%) as white semi solid.

^{1}H NMR (200 MHz, $CDCl_3$) δ :1.41 (s, 3H), 1.45 (s, 3H), 1.96 – 2.04 (m, 1H), 2.19 - 2.23 (m, 1H), 2.56 (t, *J* = 10.6 Hz, 1H), 3.03 (dd, *J* = 11.04, 4.52 Hz, 1H), 3.20 – 3.26 (dd, *J* =

12.55, 5.53, 1H), 3.27 – 3.31 (m, 2H), 3.51 (d, *J* = 9.8 Hz, 1H), 3.80 (d, *J* = 11.54 Hz, 1H), 3.81 – 3.84 (m, 1H), 4.24 (d, *J* = 11.54 Hz, 1H).; **^{13}C NMR (200 MHz, $CDCl_3$) δ:** 20.2, 26.6, 26.6, 51.6, 52.0, 63.8, 69.3, 72.1, 73.6, 85.8, 110.07.; **α $^{27}_{D}$** = + 17.7° (in $CHCl_3$);**Mass (m/z%)** : 230($M+H^+$).

Praparation of (3a*S*,7a*R*,8a*R*)-2,2-dimethyltetrahydro-3aH-azeto[1,2-a][1,3]dioxolo[4,5-d]pyridin-8(4H)-one(118):

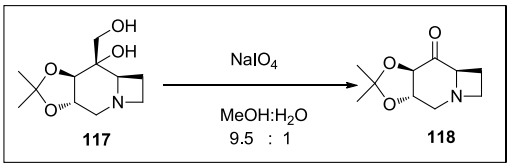

To a solution of **117** (0.4 g, 2.1 mmol) in MeOH : water (9.5 : 0.5, 10 mL) $NaIO_4$ (0. 43 g, 2.5 mmol) was added in portions during 10 min. at 0^o C. This suspension was stirred for 1 h at the same temperature and was filtered after maximum starting materials was consumed (monitored by TLC). The solvent was evaporated off to dryness and the white pasty crude mass **118** was immediately used as such for the next step.

Preparation of (3a*S*,7a*R*,8*S*,8a*S*)-2,2-dimethylhexahydro-3aH-azeto[1,2-a][1,3]dioxolo [4,5-d]pyridin-8-ol(119)

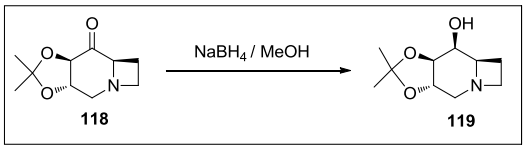

Sodium borohydride (0.072 g, 2 mmol) was added to a solution of **39** (0.2 g, 1 mmol) in dry methanol (10 mL) at 0° C. The resulting mixture was stirred for 2 h at room temperature before quenching with excess of saturated NaCl solution. This suspension was stirred for 6 h. Evaporation of methanol under reduce pressure afforded white pasty mass which was extracted with ethyl acetate (4 X 10 mL). The combined organic extracts were dried over anhydrous Na_2SO_4 and the solvent was evaporated under reduced pressure. The residue was

purified by column chromatography (silica gel, ethylacetate : MeOH 90 : 10) to afford **40** (0.042 g, 74%).

^{1}H NMR (200 MHz, $CDCl_3$) δ :1.48 (s, 3H), 1.51 (s, 3H), 2.26 – 2.29 (m, 1H), 2.39 - 2.46 (m, 1H), 2.76 – 2.81 (m, 1H), 3.03 (dd, *J* = 13.3, 4.7 Hz, 1H), 3.41 – 3.45 (m, 2H), 3.76 -3.78 (m, 1H), 3.85 – 3.87 (m, 1H), 4.30 – 4.35 (m, 1H), 4.38 (1H, m).; **^{13}C NMR (50MHz, $CDCl_3$) δ:**18.3, 26.7, 27.0, 51.0, 53.5, 63.8, 66.3, 68.6, 80.3, 110.0 (C).; **α $^{27}_D$** = + 30.5° (in $CHCl_3$); **Mass (m/z%):** 200($M+H^+$)

(3*S*, 4*R*, 5*S*, 6*R*)-1-aza-bicyclo[4.2.0]octane-3,4,5-triol. HCl (86. HCl)

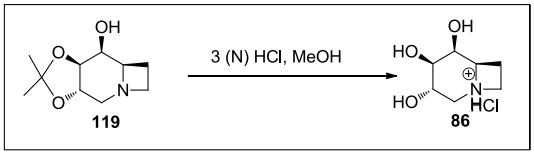

To a solution of **119** (0.025 g) in distilled methanol (2mL) was added 1(N) HCl (1mL) at room temperature and the reaction mixture was stirred for 3 h. Solvent was evaporated to dryness to afford **86**.**HCl** as a white pasty mass (0.015 g, 75%). The **86**.**HCl** was directly used for biologically testing.

^{1}H NMR (500 MHz, D_2O) δ : 2.36-2.42 (m, 1H), 2.75-2.81 (m, 1H), 3.21 (dd, *J* = 13.3, 5.7 Hz, 1H), 3.36 (dd, *J* = 13.5, 3.26 Hz, 1H), 3.42 (m, 1H), 3.51 (dd, *J* = 8.28, 5.2 Hz, 1H), 4.12 (m, 1H), 4.17 (m, 1H), 4.19 (m, 1H), 4.23 (m, 1H).; **^{13}C NMR (100MHz, D_2O) δ:** 22.0, 49.1, 58.4, 62.7, 68.1, 71.3, 73.5; **α $^{27}_D$** = + 44.1° (in MeOH); **Mass (m/z%):** 160($M+H^+$).

General procedure for enzyme inhibition assay

Inhibition assay for evaluating inhibitory potencies of the azasugars were determined by measuring the residual hydrolytic activities of the glycosidases of the corresponding *p*-nitrophenyl glycosides in the presence of azasugars spectrophotometrically.

General assay procedure

To a 10 mM solution of inhibitor in water was added appropriately diluted enzyme. 50 µL of buffer of appropriate pH was added to that. Double distilled water was added to make the final volume of the reaction mixture to 500 µL. Substrate of appropriate concentration and volume was added to that. The reaction was incubated for a suitable time period at appropriate temperature (on a water bath). It was quenched by the addition of 1.0 mL of (1M) Na_2CO_3 solution. The absorbance of the resulting solution was read at 405 nm.

Once the inhibitor was found to show inhibition to enzyme, IC_{50} (half maximal inhibitory concentration**)** was determined by checking the inhibition at various inhibitor concentrations with all other parameter remaining the same. Concentration of inhibitor was plotted against the percentage of inhibition it shows. IC_{50} was determined from the graph, which was the concentration of inhibitor showing 50% of inhibition. Dixon method was employed for the determination of *Ki* (dissociation constant of the enzymatic reaction).

In this method, hydrolytic activity of enzyme was measured in the presence of two different concentrations of substrates and varying concentrations of inhibitors. The *Ki* values were determined from the Lineweaver-Burk double reciprocal plots of 1/v versus 1/[S]. *Ki* for competitiveinhibition was determined by using the formula:

$$Ki = \frac{[I]}{\left(\frac{K_{MI}}{K_M}\right) - 1}$$

Spectra

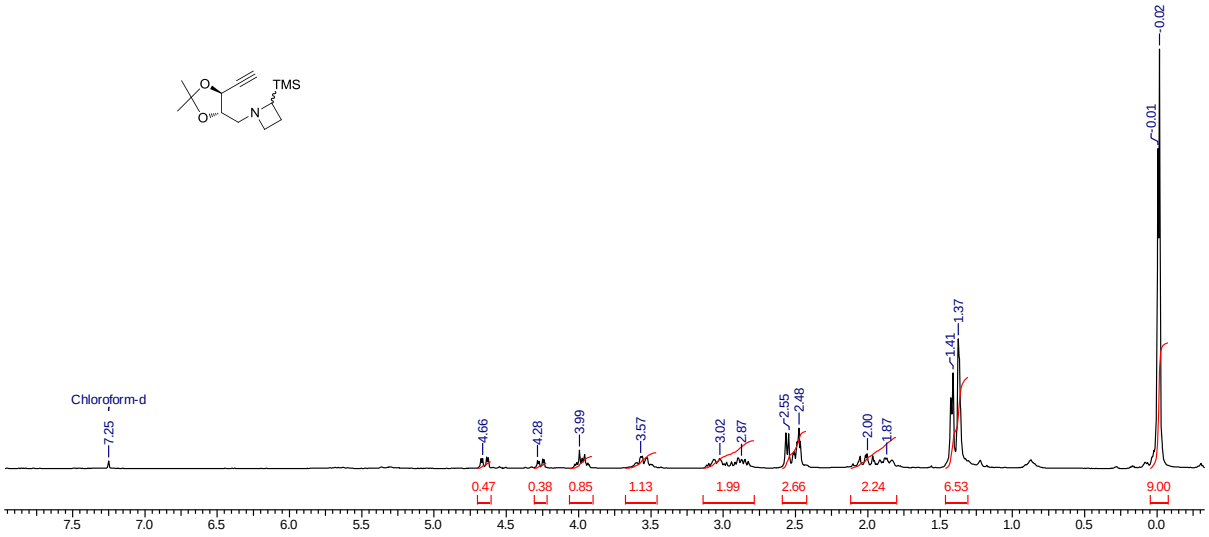
TMS
Chloroform-d
7.25
4.66
4.28
3.99
3.57
3.02
2.87
2.55
2.48
2.00
1.87
1.41
1.37
0.02
0.01
0.47
0.38
0.85
1.13
1.99
2.66
2.24
6.53
9.00

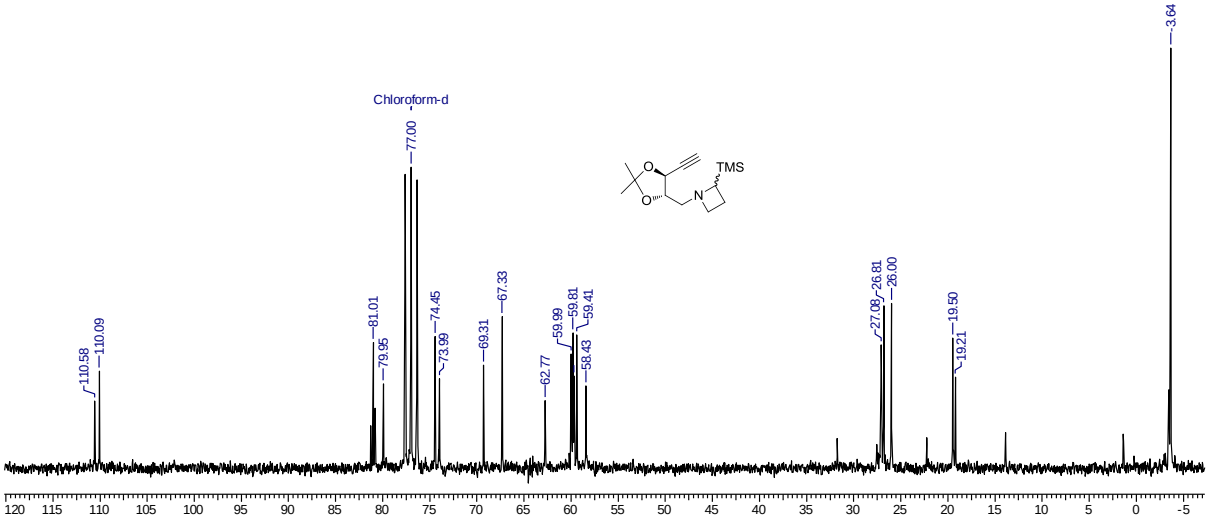
TMS
Chloroform-d
77.00
110.58
110.09
81.01
79.95
74.45
73.99
69.31
67.33
62.77
59.99
59.81
59.41
58.43
27.08
26.81
26.00
19.50
19.21
3.64

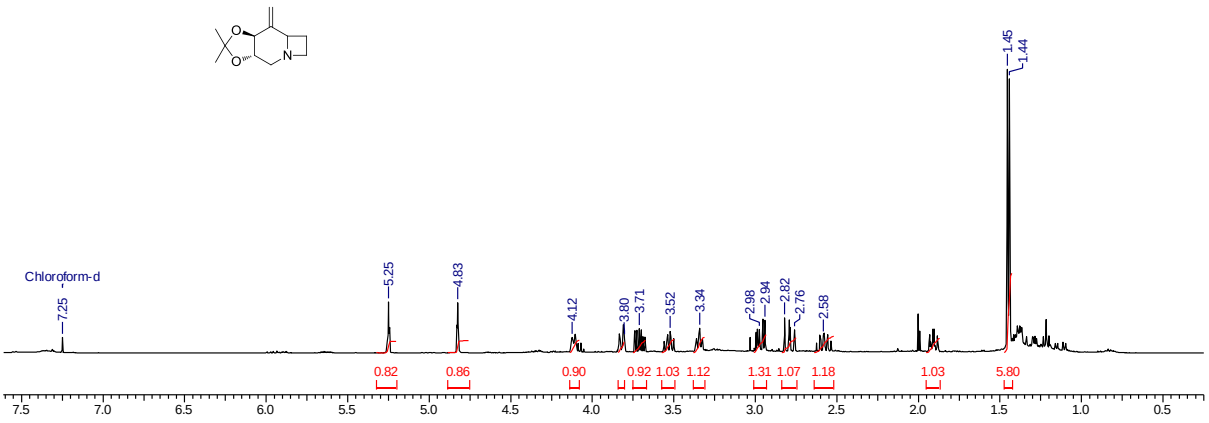
Chloroform-d
7.25
5.25
4.83
4.12
3.80
3.71
3.52
3.34
2.98
2.94
2.82
2.76
2.58
1.45
1.44
0.82
0.86
0.90
0.92
1.03
1.12
1.31
1.07
1.18
1.03
5.80

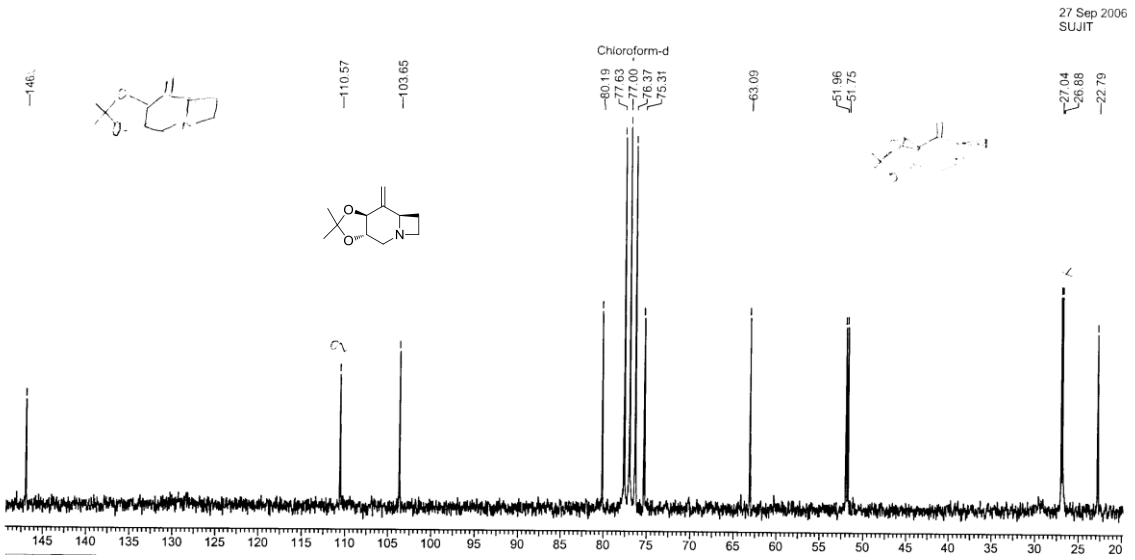
27 Sep 2006
SUJIT
Chloroform-d
146.
110.57
103.65
80.19
77.63
77.00
76.37
75.31
63.09
51.96
51.75
27.04
26.88
22.79

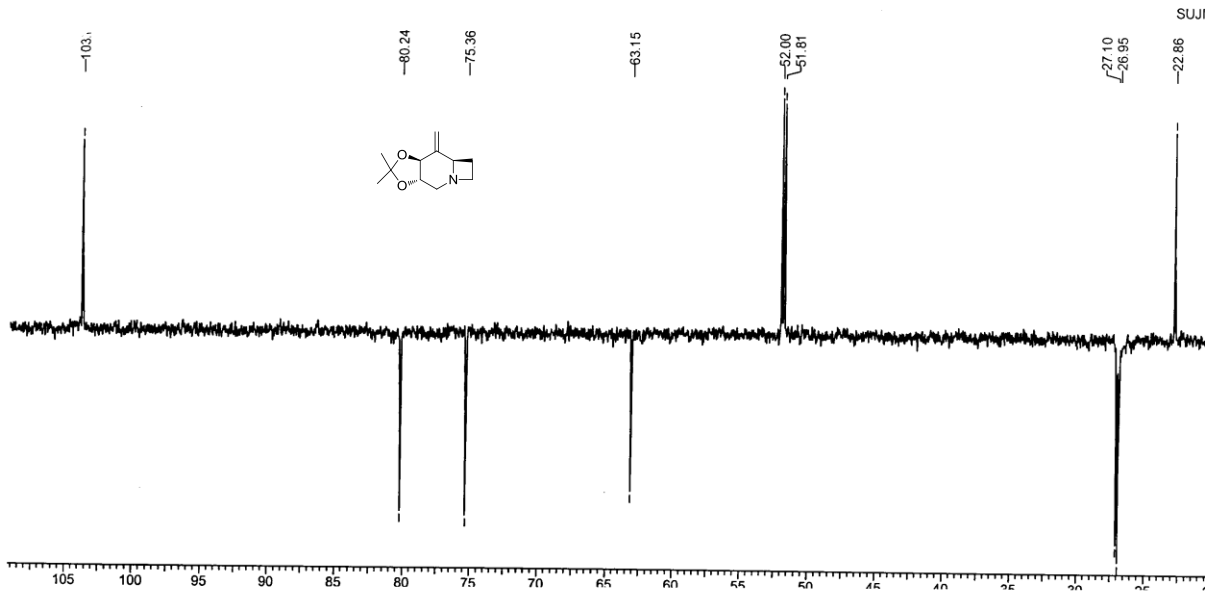
SUJI
103.
80.24
75.36
63.15
52.00
51.81
27.10
26.95
22.86
105
100
95
90
85
80
75
70
65
60
55
50

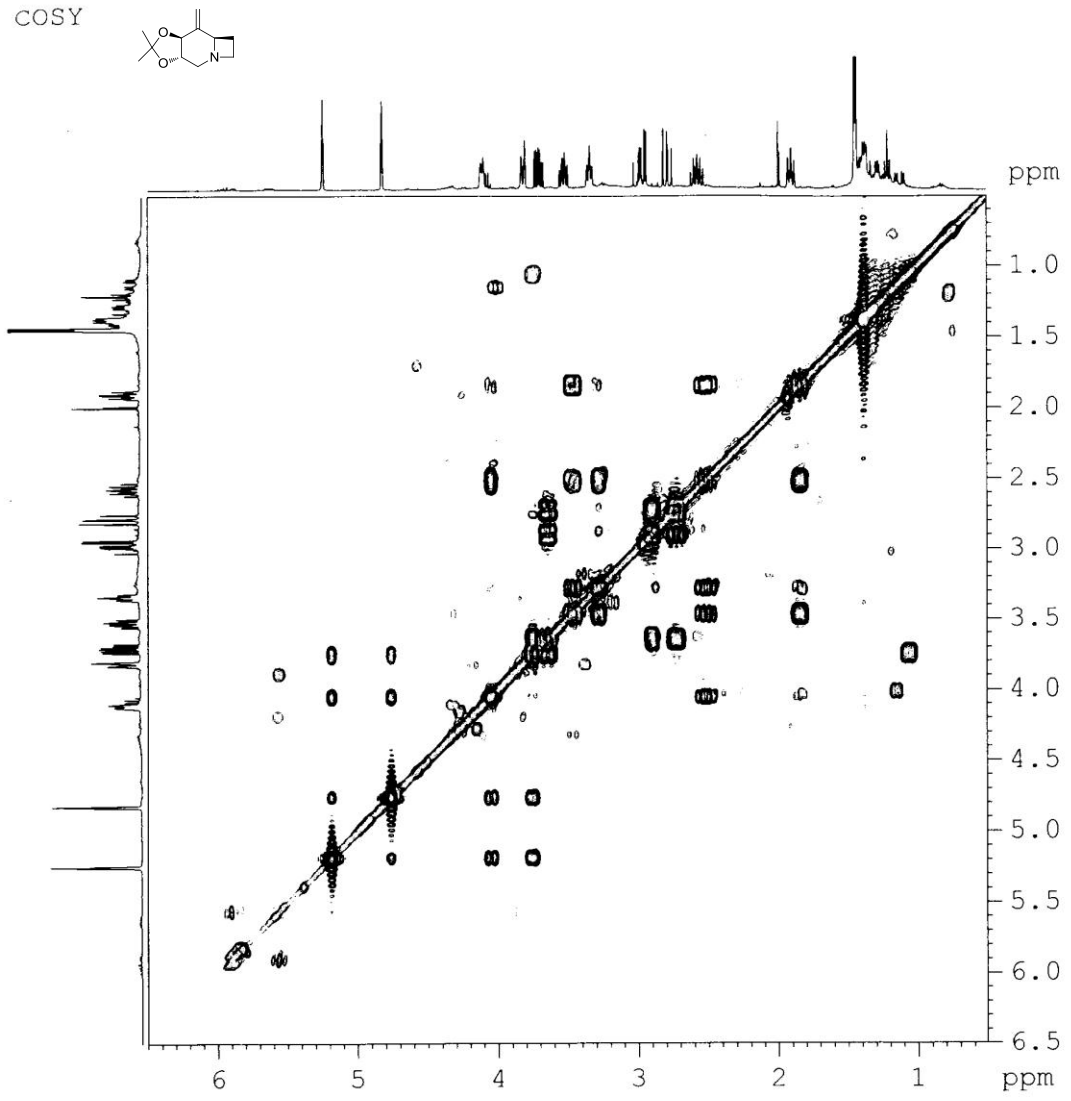
COSY
ppm
1.0
1.5
2.0
2.5
3.0
3.5
4.0
4.5
5.0
5.5
6.0
6.5
6
5
4
3
2
1
ppm

NOESY

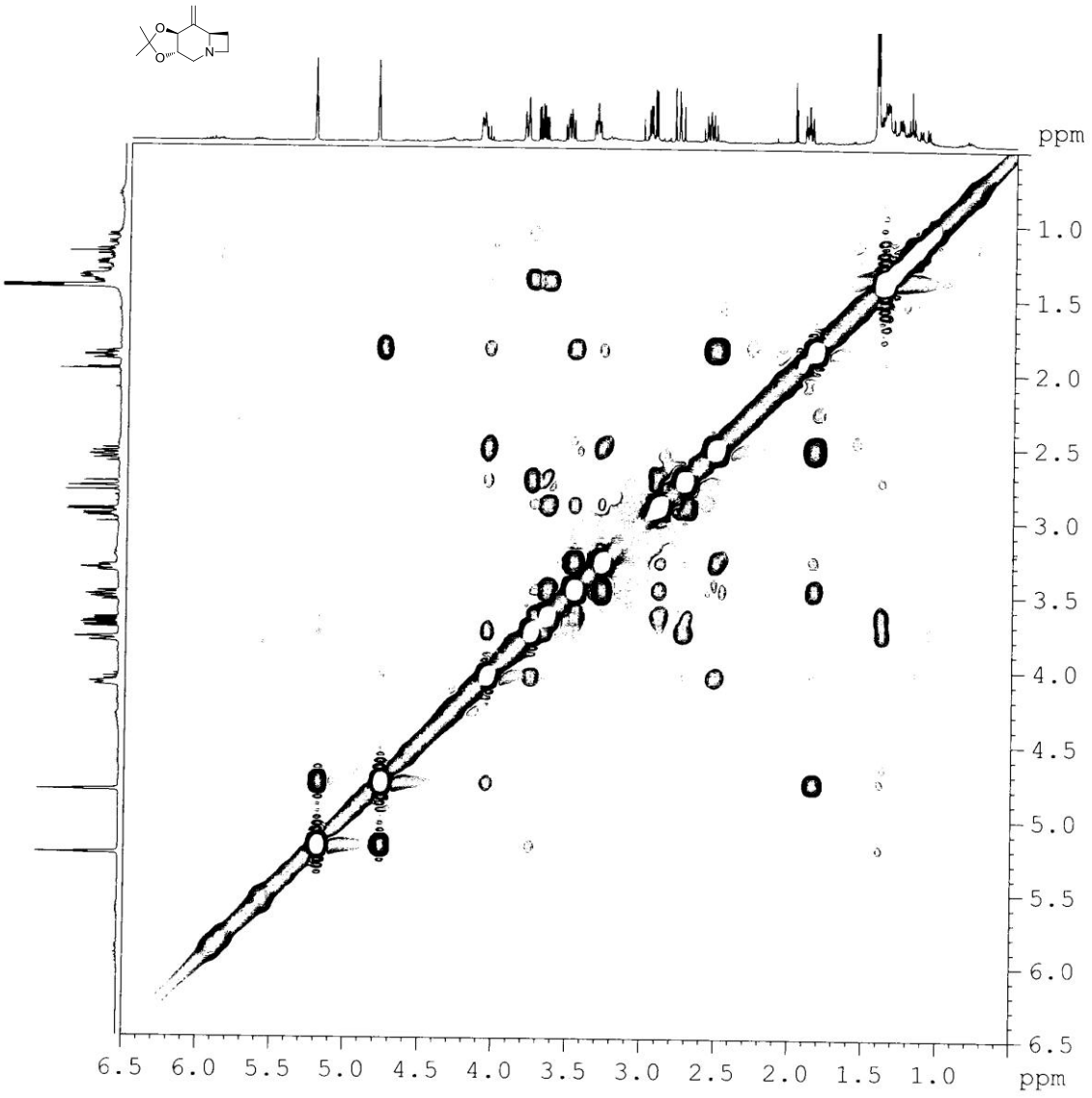
ppm
1.0
1.5
2.0
2.5
3.0
3.5
4.0
4.5
5.0
5.5
6.0
6.5
6.5 6.0 5.5 5.0 4.5 4.0 3.5 3.0 2.5 2.0 1.5 1.0
ppm

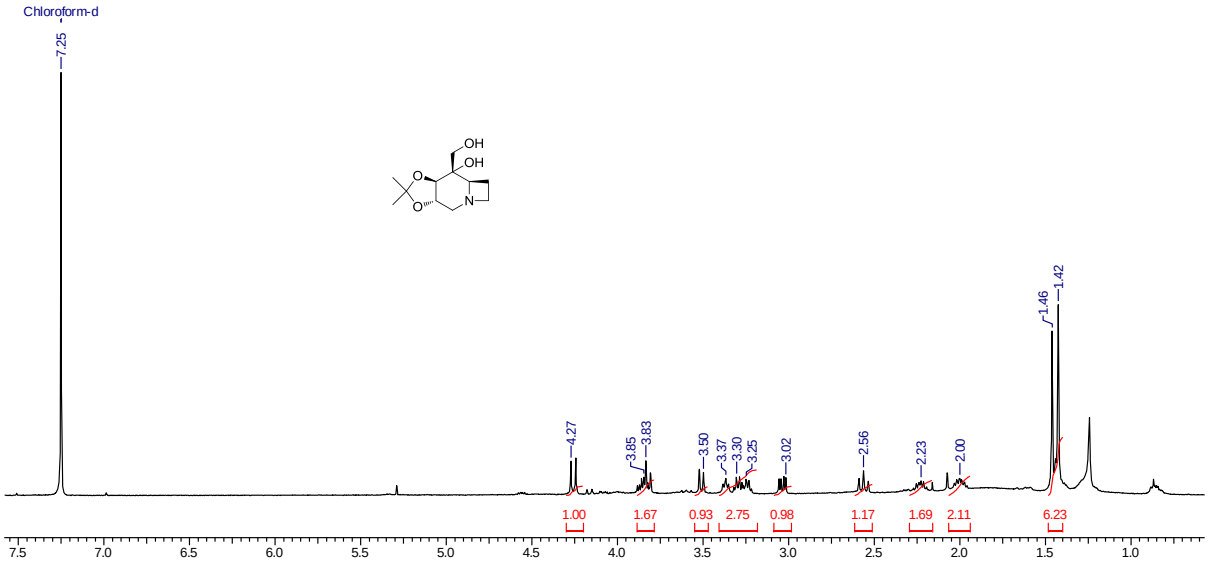
Chloroform-d
7.25
OH
OH
O
O
N
4.27
3.85
3.83
3.50
3.37
3.30
3.25
3.02
2.56
2.23
2.00
1.46
1.42
1.00
1.67
0.93
2.75
0.98
1.17
1.69
2.11
6.23
7.5
7.0
6.5
6.0
5.5
5.0
4.5
4.0
3.5
3.0
2.5
2.0
1.5
1.0

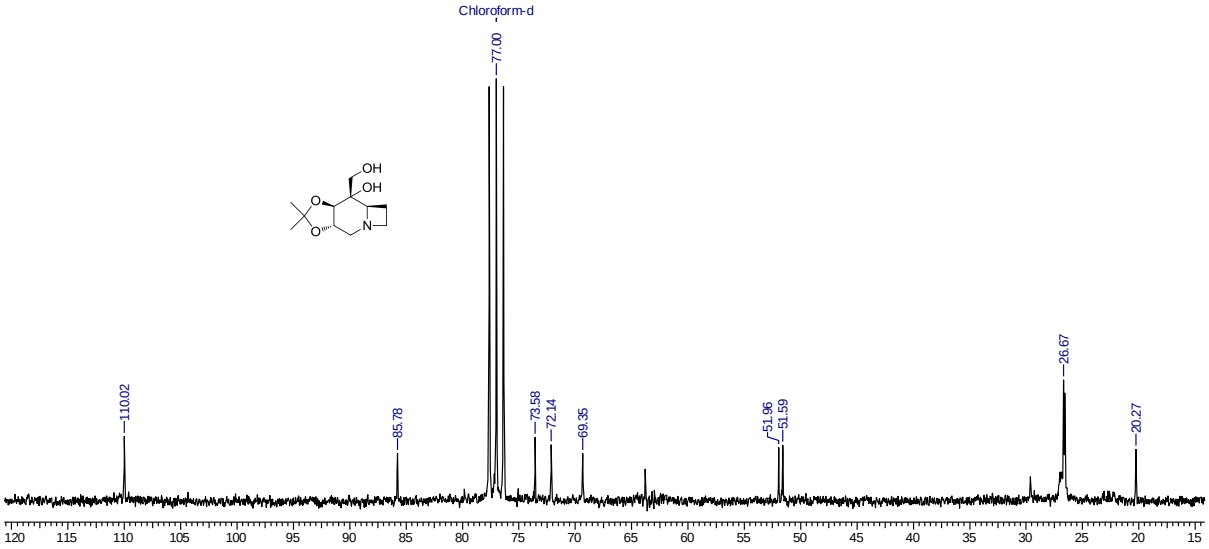
Chloroform-d
77.00
OH
OH
O
O
N
110.02
85.78
73.58
72.14
69.35
51.96
51.59
26.67
20.27
120
115
110
105
100
95
90
85
80
75
70
65
60
55
50
45
40
35
30
25
20
15

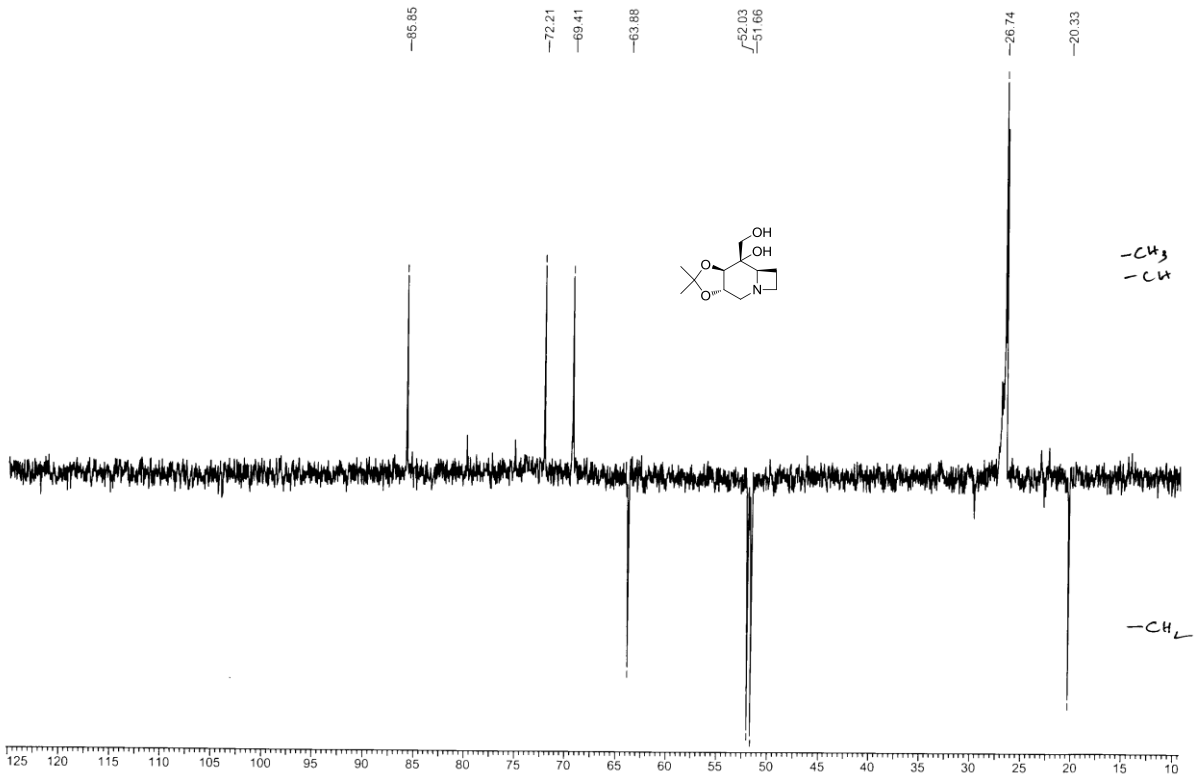
85.85
72.21
69.41
63.88
52.03
51.66
26.74
20.33
OH
OH
O
O
N
-CH3
-CH
-CH2
125 120 115 110 105 100 95 90 85 80 75 70 65 60 55 50 45 40 35 30 25 20 15 10

NOESY

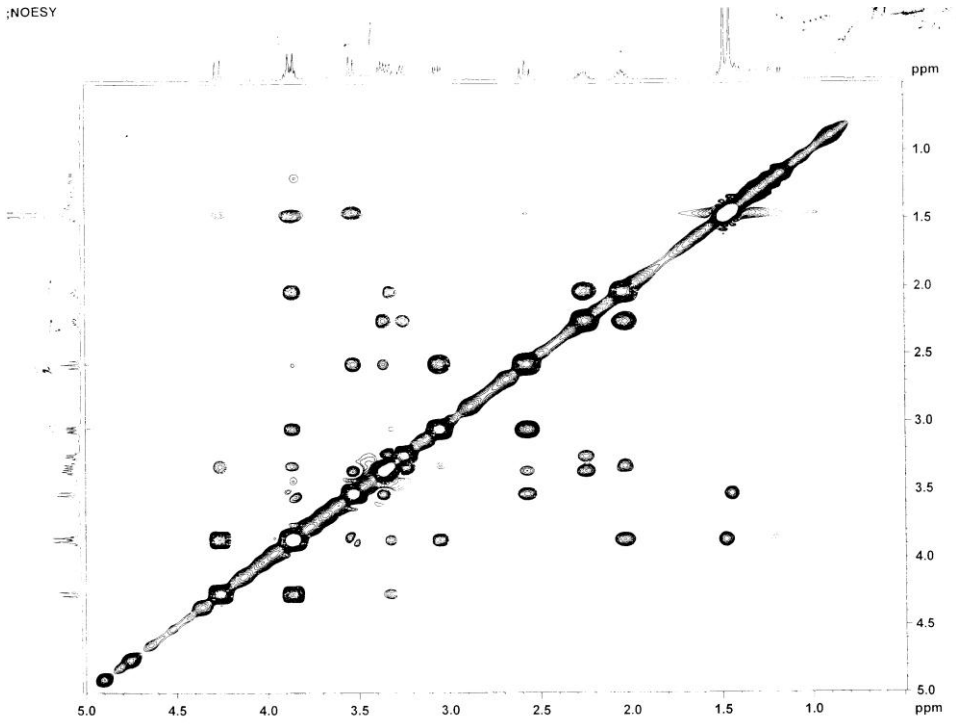
NOESY
ppm
1.0
1.5
2.0
2.5
3.0
3.5
4.0
4.5
5.0
5.0 4.5 4.0 3.5 3.0 2.5 2.0 1.5 1.0 ppm

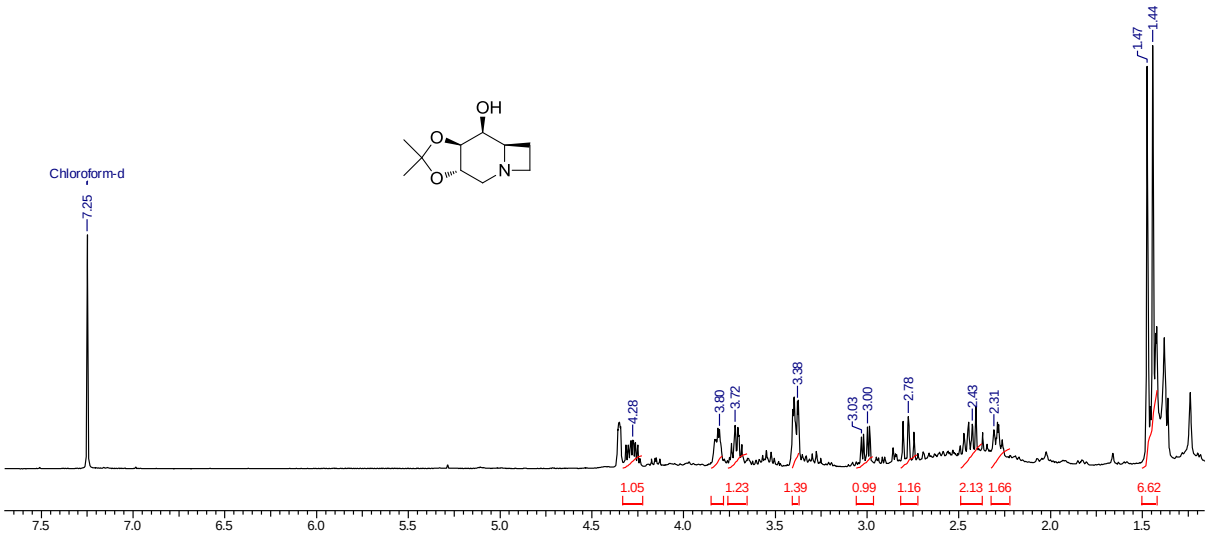
Chloroform-d
7.25
OH
O
O
N
4.28
3.80
3.72
3.38
3.03
3.00
2.78
2.43
2.31
1.47
1.44
1.05
1.23
1.39
0.99
1.16
2.13
1.66
6.62
7.5
7.0
6.5
6.0
5.5
5.0
4.5
4.0
3.5
3.0
2.5
2.0
1.5

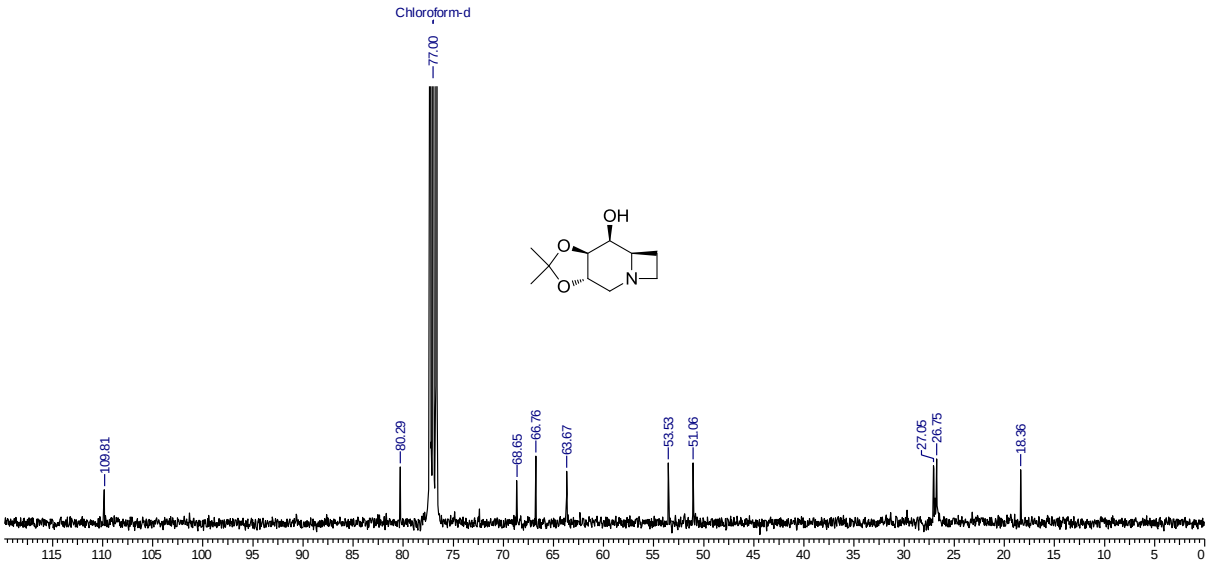
Chloroform-d
77.00
OH
O
O
N
109.81
80.29
68.65
66.76
63.67
53.53
51.06
27.05
26.75
18.36
115
110
105
100
95
90
85
80
75
70
65
60
55
50
45
40
35
30
25
20
15
10
5
0

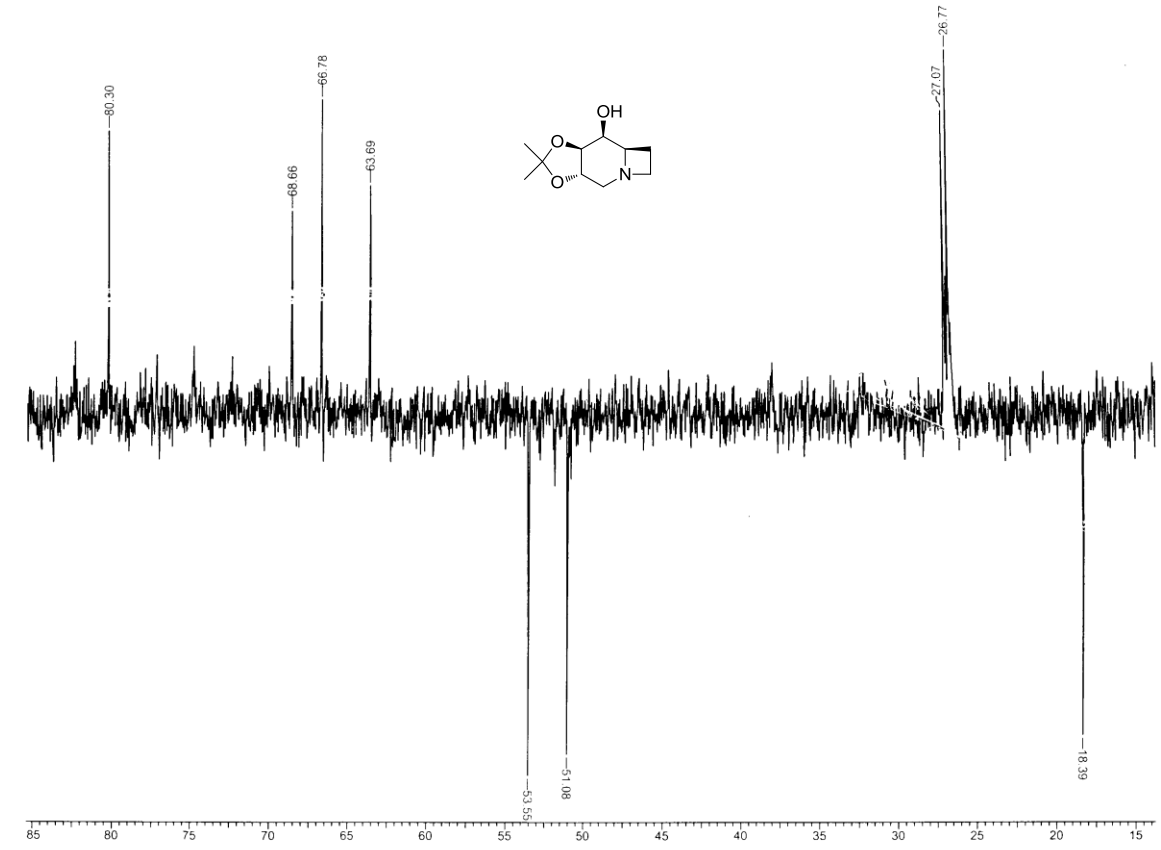
80.30
68.66
66.78
63.69
26.77
27.07
53.55
51.08
18.39
OH
O
O
N

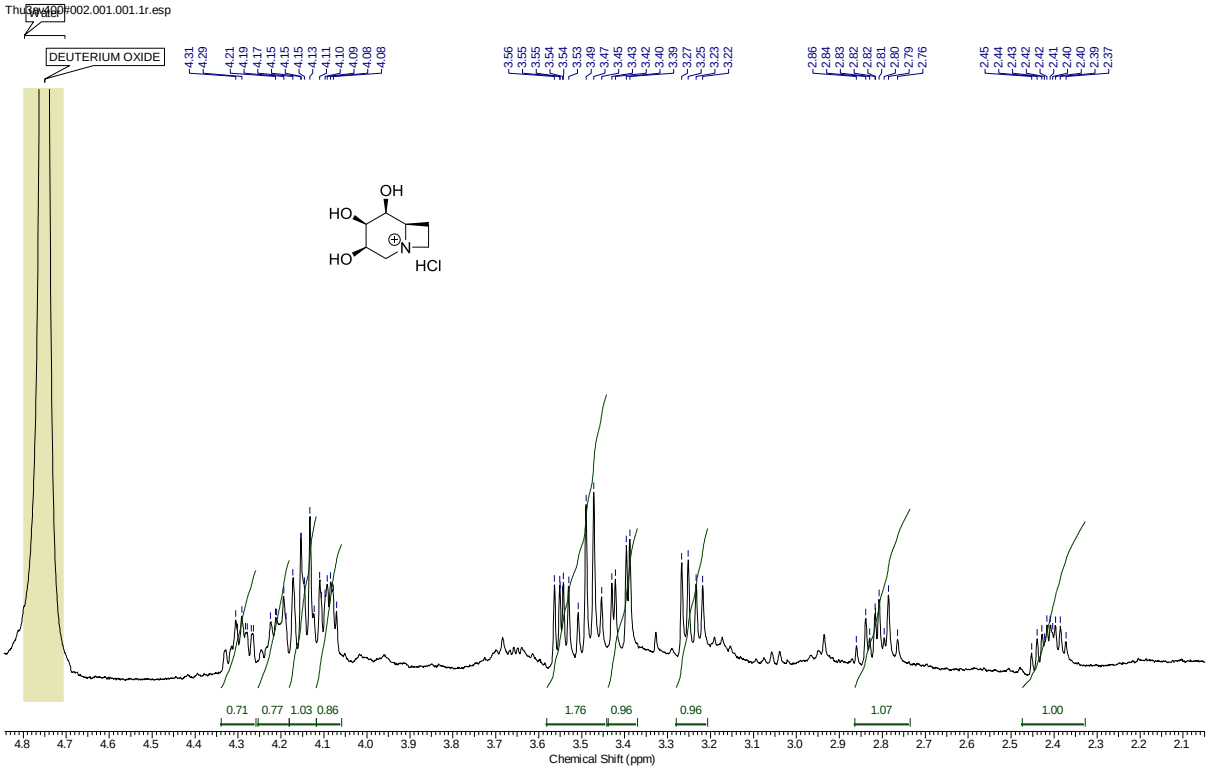
DEUTERIUM OXIDE
OH
HO
HO
HCl
0.71
0.77
1.03
0.86
1.76
0.96
0.96
1.07
1.00
Chemical Shift (ppm)

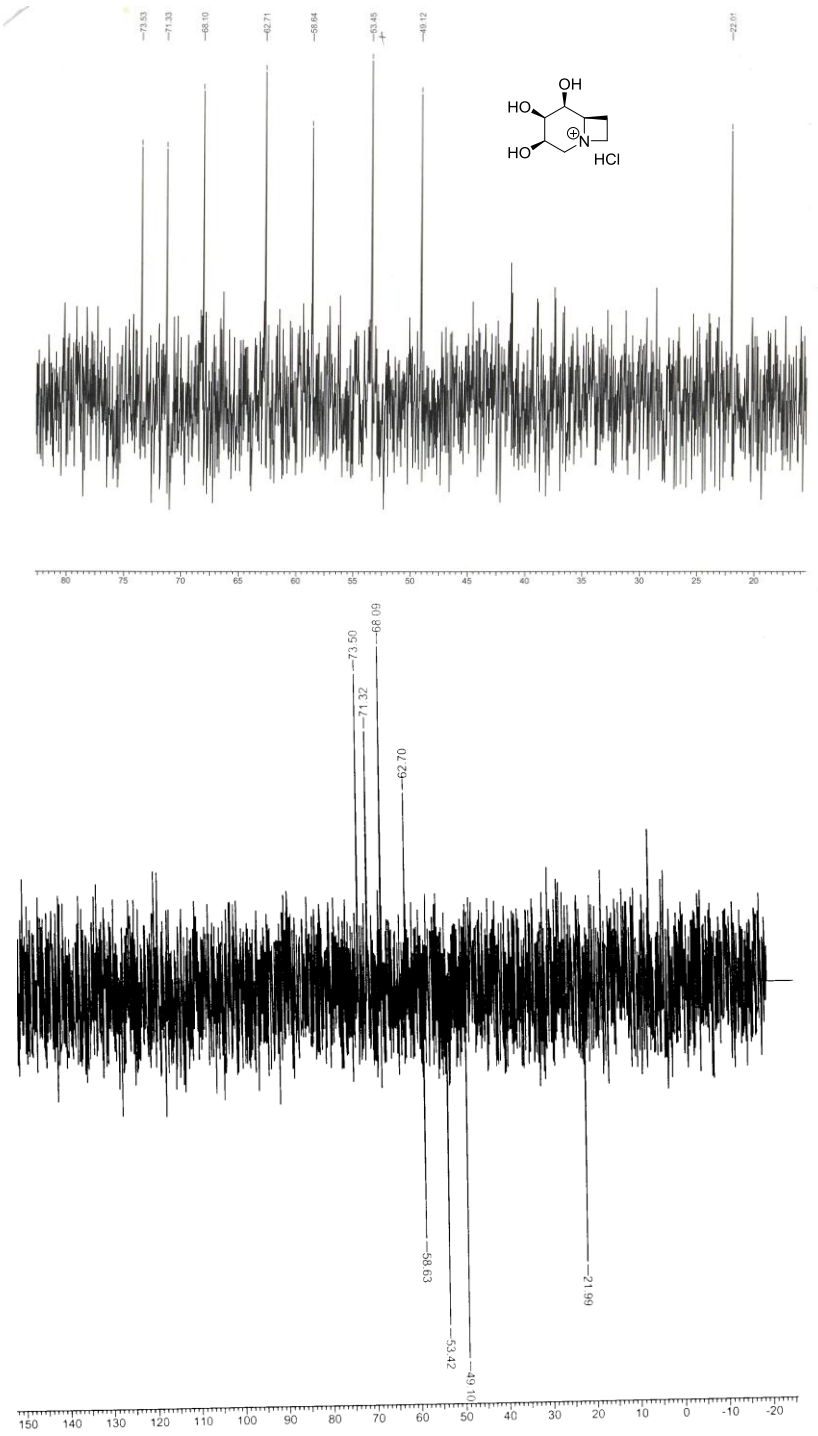
73.53
71.33
68.10
62.71
58.64
53.45
49.12
22.01
OH
HO
HO
N
HCl
80 75 70 65 60 55 50 45 40 35 30 25 20
73.50
71.32
68.09
62.70
58.63
53.42
49.10
21.99
150 140 130 120 110 100 90 80 70 60 50 40 30 20 10 0 -10 -20

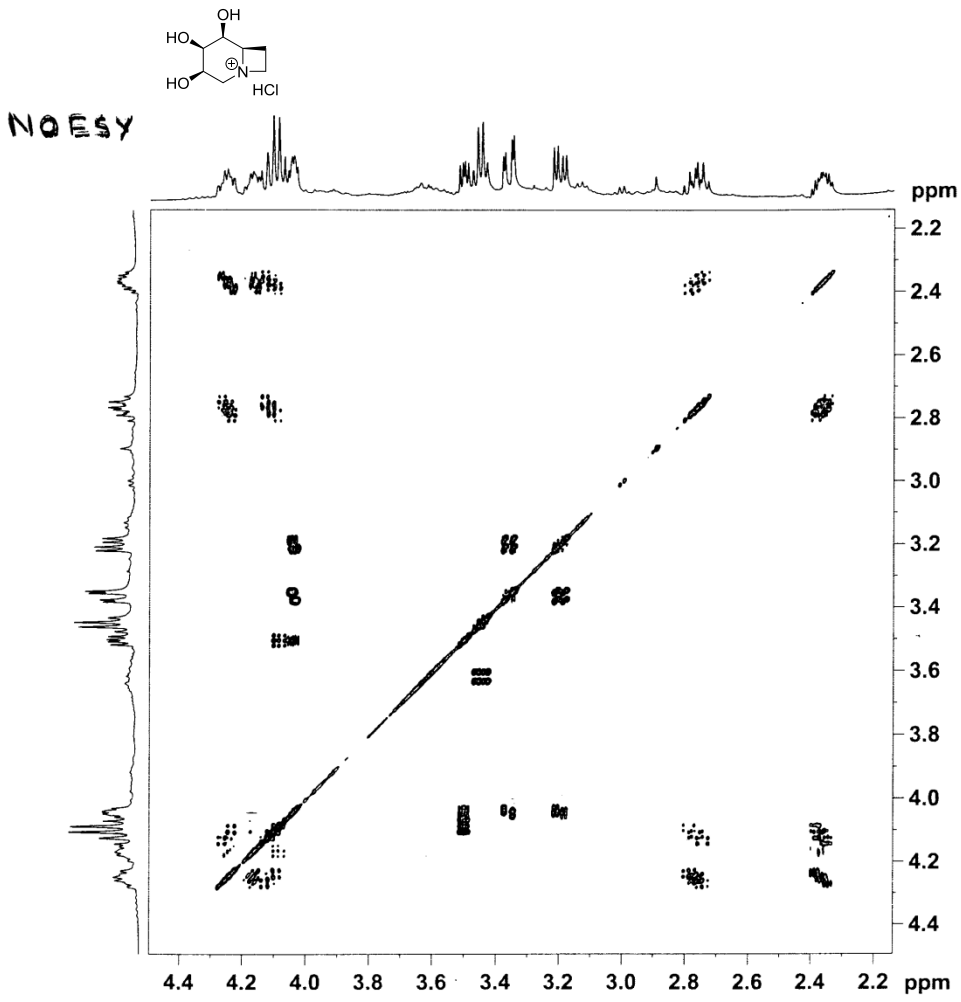
OH
HO
HO
N
HCl
NOESY
ppm
2.2
2.4
2.6
2.8
3.0
3.2
3.4
3.6
3.8
4.0
4.2
4.4
4.4 4.2 4.0 3.8 3.6 3.4 3.2 3.0 2.8 2.6 2.4 2.2 ppm

Enzymatic data for 86.HCl with β- glucosidase.

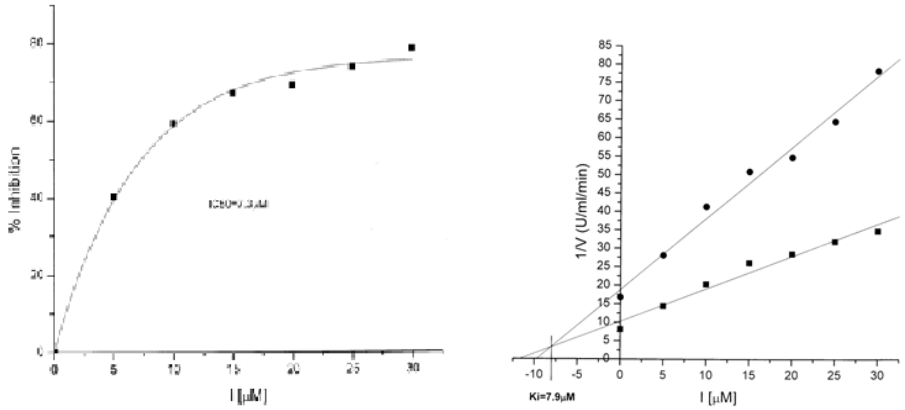

Enzymatic data for 86.HCl with β-galactoosidase.

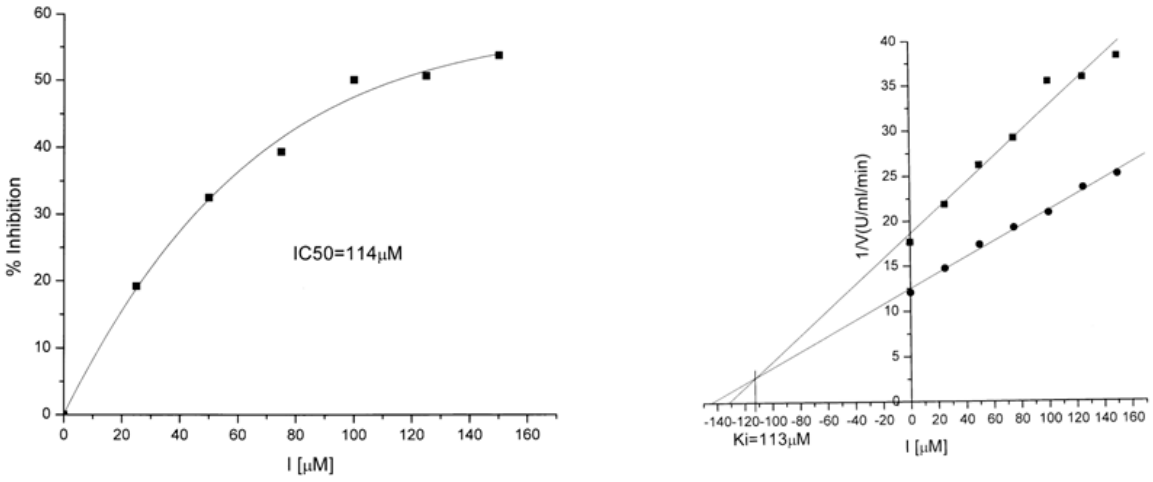

CHAPTER 3

Protecting group free Synthetic effort towards the (+)-223A

3.1 Introduction

The skin glands of amphibians are a major source of alkaloids used by them for chemical defence[1-2]. It has been reported that a wide range of alkaloids, over 20 structural classes and 500 alkaloids, are isolated from amphibian skin[3] where some of them have major biomedical impact[4-5]. Among these alkaloids, **223A**, the first member of a new trisubstituted indolizidine[6] class of amphibian alkaloids, was isolated by Daly and co – workers[4] from the skin extract of a *Panamanian* population of the frog *Dendrobates punilio Schmidt* in 1997 along with three higher homologous of **223A** (**Figure 1**). Recently, this alkaloid was shown to exhibit blocking effect on nicotinic acetylcholine receptors[7]. However, due to the scarcity of this alkaloid from natural sources, biological activities have still remained unexplored. Therefore, intensive synthetic studies have flourished towards the synthesis of these alkaloids during the past decades[8-13].

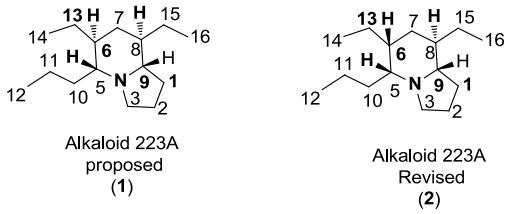

Figure 1

3.2 Literature reports:

The first total synthesis of **223A** (**1**) was attempted by Toyooka *et al*.[8] starting from (2*S*)-piperidone **3** by carrying out sequential conjugate addition of vinyl Grignard to the enaminoesters **4** and **7** followed by simple functional group transformations and cyclization as depicted in **Scheme 1**.

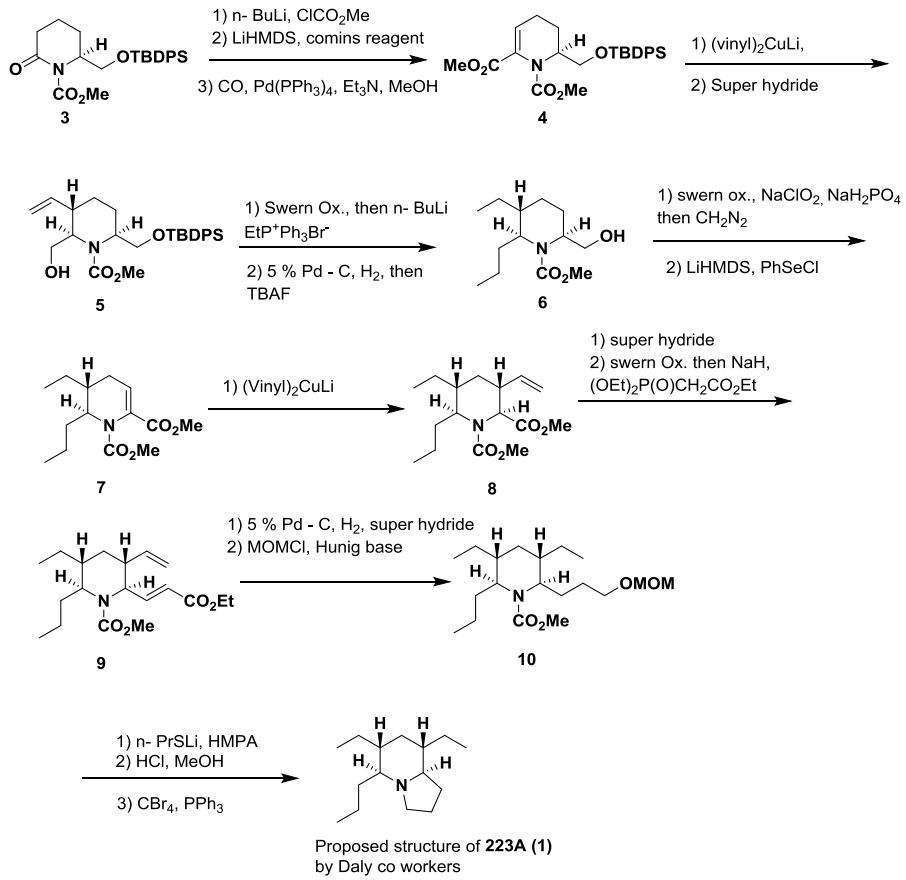

Scheme 1

However, comparison of the ^{1}H and ^{13}C NMR spectra of synthesized compound with naturally isolated **223A** turned out to be different having opposite ethyl configuration at C_6 position. Therefore, the structure of **223A** was revised as **2 (Figure 1)**. To complete the total synthesis of natural **223A** (**2**), the same has group modified their strategy as shown in **Scheme2**.

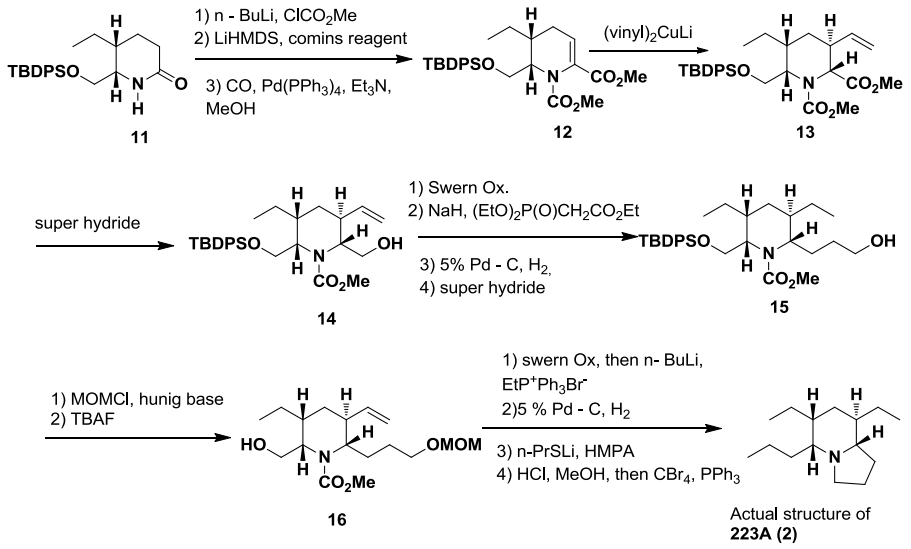

Scheme 2

Another synthesis of **223A** by Ma *et al*[9]. is reported by conjugate addition of (2*S*,3*R*)-3-amino-2-ethylhexanol (**20)**, obtained in several steps from (*E*)-2-ethylhex-2-enoic acid (**17**), to 7-(benzyloxy)hept-3-yn-2-one (**28)** followed by enamine cyclization to obtain **22** which on hydrogenation produced a mixture of isomers (**23**-**25**). The desired **25** was isolated and converted to **2** as shown in **Scheme 3** with overall 11.5% yield.

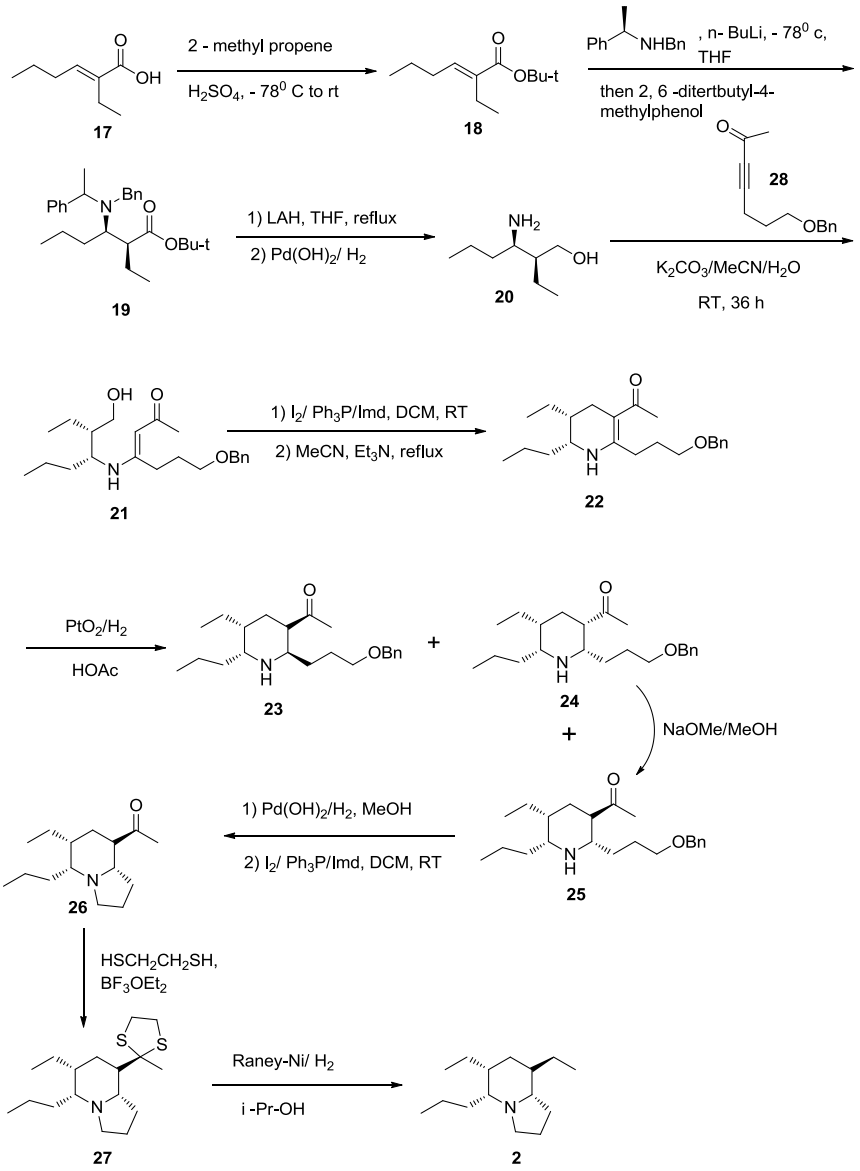

Scheme 3

Subsequently, another step economical synthetic strategy appeared by the same group[10] as shown in **Scheme 4**.

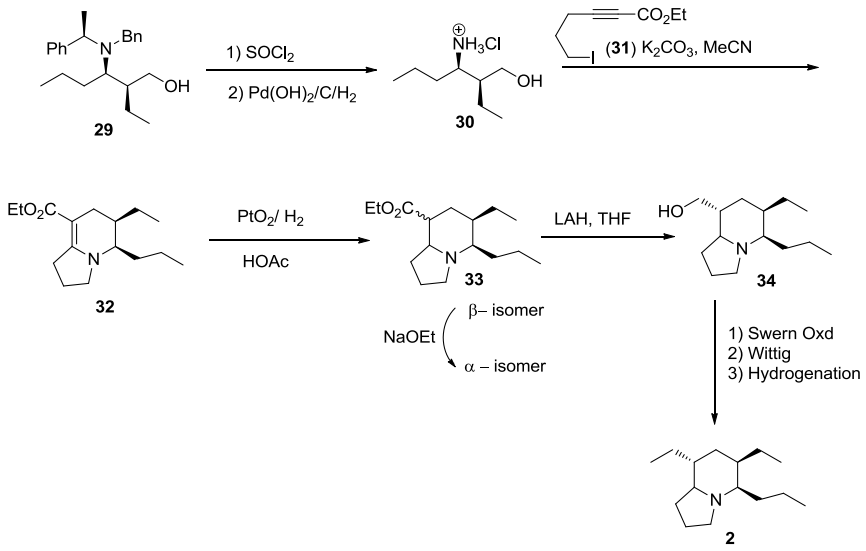

Scheme 4

Davis *et al.*[11] synthesized crucial precursor piperidone **38 (**58% yield) along with 14% minor **39** diastereoselectively by intramolecular aldol reaction of enamine **37A**, obtained by the reaction of *syn*-*α*-substituted-*β*-amino ketone (**37**) and crotonaldehyde. Compound **38** was transformed to **2** by ring closing metathesis followed by deoxygenation as shown in **Scheme 5**.

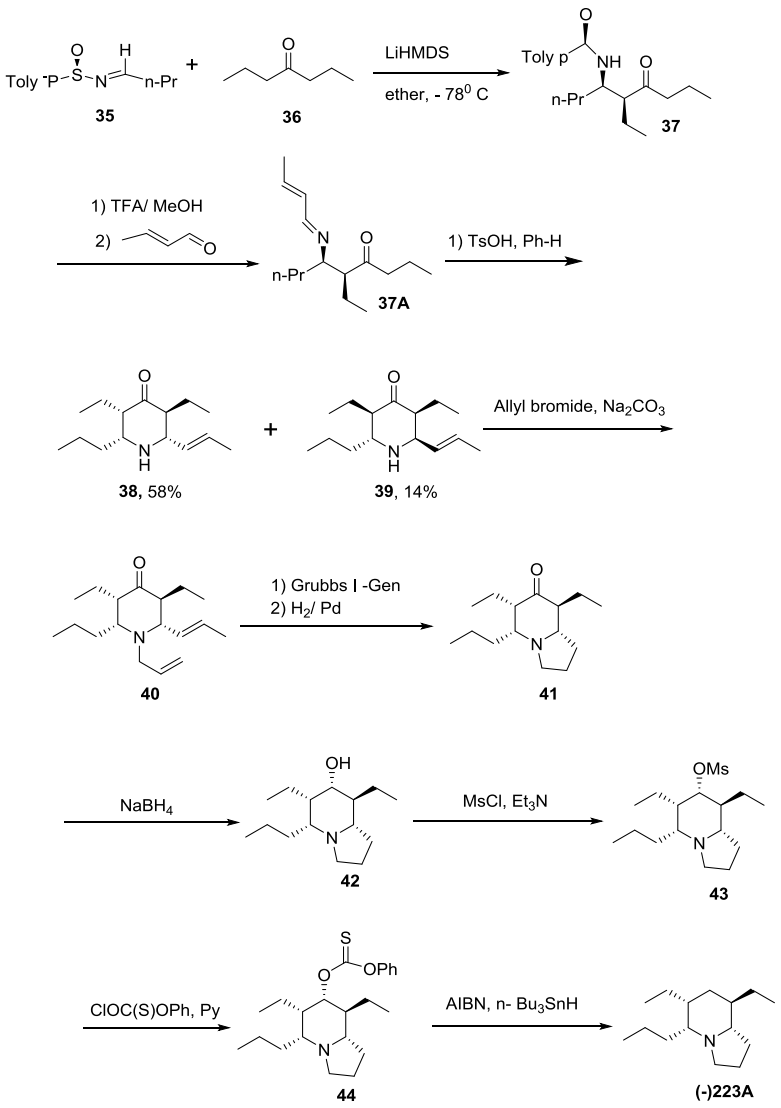

Scheme 5

Aube *et al.*[12] reported shortest synthesis of **2** by ring opening metathesis of **50**, obtained by Schmidt reaction of **49**, using Grubbs-Hoveyda catalyst followed by simple reaction sequence as shown in **Scheme 6**.

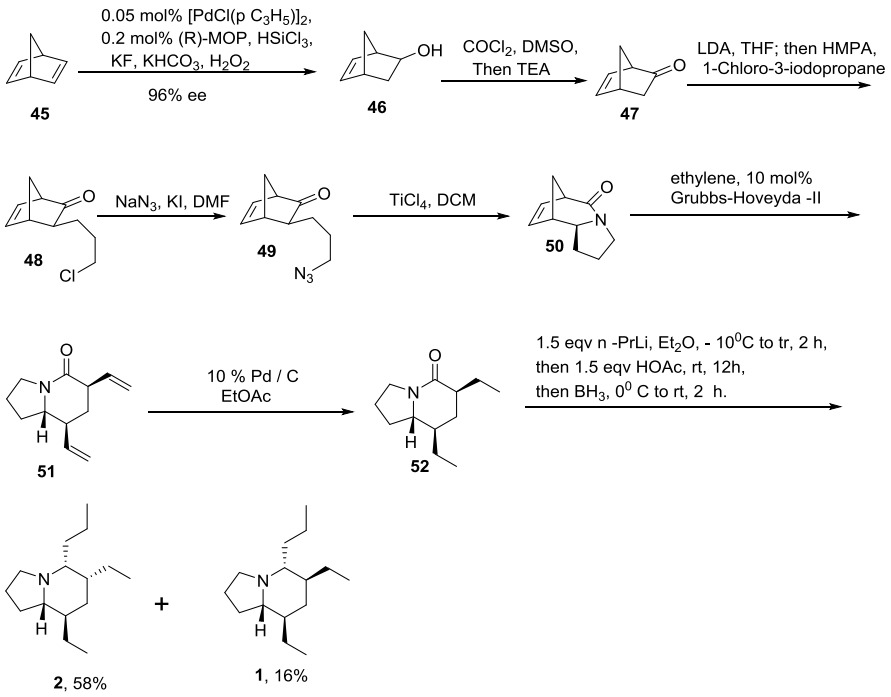

Scheme 6

Based on above introductory remarks on synthetic routes for **223A**, it becomes apparent that most of the synthetic approaches have elaborated on chiral tetrasubstituted piperidine to construct indolizidine core of the alkaloid. Although, some of the synthetic routes reported are attractive, more concise and versatile strategy is required to obtain this biologically active alkaloid in short steps.

Our success of synthesizing 7-aza bi-cyclic core by utilizing α-silylmethylamine radical cation cyclization (**Chapter 2**) encouraged us to evaluate the application of this strategy in the synthesis of indolizidines **(+)-223A** alkaloid. We envisioned that the stereoselective construction of C_9 and C_8 bond (1, 6-*trans* stereochemistry) could be made possible by the PET cyclization[14] of **61** which in turn could be synthesized from **58** and **59**. The optically active **58** could be synthesized by Grignard addition to the Wienreb amide **56**. The intermediate **55** could be easily obtained by performing Evan's alkylation[15] on **54** (**Scheme 7**).

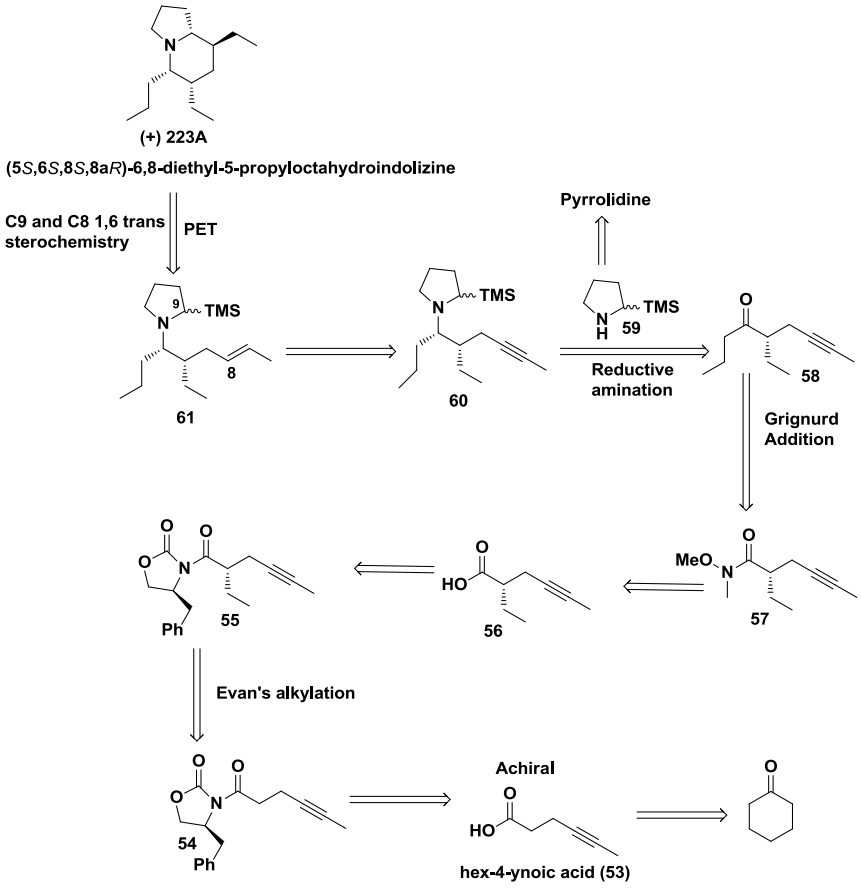

Scheme 7

3.3 Result and Discussion:

We initiated the synthesis of **2** from 4–hexynoic acid (**53**) which was synthesized by following the reported protocol[16] as depicted in **Scheme 8**. Coupling of **53** with

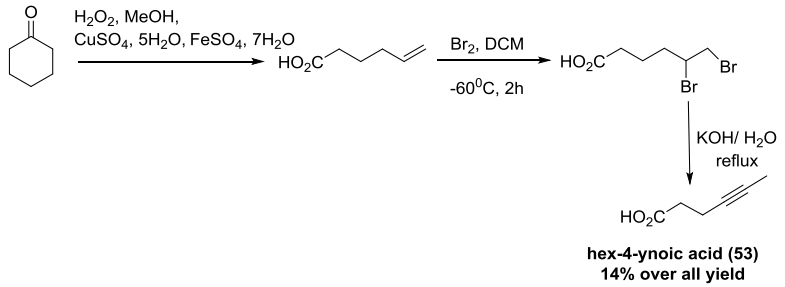

Scheme 8

(*S*)-4-benzyloxazolidin-2-one produced **54** (56% yield). Alkylation of **54** using ethyltriflate in the presence of NaHMDS as a base produced **55** in 42% yield (*de* = 96:4). The methyl protons of the ethyl group appeared in ^{1}H NMR at δ 0.95 (t, *J* = 7.46 Hz, 3H) and newly generated chiral methine proton appeared at δ 3.71 (m, 1H) indicating the success of asymmetric alkylation. The structure and stereochemistry of **55** was completely established by 2D NMR (HMBC, HSQC) spectral analysis.

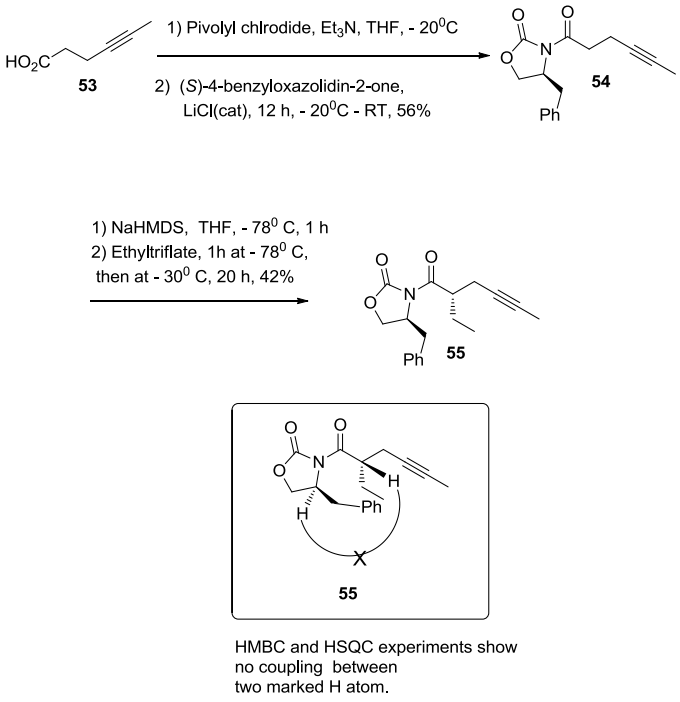

Scheme 9

Removal of the chiral auxilary from **55** by treating with LiOH/H_2O_2 at –10° C gave **56** which was subsequently converted to Wienreb amide **57**. Addition of the *n*-propyl magnesiumchloride to **57** afforded optically pure **58** (90 %, **Scheme 10**).

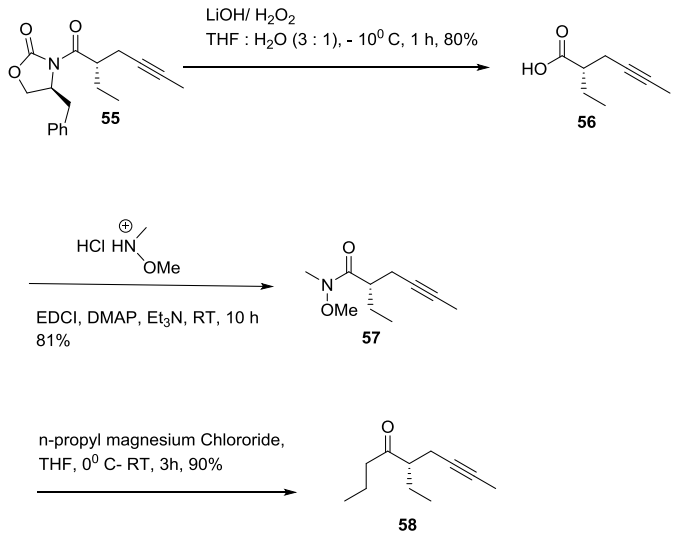

Scheme 10

The other counterpart **59** was synthesized (over all 60%) from pyrrolidine by following our established protool[17] as shown in **Scheme 11**.

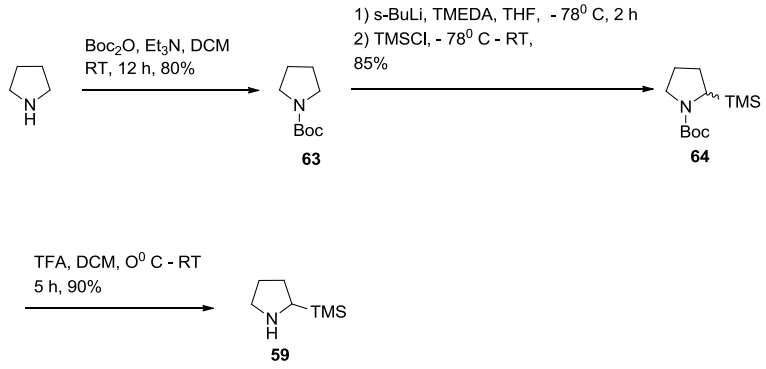

Scheme 11

Having obtained both coupling partners **58** as well as **59**, we attempted their coupling by reductive amination in the presence of $NaBH(OAc)_3$, however, to our dismay the expected **60** could not be isolated even by following repeated optimization (**Table 1**).

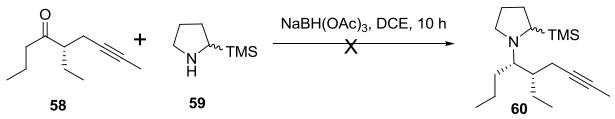

Scheme 12

Table 1 Different reductive amination condition

Entry	Condition	Remark
1	$NaBH(OAc)_3$, DCE, pH = 5, 24 h, RT	Only starting material recovered
2	TFA, DCM, 24 h, RT	**60** not formed
3	$InCl_3$, Et_3SiH, MeOH, 8 h, RT	**60** not formed
4	$SiCl_2$, $NaBH_3CN$, 18 h, RT	Sign of TMS group expulsion was observed in the isolated product.
5	2, 2, 2 –trifluroethanol, $NaBH_3CN$, reflux	Similar sign of TMS group expulsion was observed in the isolated product.
6	$NaBH(OAc)_3$, EDC, AcOH (2eqv)	Starting material recovered
7	$TiCl_4$, Et_3N, THF, RT	Starting material consumed but **60** could not able to isolate

This unanticipated failure led us to utilize **62** as a precursor for reductive amide alkylation to obtain **60** by following Huang *et al.*[18] protocol. The required **62** was synthesised by coupling of **56** and **59** utilizing EDCI.HCl as an amidating reagent (**Scheme 13**). Reaction of **62** with *n*-propylmagnesium (1M THF solution) at -78° C followed by sodium borohydride reduction of resultant imine produced **60** as a mixture of diastereomers. Further diastereomeric ratio of **60** is calculated by HPLC analysis is in under progress.

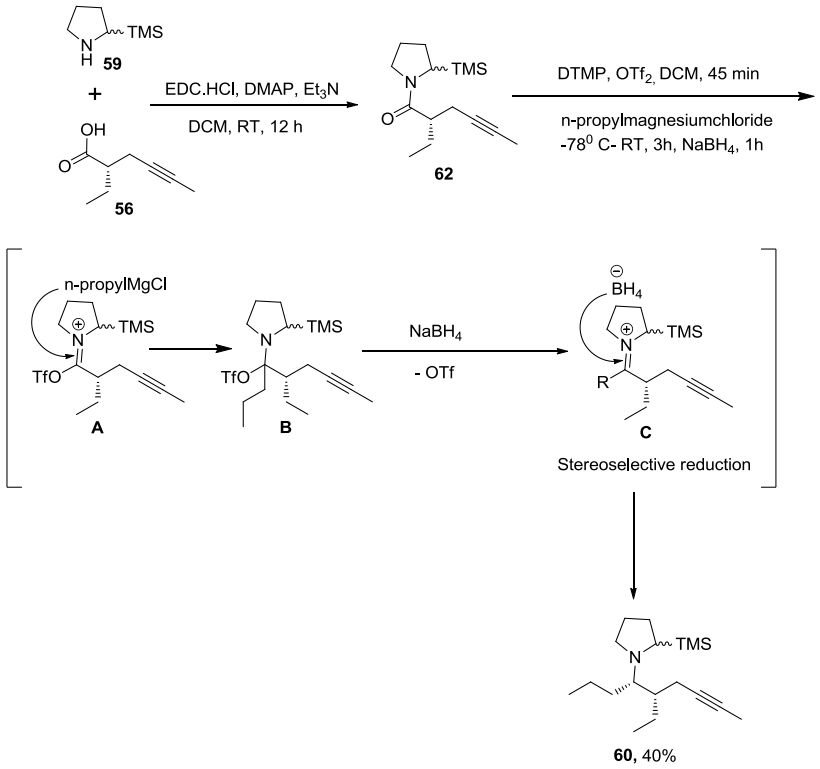

Scheme 13

Due to time constrains, the synthesis of (+)-**223A** has to be curtailed at this stage for the time being. Hopefully the synthesis would be concluded by following the remaining steps (**Scheme 14**).

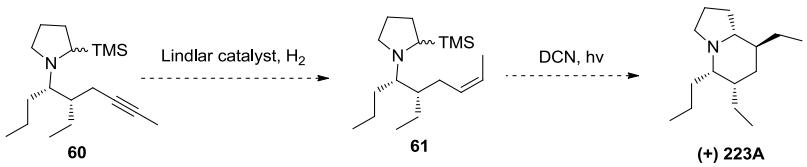

Scheme14

3.4 Summary:

In conclusion an advance precursor **60**, has been synthesized and further study to complete the synthesis of (+)-**223A** is in progress.

3.5 References:

1) Rodrıguez A; Poth D; Schulz S; Vences M. **2011**. Discovery of skin alkaloids in a miniaturized eleutherodactylid frog from Cuba.*Biology Letters*, *7*, 414-418.

2) Vences M; Schulz S; Poth D; Rodriguez A. **2011**. Defining frontiers in mite and frog alkaloid research.*Biology Letters*.*7*, 557.

3) Daly, J. W.; Spande, T. F. Alkaloids: Chemical and Biological Perspecti Ves; Pelletier S. W., Ed.; John Wiley & Sons: New York, **1986**; Vol. *4*, pp 1- 274.

4) a) Garraffo, H. M.; Jain, P.; Spande, T. F.; Daly, J. W. *J. Nat. Prod*. **1997**, *60*, 2–5.

5) Mitchinson, A..; Nadin. A. *J. Chem. Soc. Perkin. Trans 1*, **2000**, 2862.

6) a) Michael, J. P. Nat. Prod. Rep. **2007**, *24*, 191–222.; b)Michael, J. P. Simple indolizidine and quinolizidine alkaloids. In *The Alkaloids, Chemistry and Pharmacology;* Cordell, G., Ed.; Academic Press: New York, **2001**; pp 91–258.

7) a) Tsuneki, H.; You, Y.; Toyooka, N.; Kagawa, S.; Kobayashi, S.; Sasaoka, T.; Nemoto, H.; Kimura, I.; Dani, J. A. Mol. Pharm. **2004**, *66*, 1061–1069. (b) Katavic, P. L.; Venables, D. A.; Rali, T.; Carroll, A. R. J. Nat. Prod. **2007**, *70*, 872–875.

8) a)Toyooka, N.; Fukutome, A.; Nemoto, H.; Daly, J. W.; Spande, T. F.; Garraffo, H. M.; Kaneko, T. Org. Lett. **2002**, *4*, 1715–1717.

9) Pu, X.; Ma, D. J. Org. Chem. **2003**, *68*, 4400–4405.

10) Davis, F. A.; Yang, B. J. Am. Chem. Soc. **2005**, *127*, 8398–8407.

11) Zhu, W.; Dong, D.; Pu, X.; Ma, D. Org. Lett. **2005**, *7*, 705–708.

12) Ghosh. P; Judd. W. R; Ribelin. T; Aubè. J. *Org. Lett*. 2009, *11*, 4140.

13) Fellah. M; Lhommet.G; Mansuy.V. M. *Eur. J. Org. Chem*. **2012**, 463.

14) Pandey. G.; Devi Reddy. G. *Tetrahedron Lett*. *33*(43), 6533, **1992**

15) Evans D.A., Aldrichimica Acta, **1982**, *15*, 23; b) Ager D.J., Prakash I., Schaad D.R., Aldrichimica Acta, **1997**, *30*, 3.

16) E. K. Starostin, A. V. Ignatenko, M. A. Lapitskaya, K. K. Pivnitsky, G. I. Nikishin, *Russ. Chem. Bull. Int. Ed.***2001**, *50*, 833.

17) Pandey, G.; Dumbre, S. G.; Pal, S.; Khan, M. I.; Shabab, M. *Tetrahedron*, **2006**,*63*, 4756.

18) K. J. Xiao, J. M. Luo, K. Y. Ye, Y. Wang, P. Q. Huang, *Angew. Chem. Int. Ed*. **2010**, *49*, 3037-3040.

3.6 EXPERIMENTAL

Synthesis of 4 –Hexnoic acid (53):

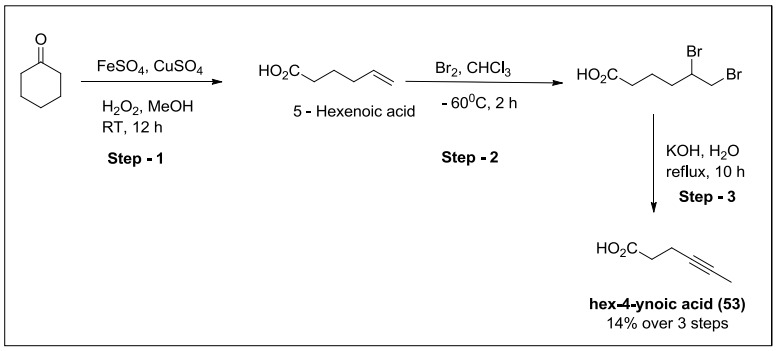

Step - 1

Hydrogen peroxide (227 mL, 30% aquous solution, 2 mol) was added over 30 min at 20 – 25 °C to a stirred solution of cyclohexanone (98 g, 1 mol) in MeOH (100 mL). The mixture was added to a stirred solution of ferrous sulphate heptahydrate (278 g, 1 mol) and cupric sulphate pentahydrate (250 g, 1 mol) in water (1.8 L), maintaining the reaction mixture at 18 – 20 °C. The reaction mixture was allowed to stir for 12 h at room temperature. The aqueous phase was separated and extracted with ethylacetate (3 X 300 mL). The organic phase was washed with 20% aq NaOH (3 X 200 mL). The alkaline extract was acidified with 20 % sulphuric acid to pH = 2 and extracted with ethylacetate (3 X 300 mL). The removal of solvent under reduced pressure produced 5-hexenoic acid (16.1 g as crude) as brownish liquid and proceeds for next step.

Step - 2

To a solution of 5–hexenoic acid (16.6 g, 145.5 mmol) in DCM (150 mL) was slowly added bromine (23.7 g, 146.9 mmol, 7.6 mL in 20 mL DCM) at –60 °C and the mixture was stirred for 2 h. The reaction was quenched at same temperature by saturated $Na_2S_2O_3$ solution (20 mL) with vigorous stirring. The aqueous layer was extracted with ethylacetate (2 X 100 mL). The combined organic layers were washed with brine, dried over anhydrous Na_2SO_4 and concentrated to obtain 5, 6 –dibromohexanoic acid as a deep reddish liquid, forwarded to next step.

Step - 3

The crude 5, 6–dibromohexanoic acid(38.4 g, 141.7 mmol) was treated with KOH (81 g, 1470 mmol) in water (132 mL) under reflux for 10 h. The reaction mixture was cooled to room temperature and was acidified with conc. HCl to pH = 3 and aqueous layer was extracted with ethylacetate (3 X 300 mL). The organic layer was dried over anhydrous Na_2SO_4 and was evaporated under reduced pressure. The residue was purified by column chromatography (silica gel, 15% ethylacetate/pet- ether) to afford 4 –Hexnoic acid (**53**, 8.2 g, 14% yield after three steps) as white solid product.

^{1}H NMR (400 MHz, $CDCl_3$) δ ppm: 9.2 (bs, 1H), 2.55 (m, 4H), 1.75 (t, *J* = 2.32 Hz, 3H); **^{13}C NMR (100 MHz, $CDCl_3$) δ ppm:** 178.3, 76.8, 76.5, 33.7, 14.9, 3.43. **HRMS:** Calc mass for $(M - H)^- C_6H_7O_2$: 111.0444, found 111.0451.

Synthesis of (*S*)-4-benzyl-3-(hex-4-ynoyl) oxazolidin-2-one (54):

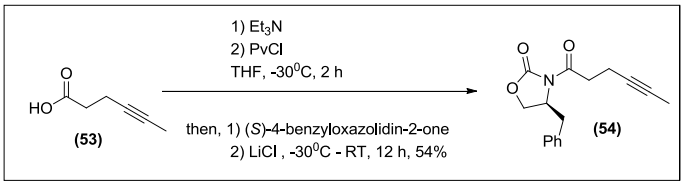

To a stirring solution of **53** (0.56 g, 5 mmol) in THF (25 mL) was added triethylamine (2.02 g, 20 mmol, 2.8 mL). To this mixture pivolyl chloride (0.623 g, 5.2mmol, 0.6 mL) was added at -20°C. The reaction mixture was allowed to stir for 2 h at same temperature. (*S*)-4–benzilidineone (0.9 g, 5.1 mmol, dissolved in 10 mL THF) was added slowly to the reaction mixture followed by LiCl (0.21 g, 5 mmol) at – 20 °C. The reaction mixture was slowly allowed to come to room temperature and stirred for another 12 h before the addition of saturated $NaHCO_3$ solution. The aqueous layer was partitioned and extracted by ethylacetate (3 X 100 mL). The organic layer was washed with brine and dried over anhydrous sodium sulphate before concentrating under reduced pressure. The resultant brown thick mass was column purified (silica gel, 10% ethylacetate /pet –ether eluent) to afford **54** (0.75 g, 56%) as a pale yellow liquid.

^{1}H NMR (400 MHz, $CDCl_3$) δ ppm: 7.33-7.18 (m, 5H), 4.70-4.68 (m, 1H), 4.18-4.01 (m, 3H), 3.22 (dd, *J* = 13.3, 2.9 Hz, 1H), 3.16-3.10 (m, 1H), 2.84-2.72 (m, 1H), 2.51 (m, 2H), 1.75 (t, *J* = 2.32 Hz, 3H); **^{13}C NMR (100 MHz, $CDCl_3$) δ ppm:** 171.6, 153.3, 135.1, 129.3,

128.9, 127.3, 126.7, 77.4, 76.5, 66.27, 55.0, 37.7, 35.28, 13.81, 3.47 ; **HRMS:** Calc mass for $[M + H]^+$ $C_{16}H_{17}NNaO_3$: 294.1106, found 294.1105; $[\alpha]^{27}_D$ = + 76.41°.

Synthesis of (*S*)-4-benzyl-3-((*S*)-2-ethylhex-4-ynoyl)oxazolidin-2-one (55):

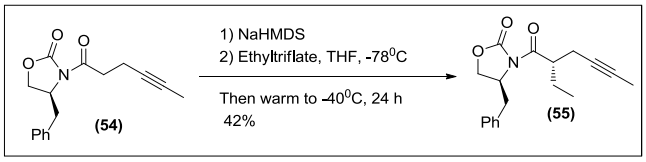

To a stirring solution of **54** (1.25 g, 4.75 mmol) in THF (50 mL) was added NaHMDS (5.6 mmol, 1 M THF solution, 5.6 mL) at - 78°C. The resulting reaction mixture was stirred for additional 1 h at same temperature; ethyltrifluoromethanesulphonate (5.0 g, 32.5 mmol in 10 mL THF) was added drop wise and further allowed stirring for 1 h at same temperature. After 1 h, reaction mixture was allowed to warm to - 40° C and was stirred for additional 20 h at -40° C. After maximum starting material had disappeared (monitored by TLC), the reaction was quenched by saturated NH_4Cl solution. The aqueous layer was extracted by ethylacetate (3 X 100 mL). The organic layer was washed with brine and dried over anhydrous sodium sulphate before evaporating under reduce pressure to afford **55** as a pale reddish liquid. The crude mixture was purified by column chromatography (silica gel, 7% ethylacetate-pet – ether) to obtain pure **55** (0.57 g, 42%) as a pale yellow liquid.

^{1}H NMR (400 MHz, $CDCl_3$) δ ppm: 7.33-7.18 (m, 5H), 4.73-4.69 (m, 1H), 4.18-4.15 (m, 2H), 3.88 (m, 1H), 3.34-3.28 (dd, *J* = 13.3, 3.5 Hz, 1H), 2.70 (dd, *J* = 13.3, 9.1 Hz, 1H), 2.41 (m, 2H), 1.80- 1.70 (m, 5H), 0.95 (t, *J* = 7.46 Hz, 3H); **^{13}C NMR (100 MHz, $CDCl_3$) δ ppm:** 174.9, 153.0, 135.2, 129.2, 128.7, 127.1, 77.6, 76.0, 65.9, 55.3, 43.5, 37.9, 24.5, 20.5, 10.8, 3.4; **HRMS:** Calc mass for $C_{18}H_{21}NNaO_3$: 322.1419, found 322.1423; **HPLC:** *The diasteromeric excess* (*de*) = 96%, by using column: Kromasil RP-18, mobile phase; acetonitrile : water = 50 : 50, flow rate 1.0 mL/ min, wavelength = 230 nm.; $[\alpha]^{27}_D$= + 70.38°.

Synthesis of (*S*)-2-ethylhex-4-ynoic acid (56):

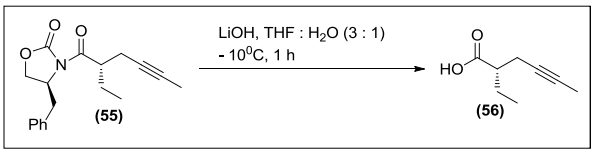

To a solution of **55** (5.1 g, 17.06 mmol) in 3:1 THF – water solution was added slowly LiOH (820 mg, 34 mmol) at – 10°C. To this reaction mixture 30 % aqueous solution of H_2O_2 (6.5 mL, 136 mmol) was added slowly over the period of 20 minute at same temperature. After completion of H_2O_2 addition, the reaction was allowed to stir for another 1h at – 10°C. After 1 h the reaction mixture was carefully quenched by Na_2SO_3 (2.0 g in 10 mL water) and 10 mL saturated $NaHCO_3$ solution was added. After complete basification was over, the reaction mixture was washed with ethylacetate and the water layer was carefully acidified by 2 (N) HCl (until pH = 2). The resulting mixture was extracted by ethylacetate (3 X 100 mL). The organic layer was dried over anhydrous sodium sulphate and the solvent was evaporated under reduce pressure to afford crude **56** (1.92 g, 80%) as a white solid product. The crude mixture was pure enough to carry forward to next step.

^{1}H NMR (400 MHz, $CDCl_3$) δ ppm: 7.71 (bs, 1H), 2.51 -2.41 (m, 3H), 1.75 (m, 5H), 0.94 (t, *J* = 7.51 Hz, 3H); **HRMS:** Calc mass for $C_8H_{12}NaO_2$: 163.0735, found 163.0727.

Synthesis of (*S*)-2-ethyl-N-methoxy-N-methylhex-4-ynamide (57):

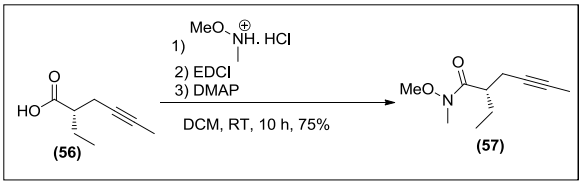

A solution of **56** (0.4 g, 2.8 mmol), DMAP (0.6 g, 0.56 mmol), Wienreb amine hydrochloride salt (0.45 g, 4.2 mmol), EDCI.HCl **(**0.85 g,4.2mmol) and triethylamine (0.51 g, 5 mmol, 0.7 mL) in 50 mL DCM at room temperature was allowed to stir for 8 h. After maximum disappearance of **56** (monitored by TLC), the reaction mixture was diluted by water and was

extracted by ethylacetate (3 X 100 mL). The organic layer was washed with dilute solution of $KHSO_4$ and brine, respectively. The organic layer was dried over Na_2SO_4 and evaporated to obtain reddish liquid which on column chromatography (silica gel, 10% ethylacetate/Pet ether) afforded **57** (0.38 g, 75%) as a pale yellow liquid.

^{1}H NMR (400 MHz, $CDCl_3$) δ ppm: 3.71 (s, 3H), 3.22 (s, 3H), 2.96 (m, 1H), 2.45 -2.15 (m, 2H), 1.74 (t, *J* = 2.32 Hz, 3H), 1.68 (m, 2H), 0.94 (t, *J* = 7.46 Hz, 3H); **^{13}C NMR (100 MHz, $CDCl_3$) δ ppm:** 76.8, 76.4, 61.3, 42.1, 32.1, 25.0, 21.5, 11.5, 3.4.; **Mass**: 184.1 $(M+H)^+$.

Synthesis of (*S*)-5-ethylnon-7-yn-4-one (58):

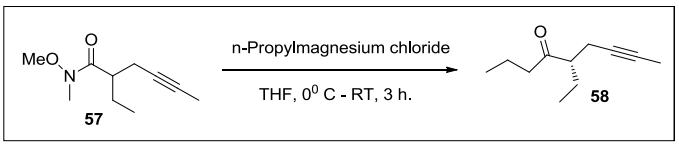

To a cooled (0°C) solution of **57** (0.18 g, 1.0 mmol) in THF (15 mL) was added drop wise 1 M THF solution of *n*-propylmagnesiumchloride (1.1 mL, 1.1 mmol). The reaction mixture was warmed slowly to room temperature and stirred for 3 h. The reaction was quenched with a saturated ammonium chloride solution and extracted with ethylacetate (2 X 100 mL). The combined organic layers were washed with brine, dried over anhydrous Na_2SO_4, filtered, and concentrated under reduced pressure. The residue was purified by column chromatography on silica gel (silica gel, 5% ethylacetate-pet ether) to afford **58** (0.15 g, 90%).

^{1}H NMR (400 MHz, $CDCl_3$) δ ppm: 2.60 -2.30 (m, 4H), 1.71 -1.47 (m, 7H), 0.96 -0.92 (m, 6H). **^{13}C NMR (100 MHz, $CDCl_3$) δppm:** 76.8, 76.5, 52.5, 44.6, 24.0, 20.2, 16.7, 13.7, 11.3, 3.3; **Mass**: 167.1 $(M+H)^+$; **$[\alpha]_D^{27}$**= + 12.26°. **HPLC:** The enantiomeric ratio: 97 : 03; column : chiralcel OD-RH, mobile phase : acetonitrile:water = 30:70, flow rate 0.5 mL/ min, wave length = 210 nm.

Synthesis of tert-butyl 2-(trimethylsilyl)pyrrolidine-1-carboxylate (64):

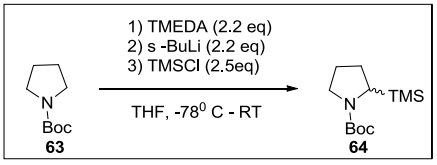

A solution of N- Boc pyrrollidine **63** (3.44 g, 20.1 mmol) in 40 mL of THF was charged into a 250 mL flask, equipped with a magnetic bar and argon gas balloon and was cooled to – 78 ° C. TMDEA (2.79 g, 24. 12 mmol) followed by *s*–BuLi (1.5 M solution in cyclohexane, 16. 1 mL, 24.12 mmol) were introduced to the stirring mixture dropwise over 15 min. The mixture was further allowed to stir for 2 h at -78° C. TMSCl (2.61 g, 24.12 mmol) was added dropwise into the flask. The reaction mixture was allowed to warm to room temperature and diluted with 15 mL of saturated aqueous NH_4Cl solution. The organic layer was concentrated and the crude oily residue was purified by column chromatography (3% ethylacetate – pet ether) to afford **64** (4.3 g, 88%) as a colourless oil.

^{1}H NMR (400 MHz, $CDCl_3$) δ ppm: 0.05 (s, 9H), 1.45 (s, 9H),,1.75-1.95 (m, 3H), 1.95 - 2.05 (m, 1H), 3.15-3.30(m, 2H), 3.35-3.60 (m, 1H); **^{13}C NMR (100 MHz, $CDCl_3$) δ ppm:** - -2.3, 27.8, 28.4, 46.7, 47.5, 78.0, 154.5; **Mass:** 243 $(M+H)^+$.

Syntheis of 2-(trimethylsilyl)pyrrolidine (59):

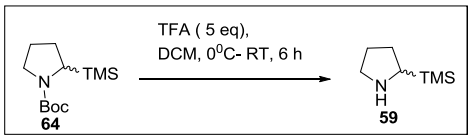

To a stirring solution of **64** (3.39 g, 13.95 mmol) in 60 mL of DCM at 0° C, TFA (5.7 g, 50.0 mmol) was added drop-wise over a period of 30 min. The mixture was allowed to warm to room temperature and allowed to stir further for 4 h. The reaction mixture was re-cooled to 0° C and was basified by saturated $NaHCO_3$ solution (pH = 8). The organic layer was separated and aqueous layer was extracted with DCM (3 X 100 mL). The combined extracts were

washed with brine, dried over Na_2SO_4 and concentrated to give crude **59**, which was utilized as such without further purification for the next step.

^{1}H NMR (400 MHz, $CDCl_3$) δ ppm: 0.00 (s, 9H), 1.48-2.07 (m, 4H), 2.50 (dd, 1H, *J* = 6.9 Hz, 12.1 Hz), 2.96-3.23 (m, 2H); **^{13}C NMR (100 MHz, $CDCl_3$) δ ppm:** - 3.8, 24.9, 27.2, 46.6, 49.1; **Mass:** 143 $(M)^+$.

Synthesis of (2S)-2-ethyl-1-(2-(trimethylsilyl)pyrrolidin-1-yl)hex-4-yn-1-one 4 (62):

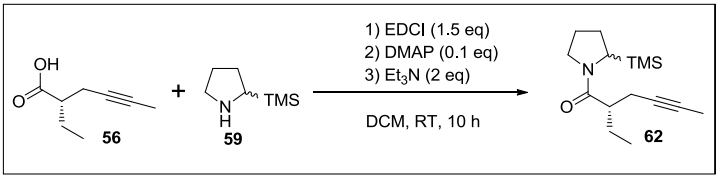

To a solution of **56** (2.39 g, 17.06 mmol) in 150 mL DCM, was added DMAP (0.2 g, 1.7 mmol) and EDCI **(**4.9 g, 25.5mmol). Amine **59** (2.7 g, 20 mmol) and triethylamine (34 mmol, 4.6 mL) were added at room temperature to the mixture. The reaction was allowed to stir for 10 h. After maximum starting materials was disappeared (monitored by TLC), the reaction mixture was quenched by adding water (20 mL).The water layer was extracted by ethylacetate (3 X 100 mL). Finally organic layer was successively washed a dilute solution of $KHSO_4$ and saturated $NaHCO_3$. The organic layer was dried over Na_2SO_4 and solvent was evaporated under reduce pressure to afford **62** as 1:1 diastereomeric mixture (3.8 g, 75%) as liquid.

^{1}H NMR (400 MHz, $CDCl_3$) δ ppm: 4.25 – 4.17 (m, 1H), 3.82 – 3.31 (m, 4H), 2.69 – 2.60 (m, 1H), 2.47 – 2.23 (m, 3H), 2.00 – 1.54 (m, 13H), 0.99 – 0.87 (m, 6H), 0.13 – 0.04 (two singlets, 9H).; **^{13}C NMR (100 MHz, $CDCl_3$) δ ppm:** 0.01 + 0.06, 5.2, 13.6, 23.6 + 23.9, 27.1 + 27.1, 28.0, 29.2, 46.9 + 47.0, 49.3 + 49.6, 50.3, 76.31, 77.15 173.8; **HRMS:** Calc mass for $C_{15}H_{28}NOSi$: 266.1940, found 266.1943.

Synthesis of 1-((4*S*, 5*S*)-5-ethylnon-7-yn-4-yl)-2-(trimethylsilyl)pyrrolidine (60)

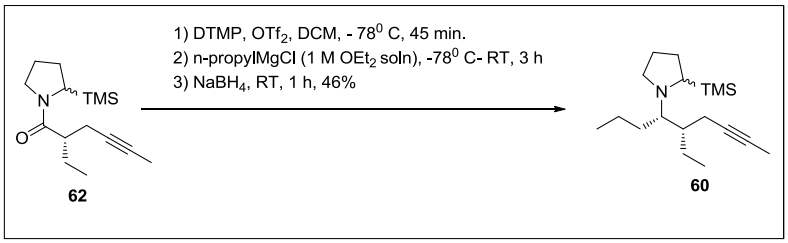

To a cooled (-78° C) solution of **62** (0.15 g, 0.57 mmol) and 2, 6 –di-*tert*-butyl-4-methylpyridine (0.17 g, 0.84 mmol) in DCM (10 mL) was added Tf_2O (0. 21 g, 0.84 mmol, 0.15 mL) in a drop wise manner and stirred at -78° C for 45 mim. A 1 M THF solution of *n* –propylmagnesiumchloride (0.84 mmol, 0.85 mL) was added dropwise to the resultant mixture. The reaction mixture was warmed slowly to room temperature and stirred for additional 2 h. After 2 h the reaction mixture was again cooled to 0° C and $NaBH_4$ (1 mmol, 0.04 mg) was added. After 1 h stirring, the reaction was quenched by saturated NH_4Cl solution and extracted with DCM (3 X 20 mL). The combined organic layers were dried over anhydrous Na_2SO_4, and concentrated under reduce pressure. The residue was purified by column chromatography (7% ethylacetate – pet ether) to afford **60** (0.06 g, 46%) as a colourless liquid.

^{1}H NMR (400 MHz, $CDCl_3$) δ ppm: 3.65 – 3.45 (m, 1H), 3.33 – 3.12 (m, 1H), 2.80 – 2.70 (m, 1H), 2.47 – 1.89 (m, 4H), 1.80 – 1.51 (m, 8H), 1.33 – 1.23 (m, 4H), 1.01 – 0.86 (m, 6H), 0.09 – 0.04 (m, 9H).; **^{13}C NMR (100 MHz, $CDCl_3$) δ ppm:** -2.1+ 2.3, 3.6 + 3.6, + 12.0 + 14.7, 20.3 + 20.3, 25.5 + 25.8, 26.3 + 26.3, 27.4 + 27.5, 30.1 + 31.4, 46.8 + 47.1, 60.3, 76.28, 76.92; **HRMS:** Calc mass for $C_{18}H_{34}NSi$: 294.1035, found 294.1032.

3.7 Spectra:

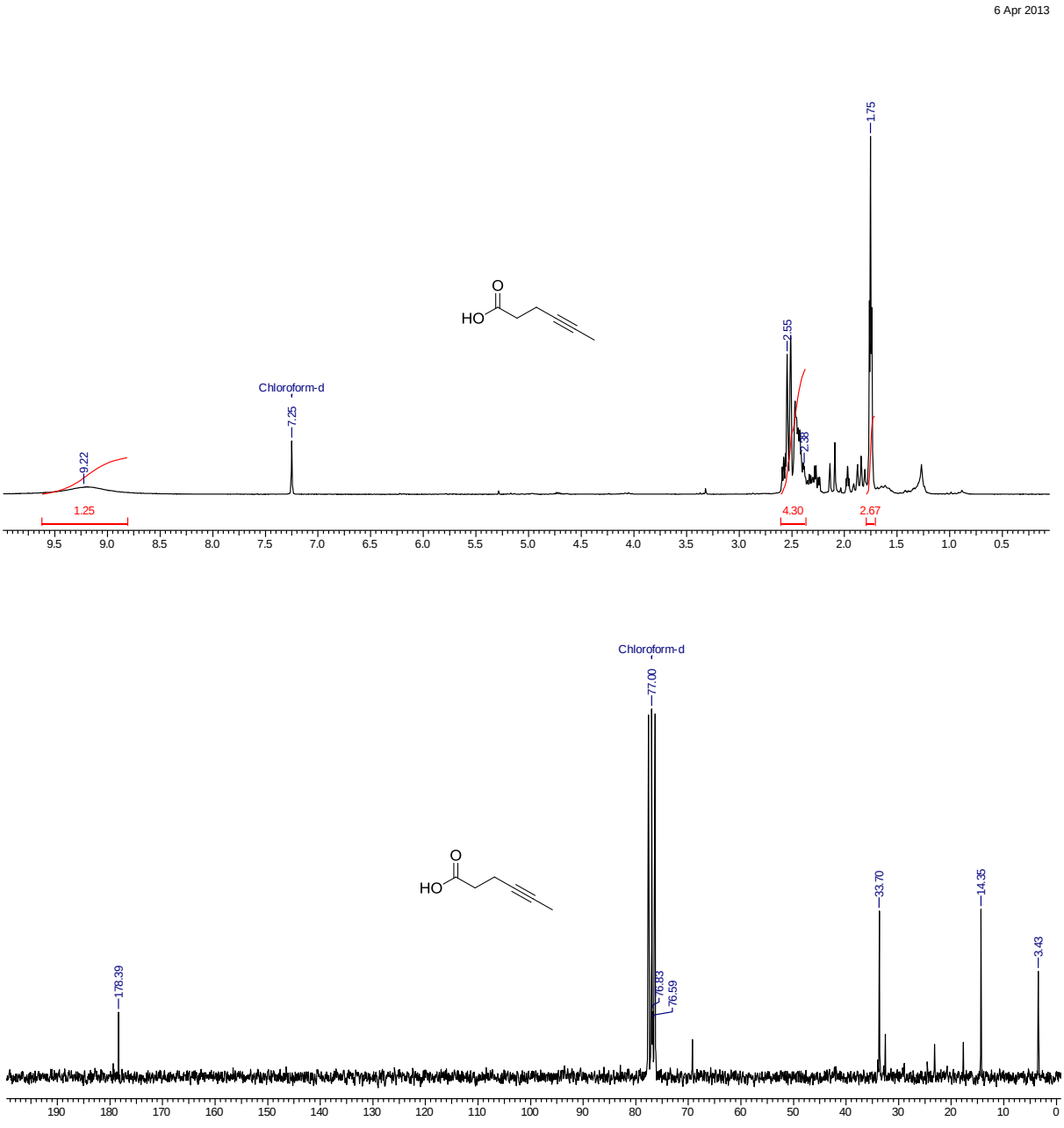
6 Apr 2013
1.75
O
HO
2.55
Chloroform-d
7.25
2.38
9.22
1.25
4.30
2.67
9.5 9.0 8.5 8.0 7.5 7.0 6.5 6.0 5.5 5.0 4.5 4.0 3.5 3.0 2.5 2.0 1.5 1.0 0.5
Chloroform-d
77.00
O
HO
33.70
14.35
3.43
178.39
76.83
76.59
190 180 170 160 150 140 130 120 110 100 90 80 70 60 50 40 30 20 10 0

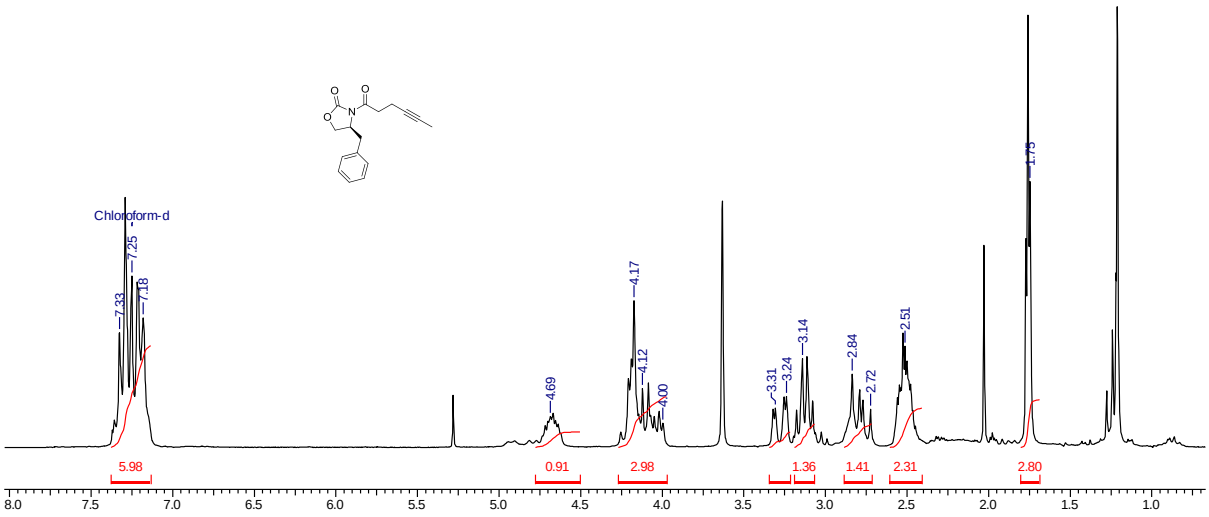
Chloroform-d
7.33
7.25
7.18
4.69
4.17
4.12
4.00
3.31
3.24
3.14
2.84
2.72
2.51
1.73
5.98
0.91
2.98
1.36
1.41
2.31
2.80

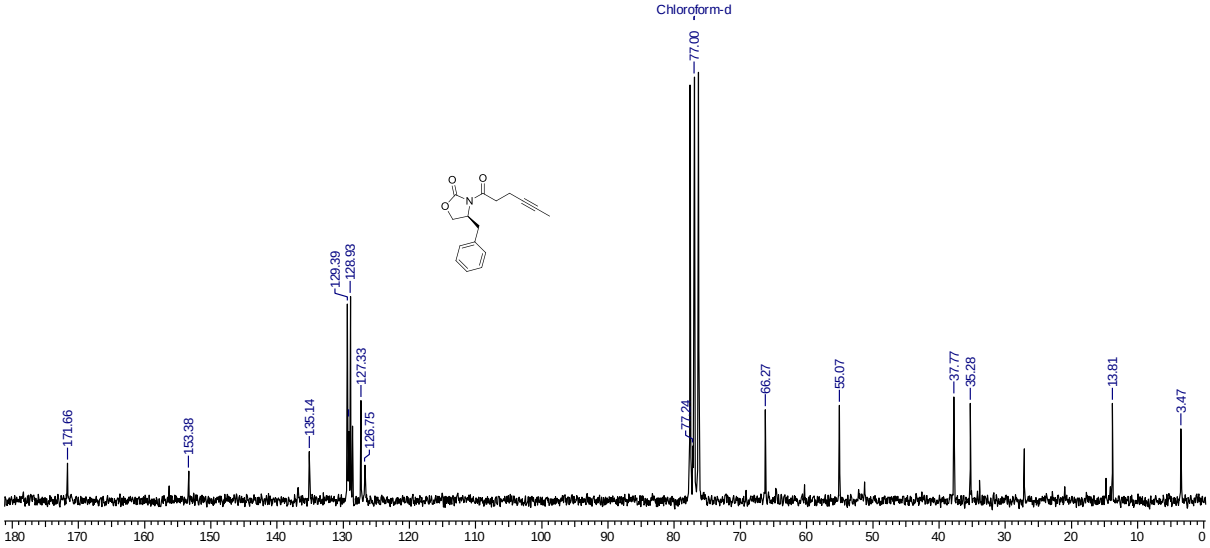
Chloroform-d
77.00
129.39
128.93
127.33
126.75
171.66
153.38
135.14
77.24
66.27
55.07
37.77
35.28
13.81
3.47

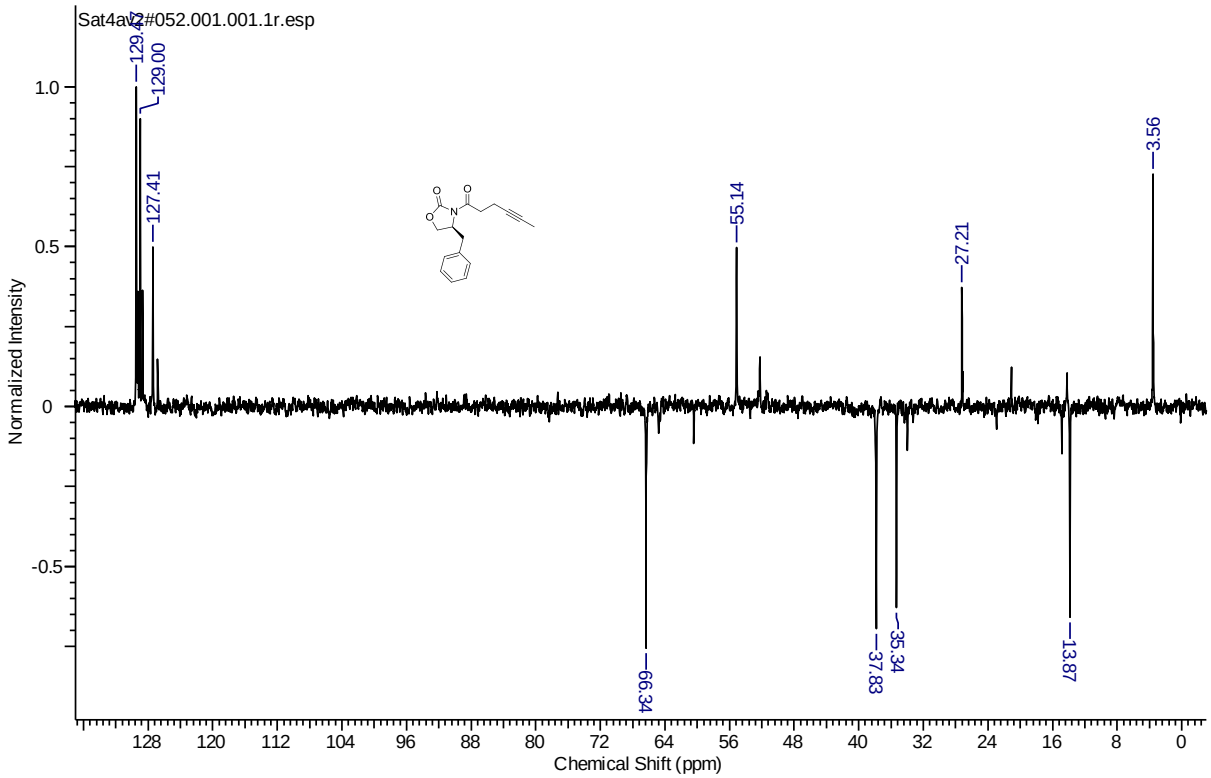
Sat4av2#052.001.001.1r.esp
129.42
129.00
127.41
55.14
27.21
3.56
69.34
37.83
35.34
13.87
Normalized Intensity
Chemical Shift (ppm)

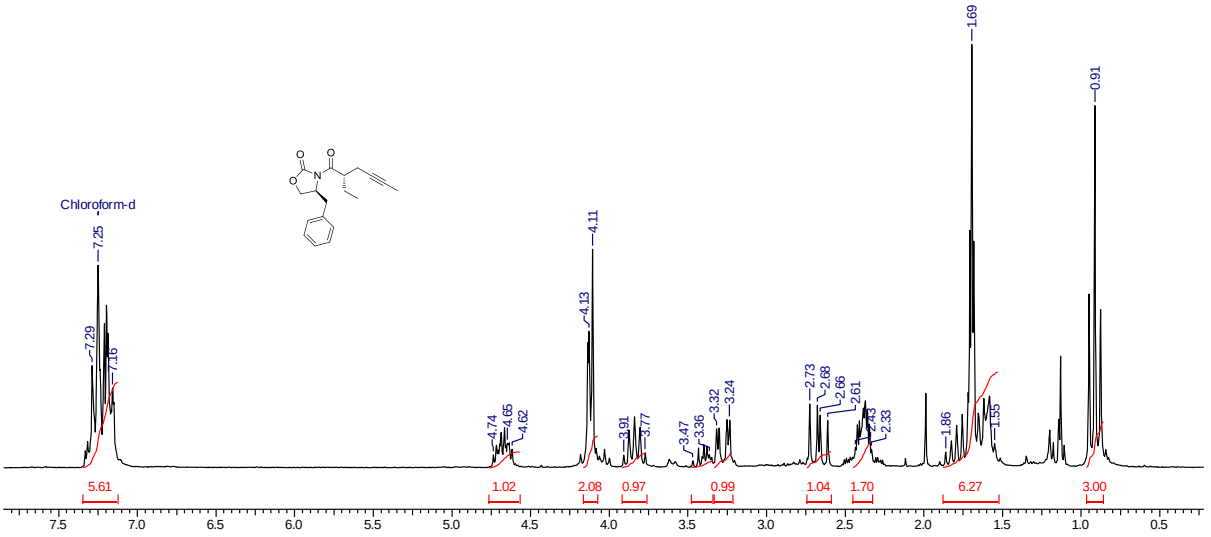
Chloroform-d
7.25
7.29
7.16
4.74
4.65
4.62
4.13
4.11
3.91
3.77
3.47
3.36
3.32
3.24
2.73
2.68
2.66
2.61
2.43
2.33
1.86
1.69
1.55
0.91
5.61
1.02
2.08
0.97
0.99
1.04
1.70
6.27
3.00

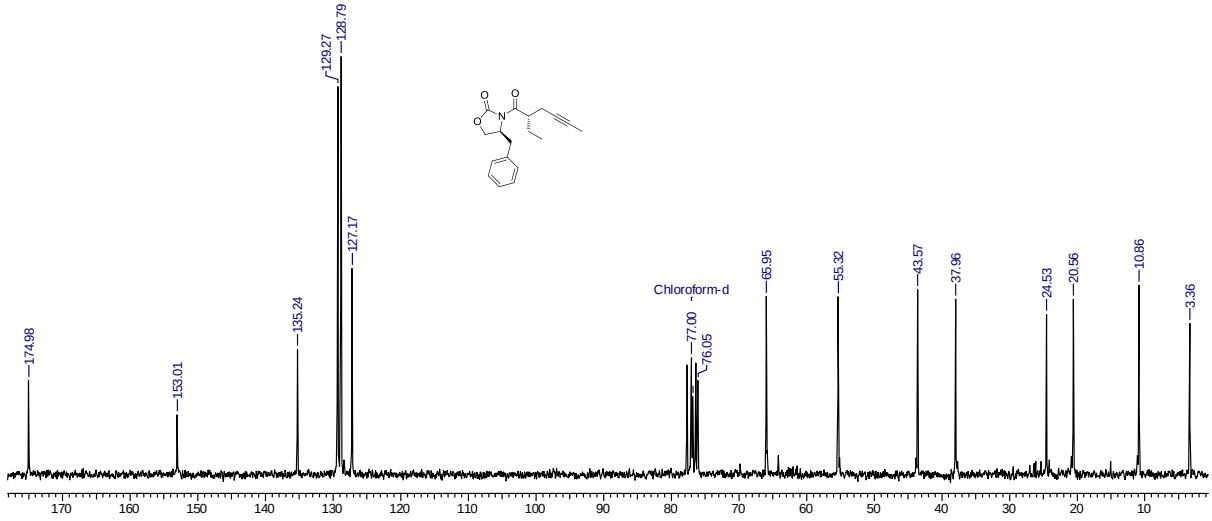
174.98
153.01
135.24
129.27
128.79
127.17
Chloroform-d
77.00
76.05
65.95
55.32
43.57
37.96
24.53
20.56
10.86
3.36

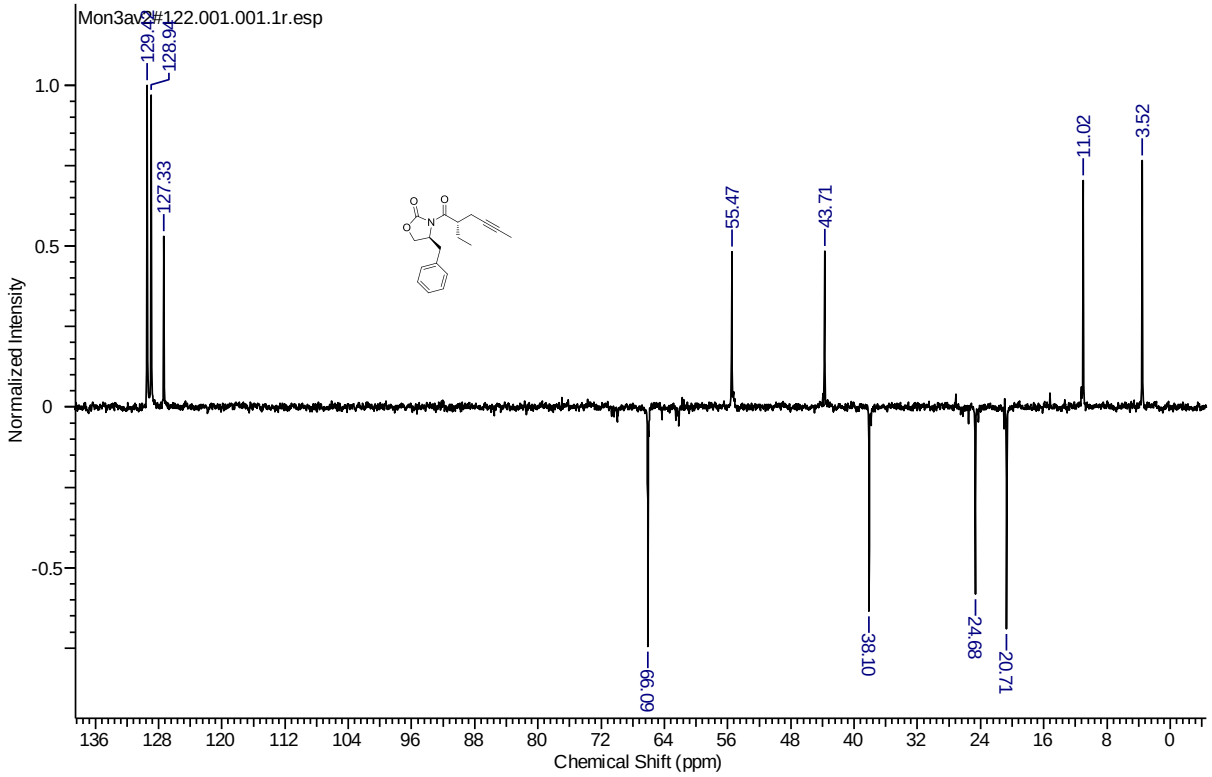
Mon3a\2#122.001.001.1r.esp
129.42
128.94
127.33
55.47
43.71
11.02
3.52
60.99
38.10
24.68
20.71
Normalized Intensity
Chemical Shift (ppm)

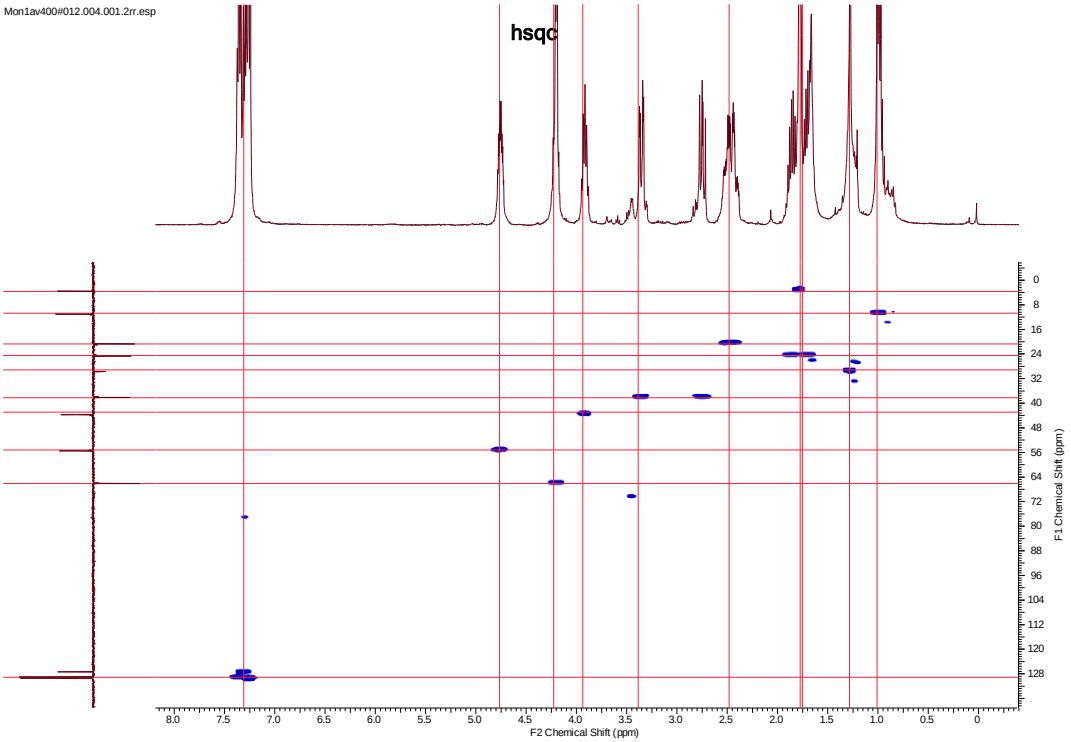
Mon1av400#012.004.001.2rr.esp
hsqc
F2 Chemical Shift (ppm)
F1 Chemical Shift (ppm)

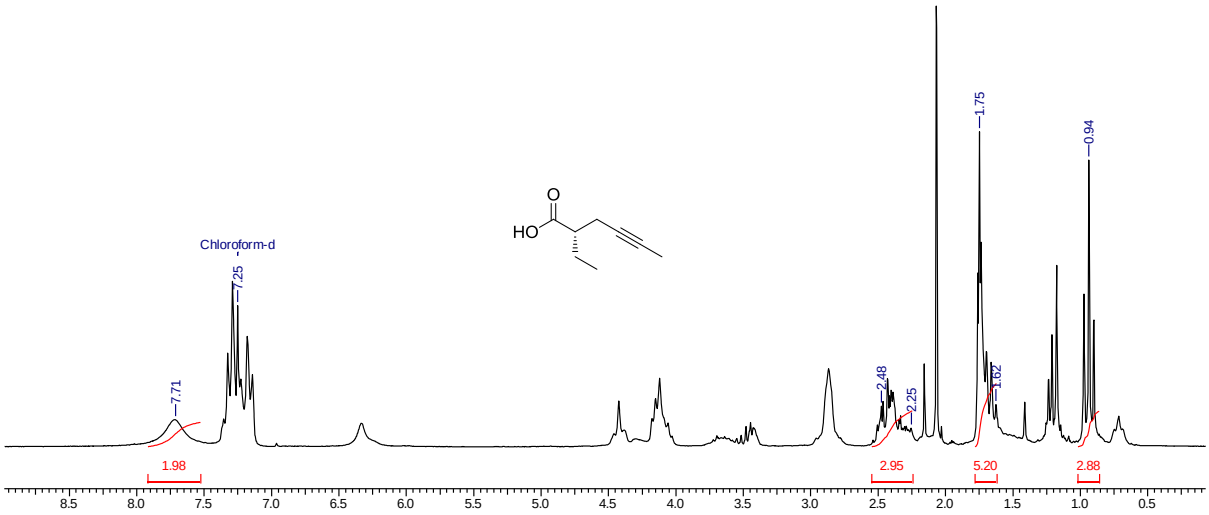
Chloroform-d
7.25
7.71
1.98
2.48
2.25
2.95
1.75
1.02
5.20
0.94
2.88
HO
O

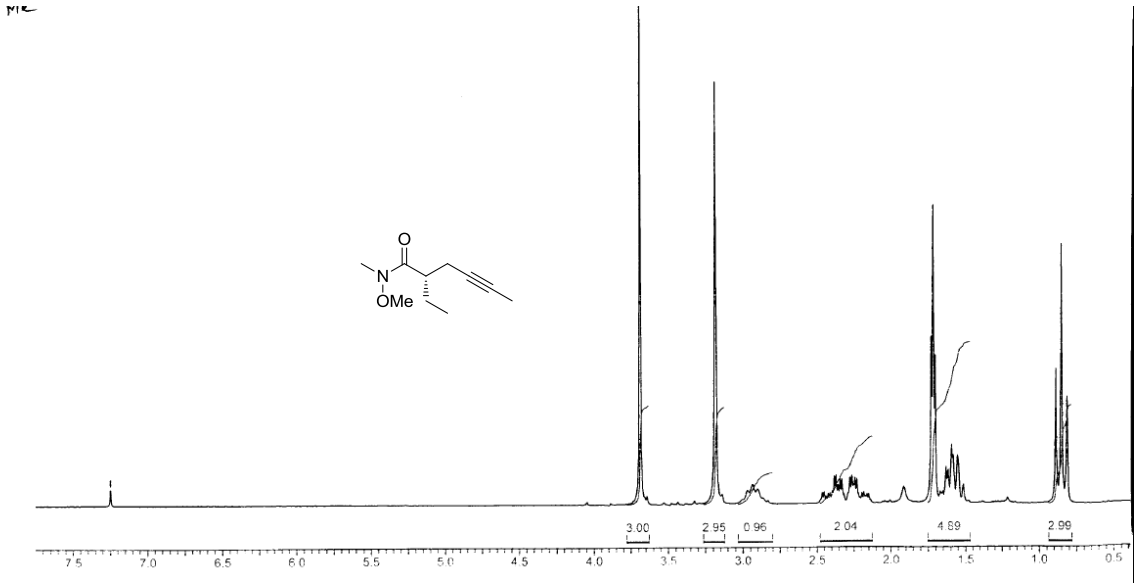
O
N
OMe
3.00
2.95
0.96
2.04
4.89
2.99
7.5
7.0
6.5
6.0
5.5
5.0
4.5
4.0
3.5
3.0
2.5
2.0
1.5
1.0
0.5

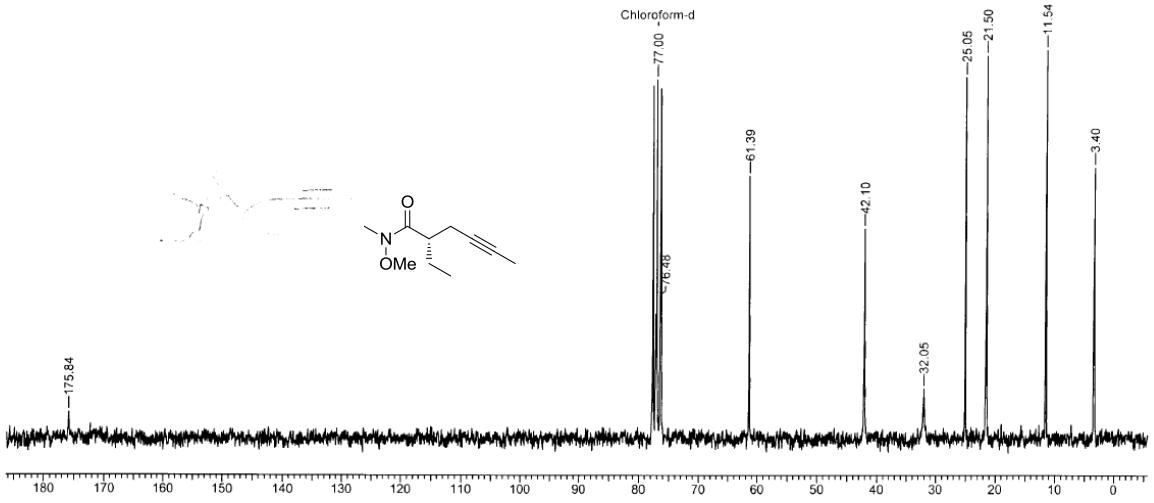
Chloroform-d
77.00
76.48
61.39
42.10
32.05
25.05
21.50
11.54
3.40
175.84
O
N
OMe
180
170
160
150
140
130
120
110
100
90
80
70
60
50
40
30
20
10
0

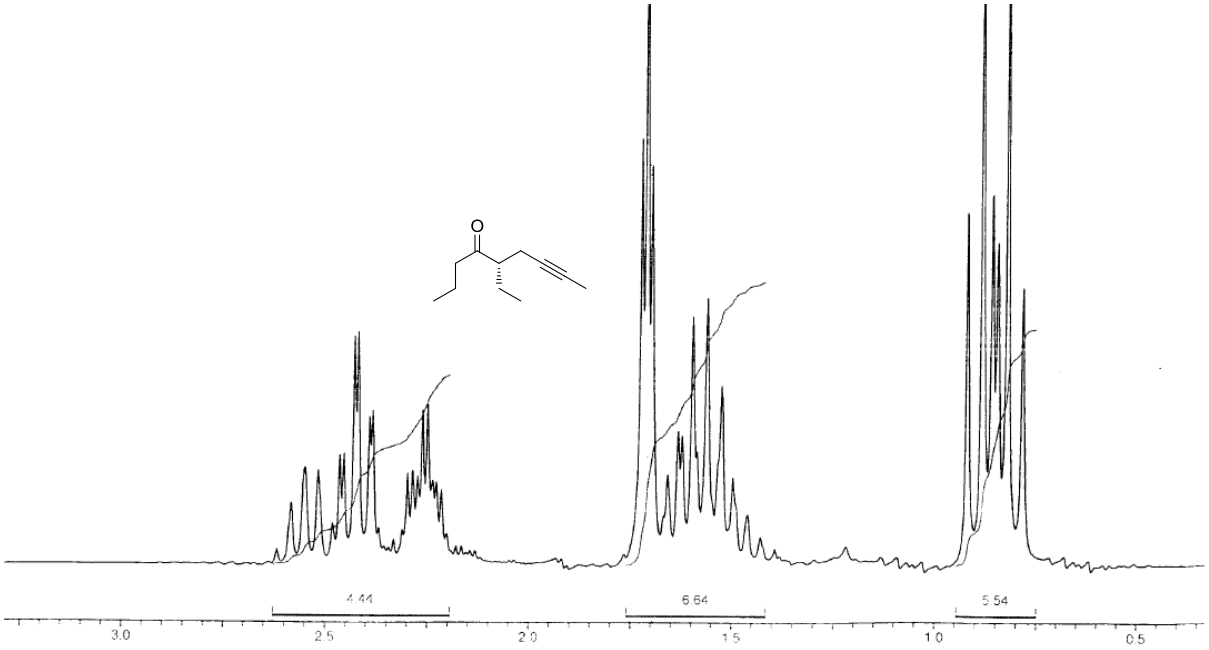
4.44
6.64
5.54
3.0
2.5
2.0
1.5
1.0
0.5

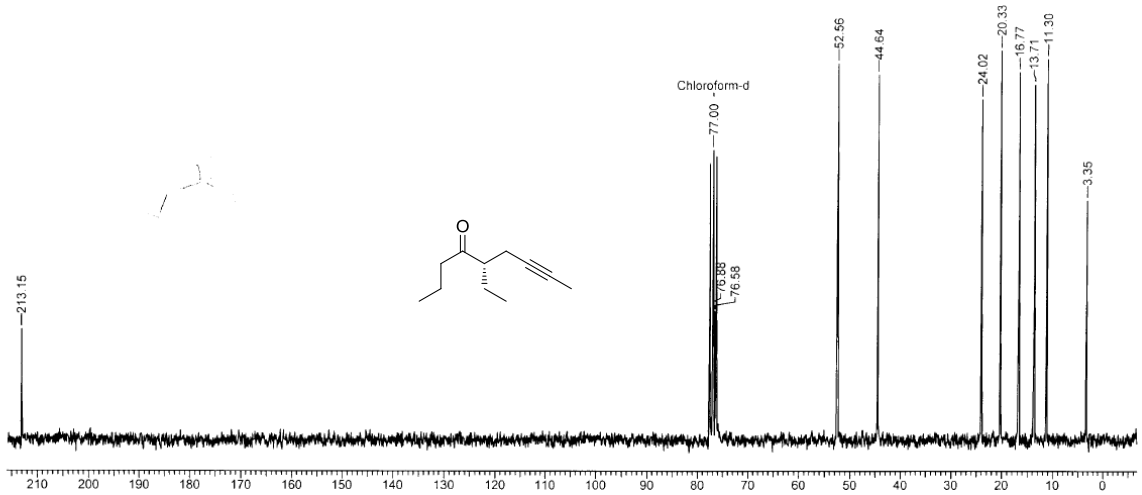
213.15
Chloroform-d
77.00
76.88
76.58
52.56
44.64
24.02
20.33
16.77
13.71
11.30
3.35

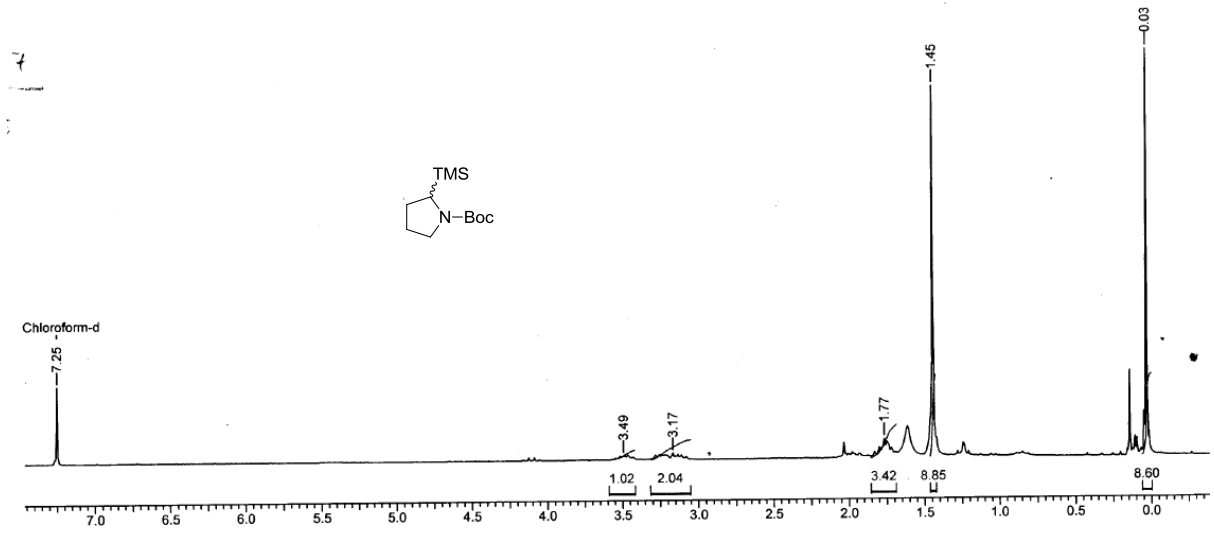
TMS
N–Boc
Chloroform-d
7.25
3.49
3.17
1.77
1.45
0.03
1.02
2.04
3.42
8.85
8.60

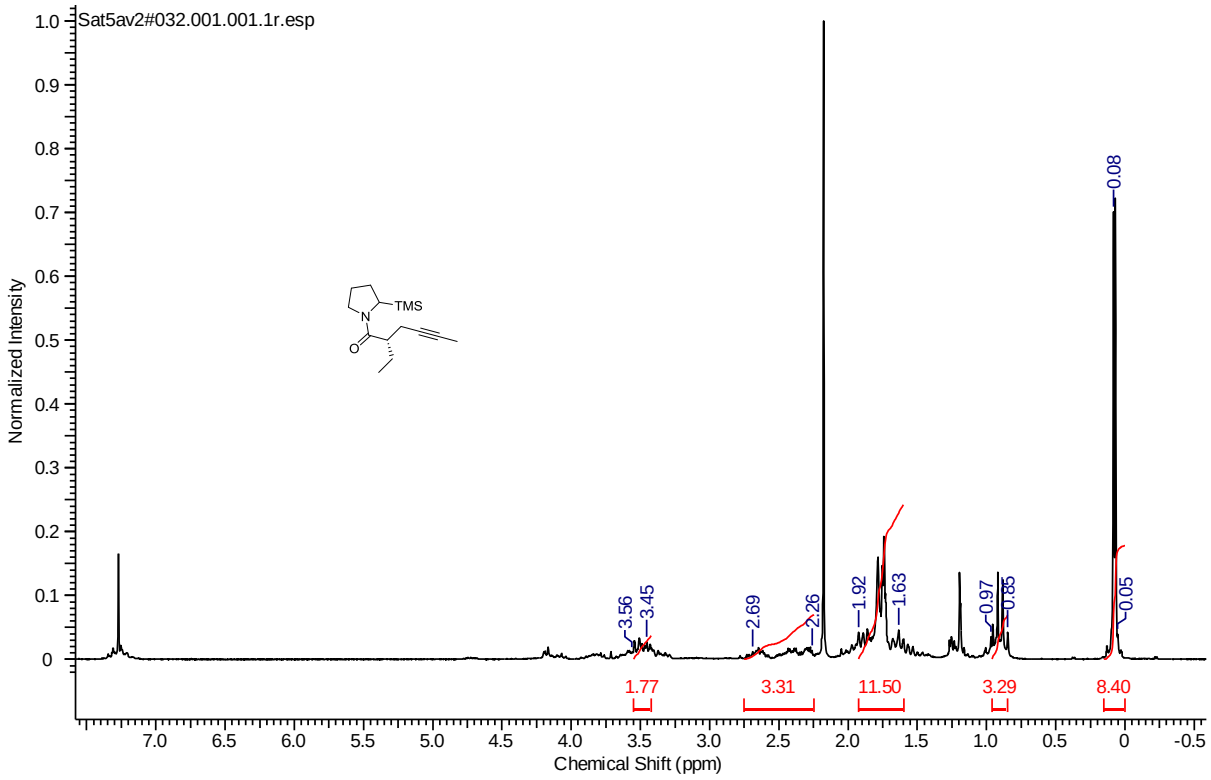
Sat5av2#032.001.001.1r.esp
TMS
Normalized Intensity
Chemical Shift (ppm)
3.56
3.45
2.69
2.26
1.92
1.63
0.97
0.85
0.08
0.05
1.77
3.31
11.50
3.29
8.40

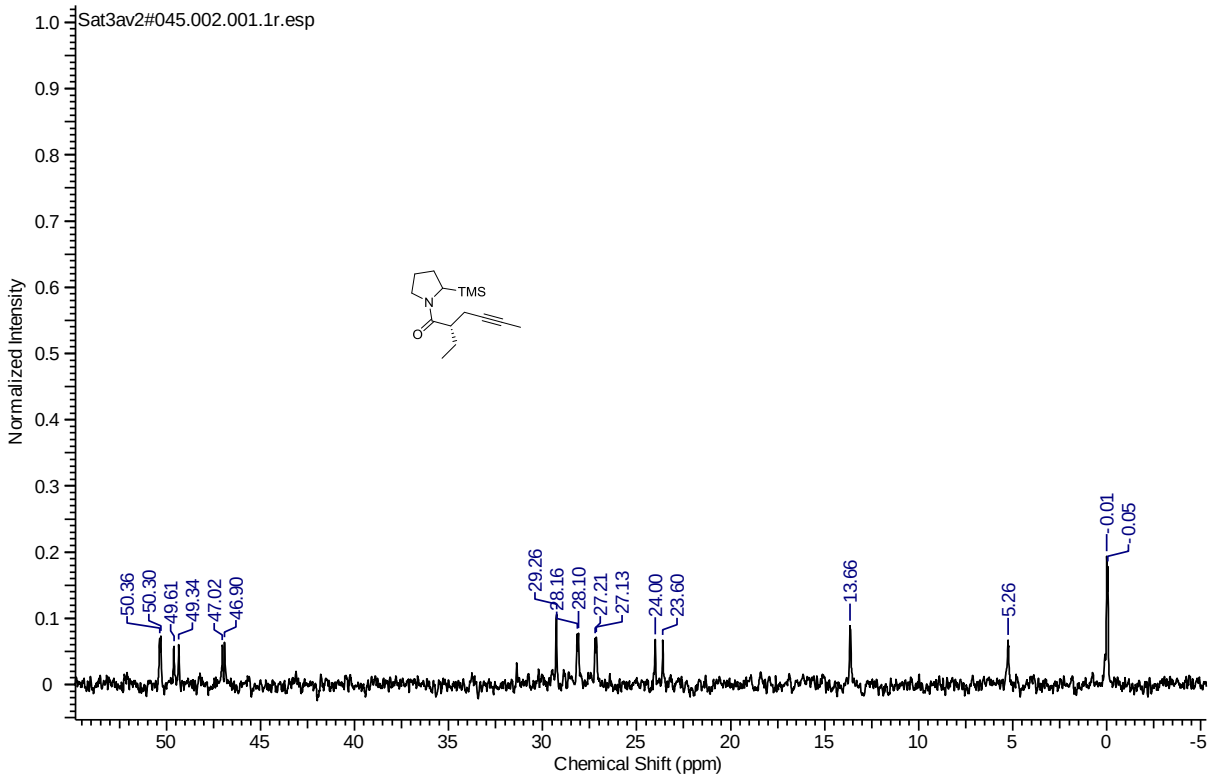
Sat3av2#045.002.001.1r.esp
Normalized Intensity
Chemical Shift (ppm)
TMS
50.36
50.30
49.61
49.34
47.02
46.90
29.26
28.16
28.10
27.21
27.13
24.00
23.60
13.66
5.26
0.01
0.05

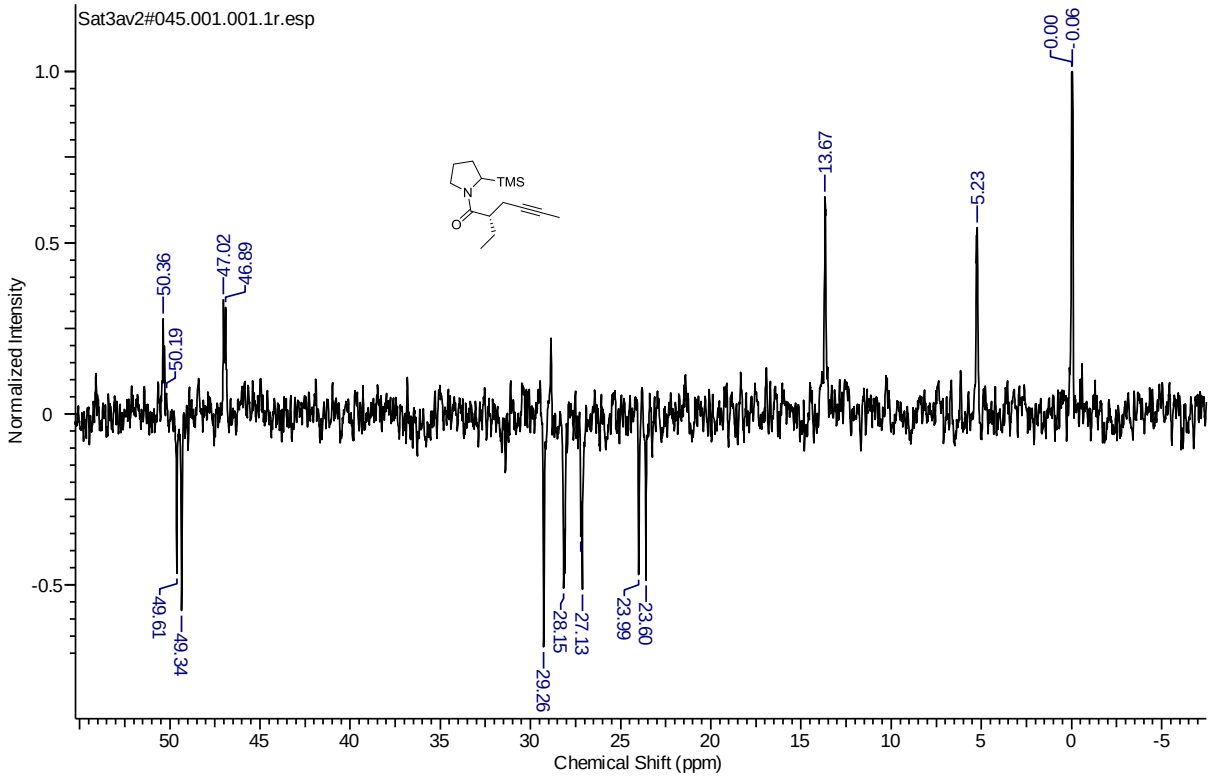
Sat3av2#045.001.001.1r.esp
Normalized Intensity
Chemical Shift (ppm)
TMS
50.36
50.19
49.61
49.34
47.02
46.89
29.26
28.15
27.13
23.99
23.60
13.67
5.23
0.00
0.06

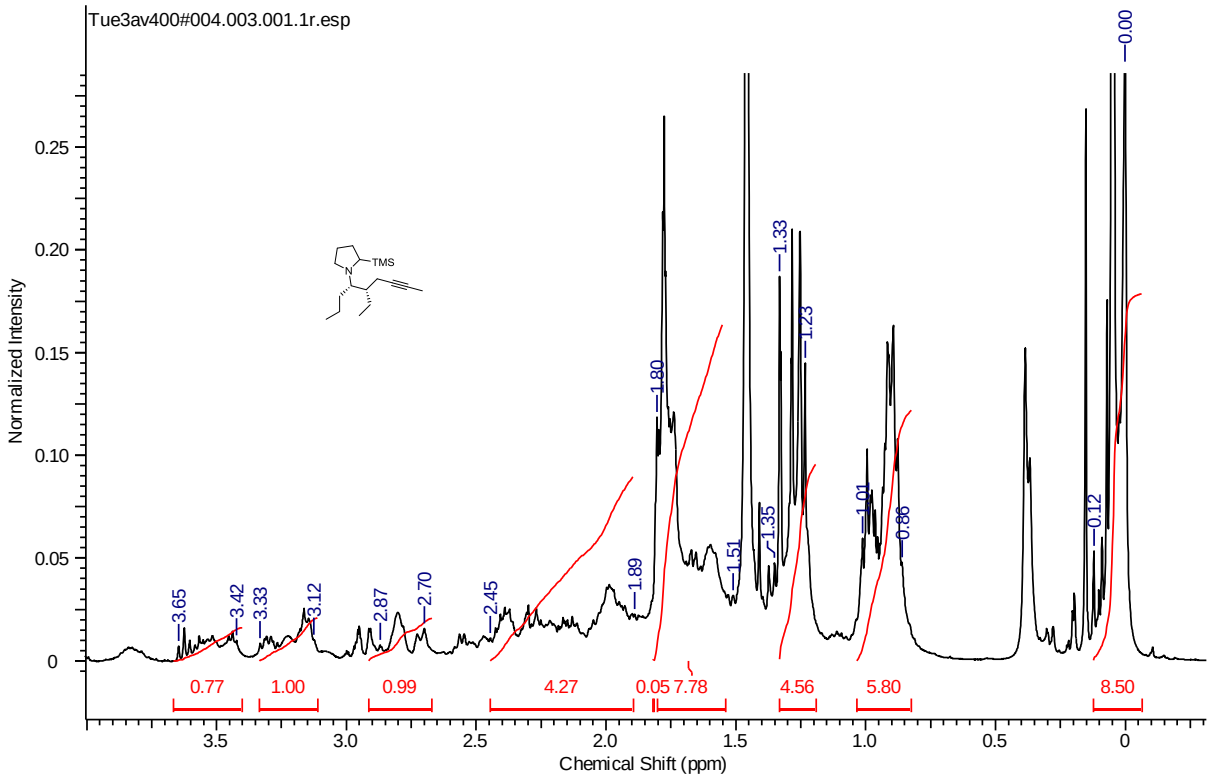
Tue3av400#004.003.001.1r.esp
Normalized Intensity
Chemical Shift (ppm)
TMS
3.65
3.42
3.33
3.12
2.87
2.70
2.45
1.89
1.80
1.51
1.35
1.33
1.23
1.01
0.86
0.12
0.00
0.77
1.00
0.99
4.27
0.05
7.78
4.56
5.80
8.50

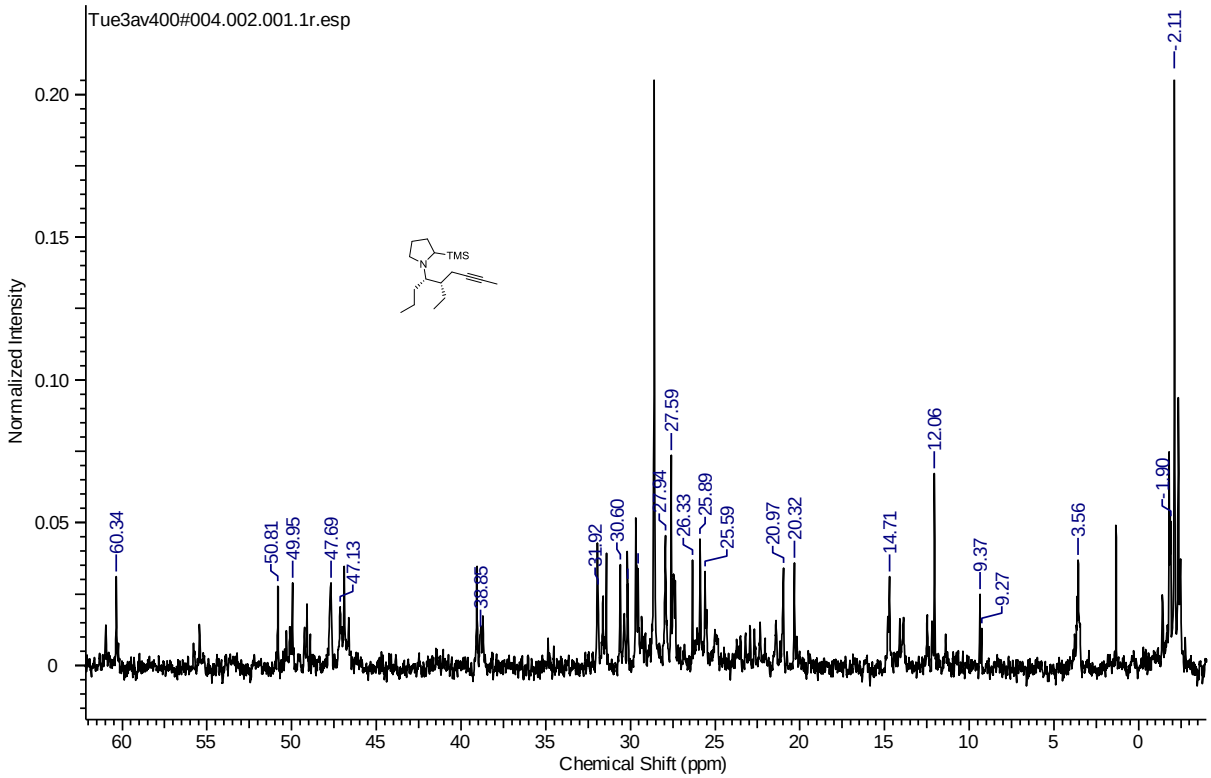
Tue3av400#004.002.001.1r.esp
Normalized Intensity
Chemical Shift (ppm)
TMS
60.34
50.81
49.95
47.69
47.13
38.85
31.92
30.60
27.94
27.59
26.33
25.89
25.59
20.97
20.32
14.71
12.06
9.37
9.27
3.56
1.90
-2.11

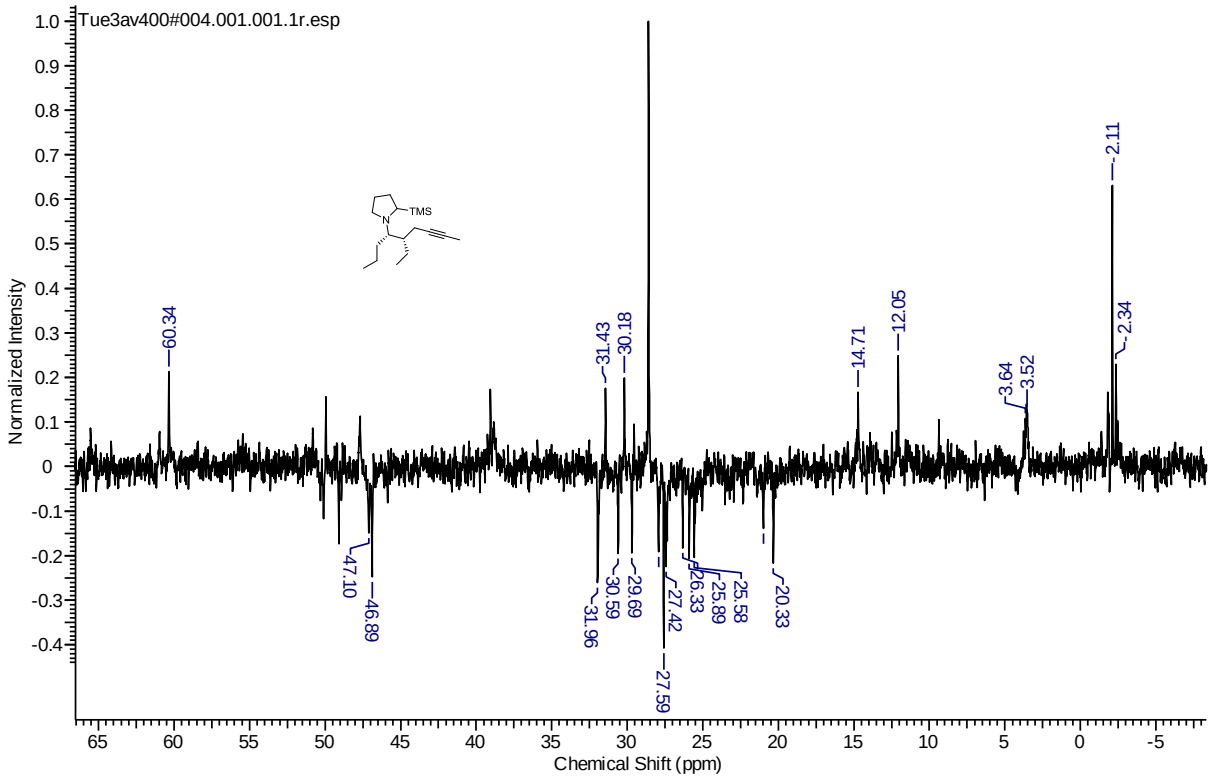
Tue3av400#004.001.001.1r.esp
TMS
Normalized Intensity
Chemical Shift (ppm)
60.34
47.10
46.89
31.96
31.43
30.59
30.18
29.69
27.59
27.42
26.33
25.89
25.58
20.33
14.71
12.05
3.64
3.52
2.34
2.11

HPLC analysis of recemic ketone **58-rac**

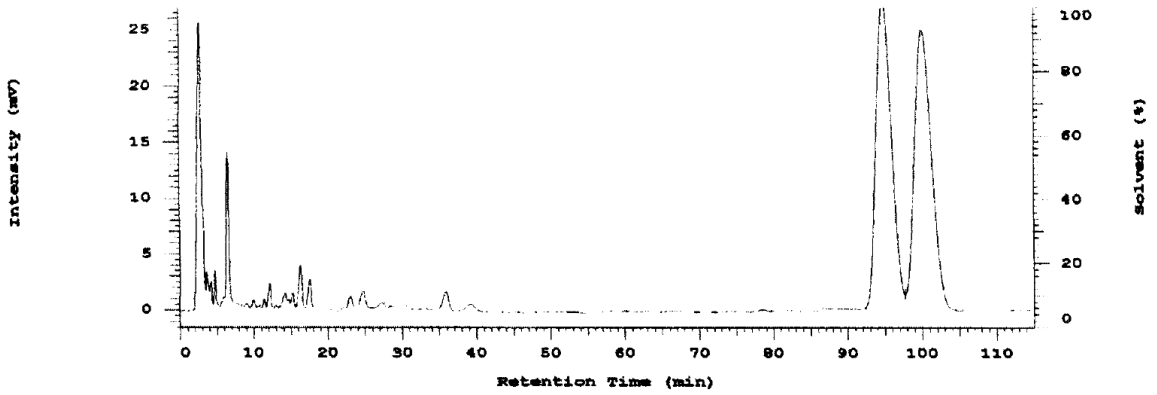

Peak Quantitation: AREA Calculation Method: AREA%

No.	RT	Height	Area	Area %
1	94.77	26934	3756622	51.837
2	100.00	23513	3490401	48.163
		50447	7247023	100.000

Peak rejection level: 0

Group Leader :Dr.Ganesh Pandey
Column :Chiralcel OD-RH (150 X 4.6 mm)
M.P. :ACN:H2O (30:70)

Flow Rate :0.5 ml/min (890 psi)
Sample conc: X mg/ 1 ml
Inj vol: 5 ul
WAVELENGTH : 210 nm

HPLC analysis of chiral ketone **58**.

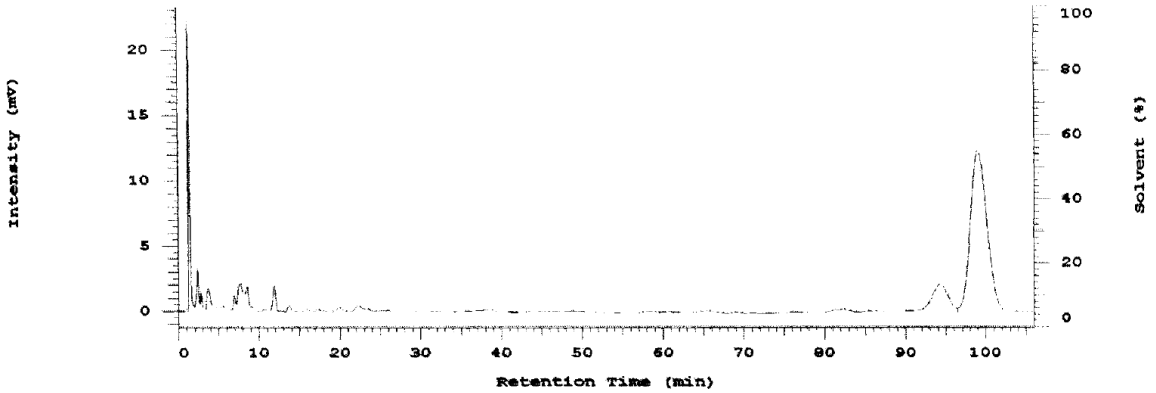

Peak Quantitation: AREA Calculation Method: AREA%

No.	RT	Height	Area	Area %
1	94.27	1213	105233	6.935
2	99.04	11088	1412100	93.065
		12301	1517333	100.000

Peak rejection level: 0

Group Leader :Dr.Ganesh Pandey
Column :Chiralcel OD-RH (150 X 4.6 mm)
M.P. :ACN:H2O (30:70)

Flow Rate :0.5 ml/min (890 psi)
Sample conc: X mg/ 1 ml
Inj vol: 5 ul
WAVELENGTH : 210 nm

HPLC analysis of **55**

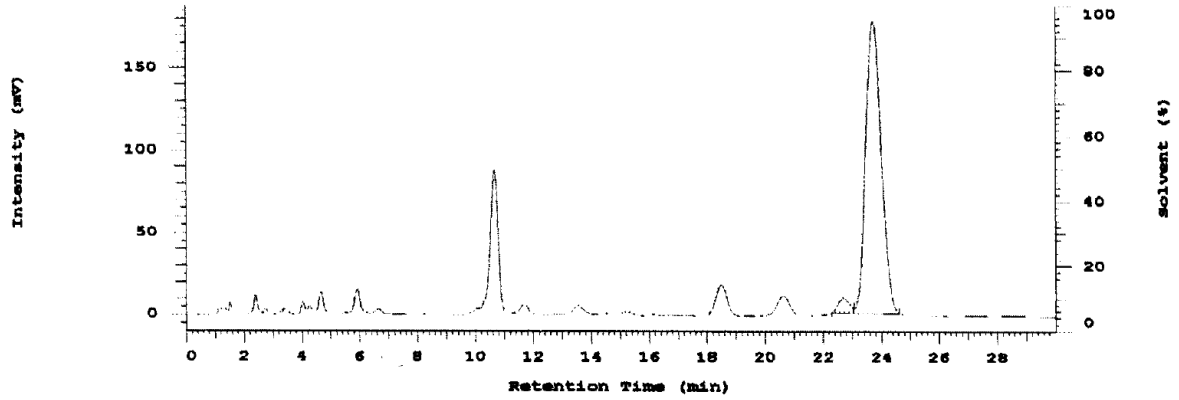

Peak Quantitation: AREA Calculation Method: AREA%

No.	RT	Height	Area	Area %
1	22.71	8907	240171	3.528
2	23.70	177151	6566938	96.472
		186058	6807109	100.000

Peak rejection level: 0

Group Leader :Dr.G.Pandey
Column : Kromasil RP-18 (150 x4.6 mm)
M.P. : ACN:H2O (50:50)

Flow Rate : 1.0 ml/min
Sample conc: 1mg/1ml
Inj vol: 10ul
WAVELENGTH : 230 nm